Apoptosis chip for drug screening

Floor Wolbers

Wolbers, Floor
Apoptosis chip for drug screening
PhD thesis University of Twente, Enschede, The Netherlands
ISBN 978-90-365-2499-5

Publisher: Wöhrmann Print Service, Zutphen, The Netherlands

Cover design by Floor Wolbers

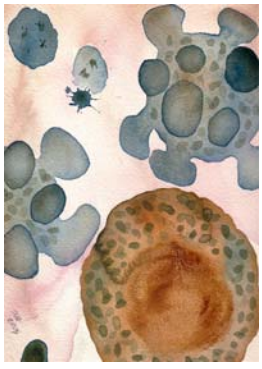

www.nick-lane.net (Ina Schuppe-Koistinen)

The cover describes the process of apoptosis in which a cell shrinks, the cytoplasm condenses and the membrane displays blebbing. The cell dissociates into small fragments, called apoptotic bodies, which are phagocytosed by surrounding macrophages. The cover is made up of small pictures describing my 4 years as a PhD. Results as well as the pictures taken during social events are included.

APOPTOSIS CHIP FOR DRUG SCREENING

PROEFSCHRIFT

ter verkrijging van
de graad van doctor aan de Universiteit Twente,
op gezag van de rector magnificus,
prof. dr. W.H.M. Zijm,
volgens het besluit van het College voor Promoties
in het openbaar te verdedigen
op vrijdag 8 juni 2007 om 13.15 uur

door

Floor Wolbers

geboren op 1 december 1979

te Enschede

The research described in this thesis was carried out at the BIOS Lab-on-a-Chip group of the MESA+ Institute for Nanotechnology of the University of Twente, Enschede, The Netherlands and the department of Clinical Chemistry, in cooperation with the department of Obstetrics and Gynaecology, of the Medisch Spectrum Twente, Hospital group, Enschede, The Netherlands. The project was financed by STW ("Stichting Technische Wetenschappen" – Dutch Technology Foundation) under project number TMM.6016 (NanoSCAN project), matching project of NanoNed project TMM.7128, Flow sensing and control in nanochannels.

Members of the committee:

Chairman	prof. dr. ir. J. van Amerongen	University of Twente
Promotors	prof. dr. ir. A. van den Berg	University of Twente
	prof. dr. I. Vermes	University of Twente/ Medisch Spectrum Twente
	prof. dr. S.M.H. Andersson	University of Twente/ RIT, Stockholm
Referent	dr. H.R. Franke	Medisch Spectrum Twente
Members	prof. dr. J. Feijen	University of Twente
	prof. dr. W. Kruijer	University of Twente
	prof. dr. A. Sturk	AMC Amsterdam
	prof. dr. J.W. Hofstraat	Philips Research

The research described in this thesis was supported by Medisch Spectrum Twente, Hospital Group, Enschede, The Netherlands

Dit proefschrift is goedgekeurd door:

Promotoren	prof. dr. ir. A. van den Berg
	prof. dr. I. Vermes
	prof. dr. S.M.H. Andersson

Contents

1

Aim and thesis outline

This chapter gives a brief introduction to the aim of this thesis, the development of an apoptosis chip for drug screening. The advantages of microfluidic lab-on-a-chip devices for cell analysis, as compared to the standard conventional assays nowadays performed in clinical laboratories are discussed. Finally, an overview of the chapters is presented.

1.1 Apoptosis chip for drug screening

Apoptosis, or programmed cell death, plays an important role in maintaining a homeostatic equilibrium between cell proliferation and cell death during embryogenesis and goes on during post-embryonic life. Suppression or enhancement of apoptosis is known to cause or contribute to many disease states, such as cancer, neurodegenerative diseases (*e.g.,* Alzheimer, Parkinson) and AIDS.[1] The process of apoptosis is characterized by a series of events, resulting in the shrinkage of the cell, condensation of the nucleus, and the fragmentation of the cell into apoptotic bodies, which are phagocytosed by nearby cells and macrophages. Nowadays, a number of techniques are available to detect cell death.[2] However, in most cases these tools are not specific or lack quantitative value. In fact the very nature of apoptotic cell death promotes the under-recognition of this phenomenon for various reasons. First, apoptosis involves single cells scattered around, with morphological changes only after the "point-of-no-return". Second, the early stages of the apoptotic process evanesce and the apoptotic bodies are small and undergo rapid phagocytosis, an inflammatory reaction remains absent. Moreover, the duration of the whole process takes no more than a few hours.

Cellular based assays are of the utmost importance to understand how cells react in a certain environment, to a certain drug or in contact with other cell types. Today there is a huge interest and much effort is taken to analyse complex biological systems such as living cells using micro- and nanotechnologies.[3-6] The main reason for this is that compared to existing conventional cell-based assays, chip technology offers great advantages. Different cell manipulation methods (sorting, detachment, staining, fixing, lysis, and others) can be integrated on one chip, which reduces the work for analysts and increases the performance. Ideally, in cases when only a few cells are available (*e.g.,* primary cells), less sample is needed. The dimensions favour single-cell analysis. Apart from, the development of cell arrays, which are analogous to DNA or protein arrays, offers the possibility for high-throughput screening. Apoptosis or programmed cell death is a process which is ideally suited to analyse on chip as apoptosis is a process that does not occur simultaneously in all the cells of a population, favouring analysis at the single-cell level. Furthermore, the apoptotic process takes no more than a few hours, hence real-time monitoring will

provide new insights in the apoptotic cascade. Only recently research groups have become interested in developing chips convenient for detecting apoptosis.[7]
Our aim is to develop a microfluidic chip convenient for monitoring the apoptotic process in the presence of various drugs, with a special interest in evaluating the apoptotic pathway in breast cancer cells, as in tumour cells the process of apoptosis is disturbed. This microfluidic chip enables dose-response analysis using different cell types and monitoring drug-specific responses in real-time at a single-cell level, demands not easily performed with conventional techniques. Eventually, this microfluidic chip can be easily implemented in various clinical settings to improve not only breast cancer therapy, but fine-tune multiple therapies and the treatment of diseases for further steps towards personalized medicine. To our best knowledge, such apoptosis experiments have not been performed on chip so far.
This project was a cooperation between the University of Twente (UT) and the hospital Medisch Spectrum Twente (MST). Work at the UT was performed at the BIOS Lab-on-a-Chip group (part of the faculty of Electrical Engineering, Mathematics and Information Technology) of the MESA+ Institute for Nanotechnology. Work at the MST was performed at the department of Clinical Chemistry, in cooperation with the department of Obstetrics and Gynaecology. The project was financed by STW ("Stichting Technische Wetenschappen" – Dutch Technology Foundation) under project number TMM.6016 (NanoSCAN project), matching project of NanoNed project TMM.7128, Flow sensing and control in nanochannels.

1.2 Thesis outline

Here, a summary is given of the subjects, which are discussed in the following chapters.

Chapter 2 describes the process of apoptosis and gives an overview of the different processes occurring along the apoptotic pathway. The conventional techniques to measure apoptosis which exist nowadays are discussed and it is explained why the move towards chip technology for cell analysis, and especially apoptosis analysis, is desired.

Chapter 3 describes the kinetics of human promyelocytic leukaemic HL60 cells and human umbilical vein endothelial cells (HUVEC) in response to different apoptotic stimuli. With the use of the fluorochrome-labeled inhibitor of caspases (FLICA) and the permeability dye propidium iodide (PI), the transition to the different phases of the apoptotic process was analysed with flow cytometry and the apoptotic cell death kinetics was determined.

In chapter 4 the measurement of autofluorescence (AF) is described as a new analytical assay to analyse the process of apoptosis. Compared to well-known fluorescent apoptosis assays, sample preparation time is reduced and cellular toxicity is avoided. This is required when long-term real-time cell based assays are performed on chip.

Chapter 5 describes the conventional apoptosis and proliferation measurements performed for screening drugs used in hormonal replacement therapy and breast cancer treatment. With these *in vitro* studies, a selection can be made of the most promising compounds that are to be used later in clinical trials. However, due to genetic variation, every patient will have his/her individual response to therapy. The promising role of microfluidics in optimizing and individualizing endocrine therapy for breast cancer patients is discussed.

In chapter 6 the effect of different environmental parameters (*e.g.,* temperature and CO_2 concentration) and the choice of chip material on the viability of HL60 cells are evaluated. This is because the chip environment is quite different from the environment used to perform conventional cell-based assays. These control viability experiments were performed to ensure proper cell analysis on chip.

Chapter 7 describes the creation of the microfluidic platform for measuring apoptosis. The cellular requirements as well as the conditions necessary for monitoring apoptosis are discussed. Different microfluidic designs are evaluated to select the one which best fits our aim.

In chapter 8, the effect on the process of apoptosis of breast cancer cells and endothelial cells treated with various stimuli is discussed. Drug-specific responses at

a single-cell level were analysed with conventional assays (flow cytometry and DELFIA®) and in real-time on chip.

Finally in chapter 9 the conclusions of the work described in the previous chapters of this thesis are summarized. Furthermore, suggestions are given for future work concerning the performance and improvement of apoptosis studies on chip for drug screening.

1.3 References

1. Vermes I, Haanen C. Apoptosis and programmed cell death in health and disease. *Adv Clin Chem* 1994; **31**: 177-246.
2. Vermes I, Haanen C, Reutelingsperger C. Flow cytometry of apoptotic cell death. *J Immunol Methods* 2000; **243**: 167-190.
3. Andersson H, van den Berg A. Microfluidic devices for cellomics: a review. *Sens Actuators B* 2003; **92**: 315-325.
4. Andersson H, van den Berg A. Microtechnologies and nanotechnologies for single-cell analysis. *Curr Opin Biotechnol* 2004; **15**: 44-49.
5. Lu X, Huang W, Wang Z, Cheng J. Recent developments in single-cell analysis. *Anal Chim Acta* 2004; **510**: 127-138.
6. El-Ali J, Sorger PK, Jensen KF. Cells on chip. *Nature* 2006; **442**: 403-411.
7. Qin J, Ye N, Lui X, Lin B. Microfluidic devices for the analysis of apoptosis. *Electrophoresis* 2005; **26**: 3780-3788.

2

ANALYSIS OF APOPTOSIS ON CHIP*

Why the move to chip technology?

Apoptosis refers to a specific form of programmed cell death, which guarantees the welfare of the whole organism through the elimination of unwanted cells. The duration of apoptosis is limited, involves single cells with morphological changes only after the "point-of-no-return", ending with phagocytosis without reaction in the neighbouring cell. Although there are a number of techniques present to measure this programmed cell death, today we are still looking for a simple, specific and sensitive technique which enables to measure apoptosis on a single-cell level, without staining, in real-time and with high-throughput. The Lab-in-a-Cell concept by using chip technology, present us with such a tool.

*parts are published in

F. Wolbers, C. Haanen, H. Andersson, A. van den Berg, I. Vermes. Analysis of apoptosis on chip: Why the move to chip technology? In "Lab-on-a-Chips for Cellomics: Micro and Nanotechnologies for Life Science", ed. H. Andersson and A. van den Berg, Kluwer Academic Publishers 2004.

F. Wolbers, H. Andersson, I. Vermes, A. van den Berg. Miniaturisation in clinical diagnostics. Clinical Laboratory International 2006; 7: 22-25.

2.1 Apoptosis

All living organisms from unicellular bacteria to multicellular animals are products of cell division. Most scientists traditionally studied proliferation and it was a given that cells survive. The role of cell death for the development, growth and survival of individuals was not considered. Not until Kerr, Wyllie and Currie[1] had discovered the existence of two different forms of cell death on the basis of morphological appearance, researchers have become aware that death is the inevitable complement to cell division. To discriminate natural cell death from accidental cell death they introduced the term apoptosis. This term is derived from the Greek: apo "apart" and ptosis "fallen" meaning the shedding of leaves from trees during autumn.

2.1.1 Physiological versus pathological cell death

There are many ways to die, but from a cell biological point of view only two forms exist: physiological and pathological cell death (Figure 2-1 and 2-2).

A **B**

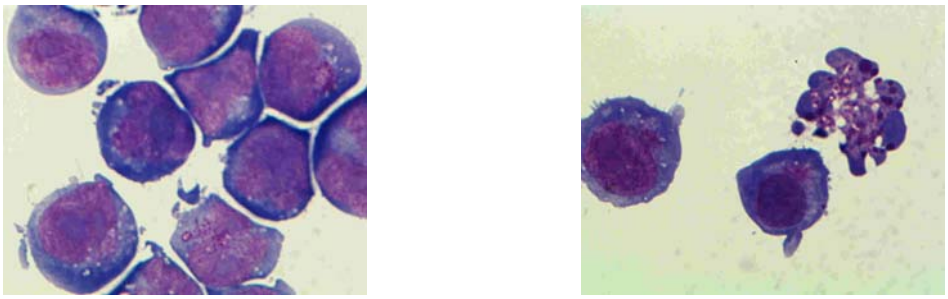

Figure 2-1. Light microscopy of **(A)** untreated control HL60 cells and **(B)** cells treated with the apoptotic inducer camptothecin for 6h *in vitro*.

Necrosis of cells occurs after physical, chemical or osmotic injury, including hypoxia and complement attack.[1-3] During this accidental cell death, the cell membrane loses its selective permeability and ion-pumping capacity. This immediately leads to swelling of the cell and its organelles and to the leaking of the cellular contents into the extracellular space, eliciting an inflammatory reaction in the adjacent viable tissues.

Apoptosis is a physiological active bio-energy-saving cell elimination mechanism by which aged, unwanted or sublethally damaged cells are abolished and their contents are reutilised by macrophages or by phagocytosing adjacent cells. Physiological cell death occurs as "programmed cell death" (PCD) during the period of embryogenesis and continues during post-embryonic life as "apoptosis", thus controlling cell numbers and organ size in a dynamic balance between cell proliferation and cell death.[4-6] Without continuously signalling by growth factors, hormones or cytokines, cells undergo apoptosis.

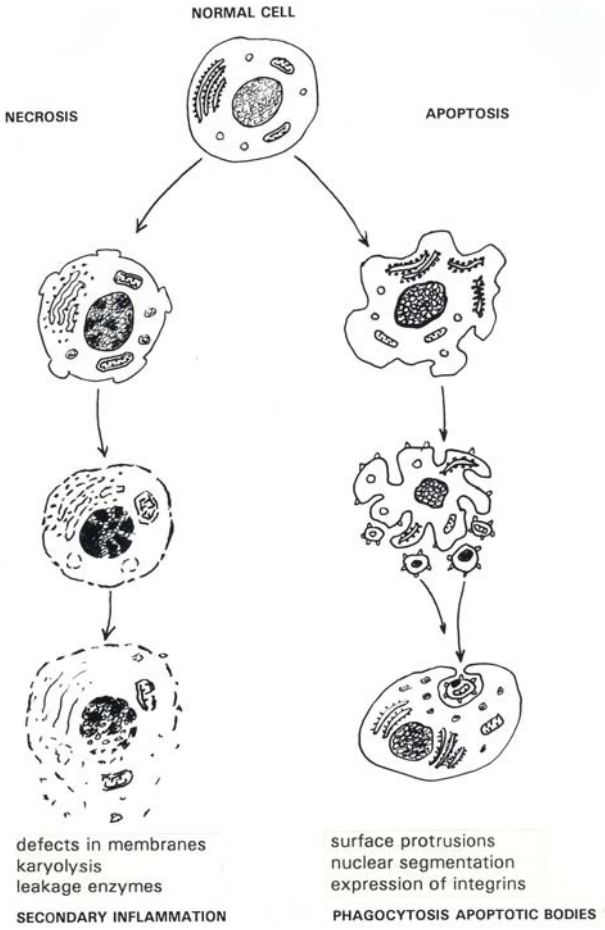

Figure 2-2. The most prominent differences between apoptosis and necrosis. From Vermes and Haanen[3] with permission of Academic Press.

During apoptosis a specific pattern of cell abolition takes place. The earliest changes include the loss of cell junctions and specialised membrane structures such as microvilli. Initially the integrity of the cell membrane and of the mitochondria remains intact, the cytoplasm condenses and the nucleus coalesces into large

masses, which then break up into fragments. The endoplasmatic reticulum transforms into vesicles which fuse with the cytoplasmic membrane. These processes result in the contraction of the cytoplasmic volume. The cell adopts a convoluted outline and subsequently the cell breaks up into small vesicles, enclosing parts of the cellular contents and apparently intact organelles. These apoptotic bodies end up in the extracellular space where they are phagocytosed by nearby cells and macrophages. The whole process takes only a few hours and the cell remnants do not elicit any inflammatory reaction (Figure 2-2).

2.1.2 Apoptosis and the plasma membrane

After external or internal death pathways are activated and the decision to die has been made, signalling routes are activated to inform the environment about the cell death decision. The environment responds with the removal of the dying cell by phagocytosis before the hydrolytic eruption inside the cell compromises the plasma membrane barrier integrity and causes leakage of inflammatory compounds into the surroundings.[7-8] In response to the cell death commitment, the plasma membrane changes its structure such that phagocytes can identify the cell as suicidal and can engulf and degrade it rapidly. Amongst these "eat me signals" on the cell surface of the apoptotic cell are sugars, thrombospondin binding sites and phosphatidylserine (PS). Phagocytes bear receptors on their cell surface, which can recognise these "eat me signals".[9] The most researched signal so far is the exposure of PS. The living cell keeps PS stringently located in the inner membrane leaflets that face the cytosol.[10] During apoptosis a phospholipid translocase is inhibited and a scramblase becomes activated.[11] The PS exposed on the cell surface is recognised by phagocytes as an "eat me signal".[12,13] This phenomenon is also exploited to detect and measure apoptosis by using Annexin V, which is a phospholipid binding protein with high affinity for PS.[14,15] In most cases, cell surface exposure of PS was found to precede the other features of apoptosis such as DNA fragmentation.[16] The molecular link between the executioner proteins and the plasma membrane has not been resolved. It appears that like the other themes of the molecular biology of apoptosis, this part of the apoptotic machinery is conserved during evolution.[17]

2.1.3 The role of the mitochondrion in apoptosis

The mitochondrion is suggested to be fundamental to the biochemistry of cell death by apoptosis for it might form the nidus where the decision of life and death is being made.[18] A crucial event of the role of the mitochondrion is the formation of permeability transition pores in its outer membrane leaflet allowing mitochondrial proteins to flux into the cytosol.[19] Amongst these proteins are Apoptotic Protease Activating Factor 2 (Apaf-2 or cytochrome c) and Apoptosis Inducing Factor (AIF).[20,21] AIF is a protease, which may be responsible for the apoptosis typical nuclear features such as chromatin condensation and internucleosomal DNA fragmentation. It was shown that Apaf-2, with the cofactors Apaf-1, Apaf-3 and dATP, could activate caspase-3.[22] Apaf-3 was identified as caspase-9.[23] The activated caspase-3 forms part of the executioner of apoptosis.[22-24] The unravelling of this mitochondrial switch from a state of reversibility into a state of irreversibility offer insights into the mechanism of action of the Bcl-2 like proteins (see: Bcl-2 family proteins). By blocking the release of Apaf-2 and AIF from the mitochondrion, Bcl-2 prevents the formation of the caspase-3 activating complex. It is also suggested that Bcl-2 interferes with this complex formation by binding to Apaf-1 and 2 directly.

2.1.4 Caspases

The proteins executing the apoptotic programme belong to a family of proteases, called the caspases, which are members of a family of cysteine proteases, bearing an active site, which cleaves specifically following aspartate residues. These proteases are indicated caspases functioning as C(ysteine) dependent ASP(artate cleaving prote)ASEs. These proteins are present as inactive pro-enzymes in all cells. The caspases can be activated to execute apoptosis under a variety of conditions including receptor-ligand coupled signal transduction, DNA damage, lack of growth factors, oxidative stress and breakage of cell-cell and cell-matrix interaction.[25]

Functionally, caspases can be divided in two major subfamilies: 1) those related to ICE, interleukin converting enzyme, (caspase-1, caspase-4, caspase-5) function in cytokine maturation, 2) the remainder mediate apoptosis. Among the latter a

further subdivision is made: 'initiator caspases' (caspase-8, caspase-9, caspase-10), which respond to pro-apoptotic stimuli and subsequently catalyse the activation of the 'effector' caspases (caspase-3, caspase-7).

The information obtained on the structures and mechanisms of caspases was exploited for development of small-molecule inhibitors of caspases. A fluorochrome-labeled inhibitor of caspases FAM-VAD-FMK (FLICA) was developed to estimate the rate of cell entrance to apoptosis and reveal the cumulative apoptotic turnover during this interval.[26-30] Exposure of cells to FLICA results in the uptake of this inhibitor followed by their covalent binding to activated caspases within the cells that undergo apoptosis. FLICA binds to activated caspases within the cell and irreversibly inactivates them, which causes the arrest of the apoptotic cascade.[26] The arrested apoptotic cells, labelled with FLICA, can be followed through the apoptotic cascade and then identified by flow cytometry.[27,28] Although various pathways for activating caspases may exist, two mechanisms have now been elucidated in detail (Figure 2-3).

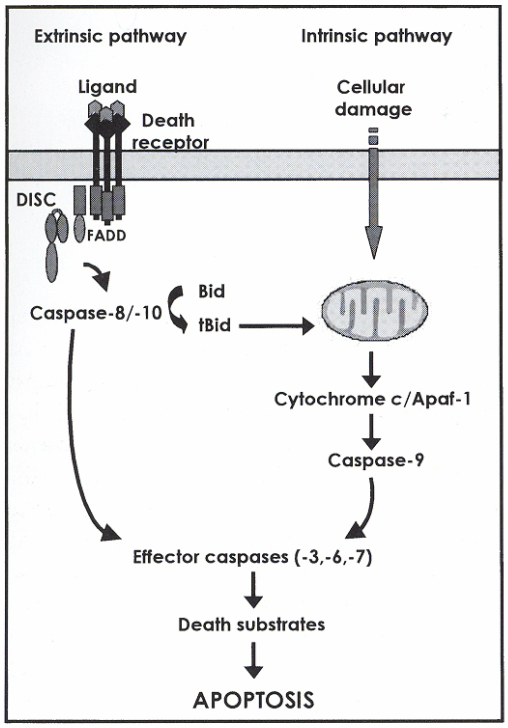

Figure 2-3. The extrinsic and intrinsic apoptotic pathways. From Frumalora and Guidotti[31] with permission of Kluwer Acad Publ.

2.1.4.1 Caspase activating mechanisms

One caspase activating mechanism is mediated by death receptors, which are present on the plasma membrane. These death receptors belong to the Tumour Necrosis Factor Receptors (TNFR) family, which use caspase activation as a signalling mechanism, thus connecting ligand binding at the cell surface to apoptosis induction within the cell.[32-34] This form of caspase activation is indicated as "the extrinsic pathway". The other caspase activation mechanism, indicated as "the intrinsic pathway", involves the participation of mitochondria, which release caspase-activating proteins into the cytosol, thereby triggering the apoptotic machinery.[31,35,36]

The extrinsic pathway

With regard to the extrinsic pathway, the ligand binding to the death receptor causes the cytosolic domain of TNFR to recruit pro-caspase-8 and -10. Caspase-8 serves in the intrinsic pathway as the apical caspase.[37-39]

The intrinsic pathway

In the intrinsic pathway permeabilization of the mitochondrial membrane (MMP) causes the release of cytochrome c from the mitochondria. Cytochrome c binds to Apaf-1 (Apoptotic Protease Activating Factor) present in the cytosol. This complex triggers activation of pro-caspase-9, which apparently serves as the apical caspase in the intrinsic pathway.[40]

2.1.4.2 Proteins controlling caspase activation

A number of proteins which control the intrinsic, extrinsic and other pathways of caspase activation are recognised and in this way are associated with apoptosis regulation. Domains, including caspase-associated recruitment domains (CARDs), death domains (DDs), death effector domains (DEDs), Bcl-2 homology (BH) domains of Bcl-2 family proteins, and the inhibitor of apoptosis proteins (IAP) commonly mediate the interaction of these proteins. All these proteins can be recognised, based on their amino acid sequence and structural similarity.[41]

Death domain proteins (DDs)

Members of the TNF family of cytokine receptors contain DDs in their cytosolic regions, including TNFR1, Fas (Apo1), DR3 (Apo2), DR4 (TrailR1), DR5 (TrailR2), DR6, Tradd, Fadd and DAP kinase. The death domain protein Fadd links the TNF receptors to the caspases.[42] Several cytoskeleton-associated proteins contain DDs, which are involved in the activation of caspase-8 after detachment of adherent cells. This may explain the phenomenon of anoikis, apoptosis induced by integrins, when the cytoskeleton of cells becomes detached from its extracellular matrix.[43] Non-caspase-activating DDs regulate apoptosis by suppressing the effect of NF-kB, which enhances the occurrence of apoptosis.[44]

Defects in the function of DDs are associated with several human diseases. Inappropriate expression of Fas and Fas ligand (FasL) on immune cells is implicated in the loss of lymphocytes in patients with HIV infection.[45] Hereditary mutation in de DD of the Fas (Apo1) gene causes an autoimmune lymphoproliferative syndrome.[46] Mutations and deletions of the Fas gene is observed in various malignancies, affording resistance of cancer cells to immune-mediated attack. A soluble version of Fas, interfering with FasL-mediated apoptosis, is associated with autoimmune lupus and resistance of cancer against immune attack of cytolytic T-cells.[47] Trail (DR4, DR5) decoy receptors are discovered, which interfere with Fas ligand binding and through which normal cells become resistant to apoptosis.[48]

Death effector domain (DED) proteins

DEDs are present in the initiator caspases, caspase-8 and caspase-10. Multiple DED-containing modulators of apoptosis have been identified, such as Fadd, pro-caspase-8, pro-caspase-10, Dredd, c-Flip, DEDD, Flash a.o.[41] Some DED proteins enhance caspase-8 activation by Fas. During Fas-induced apoptosis DEDD is translocated from the cytosol to the nucleolus.[49] Other DED proteins such as Flip suppress caspase-8 activation by competing with pro-caspases 6 and -10 for binding to Fadd. Such mechanism is used by tumours to escape apoptosis induction by cytotoxic lymphocytes.[50]

Inhibitor of apoptosis proteins (IAPs)

The IAPs represent a family of apoptosis suppressors. IAPs bind and potently inhibit activated caspases.[51] Alterations in the expression of IAPs have been discovered in patients suffering from spinal muscular atrophy.[52] Overexpression of IAPs is observed in various types of cancer and lymphomas.[53]

Bcl-2 family proteins

The mitochondrial pathway for apoptosis is modulated by Bcl-2 family proteins. The Bcl-2 family includes at least 20 different members with both pro-apoptotic (Bax, Bak, Bok, Bad, Bid, Bim, Bik, Bcl-Xs) and anti-apoptotic (Bcl-2, Bcl-XL, Mcl-1, Bfl-1, Bcl-W, Boo) effects.[54] The relative ratio of anti- and pro-apoptotic Bcl-2 proteins dictates the ultimate sensitivity or resistance of cells to apoptotic stimuli, such as growth factor deprivation, hypoxia, radiation, anti-cancer drugs, oxidants and Ca^{2+} overload.

Alterations in the quantity of these proteins are associated with a variety of pathological conditions such as cancers, malignant lymphomas, autoimmune diseases, immunodeficiency syndromes, ischemia-reperfusion injury after stroke and myocardial infarction, degenerative diseases such as Alzheimer, age related macula degeneration, etc.[41]

Bcl-2 family proteins are constitutively localised in the membranes of mitochondria. Some of these proteins are present in the endoplasmatic reticulum and the nuclear envelope. Absolutely certain is that Bcl-2 family proteins regulate the sequestration versus the release of cytochrome c from the mitochondria.[18,35,54] Bcl-2 family proteins also control the release of certain caspases (caspase-2, -3, -9), of AIF and of Smac/DIABLO (the inhibitor of AIF) in some types of cells.[55,56]

The pro-forms of cytochrome c, AIF, Smac/DIABLO are inactive in the apoptotic process, requiring modifications such as attachment of prosthetic groups (heme for cytochrome c; flavin adenine dinucleotide (FAD) for AIF) and/or proteolytic processing (AIF, Smac/DIABLO), which occurs only within the mitochondria. In this way, apoptosis is avoided during biosynthesis of the apoproteins (proteins without its characteristic prosthetic group) and is functionally linked to disruption of the mitochondrial membrane, providing cells with a suicide mechanism that can be triggered in response to mitochondrial damage.[41]

2.2 Conventional techniques to measure apoptosis

There are a variety of techniques for the detection of the two forms of cell death, apoptosis and necrosis. However, these tools either are not specific or lack quantitative values. In fact the very nature of apoptosis can explain the technical difficulty to measure programmed cell death. The duration of apoptosis is limited, involves single cells with morphological changes only after the "point-of-no-return", ending in phagocytosis without reaction in the neighbouring cell. Therefore, it is no wonder that we are still far from a reference technique to measure apoptosis in a sensitive, specific and quantitative way. In this section we briefly review the methods, which demonstrate the cellular changes during the apoptotic cascade according to the sequence in which they occur.

2.2.1 Techniques based on morphological changes

2.2.1.1 Measurement of apoptotic indices with light microscopy

Morphological evaluation is still the reference method for the detection of apoptosis.[57,58] One of the most characteristic features of apoptosis is cell shrinkage, the loss of contact with neighbouring cells as the apoptotic cell shrinks and detaches from adjacent cells. Apoptotic cells are characterised based on their specific morphological features such as bud formation, chromatin condensation and appearance of apoptotic bodies containing remnants of cell organelles and nuclei. Quantification of the number of apoptotic cells requires the scoring of great numbers of cells, since the execution phase of apoptosis is relatively short and therefore the relative frequency of apoptotic cells is expected to be low. The proportion of apoptotic cells in a population can be quantified by counting cells with light microscopy and accordingly expressed as the apoptotic index (AI), being defined as the number of microscopic features per 100 cells that can be recognised in tissue or malignant tumours, exhibiting the morphological characteristics of apoptosis.

Very recently photothermal microscopy was used for the detection and the monitoring of apoptosis in single cells.[59] Photothermal microscopy is based on optical registration of a cell response to the thermal impact that is induced in a cell due to absorption of a short laser pulse by cellular hem-proteins, such as cytochromes. For hem-proteins dissolved in cytosol, the increase in their concentration may result from a decrease in the cytosol volume due to apoptotic cell death. In this way the early stage of apoptosis can be detected directly in a single cell without any exogenous agent and with a sensitivity which exceeds the sensitivity of fluorescent methods.[59]

2.2.1.2 Electron microscopy

Electron microscopy is the method of choice for detailed examination of the structural changes within cells, but is hardly a method for routine scoring of apoptosis. Hence, this technique is primarily used to obtain qualitative information on ultrastructural changes during cell death.[58,60,61]

2.2.1.3 Changes in cell scatter pattern measured by FCM

The integrity of the cytoplasmic membrane is lost immediately during necrosis but remains largely intact during the early stage of apoptosis. Later, during the process of cell death, cytoskeletal changes occur which, in the case of apoptosis, result in the formation of apoptotic bodies. These phenomena can be exploited with flow cytometry (FCM) by the measurement of changes in the cell scatter pattern. Forward light scatter reflects the cell diameter, while right angle (side) scatter is a measure of inner cellular structures. During the initial stages of apoptosis, the cell membrane remains intact, but the cell shrinks while during necrosis cell swelling occurs immediately as a result of early failure of the cell membrane. This means that during the initial phases of apoptosis, forward light scatter diminishes, while right angle scatter temporally increases or remains stable.[62-65] Unfortunately these parameters can only be evaluated on native cells in suspension not have undergone any mechanical handling.

2.2.2 Techniques based on DNA fragmentation

2.2.2.1 Measurement of DNA content by FCM

As a result of the activation of an endonuclease, apoptotic cells exhibit a low DNA stainability as measured by flow cytometry, below the normal G0/G1 region, resulting in a sub G0/G1 peak designated as A0 cells.[62,64-69] There is circumstantial evidence that this reduced DNA stainability may be the result of progressive loss of DNA from the nuclei due to the activation of endogenous endonuclease and subsequent leakage of the low-molecular weight DNA product prior to measurement. In contrast to apoptotic cells, necrotic cells do not show an immediate reduction in DNA stainability. In contrast, by ^{3}H-thymidine labelling of the fragmented DNA (JAM-assay) one can measure the apoptotic cell death in reverse based on the detection of free DNA fragments.[70]

2.2.2.2 Labelling of DNA strand breaks

Activation of the apoptosis-associated endonuclease results in extensive DNA cleavage and thus generates a large number of DNA strand breaks. The presence of 3'hydroxyl-termini on the strand breaks can be detected by labelling with modified nucleotides (*e.g.,* biotin-dUTP, digoxigenin-dUTP, fluorescein-dUTP) in a reaction catalysed by exogenous enzymes such as terminal desoxynucleotidyl transferase (TdT)[71-73] or DNA polymerase.[74] Fluorochrome conjugated avidin or digoxigenin antibodies are used in a second step of the reaction to make individual cells suitable for detection. Commonly used techniques for the detection of apoptosis are the *in situ* nick (ISN) labelling technique or the TdT-mediated X-dUTP nick end labelling (TUNEL). Both techniques are applicable for conventional histological sections[75] and for cell-suspensions using flow cytometry (Figure 2-4).[65,72] A simplified, single-step procedure has been developed recently, utilising desoxynucleotides directly conjugated to fluorochromes.[65,76] This single-step procedure utilises Brd-UTP instead of digoxygenin or biotin conjugated triphosphodeoxynucleotides, which increases the sensitivity of the assay by giving a four-fold higher signal.

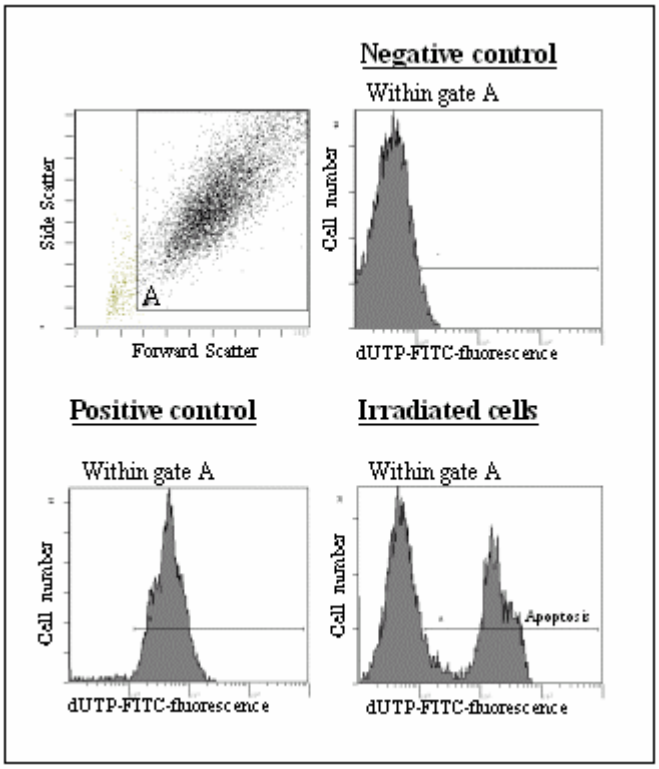

Figure 2-4. FCM of DNA double-stranded breaks: TUNEL assay. TUNEL was performed according to Gavrieli *et al.*[71] and Gorczyca *et al.*[72] One million human leukaemic T cells (HSB2) were washed twice with 1 ml PBS. The HSB2 cells were fixed with 4% (w/v) paraformaldehyde during 30 minutes on ice. After two washing steps with PBS the pellet was resuspended in 100 µl permeabilization solution (1% (v/v) Triton (Merck, Darmstadt, Germany) and 0.1 % (w/v) TriSodium Citrate dihydrate (Sigma, Deisenhofen, Germany) and incubated on ice during 2 minutes. After this incubation two wash steps with PBS followed. The cells were labelled by adding 50 µl TUNEL mix [Terminal Deoxy nucleotidyl Transferase (TdT): Deoxy Uridine triphosphate (dUTP) = 1:9] (Boehringer Mannheim, Mannheim, Germany) followed by incubation during 60 minutes at 37 °C. The samples were washed with PBS and the pellet was resuspended in 250 µl PBS. The samples were analysed by flow cytometry. Cells incubated without TdT used as negative control (right upper panel) and cells incubated with DNase (left lower panel) used as positive control. Activation of the cell death program was induced by 10 Gray irradiation. 8 hours after irradiation samples were harvested (right lower panel). From Vermes *et al.* [68] with permission of Elsevier Sci.

2.2.3 Techniques based on membrane alterations

2.2.3.1 Measurement of dye exclusion

During the initiating phase of apoptosis the fine architecture of the cell membrane is changed, but unlike necrosis, during apoptosis the integrity of the cytoplasmic membrane and a number of its basic functions remain intact. One of these functions is the active membrane transport. Accordingly, apoptotic cells exclude dyes such as Trypan Blue or Propidium Iodide (PI) while necrotic cells do not.[14,58,62,66] Recently, a two colour, fluorescence-based microplate assay has been

published by using DNA intercalating dyes.[77] This assay is particularly suitable for high-throughput applications but unfortunately is not quantitative and specific enough.

2.2.3.2 Probing for phospholipid redistribution: Annexin V assay

A change of the architecture of the plasma membrane during apoptosis involves the redistribution of the various phospholipid species between the two leaflets of the membrane. Under viable conditions the cell maintains lipid asymmetry over these two leaflets. The most pronounced feature of this asymmetry is the almost complete absence of phosphatidylserine (PS) in the outer leaflet of the plasma membrane. Fadok and colleagues were the first to show that cell surface exposure of PS occurs in nucleated cell types during apoptosis.[12] The observations of Fadok inspired Vermes *et al.*[14] to study the interaction of Annexin V with apoptotic cells. The rationale for this study came from the knowledge that Annexin V specifically binds to the phospholipid membrane in the presence of Ca^{2+}-ions when PS is exposed.[78]

Annexin V appears to be a potent discriminator between viable and apoptotic cells.[14,79] Using Annexin V as a FITC conjugate, in combination with PI, one can distinguish between viable, apoptotic and secondary necrotic cells (Figure 2-5). This outstanding result arising from using this technology indicates that PS exposure is a universal phenomenon of apoptosis occurring in all cell types, independent of the initiating trigger.[14-16]

Due to its high affinity for PS containing membranes, the Annexin V assay is easy to perform. Cells of interest and Annexin V-FITC are mixed in the presence of calcium. PI can be added to this mixture in order to specifically stain the cells, which have compromised plasma membrane integrity. Annexin V-FITC will bind immediately to cells which have surface exposed PS. Hence, after having prepared the reaction mixture it can be analysed almost instantaneously, requiring neither prolonged incubation periods nor washing steps. Analysis can be carried out using fluorescence microscopy and flow cytometry. By these means viable and dead cells can be recognised easily.

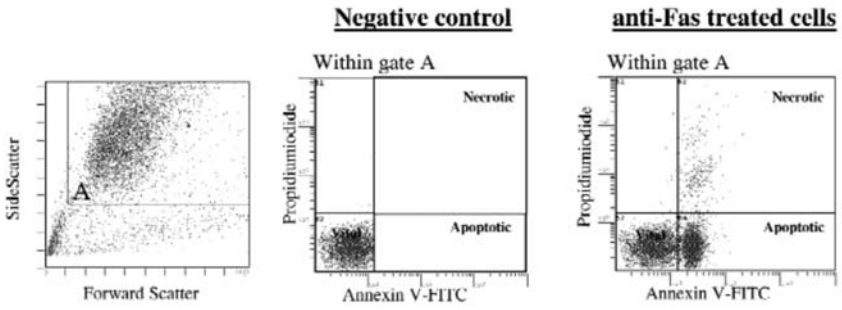

Figure 2-5. FCM of phospholipid redistribution: Annexin V/ Propidium iodide assay. The technique was performed according to Vermes *et al.*[14] Jurkat cells were cultured for 8 hours in the presence (right panel) and the absence (middle panel) of anti-Fas (100 ng/ml). One million cells were washed twice with 1 ml PBS. The pellet was resuspended in 740 µl calcium containing binding buffer (10 mM Hepes +140 mM NaCl + 2.5 mM $CaCl_2$, pH = 7.4), 1.0 µg/ml (final concentration) FITC-Annexin V (APOPTEST™-FITC, NeXins Research B.V. Hoeven, The Netherlands) and 1.0 µg/ml (final concentration) PI (Sigma, St. Louis, Missouri, USA.). The samples were analysed for green fluorescence (FITC) and for red fluorescence (PI) by flow cytometry. Cells incubated without calcium served as a negative control (middle panel). The assay gives not only information about the numbers of vital (AV-/PI-) versus apoptotic (AV+/PI-) cells, but concurrently provides also the number of secondary necrotic cells (AV+/PI+). From Vermes *et al.*[68] with permission of Elsevier Sci.

Viable cells will not contain either stain. Cells in apoptosis with intact plasma membrane integrity are stained only by Annexin V-FITC, whereas cells in secondary necrosis, the phase consecutive to apoptosis *in vitro*, contain both stains.[14,16,79] A new flow-cytometry-based ratiometric method which uses an internal reference standard of microbeads combined with Annexin V-FITC binding has recently been published to measure apoptotic rate *in vitro*.[80] In an other modified assay cells are prefixed with methanol free formaldehyde and labelled with FITC-Annexin V and with PI in the presence of digitonin.[81] Formaldehyde crosslinks DNA and hence prevents leakage of fragmented DNA from apoptotic cells. This allows us to identify the cell cycle position of apoptotic cells. Therefore this assay is suitable to study cell cycle-specific apoptosis.[81]

2.2.4 Techniques based on cytoplasmic changes

2.2.4.1 Changes in intracellular enzyme activity

Measurement of the endonuclease activity

Degradation of nuclear DNA into nucleosomal units is one of the hallmarks of apoptosis.[69] Molecular characterisation of this process identified a specific DNase (CAD, caspase-activated DNase) which cleaves chromosomal DNA.[82,83] This type of assay is the most common biochemical method used for the detection of apoptosis rate. As a substrate, either exogenous DNA (a relatively large nucleic acid

substrate isolated from non-apoptotic tissue nuclei)[84-86], or endogenous DNA, when the substrate is the chromatin of the apoptotic nuclei[87], can be used. The direct measurement of the endonuclease-induced endogenous DNA fragmentation in extracts of apoptotic cells which was until recently thought to be the specific hallmark of apoptosis, is the most common method to detect apoptosis.[88] It was believed that the linker regions between nucleosomes were the only DNA targets for the apoptotic-endonuclease attack, resulting in fragments of 180-200 bp and multiples of this unit length. This type of cleavage can be assessed by the appearance of a ladder of bands on a conventional agarose gel[87,89], by using pulsed-field gel-electrophoresis[90,91] or by 2D-electrophoresis.[90] Unfortunately this type of assay is not sensitive enough to detect apoptosis in individual cells and needs large number of cells which precludes usage of this assay to study apoptosis *in vivo*. An application of the Southern blot technique was described as an assay to improve the sensitivity of DNA fragmentation.[89,92] It is important to note that, although non-random DNA fragmentation is widely used as a marker for apoptosis, some exceptions have been observed. It is therefore important to verify the occurrence of apoptosis by other criteria such as cell morphology.[87] Accordingly, the DNA degradation detected by these techniques have to be viewed as a marker of the apoptotic process rather than a critical component of the death process itself.[91]

Measurement of caspases

During the execution-phase of apoptosis, intracellular enzymes are playing a key role in the cell death program.[25,36] As previously described the caspase activity is vital to their role in apoptosis. Each of the caspase family members is a cysteine protease that possesses the unusual ability to cleave substrates after aspartate residues. Recently, by mapping the cleavage site of PARP, Nicholson *et al.*[93] have identified the tetrapeptide, Asp-Glu-Val-Asp (DEVD) as a consensus cleavage site for caspase-3. Conjugation of a fluorometric (7-amino-4-trifluoromethyl coumarin, AFC) or a colorimetric (p-nitroanilide, pNA) moiety to DEVD provides a potential substrate for analysing caspase-3 activity.[94] This protease assay is simple, quick and sensitive to measure caspase-3 activity of crude cell lysate of 10^6 suspended or adherent cells.[95,96] Recently, more sensitive homogenous caspase-3 time resolved fluorescence assays suitable for high-throughput usage by screening small molecule compounds have been published.[97,98]

Exposure of cells to a fluorescent inhibitor of caspases FAM-VAD-FMK (FLICA) stains viable cells supravitally.[27-29] When these cells enter apoptosis, the intracellular FLICA blocks the activation of caspases and arrests further progress of the apoptotic cascade and prevents cellular disintegration. The arrested apoptotic cells, labelled with FLICA, can be followed through the apoptotic cascade and identified by flow cytometry[99-101] or by laser scanning cytometry.[102] The fluorescent FLICA labelling of cells that enter into apoptosis and the labelling of dead cells with propidium iodide offer the possibility to estimate the rate of cell entrance into apoptosis, to measure the cumulative apoptotic turnover in time and to follow the occurrence of cell death in time.[100] Accordingly, this assay allows the measuring of the rate-constants between the different stages of the apoptotic cascade and the pattern of the apoptotic process.[101]

Measurement of tissue transglutaminase

It has been demonstrated that activation of tissue transglutaminase (tTG) is part of the apoptotic machinery.[103] tTG is activated in dying cells to form cross-linked protein polymers/envelopes, which can be extracted from cells with a significant rate of physiological cell death.[104] When the apoptotic bodies are degraded after a rapid phagocytosis, the cross-link itself is not cleaved but released, and the end product can be measured in the extracellular space. Measurement of tTG activity can be done based on the incorporation of radioactive putrescin into casein[104], and with a sensitive enzyme-linked immunosorbent assay.[105] There are several antibody preparations raised against tTG which are used to detect and localise the tTG protein in apoptotic cells by immunohistochemistry and by immunoelectron-microscopy.[104] In addition, the detection and localisation of tTG mRNA expression has been demonstrated by using TaqMan-based real-time RT-PCR, a semi-quantitative RT-PCR technique.[106] It is shown that tTG mRNA expression increases significantly in response to apoptosis inducing treatment in a dose- and time-dependent manner. Accordingly, tTG expression can be used as a trace marker for the detection and the quantification of apoptosis.[106]

2.2.4.2 Measurement of calcium flux

Elevations in the cytosolic Ca^{2+} level are also a result of the apoptotic process.[107,108] Energy-dependent Ca^{2+} transport systems maintain the cytosolic Ca^{2+} concentration at 100 nM, at least four orders of magnitude below that found in the extracellular milieu under physiological conditions. The increase of the cytosolic Ca^{2+} concentration, measured by using Ca^{2+}-selective fluorescent probes may be used as a sensitive indicator of cell death.[86,109]

2.2.4.3 Measurement of mitochondrial dysfunction

Although the absence of mitochondrial changes was taken as a hallmark of apoptosis for a long time, mitochondria are today considered as the central executioners of PCD.[6,110] Decrease in mitochondrial membrane potential (DeltaPsim) is an early universal event of apoptosis. A fall of the mitochondrial membrane potential occurs before the DNA fragmentation and this drop in mitochondrial membrane potential marks the "point-of-no-return" of a cell committed to die.[111-112] Several cell viability assays are based on the fact that fluorochromes such as Rhodamine 123, $DiOC_6$ (3,3'-dihexyloxacarbocyanine iodide), CMXRos (chloromethyl-X-rosamine), JC-1(5,5',6,6'-tetrachloro-1,1'3,3'-tetraethyl-benzimidazolcarbocyanine iodide) accumulate in mitochondria of live cells as a result of transmembrane potential. An early event of apoptosis is a decrease in DeltaPsim, which is reflected by a loss of the ability of the cell to accumulate these fluorochromes.[113,114]

It was shown that a mitochondrial membrane protein designated 7A6-antigen appears to be exposed on cells undergoing apoptosis.[115] Accordingly, the antibody against this 38-kDa mitochondrial protein, APO2.7 (anti-7A6) can be used as a probe for the quantification of apoptotic cells. Phycoerythrin-labelled monoclonal APO2.7 antibody can be used in a FCM assay to demonstrate anti-Fas or radiation induced apoptosis in Jurkat cells.[116,117] It has been demonstrated that APO2.7 identifies the early apoptotic response, but it is not specific for apoptosis because the 7A6 protein becomes exposed also in necrotic cells.[79,117]

The release of cytochrome c by mitochondria is an essential step in the cell death cascade.[6,34,110,118,119] In addition to the release of cytochrome c, mitochondrial alterations in apoptosis include the release of other pro-apoptotic factors, including

Smac/DIABLO, apoptosis-inducing-factor (AIF), CIDE-B (cell death-inducing DFF45-like effector protein B) and several caspases. All of these events surrounding cytochrome c release have been researched in intact cells by flow cytometry and fluorescence microscopy and in reconstituted systems using isolated mitochondria and recombinant proteins or cytosolic extracts.[6,34,110,118,119] Another method for detecting cytochrome c release which is gaining in popularity is the use of green fluorescent protein (GFP)-tagged cytochrome c. The advantage of this system is that cytochrome c release can be observed in living cells.[119]

A new flow cytometric assay simultaneously detects independent apoptotic parameters in one single cytofluorometric assay.[120] Mitochondrial dysfunction is assessed by using mitochondrion-permeable, voltage-sensitive dyes which accumulate in the organelle matrix of healthy cells, but not in the matrix of depolarised mitochondria. Analysis of cell morphology changes is performed following variations of the forward and side light scatter parameters. Plasma membrane alterations are researched by FITC-Annexin V and with PI staining. In this way, the same cell sample can be used to visualise early apoptotic events, such as mitochondrial dysfunction, mid steps, such as cell shrinkage and PS externalisation, and the late hallmarks of apoptosis, such as plasma membrane permeabilization to PI within one assay.[120]

2.2.5 Why the move to chip technology?

At present there are about 300 different apoptosis–related kits and techniques that have been developed for apoptosis detection and quantification. However, these techniques have a number of limitations. First of all, cells must be stained, fixed or destroyed in order to analyse them, so intact single cells cannot be analysed. This is a crucial point when studying apoptotic cell death. Minimal manipulation of cells (*e.g.,* detachment of adherent cells with trypsin, which is a frequently used tool) can induce apoptosis and staining with for example fluorescent dyes, kills the cells. Accordingly, a number of techniques are dealing with artefacts. In addition, cell preparation for analysis requires additional time (at least 15-30 min) and therefore real-time monitoring of the cell death cascade is not available. Furthermore, all these techniques reviewed here, need highly sophisticated equipment and people to perform these measurements which are very labour intensive and expensive to

perform in clinical laboratories. In the nineties the term micro total analysis systems (μTAS) was introduced, to describe a complete microsystem which integrates sample handling, analysis and detection into a single device, also called Lab-on-a-Chip (LOC) device.[121-123] The Lab-on-a-Chip concept defines the scaling down of a single or multiple lab processes into a chip format with dimensions as small as a stamp. Scaling down offers many advantages, such as less sample, reagent and waste volume, faster analysis, integration of many analytical processes within one device, lower cost, to name a few, but first of all very simple handling. These advantages meet the actual demands of clinical laboratories, which are dealing with an increasing workload and decreased funding. Furthermore, microfluidic dimensions (10-100μm) equal the size of cells, making these devices very suitable for the analysis of many different biochemical processes even on a single-cell level.[124-126] Hence, there are many reasons why microtechnology is advantageous compared to the existing conventional analysis methods, especially in the case of cellular based assays, to understand how cells react in a certain environment, to a certain drug or in contact with other cell types. Different cell manipulation methods (sorting, detachment, staining, fixing, lysis a.o.) can be integrated on one chip, less sample is needed ideally when only a few cells are available (*e.g.,* primary cells), and the dimensions favour single-cell analysis. Further, optical detection techniques can be automated and in some cases be replaced by electrical on-chip detection techniques. Moreover, development of cell arrays, which are analogous to DNA or protein arrays, offer the possibility for high-throughput screening. Recent technological developments enable detailed cellular studies, defining a new concept Lab-in-a-Cell. In this concept the cell is used as a laboratory to perform complex biological operations. Micro- and even nanotechnological tools are employed to access and analyse this laboratory and interface it with the outside world.[125] Apoptosis or programmed cell death is a process which is ideally suited to analyse on chip as apoptosis is a process that does not occur simultaneously in all the cells of a population, favouring analysis at the single-cell level. Furthermore, the apoptotic process takes no more than a few hours, hence real-time monitoring will provide new insights into the apoptotic cascade. Specific for apoptosis, integration of different detection techniques (electrical properties, cell size/morphology, and released cell content) can overcome the technical difficulties now existing to measure programmed cell

death. The different stages of the apoptotic cascade can in this way be monitored with high specificity on one chip device. Accordingly there is a real need for simple chip technology to study apoptosis in real time on single-cell level with high-throughput.

2.3 Apoptosis on chip

As stated above, the conventional methods, which are now available to detect apoptosis have many limitations. Apoptosis is one of the most important topics in the field of cellular science, however it was not until recently that research groups have become interested in developing chips convenient for detecting apoptosis.[127] The advantages of microfluidic devices are numerous such as the possibilities for non-destructive real-time analysis of apoptosis. In the section below we will present a few examples of chips for apoptosis analysis that have been presented until so far.

With confocal microscopy, characteristic events in the apoptotic cascade (*e.g.,* loss of mitochondrial transmembrane potential, exposure of PS, membrane blebbing and permeabilization of the cell membrane) have been analysed on chip, in real-time at a single-cell level.[128] Human U937 myeloid leukaemic cells were trapped in a microfluidic chip in the presence of apoptotic inducer and the appropriate fluorescent dyes to monitor the apoptotic cascade. In response to the apoptotic stimuli anti-Fas (via death receptors) and etoposide (inhibits the enzyme topo-isomerase II in the nucleus, widely used as a chemotherapeutic drug), heterogeneity in the apoptotic phenotype has been observed in time (Figure 2-6). Moreover, this microfluidic cell trap device was used to study the apoptotic cell death dynamics of human promyelocytic leukaemic HL60 cells in the presence of the stimulus tumour necrosis factor (TNF)-α in combination with the protein synthesis inhibitor cycloheximide (CHX).[129] With the use of the appropriate fluorescent dyes, FLICA and PI, the onset of apoptosis and the different phases of the apoptotic process could be monitored in real-time (see also chapter 3). To improve live cell imaging and time-lapse recording, photostable dyes such as quantum dots (Qdots) can be used.[130] Fast events, as those occurring during the apoptotic process, can be visualized, which might be missed using organic dyes which are prone to bleaching phenomena. Moreover, more than six Qdots can be visualised simultaneously,

hence favouring the staining of multiple targets for the detailed study of complex biological processes within cells, such as apoptosis.

A

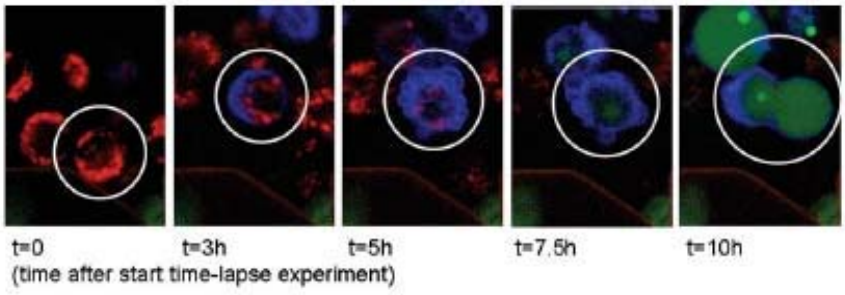

B

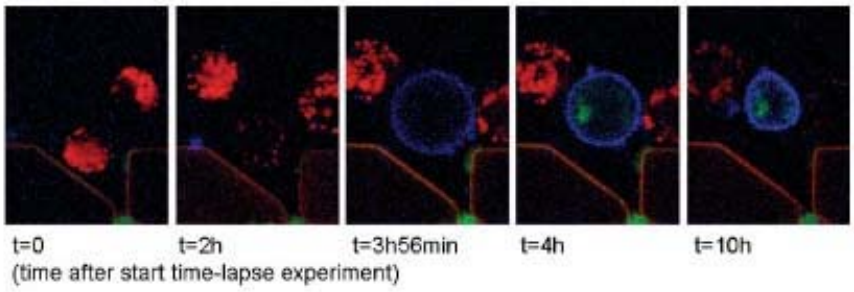

Figure 2-6. Real-time monitoring of the apoptotic cascade at the single-cell level after treatment with etoposide (A) and anti-FAS (B). Red corresponds to the TMRE signal (mitochondrial transmembrane potential), green to YOPRO-1 (permeabilization), and blue to Annexin V (PS exposure). Published with permission of Munoz-Pinedo *et al.*[128]

As single-cell imaging using confocal microscopy proved very useful, the fluorescent labelling molecules used may possibly affect the biochemical pathways in the cell. Therefore Tamaki *et al.*[131] developed a microsystem for cell experiments consisting of a scanning thermal lens microscope detection system and a cell culture microchip. This system is able to detect non-fluorescent biological substances with extremely high sensitivity without any labelling materials. They succeeded in monitoring the cytochrome c distribution during apoptosis in a single neuroblastoma-glioma hybrid cell, cultured in a microflask (1 mm x 10 mm x 0.1 mm; 1μl), fabricated in a glass microchip. The absolute amount of cytochrome c detected within this system was estimated to be ~ 10 zmol. As morphological evaluation is still the reference method for the detection of apoptosis, flow cytometry is widely used to analyse the different stages of the apoptotic process. Nowadays, there is growing interest in flow cytometry performed in microfluidic devices, especially for using primary cells. Primary cells are prepared directly from

fresh tissues or fluids of an organism and often display most of the differentiated properties of the original source. Chan *et al.*[132] developed a microfluidic system allowing flow cytometric analysis of apoptosis and protein expression with a minimum number of fluorescently stained lymphocytes, endothelial cells and dermal fibroblasts. The cells move by pressure driven flow (as in conventional flow cytometry) inside a network of microfluidic channels and are analysed individually by two-channel fluorescence detection. Results obtained with this microfluidic device are consistent with conventional flow cytometry, at the same time having the advantages of working on a smaller scale. Furthermore, on-chip staining reduces cell and reagent consumption and time-consuming work.

DNA fragmentation is another hallmark of apoptosis, resulting from the activation of a nuclear endonuclease, which selectively cleaves the DNA at sites located between nucleosomal units. Though DNA size-based analysis is not possible with flow cytometry and therefore capillary electrophoresis is used. Klepárník *et al.*[133] have developed a CD-like plastic disc for single-cell handling in a vacuum-driven flow, alkaline lysis and denaturing, and electrophoretic separation. The migration of fluorescently stained DNA fragments is monitored with confocal microscopy. The relatively high differences in sizes of the apoptotic fragments allow their electrophoretic separation on a very short migration distance. Increasing intracellular concentrations of doxorubicin in cardiac myocytes caused a rapid onset of DNA fragmentation. After 24h doxorubicin treatment, necrosis is the prevalent mechanism of destruction of cardiomyocytes.

Optical detection techniques have been replaced by electrical on-chip detection techniques. Kurita *et al.*[134] have developed a chip-based biosensor enabling the continuous monitoring of neurotransmitters and metabolites. This microfabricated device consist of two glass plates and two glass capillaries, integrated with four electrodes, designed to evaluate the effect of an endocrine disrupter tributyltin (TBT) on the secretion of glutamate and hydrogen peroxide via an increase in the intracellular calcium concentration. High concentrations of TBT show apoptosis like features.

Our focus is developing a microfluidic chip for high-throughput drug screening in a clinical setting. The effect of various drugs on the apoptotic pathway will be analysed in real-time on different cell types, such as cancer cells, immortalized cells and primary cells. Differences in autofluorescent (AF) intensity are used to

discriminate viable from apoptotic cells, as described in chapter 4. In short, measurement of AF reduces sample preparation time and avoids cellular toxicity due to the fact that no labelling is required. This offers us the possibility to measure apoptotic cell death without manipulation of the cells and monitor the apoptotic cascade in real-time at a single-cell level. Furthermore, using the microfluidic cell trap chip (discussed in chapter 7), optical detection of a decrease in AF intensity during apoptosis, can be combined with a change in the mechanical properties (*e.g.,* size) of the trapped cells, which can, due to cell shrinkage, pass the capture position.

In clinical settings, every patient has his/her own response to certain medications. The goal is to select the best individual therapy to treat symptoms and cure diseases. The ability to measure the balance between apoptosis and proliferation on a chip using the patients' own cells offers the possibility to make optimal selection of cytotoxic treatment for a cancer patient which is an important step towards personalized medicine. We have developed a microfluidic chip to culture different adherent cells and analyse the effect of various drugs on the apoptotic pathway, with a special interest in the detachment of adherent cells from their surface, a process called anoikis ("homelessness"). Conventionally, different (combinations) of drugs, such as steroid hormones, used to treat breast cancer patients and postmenopausal women have been analysed for their effect on proliferation and apoptosis (chapter 5). However, performing these assays on chip will obtain a lot of advantages. Fewer cells are needed, hence ideal for using primary (patient's own) cells. Moreover, using patient's own cells at different positions on the chip, different (combinations of) drugs can be analysed at the same time, as performing dose-response assays to explore drug specific pharmacokinetics, leading to high-throughput analysis. First attempts have been made to develop a microfluidic chip to explore the apoptotic effect of various drugs using breast cancer cells and the results will be discussed in chapter 8.

2.4 Conclusion

The references described above give a brief summarisation of what has been accomplished in the past few years for detecting apoptosis in a chip-based system. However, up till now still little has been done. The development of new micro-

and nanotechnological tools, better understanding of single cells and promoting interest among scientist will create new opportunities for realising new micro- or nanofluidic devices to detect apoptosis, which cannot only replace the conventional analytical methods now available, but will also provides us with detailed single-cell analysis of the different apoptotic characteristics within a single microfluidic device.

2.5 References

1. Kerr JFR, Wyllie AH, Currie AR. Apoptosis: A basic biological phenomenon with wide-ranging implications in tissue kinetics. *Br J Cancer* 1972; **26**: 239-257.
2. Wyllie AH, Kerr JFR, Currie AR. Cell death: The significance of apoptosis. *Int Rev Cytol* 1980; **68**: 251-300.
3. Vermes I, Haanen C. Apoptosis and programmed cell death in health and disease. *Adv Clin Chem* 1994; **31**: 177-246.
4. Fadeel B. Programmed cell clearance. *Cell Mol Life Sci* 2003; **60**: 2575-2585.
5. Ravichandran KS. "Recruitment Signals" from apoptotic cells to a quiet meal. *Cell* 2003; **113**: 817-820.
6. Daniel NN, Korsmeyer SJ. Cell death: Critical control points. *Cell* 2004; **116**: 205-219.
7. Savill J. Apoptosis in resolution of inflammation. *J Leukoc Biol* 1997; **61**: 375-380.
8. Savill J, Gregory C, Haslett C. Cell biology. Eat me or die. *Science* 2003; **302**: 1516-1517.
9. Pearson AM. Scavenger receptors in innate immunity. *Curr Opin Immunol* 1996; **8**: 20-28.
10. Diaz C, Schroit AJ. Role of translocases in the generation of phosphatidylserine asymmetry. *J Membrane Biol* 1996; **151**: 1-9.
11. Zhou Q, Zhao J, Stout JG, Luhm RA, *et al.* Molecular cloning of human plasma membrane phospholipid scramblase. A protein mediating transbilayer movement of plasma membrane phospholipids. *J Biol Chem* 1997; **272**: 18240-18244.

12. Fadok VA, Voelker DR, Campbell PA, Cohen JJ, *et al.* Exposure of phosphatidylserine on the surface of apoptotic lymphocytes triggers specific recognition and removal by macrophages. *J Immunol* 1992; **148**: 2207-2216.
13. Fadok VA, Henson PM. Apoptosis: Giving phosphatidylserine recognition an assist - with a twist. *Curr Biol* 2003; **13**: R655-657.
14. Vermes I, Haanen C, Steffens-Nakken H, Reutelingsperger C. A novel assay for apoptosis - Flow cytometric detection of phosphatidylserine expression on early apoptotic cells using fluorescein labelled Annexin V. *J Immunol Methods* 1995; **184**: 39-51.
15. van Engeland M, Nieland LJW, Ramaekers FCS, Schutte B, Reutelingsperger CPM. Annexin V-affinity assay: A review on an apoptosis detection system based on phosphatidylserine exposure. *Cytometry* 1998; **31**: 1-9.
16. Martin SJ, Reutelingsperger CP, McGahon AJ, Rader JA, *et al.* Early redistribution of plasma membrane phosphatidylserine is a general feature of apoptosis regardless of the initiating stimulus: Inhibition by overexpression of Bcl-2 and Abl. *J Exp Med* 1995; **182**: 1545-1556.
17. van den Eijnde SM, Boshart L, Baehrecke EH, de Zeeuw CI, *et al.* Cell surface exposure of phosphatidylserine during apoptosis is phylogenetically conserved. *Apoptosis* 1998; **3**: 9-16.
18. Kroemer G, Reed JC. Mitochondrial control of cell death. *Nat Med* 2000; **6**: 513-519.
19. Marchetti P, Castedo M, Susin SA, Zamzami N, *et al.* Mitochondrial permeability transition is a central coordinating event of apoptosis. *J Exp Med* 1996; **184**: 1155-1160.
20. Kluck R, Bossy Wetzel ME, Green DR, Newmeyer DD. The release of cytochrome c from mitochondria: a primary site for Bcl-2 regulation of apoptosis. *Science* 1997; **275**: 1132-1136.
21. Reed JC. Cytochrome c: Can't live with it; can't live without it. *Cell* 1997; **91**: 559-562.
22. Zou H, Henzel WJ, Liu X, Lutschg A, Wang X. Apaf-1, a human protein homologous to C. elegans CED-4, participates in cytochrome c - dependent activation of caspase-3. *Cell* 1997; **90**: 405-413.

23. Li P, Nijhawan D, Budihardjo I, Srinivasula SM, *et al.* Cytochrome c and dATP-dependent formation of Apaf-1/caspase-9 complex initiates an apoptotic protease cascade. *Cell* 1997; **91**: 479-489.
24. Vaux DL. CED-4 - The third horseman of apoptosis. *Cell* 1997; **90**: 389-390.
25. Degterev A, Boyce M, Yuan J. A decade of caspases. *Oncogene* 2003; **22**: 8543-8567.
26. Bedner E, Smolewski P, Amstad P, Darzynkiewicz Z. Activation of caspases measured in situ by binding of fluorochrome-labeled inhibitors of caspases (FLICA): Correlation with DNA fragmentation. *Exp Cell Res* 2000; **259**: 308-313.
27. Smolewski P, Grabarek J, Phelps DJ, Darzynkiewicz Z. Stathmo-apoptosis: Arresting apoptosis by fluorochrome-labeled inhibitor of caspases. *Int J Oncol* 2001; **19**: 657-663.
28. Smolewski P, Grabarek J, Halicka HD, Darzynkiewicz Z. Assay of caspase activation in situ combined with probing plasma membrane integrity to detect three distinct stages of apoptosis. *J Immunol Meth* 2002; **265**: 111-121.
29. Grabarek J, Amstad P, Darzynkiewicz Z. Use of fluorescently labeled caspase inhibitors as affinity labels to detect activated caspases. *Hum Cell 2002*; **15**: 1-12.
30. Teodori L, Grabarek J, Smolewski P, Ghibelli L, *et al.* Exposure of cells to static magnetic field accelerates loss of integrity of plasma membrane during apoptosis. *Cytometry* 2002; **49**: 113-118.
31. Fumarola C, Guidotte GG. Stress-induced apoptosis: Toward a symmetry with receptor-mediated cell death. *Apoptosis* 2004; **9**: 77-82.
32. Yuan J. Transducing signals of life and death. *Curr Opin Cell Biol* 1997; **9**: 247-251.
33. Wallach D, Varfolomeev EE, Malinin NL, Goltsev YV, *et al.* Tumor necrosis factor receptor and Fas signaling mechanisms. *Ann Rev Immunol* 1999; **17**: 331-367.
34. Ashe PC, Berry MD. Apoptotic signaling cascades. *Progr Neuro-psychopharmacol Biol Psychiatry* 2003; **27**: 199-214.

35. Green DR, Reed JC. Mitochondria and apoptosis. *Science* 1998; **281**: 1309-1312.
36. Boatright KM, Salvesen GS. Mechanisms of caspase activation. *Curr Opin Cell Biol* 2003; **15**: 725-731.
37. Juo P, Kuo CJ, Yuan J, Blenis J. Essential requirement for caspase-8/Flice in the initiation of the Fas-induced apoptotic cascasde. *Curr Biol* 1998; **8**: 1001-1008.
38. Hakem R, Hakem A, Duncan GS, Henderson JT, *et al.* Differential requirement for caspase 9 in apoptotic pathways in vivo. *Cell* 1998; **94**: 339-352.
39. Muzio M, Stockwell BR, Stennicke HR, Salvesen GS, Dixit VM. An induced proximity model for caspase-8 activation. *J Biol Chem* 1998; **273**: 2926-2930.
40. Saleh A, Srinivasula S, Acharya S, Fishel R, Alnemri E. Cytochrome c and dATP-mediated oligomerization of Apaf-1 is a prerequisite for procaspase-9 activation. *J Biol Chem* 1999; **274**: 17941-17945.
41. Reed J. Mechanisms of apoptosis. *Am J Pathol* 2000; **157**: 1416-1430.
42. Kischkel FC, Lawrence DA, Chuntharapai A, Schow P, *et al.* Apo2L/TRAIL-dependent recruitment of endogenous FADD and caspase-8 to death receptors 4 and 5. *Immunity* 2000; **12**: 611-620.
43. Frisch S. Evidence for a function of death-receptor-related, death-domain-containing proteins in anoikis. *Curr Biol* 1999; **9**: 1047-1049.
44. Liu ZG, Hsu H, Goeddel DV, Karin M. Dissection of TNF receptor 1 effector functions: JNK activation is not linked to apoptosis while NF-kB activation prevents cell death. *Cell* 1996; **87**: 565-576.
45. Gougeon M, Montagnier L. Apoptosis in Aids. *Science* 1993; **260**: 1269-1270.
46. Fisher GH, Rosenberg FJ, Straus SE, Dale JK, *et al.* Dominant interfering fas gene mutations impair apoptosis in a human autoimmune lymphoproliferative syndrome. *Cell* 1995; **81**: 935-946.
47. Hohlbaum AM, Moe S, Marshak-Rotstein A. Opposing effects of transmembrane and soluble fas ligand expression on inflammation and tumor cell survival. *J Exp Med* 2000; **191**: 1209-1219.

48. Gura T. How TRAIL kills cancer cells, but not normal cells. *Nat Med* 1997; **277**: 768.
49. Stegh AH, Schickling O, Ehret A, Scaffidi C, *et al.* DEDD, a novel death effector domain-containing protein, targeted to the nucleolus. *EMBO J* 1998; **17**: 5974-5986.
50. Tschopp J, Irmler M, Thome M. Inhibition of Fas death signals by Flips. *Curr Opin Immunol* 1998; **10**: 552-558.
51. Deveraux QL, Roy N, Stennicke HR, Van Arsdale T, *et al.* IAP's block apoptotic events induced by caspase-8 and cytochrome c by direct inhibition of distinct caspases. *EMBO J* 1998; **17**: 2215-2223.
52. Roy N, Deveraux QL, Takashashi R, Salvesen GS, Reed JC. The c-IAP-1 and c-IAP-2 proteins are direct inhibitors of specific caspases. *EMBO J* 1997; **16**: 6914-6925.
53. Ambrosini G, Adida C, Altieri D. A novel anti-apoptosis gene, survivin, expressed in cancer and lymphoma. *Nat Med* 1997; **3**: 917-921.
54. Gross A, McDonnell J, Korsmeyer S. Bcl-2 family members and the mitochondria in apoptosis. *Genes Dev* 1999; **13**: 1899-1911.
55. Krajewski S, Krajewski M, Ellerby LM, Welsch K, *et al.* Release of caspase-9 from mitochondria during neuronal apoptosis and cerebral ischemia. *Proc Natl Acad Sci USA* 1999; **96**: 5752-5757.
56. Susin SA, Lorenzo HK, Zamzami N, Marzo I, *et al.* Mitochondrial release of caspase-2 and -9 during the apoptotic process. *J Exp Med* 1999; **189**: 382-394.
57. Smyth PG, Berman SA, Bursztajn S. Markers of apoptosis: Methods for elucidating the mechanism of apoptotic cell death from the nervous system. *BioTechniques* 2002; **32**: 648-665.
58. Watanabe M, Hitomi M, van der Wee K, Rothenberg F, *et al.* The pros and cons of apoptosis assays for use in the study of cells, tissues, and organs. *Microsc Microanal* 2002; **8**: 375-391.
59. Lapotko D. Monitoring of apoptosis in intact single cells with photothermal microscopy. *Cytometry* 2004; **58A**: 111-119.
60. Gorman A, McCarthy J, Finucane D, Reville W, Cotter T. Morphological assessment of apoptosis. In "Techniques in apoptosis. A user's guide" ed. TG Cotter, SJ Martin, London, Portland Press Ltd., 1996.

61. Otsuki Y. Various methods of apoptosis detection. *Acta Histochem Cytochem* 2000; **33**: 235-241.
62. Darzynkiewicz Z, Bruno S, DelBino G, Gorczyca W, *et al.* Features of apoptotic cells measured by flow cytometry. *Cytometry* 1992; **13**: 795-808.
63. Darzynkiewicz Z, Juan G, Li X, Gorczyca W, *et al.* Cytometry in cell necrobiology: Analysis of apoptosis and accidental cell death (necrosis). *Cytometry* 1997; **27**: 1-20.
64. Darzynkiewicz Z, Bedner E, Smolewski P. Flow cytometry in analysis of cell cycle and apoptosis. *Semin Hematol* 2001; **38**: 179-193.
65. Darzynkiewicz Z., Li X. Measurements of cell death by flow cytometry. In "Techniques in apoptosis. A user's guide" ed. T.G. Cotter, S.J. Martin, London, Portland Press Ltd., 1996.
66. Nicoletti I, Migliorati G, Pagliacci MC, Grignani F, Riccardi C. A rapid and simple method for measuring thymocyte apoptosis by propidium iodide staining and flow cytometry. *J Immunol Meth* 1991; **139**: 271-279.
67. Telford WG, King LE, Fraker PJ. Comparative evaluation of several DNA binding dyes in the detection of apoptosis-associated chromatin degradation by flow cytometry. *Cytometry* 1992; **13**: 137-143.
68. Vermes I, Haanen C, Reutelingsperger C. Flow cytometry of apoptotic cell death. *J Immunol Meth* 2000; **243**: 167-190.
69. Zhang J, Xu M. Apoptotic DNA fragmentation and tissue homeostasis. *Trends Cell Biol* 2002; **12**: 84-89
70. Hoves S, Krause SW, Schölmerich J, Fleck M. The JAM-assay: Optimized conditions to determine death-receptor-mediated apoptosis. *Methods* 2003; **31**: 127-134.
71. Gavrieli Y, Sherman Y, Ben-Sasson SA. Identification of programmed cell death in situ via specific labelling of nuclear DNA fragmentation. *J Cell Biol* 1992; **119**: 493-501.
72. Gorczyca W, Gong J, Darzynkiewicz Z. Detection of DNA strand breaks in individual apoptotic cells by the in situ terminal deoxynucleotidyl transferase and nick translation assays. *Cancer Res* 1993; **53**: 1945-1951.
73. Gorczyca W, Bruno S, Darzynkiewicz RJ, Gong J, Darzynkiewicz Z. DNA strand breaks occurring during apoptosis: Their early in situ detection by

the terminal deoxynucleotidyl transferase and nick translation assays and prevention by serine protease inhibitors. *Int J Oncol* 1992; **1**: 639-648.

74. Meyaard L, Otto SA, Jonker RR, Mijnster MJ, *et al.* Programmed death of T cells in HIV-1 infection. *Science* 1992; **257**: 217-219.
75. Wijsman JH, Jonker RR, Keijzer R, van de Velde CJH, *et al.* A new method to detect apoptosis in paraffin sections: In situ end-labelling of fragmented DNA. *J Histochem Cytochem* 1993; **41**: 7-12.
76. Li X, Darzynkiewicz Z. Labelling DNA strand breaks with BdrUTP. Detection of apoptosis and cell proliferation. *Cell Prolif* 1995; **28**: 571-579.
77. Wronski R, Golob N, Grygar E, Windisch M. Two-color, fluorescence-based microplate assay for apoptosis detection. *BioTechniques* 2002; **32**: 666-668.
78. Andree HAM, Reutelingsperger CPM, Hauptmann R, Hemker HC, *et al.* Binding of vascular anticoagulant a (VACa) to planar phospholipid bilayers. *J Biol Chem* 1990; **265**: 4923-4928.
79. Overbeeke R, Yildirim M, Reutelingsperger CPM, Haanen C, Vermes I. Sequential occurrence of mitochondrial and plasma membrane alterations, fluctuations in cellular Ca2+ and pH during initial and later phases of cell death. *Apoptosis* 1999; **4**: 455-460.
80. Prieto A, Diaz D, Barcenilla H, Garcia-Suārez J, *et al.* Apoptotic rate: A new indicator for the quantification of the incidence of apoptosis in cell culture. *Cytometry* 2002; **48**:185-193.
81. Tao D, Wu J, Feng Y, Qin J, *et al.* New method for the analysis of cell cycle-specific apoptosis. *Cytometry* 2004; **57A**: 70-74.
82. Nagata S. Apoptotic DNA fragmentation. *Exp Cell Res* 2000; **256**:12-18.
83. Nagata S, Nagase H, Kawane K, Mukae N, Fukuyama H. Degradation of chromosomal NDA during apoptosis. *Cell Death Diff* 2003; **10**: 108-116.
84. Compton MM. Development of an apoptosis endonuclease assay. *DNA Cell Biol* 1991; **10**: 133-141.
85. Compton MM, Cidlowski JA. Thymocyte apoptosis. A model of programmed cell death. *Trends Endocrinol Metab* 1992; **3**: 17-23.
86. Eastman A. Assays for DNA fragmentation, endonucleases, and intracellular pH and Ca2+ associated with apoptosis. *Methods Cell Biol* 1995; **46**: 41-55.

87. Wolfe JT, Pringle JH, Cohen GM. Assays for the measurement of DNA fragmentation during apoptosis. In "Techniques in apoptosis. A user's guide" ed. T.G. Cotter, S.J. Martin, London, Portland Press Ltd., 1996.
88. Lecoeur H. Nuclear apoptosis detection by flow cytometry: Influence of endogenous endonucleases. *Exp Cell Res* 2002; **277**: 1-14.
89. Wu CF, Bishopric NH, Pratt RE. Nonradioactive method for the determination of internucleosomal cleavage associated with apoptosis. *BioTechniques* 1997; **23**: 840-843.
90. Walker PR, Leblanc J, Smith B, Pandey S, Sikorska M. Detection of DNA fragmentation and endonucleases in apoptosis. *Methods* 1999; **17**: 329-338.
91. Kaufmann SH, Mesner PW, Samejima K, Toné S, Earnshaw WC. Detection of DNA cleavage in apoptotic cells. *Methods Enzymol* 2000; **322**: 3-15.
92. Facchinetti A, Tessarollo L, Mazzocchi M, Kingston R, *et al.* An improved method for the detection of DNA fragmentation. *J Immunol Meth* 1991; **136**: 125-131.
93. Nicholson DW, Ali A, Thornberry NA, Vaillancourt JP, *et al.* Identification and inhibition of the ICE/CED-3 protease necessary for mammalian apoptosis. *Nature* 1995; **376**: 37-43.
94. Gurtu V, Kain SR, Zhang G. Fluorometric and colorometric detection of caspase activity associated with apoptosis. *Anal Biochem* 1997; **251**: 98-102.
95. Saunders PA, Cooper JA, Roodell MM, Schroeder DA, *et al.* Quantification of active caspase 3 in apoptotic cells. *Anal Biochem* 2000; **284**: 114-124.
96. Zeng L, Smith LD. Caspase-3 colorimetric assay. *BioTechniques* 2002; **33**: 1196-1197.
97. Karvinen J, Hurskainen P, Gopalakrishnan S, Burns D, *et al.* Homogeneous time-resolved fluorescence quenching assay (LANCE) for caspase-3. *J Biomol Screen* 2002; **7**: 223-231.
98. Préaudat M, Ouled-Diaf J, Alpha-Bazin B, Mathis G, *et al.* A homogeneous caspase-3 activity assay using HTRF® technology. *J Biomol Screen* 2002; **7**: 267-274.
99. King MA, Radicchi-Mastroianni MA. Effect of caspase inhibition on camptothecin-induced apoptosis of HL-60 cells. *Cytometry* 2002; **49**: 28-35.

100. Smolewski P, Grabarek J, Lee BW, Johnson GL, Darzynkiewicz Z. Kinetics of HL60 cell entry to apoptosis during treatment with TNF-α or camptothecin assayed by the stathmo-apoptosis method. *Cytometry* 2002; **47**: 143-149.

101. Wolbers F, Buijtenhuijs P, Haanen C, Vermes I. Apoptotic cell death kinetics in vitro depend on the cell types and the inducers used. *Apoptosis* 2004; **9**: 385-392.

102. Smolewski P, Bedner E, Du L, Hsieh T, *et al.* Detection of caspase activation by fluorochrome-labeled inhibitors: Multiparameter analysis by laser scanning cytometry. *Cytometry* 2001; **44**: 73-82.

103. Fesus L, Davies PJA, Piacentini M. Apotosis: Molecular mechanisms in programmed cell death. *Eur J Cell Biol* 1991; **56**:170-177.

104. Fesus L, Nemes Z, Piredda L, Madi A, *et al.* Measurement of the induction, activity and products of tissue transglutaminase in cells undergoing apoptosis. In "Techniques in apoptosis. A user's guide" ed. T.G. Cotter, S.J. Martin, London, Portland Press Ltd., 1996.

105. Vermes I, Steur EN, Jirikowski GF, Haanen C. Elevated concentration of cerebrospinal fluid tissue transglutaminase in Parkinson's disease indicating apoptosis. *Mov Disord* 2004; **19**: 1252-1254.

106. Volokhina EB, Hulshof R, Haanen C, Vermes I. Tissue transglutaminase mRNA expression in apoptotic cell death. *Apoptosis* 2003; **8**: 673-679.

107. Hajnóczky G, Davies E, Madesh M. Calcium signalling and apoptosis. *Biochem Biophys Res Commun* 2003; **304**: 445-454.

108. Orrenius S, Zhivotovsky B, Nicotera P. Regulation of cell death: The calcium-apoptosis link. *Nature Rev Mol Cell Biol* 2003; **4**: 552-565.

109. McConkey DJ. Calcium flux measurement in cell death. In "Techniques in apoptosis. A user's guide" ed. T.G. Cotter, S.J. Martin, London, Portland Press Ltd., 1996.

110. Shi Y. A structural view of mitochondria-mediated apoptosis. *Nature Struct Biol* 2001; **8**: 394-401.

111. Tsujimoto Y, Shimizu S. The voltage-dependent anion channel: An essential player in apoptosis. *Biochimie* 2002; **84**: 187-193.

112. Ly JD, Grubb DR, Lawen A. The mitochondrial membrane potential (Δψ m) in apoptosis: An update. *Apoptosis* 2003; **8**: 115-128.

113. Kroemer G, Zamzami N, Susin SA. Mitochondrial control of apoptosis. *Immunol Today* 1997; **18**: 44-51.
114. Mignotte B, Vayssiere JL. Mitochondria and apoptosis. *Eur J Biochem* 1998; **252**: 1-15.
115. Zhang C, Ao Z, Seth A, Schlossman SF. A mitochondrial membrane protein defined by a novel monoclonal antibody is preferentially detected in apoptotic cells. *J Immunol* 1996; **157**: 3980-3987.
116. Koester SK, Roth P, Mikulka WR, Schlossman SF, *et al.* Monitoring early cellular responses in apoptosis is aided by the mitochondrial membrane protein-specific monoclonal antibody APO2.7. *Cytometry* 1997; **29**: 306-312.
117. Overbeeke R, Steffens-Nakken H, Vermes I, Reutelingsperger C, Haanen C. Early features of apoptosis detected by four different flow cytometry assays. *Apoptosis* 1998; **3**: 115-121.
118. Arnoult D, Parone P, Martinou J, Antonsson B, *et al.* Mitochondrial release of apoptosis-inducing factor occurs downstream of cytochrome c release in response to several apoptotic stimuli. *J Cell Biol* 2002; **6**: 923-929.
119. Gottlieb RA, Granville DJ. Analyzing mitochondrial changes during apoptosis. *Methods* 2002; **26**: 341-347.
120. Rasola A, Geuna M. A flow cytometry assay simultaneously detects independent apoptotic parameters. *Cytometry* 2001; **45**: 151-157.
121. Reyes D, Iossifidis D, Auroux P, Manz A. Micro total analysis systems. 1. Introduction, theory, and technology. *Anal Chem* 2002; **74**: 2623-2636.
122. Aroux P, Iossifidis D, Reyes D, Manz A. Micro total analysis systems. 2. Analytical standard operations and applications. *Anal Chem* 2002; **74**: 2637-2652.
123. van den Berg A, Lammerink T. Micro total analysis systems: microfluidic aspects, integration concept and applications. *Top Curr Chem* 1998; **194**: 21-49.
124. Andersson H, van den Berg A. Microfluidic devices for cellomics: a review. *Sens Actuators B* 2003; **92**: 315-325.
125. Andersson H, van den Berg A. Microtechnologies and nanotechnologies for single cell analysis. *Curr Opin Biotechnol* 2004; **15**: 44-49.
126. El-Ali J, Sorger PK, Jensen KF. Cells on chip. *Nature* 2006; **442**: 403-411.

127. Qin J, Ye N, Lui X, Lin B. Microfluidic devices for the analysis of apoptosis. *Electrophoresis* 2005; **26**: 3780-3788.
128. Munoz-Pinedo C, Green DR, van den Berg A. Confocal restricted-height imaging of suspension cells (CRISC) in a PDMS microdevice during apoptosis. *Lab Chip* 2005; **5**: 628-633.
129. Valero A, Merino F, Wolbers F, Luttge R, *et al.* Apoptotic cell death dynamics of HL60 cells studied using a microfluidic cell trap device. *Lab Chip* 2005; **5**: 49-55.
130. Le Gac S, Vermes I, van den Berg A. Quantum dots based probes conjugated to annexin V for photostable apoptosis detection and imaging. *Nano Lett* 2006; **6**: 1863-1869.
131. Tamaki E, Sato K, Tokeshi M, Sato K, *et al.* Single-cell analysis by a scanning thermal lens microscope with a microchip: Direct monitoring of cytochrome c distribution during apoptosis process. *Anal Chem* 2002; **74**: 1560-1564.
132. Chan SDH, Luedke G, Valer M, Buhlmann C, Preckel T. Cytometric analysis of protein expression and apoptosis in human primary cells with a novel microfluidic chip-based system. *Cytometry* 2003; **55A**: 119-125.
133. Klepárník K, Horky M. Detection of DNA fragmentation in a single apoptotic cardiomyocyte by electrophoresis on a microfluidic device. *Electrophoresis* 2003; **24**: 3778-3783.
134. Kurita R, Hayashi K, Torimitsu K, Niwa O. Continuous measurement of glutamate and hydrogen peroxide using a microfabricated biosensor for studying the neurotoxicity of tributyltin. *Anal Sciences* 2003; **19**: 1581-1585.

3

Apoptotic cell death kinetics *in vitro* depend on the cell types and the inducers used*

In vitro exposure of cells to a fluorochrome-labeled inhibitor of caspases (FLICA) labels cells after caspase activation and arrests further progress of apoptotic cell death, thereby preventing cell disintegration. The labelled apoptotic cells can be quantified in relation to time of apoptosis induction with flow cytometry. Loss of membrane integrity (late apoptosis and necrotic cell death) was measured with exposure to propidium iodide (PI). From the obtained labelling patterns with FLICA and PI, the apoptotic cell death kinetics of leukaemic cells (HL60) cells and endothelial cells (HUVEC) were calculated. This study shows that the apoptotic turnover rate depends on the stimulus used to induce apoptosis, while the type of cell determines the route of the transition through the apoptotic cascade.

*modified from
F. Wolbers, P. Buijtenhuijs, C. Haanen, I. Vermes. Apoptosis 2004;9:385-392
Department of Clinical Chemistry, Medisch Spectrum Twente, Hospital Group, Enschede, The Netherlands

3.1 Introduction

Apoptosis is a kinetic event.[1] The entire duration of apoptosis, from onset to total disintegration of the cell is relatively limited and of variable length in comparison to the duration of the cell cycle.[2] The time-window during which individual apoptotic cells display their characteristic features varies. The assay that is being used, the cell type, the nature of the apoptotic stimuli and the environmental factors the cells is exposed to, might shorten or prolong the apoptotic process. So, determining the apoptotic index does not accurately represent the incidence of apoptosis, and therefore a new assay using fluorescent caspase inhibitors is introduced which enables us to sophistically measure the apoptotic cell death kinetics.[3]

The various inducers of apoptosis start the process by activation of intracellular cysteine-aspartic acid specific proteases (caspases).[4,5] The process of their activation is considered to be the key event of apoptosis.[6,7] Caspases bring about most of the morphological changes that characterize apoptotic cell death, for example shrinkage, membrane blebbing, dissociation from surrounding cells and disintegration into apoptotic bodies. Caspases are constitutively expressed as inactive precursors (zymogens) in the cell. Apoptotic stimuli convert them rapidly into mature active enzymes via auto- or trans-catalytic cleavage, forming a heterotetramer of two large subunits and two small subunits with two active centers. Caspases are among the most specific proteases, as cleavage is performed after aspartic acid and the specific recognition of four amino-acids in front of the cleavage site is required for efficient catalysis.[4,5] Exposure of cells to a fluorescent inhibitor of caspases FAM-VAD-FMK (FLICA) stains viable cells supravitally.[3,8] FAM refers to the fluorochrome label carboxyfluorescein, VAD to the three-amino-acid peptide and FMK to the fluoromethyl ketone which binds to the cysteine of the active center. As stated above, the specificity of caspase recognition is dependent on four amino-acids in front of the cleavage site, therefore the three-amino-acid (VAD) peptide is not specific for any particular caspase, and therefore FAM-VAD-FMK is a pan-caspase reacting with all caspases, with the exception of caspase 2.[7] Binding of FLICA to activated caspases precedes the binding of annexin V to phosphatidylserine, chromatin condensation and DNA fragmentation and therefore this assay is very sensitive to detect early apoptotic cells. Prior to FLICA binding, loss of mitochondrial membrane potential occurs, which might be a

prerequisite for the binding of FLICA to activated caspases.[9] When cells enter apoptosis, the intracellular FLICA blocks the activation of caspases and arrests further progress through the apoptotic cascade, preventing cellular desintegration.[3,8] The arrested apoptotic cells, labeled with FLICA, can be followed through the apoptotic cascade and identified by flow cytometry.[3,7-11] The analysis of caspase activation is combined with the probe propidium iodide to measure the loss of membrane integrity. PI is excluded by viable and early apoptotic cells, but not by late apoptotic and necrotic cells. The fluorescent labelling of cells that enter into apoptosis and the combined labelling of FLICA and PI offers the possibility to estimate the rate of cell entrance into apoptosis, to measure the cumulative apoptotic turnover in time and to follow the occurrence of cell death in time.[3,6-13] Accordingly, this assay allows to measure the rate-constants between the different stages of the apoptotic cascade and the pattern of the apoptotic process.[10] We compared the cell death kinetics of leukaemic HL60 cells and human umbilical vein endothelial cells (HUVEC) by using different inducers, which have their specific point of action, to initiate apoptotic cell death *in vitro*.

3.2 Materials and Methods

3.2.1 HL60 cells

Human promyelocytic leukaemic HL60 cells were obtained from the German Collection of Microorganisms (Braunschweig, Germany). Tissue culture equipment was supplied by Corning (Badhoeverdorp, The Netherlands). HL60 cells were cultured in RPMI-1640 medium supplemented with 10% heat-inactivated and filter-sterilised Foetal Bovine Serum , 100 IU/ml penicillin, 100 μg/ml streptomycin, 2 mM L-Glutamine and 0.4 μg/ml fungizone (= RPMI+ medium). RPMI-1640 medium was obtained from BioWhittaker (Verviers, Belgium). Supplements and antibiotics were all obtained from Life Technologies (Grand Island, NY, USA). Cell cultures were sustained in a humidified atmosphere at 37°C at 5% CO2. Medium was refreshed every 3-4 days. Exponentially growing cells were used in the experiments.

3.2.2 Human umbilical vein endothelial cells (HUVEC)

HUVEC were isolated from an umbilical vein, by the method of Jaffe *et al.*[14], using trypsin solution (0.05% trypsin/0.02% EDTA in PBS; BioWhittaker, Verviers, Belgium). The obtained endothelial cells were cultured on 1% gelatin-coated culture flasks. Culture medium consisted of 50% Medium 199 (with Hanks salts, L Glutamine and 25 mM HEPES; Life Technologies, Grand Island, NY, USA) and 50% RPMI-1640 medium without L-glutamine, supplemented with 20% heat-inactivated and filter-sterilised Human Pooled Serum, 100 IU/ml penicillin, 100 μg/ml streptomycin and 2 mM L-glutamine. Cell cultures were sustained in a humidified atmosphere at 37°C and 5% CO_2. Medium was refreshed every 3-4 days. Confluent cultures were subcultured for up to 5 passages with use of trypsin solution.

3.2.3 Modulation of apoptosis

Camptothecin (CPT) or tumour necrosis factor (TNF)-α and cycloheximide (CHX) (all from Sigma, St. Louis, MO, USA) were used in a final concentrations of 0.15 μM, 3 nM and 50 μM, respectively. Lyophilized FAM-VAD-FMK was obtained from Intergen Co. (Purchase, NY, USA). The solution of FAM-VAD-FMK was mixed with a solution of the unlabeled inhibitor z-VAD-FMK (R&D Systems, Inc. Minneapolis, MN, USA) in a 1:4 molar ratio. The z-VAD-FMK/FAM-VAD-FMK mixture (FLICA) was added to the cell cultures to yield a 20 μM final concentration of the inhibitor.

3.2.4 HL60 cell staining

HL60 cells ($0.5x10^6$ cells/ml) were treated with either CPT (0.15 μM) or TNF-α/CHX (3 nM /50 μM) in the continuous presence of FLICA (20 μM) for different periods of time, as specified under results. After incubation, cells were washed twice, resuspended in 0.5 ml PBS and stained with 1 μg/ml propidium iodide (PI; Sigma, St. Louis, MO, USA) for 30 seconds before measurement. Samples were kept on ice until flow cytometry analyses.

3.2.5 HUVEC staining

HUVEC grown to 80% confluence, were treated with either CPT (0.15 μM) or TNF-α/CHX (3 nM/50 μM) in the continuous presence of FLICA (20 μM) for different periods of time. During the final 30 minutes of incubation, 50 μg/ml PI was added to the cultering medium. After incubation supernatants were collected, and adherent cells were detached with trypsin solution. After centrifugation, supernatants and detached cells were pooled, washed twice and resuspended in PBS. Samples were kept on ice until flow cytometry analyses.

3.2.6 Flow cytometry

Green FLICA fluorescence and red PI fluorescence of individual cells were measured with a Coulter Epics XL flow cytometer, using System IITM software with the XL-2 or DOS configuration. Excitation was elicited with the Argon laser at 488 nm and measured using the standard band pass (530nm±20 nm) and long pass (>570 nm) filters. In each sample 10,000 events were measured. Flow cytometry data were analysed with the computerprogram Expo II and gates were set with several controls (e.g., untreated cells stained with either FLICA or PI or the combination, cells treated with apoptotic inducer and stained with either FLICA or PI).

3.2.7 Statistical analysis

Results are shown as mean ± standard deviation of the mean of 1 to 4 separate experiments of each time point. The kinetics of HL60 cells and HUVEC revealed exponential curves. Two tangents were drawn and slopes were determined with linear regression.

3.3 Results

3.3.1 HL60 cells

Apoptosis was initiated in HL60 cells by incubation with 0.15 μM camptothecin (CPT) or by incubation with a mixture of tumour necrosis factor-α (TNF-α) and cycloheximide (CHX) in final concentrations of 3 nM and 50 μM, respectively. CPT initiates apoptosis via its binding to topo-isomerase I-DNA complexes in the nucleus. The interaction between CPT-stabilized complexes and advancing replication forks in S-phase cells, causes double-stranded DNA breaks which activate the apoptotic machinery. TNF-α initiates apoptosis through the death-receptor pathway. Cycloheximide inhibits the protein synthesis resulting in cell growth arrest and cell death. Figure 3-1A shows light microscopy pictures of untreated cells and cells treated with CPT for 6h with and without FAM-VAD-FMK (FLICA). Figure 3-1B shows the bivariate distributions of green and red fluorescence intensity levels from cells 'supravitally' stained with FLICA and PI. Four distinct subpopulations, which differ in fluorochrome binding, can be identified: Viable, or non-apoptotic cells, show neither FLICA nor PI fluorescence (Figure 3-1B, t=0h, quadrant B). Because HL60 cells have the propensity to spontaneously differentiate, some cells in cultures may represent dying cells that were terminally differentiated (Figure 3-1B, t=0h, quadrant C-E). In the initial phase of apoptosis, the caspases become enzymatically activated and FLICA binds to these activated caspases. In this early phase the plasma membrane is still able to exclude PI. In the initial phase of apoptosis, HL60 cells are $FLICA^+/PI^-$, also called early apoptotic (Figure 3-1B, t= 6-24h, quadrant C). Subsequently, HL60 cells lose their plasma membrane integrity and their ability to exclude PI. These late apoptotic cells are $FLICA^+/PI^+$ (Figure 3-1B, t= 6-24h, quadrant D). Finally, HL60 cells lose their ability to bind FLICA, because the caspases are either inhibited or degraded, and become $FLICA^-/PI^+$. This phase is called the 'necrotic stage' of apoptosis (Figure 3-1B, t= 6-24h, quadrant E). In the continuous presence of FLICA during the entire culturing period, the transition from $FLICA^+/PI^+$ (late apoptotic) to $FLICA^-/PI^+$ (necrotic) was prevented (Figure 3-1B). The same transitions of HL60 cellls were observed when apoptosis was induced by TNF-α/CHX treatment.

A

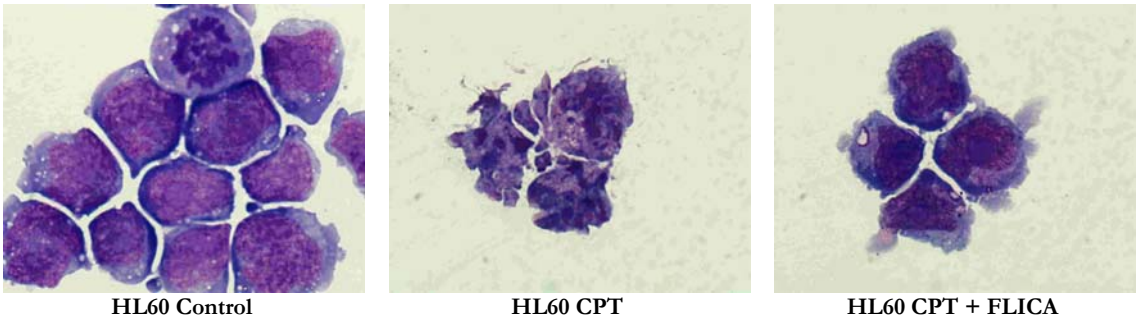

HL60 Control **HL60 CPT** **HL60 CPT + FLICA**

B

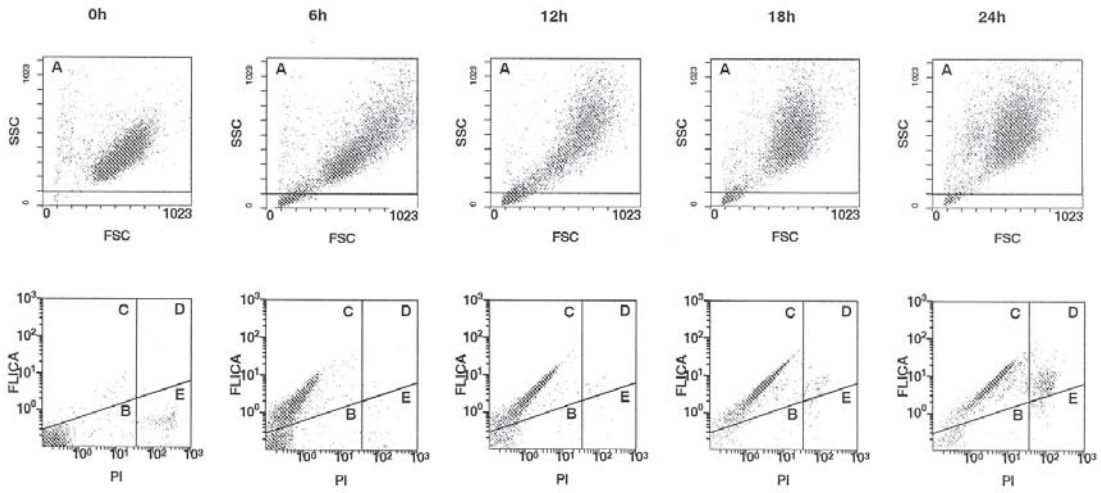

Figure 3-1. HL60 cells treated with camptothecin (CPT) in the presence of fluorochrome labeled inhibitor of caspases (FLICA). **(A)** Light microscopy (LM) of untreated HL60 cells (HL60 Control), HL60 cells treated with 0.15 μM CPT (HL60 CPT)) and treated with CPT in the presence of FLICA (HL60 CPT+FLICA) for 6h. HL60 cells were stained with May Grünwald Giemsa staining. Magnificance of the LM pictures is 100x. **(B)** Dual fluorescence staining of HL60 cells. HL60 cells were incubated with CPT to initiate apoptosis in the continuous presence of 20 μM FAM-VAD-FMK (FLICA) for 0, 6h, 12h, 18h and 24h and were supravitally stained with propidium iodide (PI). The cells presented in gate A are used to plot FLICA fluorescence in relation to PI fluorescence. Four cell subpopulations (B-E) can be identified on these scattergrams, differing in their capability to bind FLICA and PI. Scatterdiagrams show results from a representative experiment.

The results from the scatterdiagrams obtained from 3 different experiments, with either one of the inducers of apoptosis, are plotted as a function of time (Figure 3-2). The plots represent the averaged number of events (%) of each quadrant in relation to CPT incubation (Figure 3-2A) and TNF-α/CHX treatment (Figure 3-2B).

The maximum number of early apoptotic cells inititated, was at 6h during TNF-α/CHX and 18h during CPT treatments. Furthermore, figure 3-2 clearly shows that in both cases the transition of cells from FLICA$^+$/PI$^+$ (late apoptotic) to FLICA$^-$/PI$^+$ (necrotic) was prevented in the continuous presence of FLICA. The apoptotic cascade was thus halted at the late apoptotic stage (FLICA$^+$/PI$^+$).

A

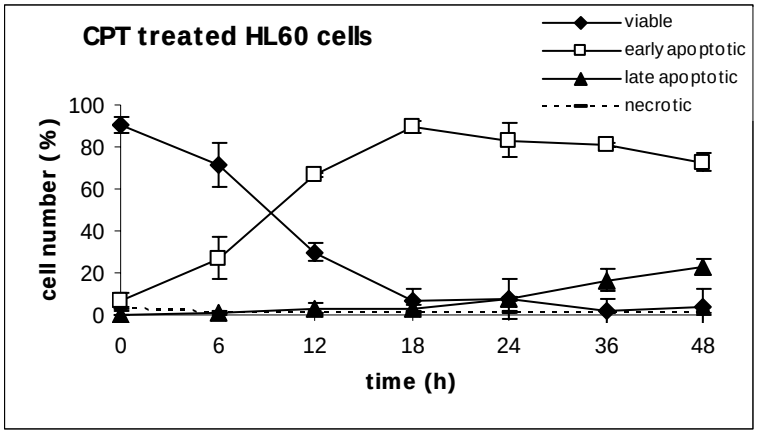

B

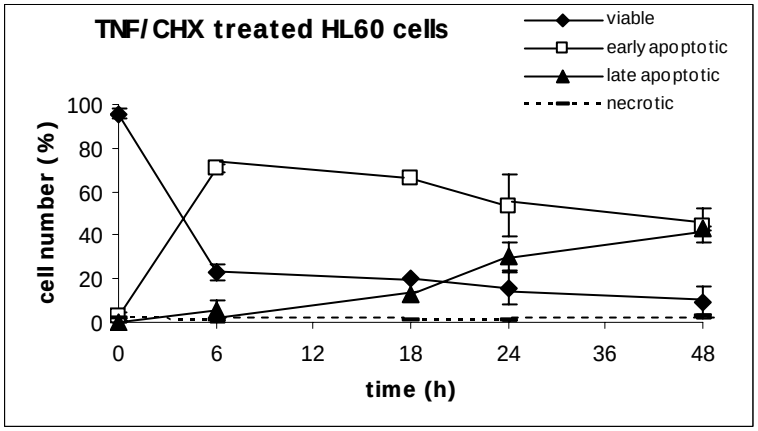

Figure 3-2. The relative amounts of viable, early apoptotic, late apoptotic and necrotic HL60 cells during apoptosis. The different cell populations of the quadrants shown in figure 1B are plotted as a function of time after CPT **(A)** or TNF-α/CHX **(B)** treatments in the continuous presence of FLICA. The plots represent the averaged cell numbers of 3 experiments of each time point.

The kinetics of cell accumulation during treatment with CPT or TNF-α/CHX were measured by plotting the accumulation of apoptotic cells (quadrant C and D, FLICA$^+$ cells) as a function of time. The slope of the plot provides an estimation of the cell transition into apoptosis, as shown in figure 3-3. This figure reveals two different slopes, representing different rates of cell transition into apoptosis. During

the first 18h of incubation with CPT 92% of the HL60 cells underwent apoptosis at an approximate rate of 5% per hour. The remaining cells underwent apoptosis between 18 and 48h at an approximate rate of 0.2% per hour (Figure 3-3A). When HL60 cells were treated with a mixture of TNF-α/CHX to initiate apoptosis (Figure 3-3B), 76% of the cells underwent apoptosis at an approximate rate of 12% of cells per hour during the first 6h of incubation. The remaining cells underwent apoptosis between 6 and 48h at an approximate rate of 0.3% of cells per hour.

A

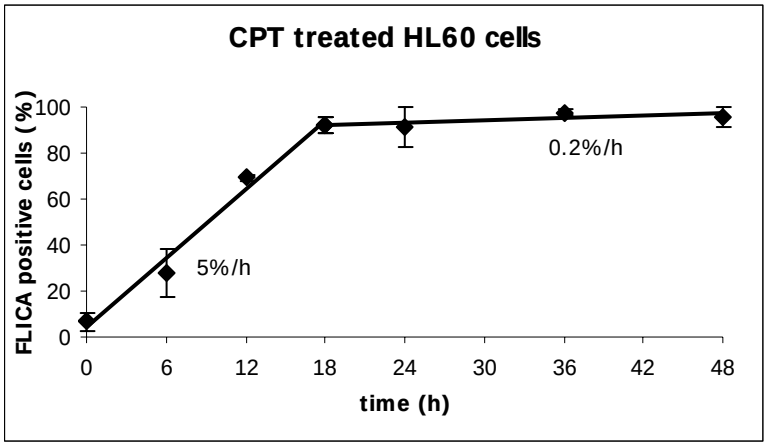

B

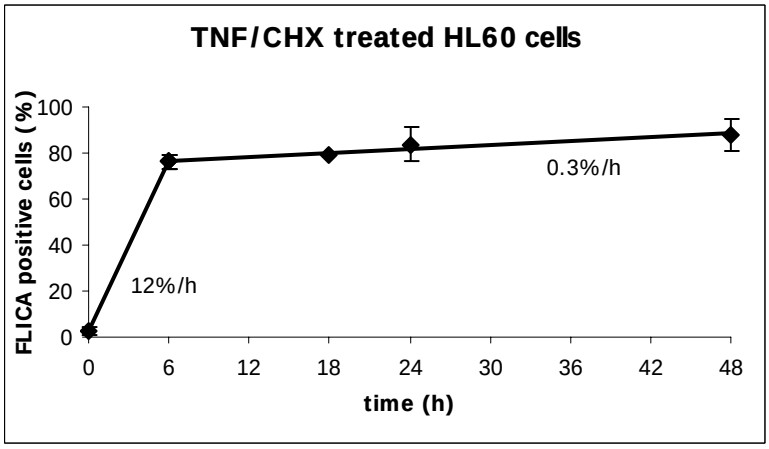

Figure 3-3. Kinetics of FLICA labeled cell accumulation in HL60 cultures treated with CPT **(A)** or TNF-α/CHX **(B)** in the continuous presence of FLICA. The percentages of FLICA positive cells (quadrant C and D) are plotted as a function of time and represent the averaged cell numbers of 3 experiments of each time point.

3.3.2 HUVEC

Incubation with a mixture of TNF-α/CHX initiated apoptosis also in HUVEC (Figure 3-4A).

A

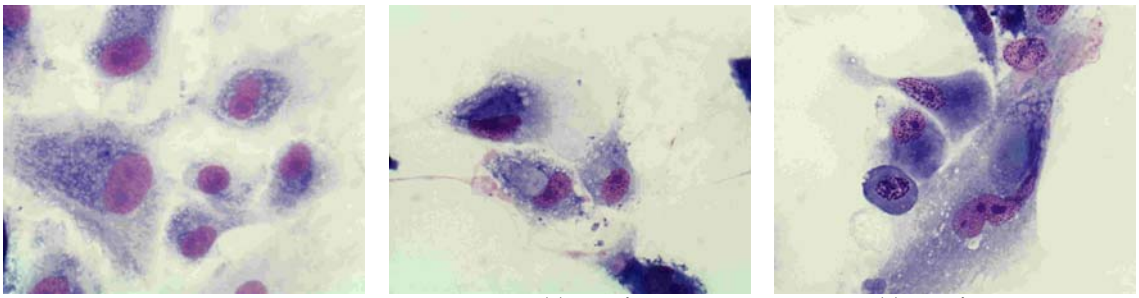

HUVEC control **HUVEC TNF-α/CHX** **HUVEC TNF-α/CHX + FLICA**

B

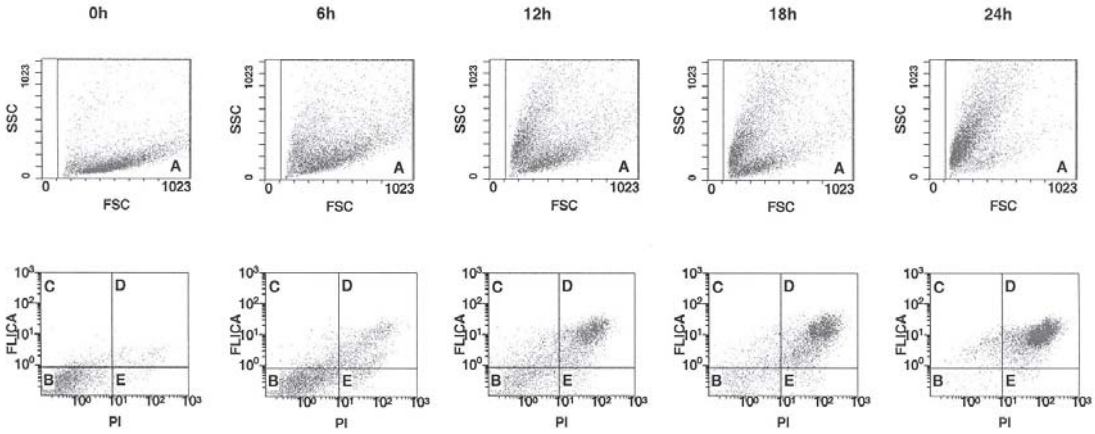

Figure 3-4. HUVEC treated with TNF-α/CHX in the presence of FLICA. **(A)** Light microscopy (LM) of untreated HUVEC, HUVEC treated with 3 nM TNF-α and 50 μM CHX and treated with TNF-α/CHX in the presence of FLICA for 6 h. HUVEC were stained with May Grünwald Giemsa staining. Magnificance of the LM pictures is 50x. **(B)** Dual fluorescence staining of HUVEC. HUVEC were incubated with TNF-α/CHX in the continuous presence of 20 μM FLICA for 0, 6h, 12h, 18h and 24h, and were stained with propidium iodide (PI) The cells presented in gate A are used to plot FLICA fluorescence in relation to PI fluorescence. Four cell subpopulations (B-E) can be identified on these scattergrams, differing in their capability to bind FLICA and PI. Scatterdiagrams show results from one a representative experiment.

In the continuous presence of FLICA, TNF-α/CHX induced a direct transition from $FLICA^-/PI^-$ (viable quadrant) to the $FLICA^+/PI^+$ (late apoptotic) quadrant (Figure 3-4B, t= 6-24h, quadrant D) in HUVEC.

The results from the scatterdiagrams obtained from 1 to 4 different experiments of each time point are plotted as function of time (Figure 3-5)

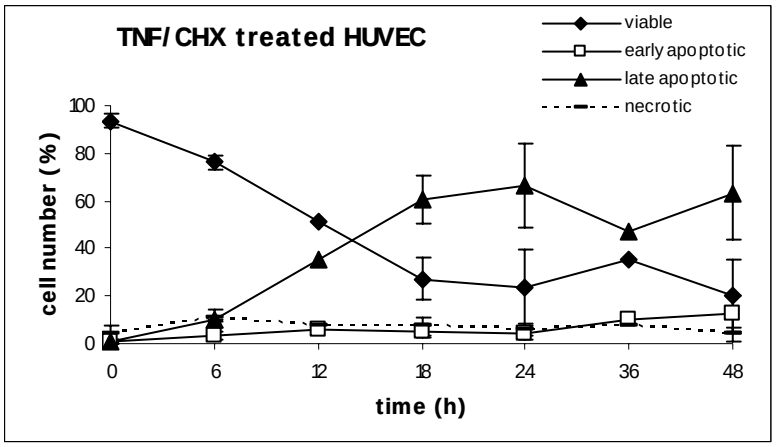

Figure 3-5. The relative amounts of viable, early apoptotic, late apoptotic and necrotic HUVEC during TNF)-α/CHX induced apoptosis. The different cell populations of the quadrants as shown in figure 4B are plotted as a function of time in the continuous presence of FLICA. The plots represent the averaged cell numbers of 1-4 experiments of each time point.

The kinetics of cell accumulation during treatment with TNF-α and CHX were measured by plotting accumulation of apoptotic cells (quadrant C and D, FLICA$^+$ cells) as a function of time with TNF-α and CHX. The slope of the plot provides an estimation of the cell transition into apoptosis. Figure 3-6 shows two different slopes, revealing different rates of cell transition into apoptosis. During the first 18h of incubation 65% of the HUVEC underwent apoptosis, at an approximate rate of 3.7% of cells per hour. The remaining cells underwent apoptosis between 18 and 48h at an approximate rate of 0.2% of cells per hour.

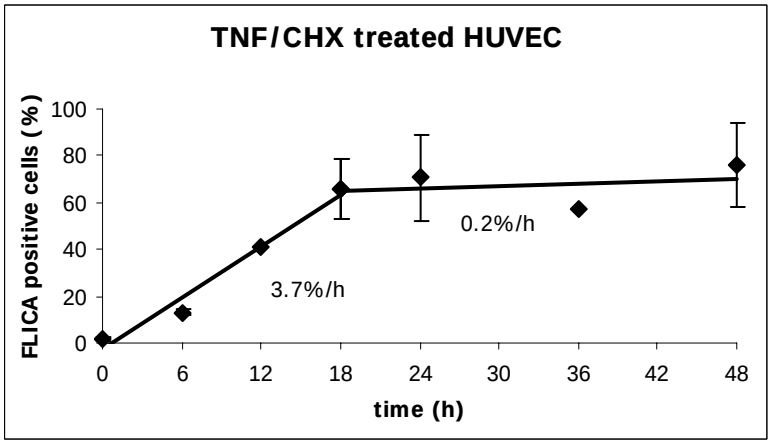

Figure 3-6. Kinetics of FLICA labeled cell accumulation in HUVEC cultures treated with TNF-α/CHX in the continuous presence FLICA. The percentages of FLICA positive cells (quadrant C and D) are plotted as a function of time and represents the averaged cell number of 1-4 experiments of each time point.

3.4 Discussion

In this study, the cell death kinetics of HL60 cells were compared to HUVEC by using different inducers to initiate apoptosis. When cells were incubated with CPT, 92% of the HL60 cells underwent apoptosis during the first 18h of incubation at an approximate rate of 5% of cells per hour. Incubation with TNF-α/CHX proved to be a stronger inducer of apoptosis, because 76% of the cells underwent apoptosis during the first 6h of incubation at an approximate rate of 12% of cells per hour. The remaining cells underwent apoptosis between 6 and 48h at an approximate rate of 0.2-0.3% of cells per hour (Figure 3-3). These results are equivalent to the results obtained by Darzynkiewicz and colleagues.[2,3,7,10] These authors found that HL60 cells underwent apoptosis at an approximate rate of 7% of cells per hour during the initial 8h of incubation with CPT. The remaining cells entered apoptosis at a rate of 1 % of cells per hour for up to 48h. When HL60 cells were incubated with TNF-α/CHX, 50% of the cells underwent apoptosis during the initial 6h at an approximate rate of 8% of cells per hour. The remaining cells underwent apoptosis between 6 and 24h at a rate approximating 2.5 % of cells per hour. In our study, 65% of the HUVEC underwent apoptosis at an approximate rate of 3.7% of cells per hour during the first 18h of incubation with TNF-α/CHX. The remaining HUVEC underwent apoptosis for up to 48h at a rate of 0.2 % of cells per hour (Figure 3-6). Accordingly, quantitiatively there was not much difference in the number of apoptotic cells comparing HL60 cells with HUVEC, though the entrance rate into the apoptotic cascade was higher for HL60 cells then for HUVEC both treated with TNF-α/CHX (6h vs 18h; figure 3-3B and figure 3-6). Furthermore, HL60 cells and HUVEC showed a different pattern of transition during the course of the cell death cascade. CPT-treated and TNF-α/CHX-treated HL60 cells, in the continuous presence of FLICA, transited from the viable quadrant to the early apoptotic quadrant and then to the late apoptotic quadrant (Figure 3-1B). The transition from the viable quadrant to the early apoptotic quadrant was skipped when HUVEC, in the continuous presence of FLICA, were incubated with TNF-α/CHX (Figure 3-4B). We speculate, that at the time the caspases were activated in HUVEC, the plasma membrane had lost already part of its integrity, and therefore behaved as a population in the late apoptotic quadrant. A possible explanation for the difference between HL60 and HUVEC, shown in the

scatterdiagrams might be the phenomenon of anoikis.[15-19] Anoikis ('homelessness') induces apoptosis due to inadequate cell-matrix interactions. One of the questions in anoikis research is how the caspase cascade is initially activated by simple detachment of cells. It was reported that anoikis in HUVEC requires interaction between the death receptor Fas and Fas ligand.[16] Adherent endothelial cells are resistant to Fas-mediated apoptosis, because Fas-L and Fas do not interact. However, in response to specific stimuli (TNF-α) or injury, which cause cell detachment, endothelial cells become sensitized to Fas-mediated apoptosis, via an increase in Fas expression and Fas receptor surface levels.[16] However, enhanced Fas expression alone is not sufficient to sensitize adherent HUVEC for Fas-mediated killing. One additional step in Fas-signaling seems necessary in the regulation of anoikis. The down-modulation of the endogenous caspase-8 inhibitor (c-Flip) during cell detachment may be a causal event in detachment-induced caspase-8 activation and HUVEC anoikis. In our study, HUVEC were treated with TNF-α/CHX in the continuous presence of FLICA, which prevents anoikis, because caspase activation is inhibited. Anoikis may explain the difference seen in the transition-scatterdiagrams between HL60 cells and HUVEC, but further study is needed in order to reveal the exact mechanism. First attempts have been made to follow the apoptotic cell death cascade in real-time at a single-cell level within a newly developed microfluidic cell trap device.[20] Apoptosis is ideally suited to analyse on chip as apoptosis is a process that does not occur simultaneously in all cells of a population, favouring analysis at the single-cell level. Furthermore, the apoptotic process takes no more than a few hours, hence real-time monitoring will provide new insights in the apoptotic cascade. As confirmed by literature and results presented in this chapter, TNF-α/CHX treated HL60 cells in the continuous presence of FLICA transited from the viable, to the early – and then to the late apoptotic quadrant. Adapting the present conventional techniques to chip technology will offer many benefits and will obtain new insights into the apoptotic cascade.

3.5 Conclusion

FLICA induces an arrest of cells in apoptosis (stathmo-apoptosis) and makes it possible to measure the number of cells present in different stages of the apoptotic cascade and to calculate cell death kinetics. This technique allows us to measure apoptotic cell death rate not only in cultured cells in suspension but in adherent cells as well. The rate of apoptotic cell death depends on the stimulus used to induce apoptosis. TNF-α/CHX showed to be a stronger inducer of apoptosis than CPT in HL60 cells. Accordingly, quantitiatively there was not much difference in the number of apoptotic cells comparing HL60 cells with HUVEC, though the entrance rate into the apoptotic cascade was higher for HL60 cells then for HUVEC both treated with TNF-α/CHX. Furthermore, different transitions during the course of the cell death cascade were seen when the same inducer (TNF-α/CHX) is used. TNF-α/CHX-treated HL60 cells, in the continuous presence of FLICA, transited from the viable quadrant to first the early apoptotic quadrant and then to the late apoptotic quadrant. When HUVEC were treated with TNF-α/CHX, in the continuous presence of FLICA, a direct transition from the viable to the late apoptotic quadrant was seen. Accordingly, cell death kinetics depend on the type of the cell in a qualitative manner and on the stimulus used to induce apoptosis in a quantitative manner.

3.6 References

1. Vermes I, Haanen C, Reutelingsperger C. Flow cytometry of apoptotic cell death. *J Immunol Meth* 2000; **243**: 167-190.
2. Darzynkiewicz Z, Bedner E, Smolewski P. Flow cytometry in analysis of cell cycle and apoptosis. *Semin Hematol* 2001; **38**: 179-193.
3. Smolewski P, Grabarek J, Phelps DJ, Darzynkiewicz Z. Stathmo-apoptosis: Arresting apoptosis by fluorochrome-labeled inhibitor of caspases. *Int J Oncol* 2001; **19**: 657-663.
4. Thornberry NA, Lazebnik Y. Caspases: Enemies within. *Science* 1998; **281**: 1312-1316.
5. Hengartner MO. The biochemistry of apoptosis. *Nature* 2000; **407**: 770-776.

6. Grabarek J, Amstad P, Darzynkiewicz Z. Use of fluorescently labeled caspase inhibitors as affinity labels to detect activated caspases. *Hum Cell* 2002; **15**: 1-12.
7. Grabarek J, Darzynkiewicz Z. In situ activation of caspases and serine proteases during apoptosis detected by affinity labeling their enzyme active centers with fluorochrome-tagged inhibitors. *Exp Hematol* 2002; **30**: 982-989.
8. Smolewski P, Bedner E, Du L, Hsieh T, *et al.* Detection of caspase activation by fluorochrome-labeled inhibitors: Multiparameter analysis by laser scanning cytometry. *Cytometry* 2001; **44**: 73-82.
9. Pozarowski P, Hunag X, Halicka DH, Lee B, *et al.* Interactions of fluorochrome-labeled caspase inhibitors with apoptotic cells: A cuation in data interpretation. *Cytometry* 2003; **55A**: 50-60.
10. Smolewski P, Grabarek J, Lee BW, Johnson GL, Darzynkiewicz Z. Kinetics of HL60 cell entry to apoptosis during treatment with TNF-α or camptothecin assayed by the stathmo-apoptosis method. *Cytometry* 2002; **47**: 143-149.
11. Smolewski P, Grabarek J, Halicka HD, Darzynkiewicz Z. Assay of caspase activation in situ combined with probing plasma membrane integrity to detect three distinct stages of apoptosis. *J Immunol Meth* 2002; **265**: 111-121.
12. Bedner E, Smolewski P, Amstad P, Darzynkiewicz Z. Activation of caspases measured in situ by binding of fluorochrome-labeled inhibitors of caspases (FLICA): Correlation with DNA fragmentation. *Exp Cell Res* 2000; **259**: 308-313.
13. Teodori L, Grabarek J, Smolewski P, Ghibelli L, *et al.* Exposure of cells to static magnetic field accelerates loss of integrity of plasma membrane during apoptosis. *Cytometry* 2002; **49**: 113-118.
14. Jaffe EA, Nachman RL, Becker CG, Minick CR. Culture of human endothelial cells derived from umbilical veins. Identification by morphologic and immunologic criteria. *J Clin Invest* 1973; **52**: 2745-2756.
15. Ruoslathi E, Reed JC. Anchorage dependence, integrins, and apoptosis. *Cell* 1994; **77**: 477-478.
16. Aoudjit F, Vuori K. Matrix attachment regulates Fas-induced apoptosis in endothelial cells: A role for c-Flip and implications for anoikis. *J Cell Biol* 2001; **152**: 633-644.
17. Frisch SM, Screaton RA. Anoikis mechanisms. *Curr Opin Cell Biol* 2001; **13**: 555-562.

18. Grossmann J. Molecular mechanisms of "detachment-induced apoptosis–Anoikis". *Apoptosis* 2002; **7**: 247-260.
19. Valentijn AJ, Zouq N, Gillmore AP. Anoikis. *Biochem Soc Trans* 2004; **32**: 421-425.
20. Valero A, Merino F, Wolbers F, Luttge R, *et al.* Apoptotic cell death dynamics of HL60 cells studied using a microfluidic cell trap device. *Lab Chip* 2005; **5**: 49-55.

4

Apoptosis induced kinetic changes in autofluorescence of cultured HL60 cells*

The measurement of natural cellular fluorescence (autofluorescence, AF) presents a new way to study apoptosis. Compared to well-known fluorescent apoptosis assays, sample preparation time is reduced and cellular toxicity is avoided, due to the fact that no labelling is required. Induction of apoptosis resulted in a decrease in AF intensity compared to untreated HL60 cells, especially seen in the late apoptotic subpopulation. The AF intensity was found to decrease significantly in time (between 2h and 24h) for all the four apoptotic inducers used. These results open a door to future developments in single-cell analysis, since with chip technology it is possible to trap single cells at a certain position and analyse their responses to certain drugs. For long-term real-time cellular based assays, toxicity of fluorescent dyes need to be avoided and measuring the AF intensity in time provides us with new possibilities to analyse the process of apoptosis.

*modified from

F. Wolbers[1,2], H. Andersson[2,3], A. van den Berg[2], I. Vermes[1]. Apoptosis 2004; 9: 749-755

[1]*Department of Clinical Chemistry, Medisch Spectrum Twente, Hospital Group, Enschede, The Netherlands*

[2]*Department of Sensorsystems for Biomedical and Environmental Applications, MESA+ Institute for Nanotechnology, University of Twente, Enschede, The Netherlands*

[3]*Department of Signals, Sensors and Systems, Royal Institute of Technology, Stockholm, Sweden*

4.1 Introduction

There are a number of techniques available to detect cell death. However, these tools are in most cases not specific or lack quantitative value.[1] In fact the very nature of apoptotic cell death promotes the underrecognition of this phenomenon for various reasons. First, apoptosis involves scattered single cells. Second, the early stages of the apoptotic process evanesce and the apoptotic bodies are small and undergo rapid phagocytosis, an inflammatory reaction remains absent. Moreover, the duration of the whole process takes no more than a few hours.[2] Nowadays, we are still seeking a simple technique, which will enable us to measure apoptotic cell death without manipulation of cells (*e.g.,* staining which kills cells) and which will monitor the apoptotic cascade in real time.[1]

During the past decade, chip technology has shown its great value for chemical analysis in so-called Lab-on-a-Chip systems.[3-5] Recently, the use of microtechnologies for cell biology applications receives rapidly growing attention.[6,7] The main reason for this is the manipulation of single cells in microfluidic structures and the possibilities for electrical characterisation and detection using microfabricated devices.[8-10]

A new method is presented here which uses autofluorescence (AF) to study the process of apoptosis. Natural cellular fluorescence can be a useful tool in unravelling intracellular pathophysiological processes and distinguish normal from diseased tissue.[11] Many cellular metabolites exhibit autofluorescence, all having their specific emission and excitation wavelengths.[12] Collagen and elastin in a cell's connective tissue and lipofuscin exhibit strong autofluorescence, in the blue-green and yellow spectral regions, respectively.[13] Nicotin-amide adenine dinucleotide (NAD(P)H) is the main fluorochrome excited by UVA, whereas NAD(P)+ is not fluorescent. NAD(P)H shows intracellular fluorescence in the blue spectral region and can be used as an indicator of redox state. The flavins, when oxidised, have strong autofluorescence in the yellow-green spectral region, and therefore can be considered as the main fluorochromes emitting above 500 nm.[13-15] Both components are actively involved in a number of metabolic processes within the cell and play an important role in the energy household of the cell. Autofluorescence colocalizes strongly within the mitochondria and in some extent within the lysosomes, while the nucleus remains dark.[16] The flavins and NAD(P)H

are mainly responsible for this mitochondrial autofluorescence and therefore this autofluorescence can be used to give an indication of the metabolic activity of the cell.[11,13,14,17,18] In most cases autofluorescence is seen as a nuisance which can obscure the fluorescence of various fluorescent probes used in optical techniques.[12-14] However, measurement of autofluorescence can be very advantageous because labelling is not required which reduces sample preparation time and avoids cellular toxicity. In this study, human promyelocytic leukaemic HL60 cells were incubated with various apoptotic inducers and autofluorescence was measured at the flow cytometer.

4.2 Materials and methods

4.2.1 HL60 cells

Human promyelocytic leukaemic HL60 cells were obtained from the German Collection of Microorganisms (Braunschweig, Germany). Tissue culture equipment was supplied by Corning (Badhoeverdorp, The Netherlands). HL60 cells were cultured in RPMI-1640 medium supplemented with 10% heat-inactivated and filter-sterilised Foetal Bovine Serum, 100 IU/ml penicillin, 100 μg/mL streptomycin, 2 mM L-glutamine and 0.4 μg/mL fungizone (= $RPMI^+$ medium). RPMI-1640 medium was obtained from BioWhittaker (Verviers, Belgium). Supplements and antibiotics were all obtained from Life Technologies (Grand Island, NY, USA). Cell cultures were sustained in a 5% CO_2 humidified atmosphere at 37°C. The medium was refreshed every 3-4 days. Exponentially growing cells were used in the experiments.

4.2.2 Modulation of HL60 cells

4.2.2.1 Induction of apoptosis

Irradiation. Cells at a concentration of 0.5 x 10^6 cells/ml in a 24-wells plate were irradiated at a mean distance to target of 100 cm and a dose rate of 4.0 Gray/min with use of a linear accelerator (Varian Clinac 2100.C, Varian, Palo, Alto, CA) with an energy of 6 MV, to a dose of 6 and 10 Gray.

Incubation with camptothecin. Apoptosis was induced by the incubation of cells under culturing conditions with 0.15 μM camptothecin (CPT, Sigma, St. Louis, MO, USA) during increasing time periods, varying from 0 to 48h.

Incubation with tumour necrosis factor-α and cycloheximide. Apoptosis was induced by the incubation of cells under culturing conditions with 3 nM tumour necrosis factor (TNF)- α and 50 μM cycloheximide (CHX) (Sigma, St. Louis, MO, USA) during increasing time periods, varying from 0 to 24h.

4.2.2.2 Induction of necrosis

HL60 cells were heated for 2h at 57°C to induce necrosis. After heating, the cells were cultured in a 24-wells plate during increasing time periods, varying from 0 to 24h.

4.2.2.3 Glucose

HL60 cells were incubated with 5 mM and 15 mM D(+)-Glucose (Merck, Darmstadt, Germany) during increasing time periods, varying from 0 to 48h.

After incubation/irradiation, HL60 cells were washed twice and resuspended in 0.5 mL PBS. Samples were kept on ice until flow cytometry.

4.2.3 Flow cytometry

Autofluorescence of individual cells was measured with a Coulter Epics XL flow cytometer, using System II™ software with the XL-2 or DOS configuration. Excitation was elicited with the Argon laser at 488 nm and measured using the FL-1 (peak 525 nm) and FL-2 (peak 575 nm) channels. In each sample 10,000 events were measured. Flow cytometry data were analysed with the computer programme Expo II and gates/markers were set with untreated HL60 cells. No difference in AF was seen between the FL-1 and FL-2 channel, therefore only the results obtained in the FL-1 channel are shown.

4.2.4 Autofluorescence intensity and statistical analysis

Autofluorescence intensity (AF intensity) is defined as the ratio of the mean fluorescence of the early apoptotic (region 1), late apoptotic (region 2) or necrotic (region 3) subpopulation as compared to the mean fluorescence of the viable population (eq. 4-1). The area defines the number of cells in the region. Standard deviations are given as the standard error of the mean (SEM).

$$\text{AF intensity} = \frac{\text{Mn X m-1, m-2 or m-3}}{\text{Mn X v}} \qquad \text{eq. 4-1}$$

in which

$$\text{Mn X} = \frac{\Sigma(\text{intensity number x count in the position})}{\text{area}}$$

$$\text{AF}^{24/2}\text{ factor} = \frac{\text{AF intensity t=24h (region 1, 2 or 3)}}{\text{AF intensity t=2h (region 1, 2 or 3)}} \qquad \text{eq. 4-2}$$

To analyse the AF intensity in time, the $AF^{24/2}$ factor is measured which defines the ratio of the minimal AF intensity (t=24h) compared to the maximal AF intensity (t=2h) (eq. 4-2).

4.3 Results

HL60 cells were incubated with various cell death inducers. Irradiation with 6 Gray activated the apoptotic cascade in HL60 cells, which resulted in cellular de-fragmentation and the formation of apoptotic bodies (Figure 4-1A 24h).

Figure 4-1B shows the scatterdiagrams of untreated HL60 cells (control) and HL60 cells 24 and 48h after irradiation with 6 Gray. Four subpopulations are shown, respectively viable, early apoptotic (region 1), late apoptotic (region 2) and the necrotic (region 3) subpopulation, corresponding to the different stages of the apoptotic cascade *in vitro*. Furthermore, for each subpopulation the fluorescence intensity histograms are shown.

A

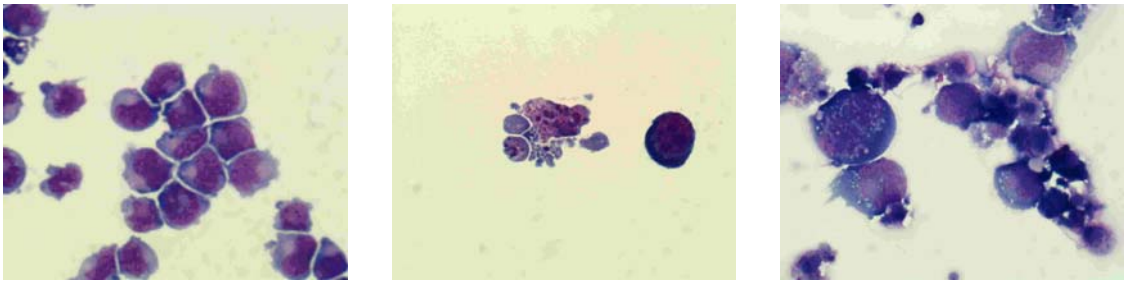

Control **24h** **48h**

B

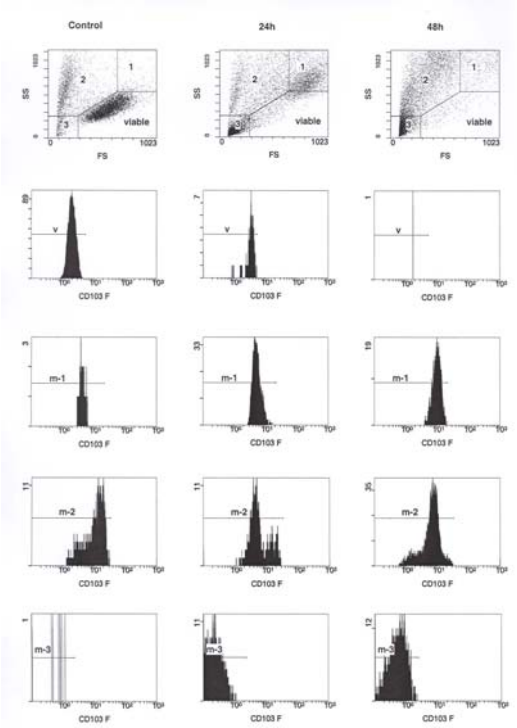

Figure 4-1. (A) Light microscopy (LM) of untreated HL60 cells (control) and HL60 cells 24 and 48h after irradiation with 6 Gray. HL60 cells were stained with May Grünwald Giemsa staining. Magnificance of the LM pictures is 50x. **(B)** Scatterdiagrams and fluorescence intensity histograms of untreated HL60 cells (control) and HL60 cells 24 and 48h after irradiation with 6 Gray. Four cell subpopulations (viable, early apoptotic (1), late apoptotic (2), and necrotic (3) can be identified on these scatterdiagrams, differing in their AF intensity, as shown in the fluorescence intensity histograms. Scatterdiagrams show results from a representative experiment.

The results from the scatterdiagrams are plotted as function of time for each individual apoptotic inducer (Figure 4-2A-D). Untreated HL60 cells showed only minor fluctuations in time (Figure 4-3), and could be seen as a stable control population.

A

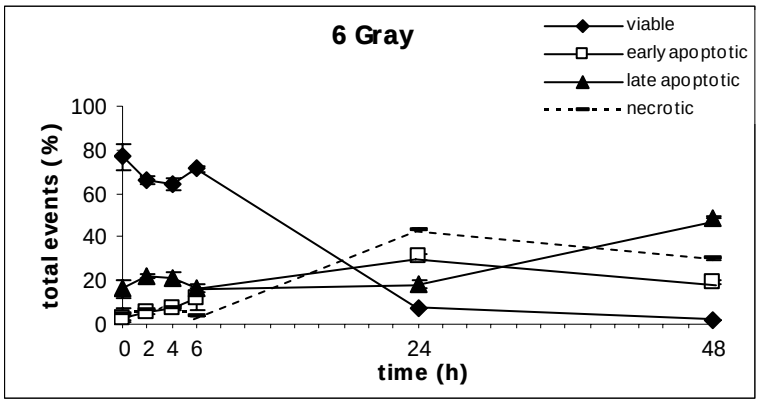

B

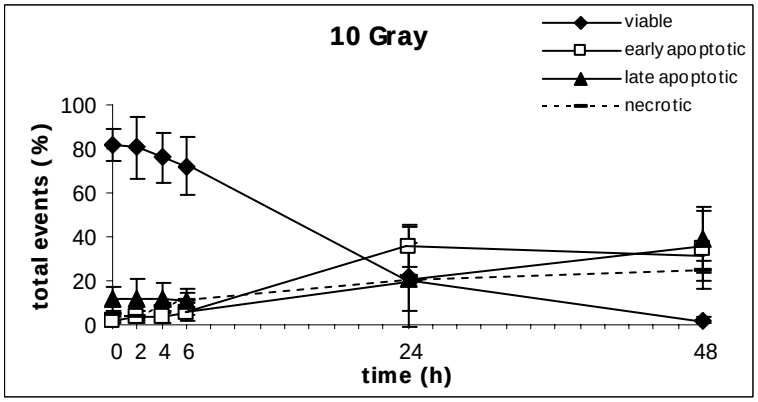

C

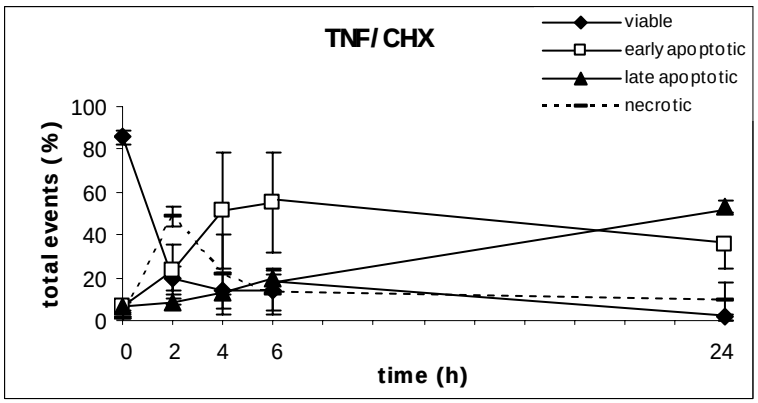

D

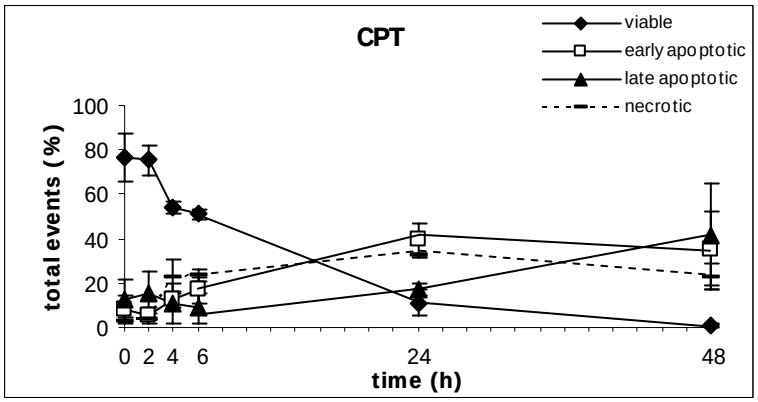

Figure 4-2. The relative amount of viable, early apoptotic, late apoptotic and necrotic HL60 cells during apoptosis. The different cell populations of the quadrants shown in Figure 4-1B (for 6 Gray) are plotted as a function of time after irradiation with 6 Gray **(A)**, 10 Gray **(B)**, and incubation with a mix of 3 nM TNF/50 μM CHX **(C)** and 0.15 μM CPT **(D)**. The plot represents the averaged cell number of 1-3 experiments performed in triple.

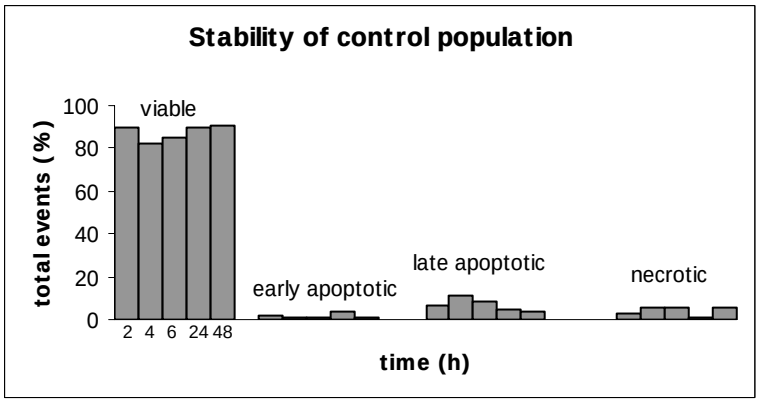

Figure 4-3. The relative amount of viable, early apoptotic, late apoptotic and necrotic HL60 cells. The different cell populations of the quadrants are plotted as function of time for untreated HL60 cells (control population). The plot represents the averaged number of one experiment.

Figure 4-2 shows that after the induction of apoptosis with either irradiation (Figure 4-2A-B) or chemicals (Figure 4-2C-D), HL60 cells in time transited form the viable quadrant to the early - , late apoptotic and necrotic quadrant.

Autofluorescence intensity was measured, using the markers shown in the histograms of figure 4-1B for irradiation with 6 Gray (marker v, m-1, m-2 and m-3). In the first 2h, induction of apoptosis resulted in a slight increase followed by a decrease in AF intensity up to 24h. This decrease in AF intensity was mainly seen in the late apoptotic subpopulation (Figure 4-4A). Between 24 and 48h the AF intensity increased again, especially in the early apoptotic region. The other

apoptotic inducers (10 Gray, TNF-α/CHX and CPT) gave similar results, though TNF-α/CHX was only analysed for a time period of 24h (Figure 4-4B-D).

A

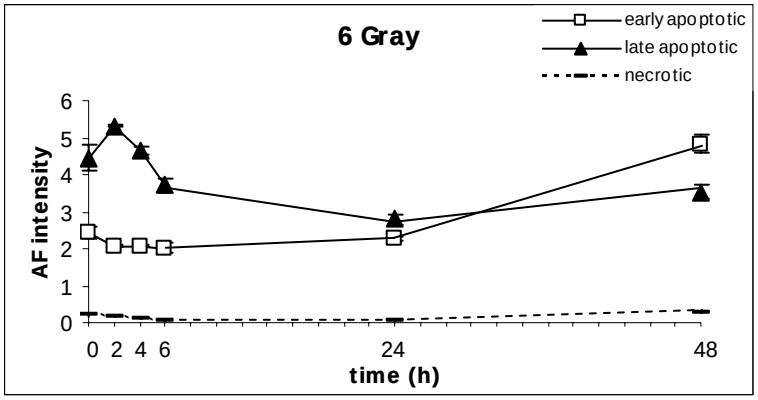

B

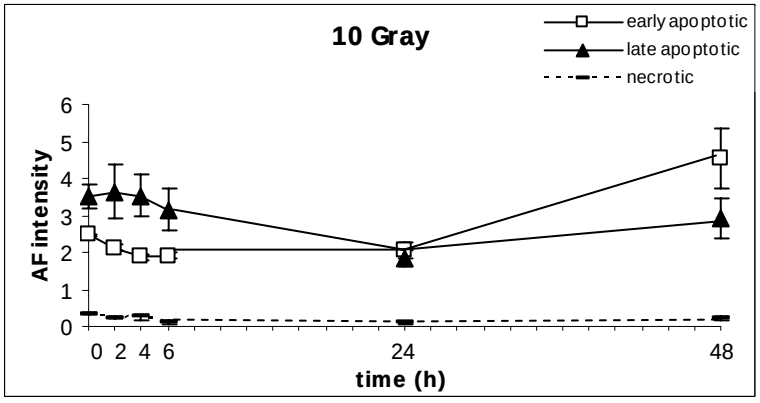

C

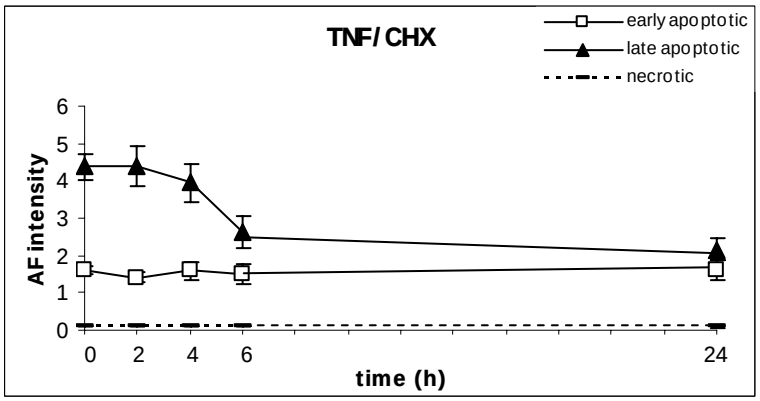

D

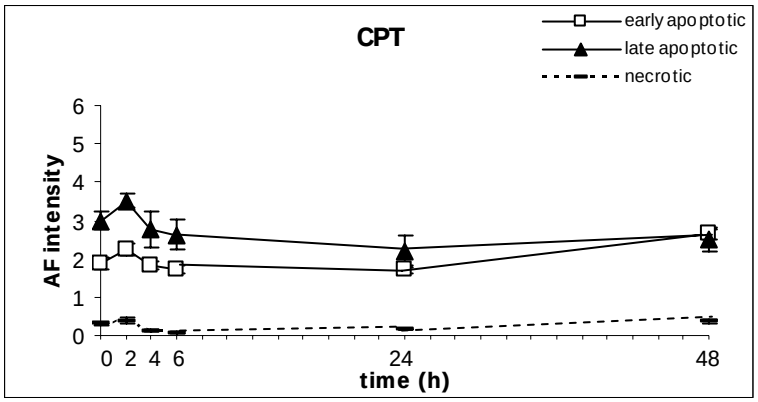

Figure 4-4. Autofluorescence (AF) intensity of HL60 cells irradiated with 6 Gray **(A)**, 10 Gray **(B)**, or treated with a mix of 3 nM TNF-α/50 μM CHX **(C)** or 0.15 μM CPT **(D)**. AF intensity is defined as the ratio of the mean fluorescence of the early apoptotic (region 1), late apoptotic (region 2) or necrotic (region 3) subpopulation as compared to the mean fluorescence of the viable population (eq. 4.1). The plot represents the averaged number of 1-3 experiments performed in triple.

Further, the AF intensity was changing in time, with a maximum at t=2h and a minimum at t=24h. The $AF^{24/2}$ factor of each region was measured for all four apoptotic inducers used. Figure 4-5 shows a decrease in $AF^{24/2}$ factor in each region compared to untreated HL60 cells ($AF^{24/2}$ factor for untreated HL60 cells is set at 1), except for the measured $AF^{24/2}$ factor of HL60 cells incubated with TNF-α/CHX or irradiated with 6 Gray in the early apoptotic region. A slight increase in $AF^{24/2}$ factor compared to untreated HL60 cells was seen here.

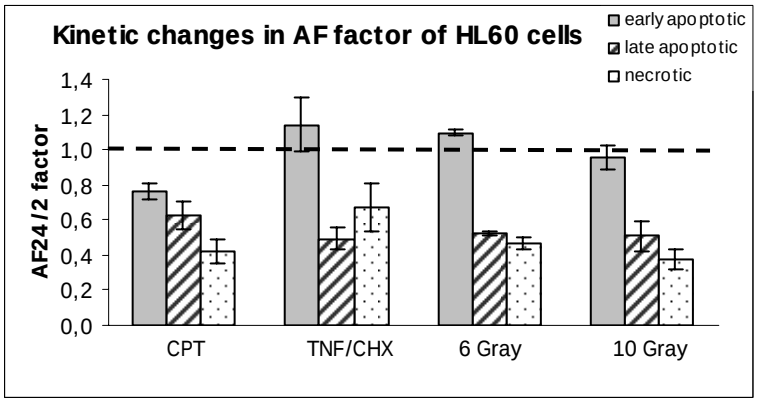

Figure 4-5. $AF^{24/2}$ factor of HL60 cultures treated with 0.15 μM CPT or 3 nM TNF-α in combination with 50 μM CHX, or irradiated with 6 Gray or 10 Gray. The $AF^{24/2}$ factor is defined as the ratio of the minimal AF intensity (t=24h) compared to the maximal AF intensity (t=2h) (eq. 4-2). The $AF^{24/2}$ factor of untreated HL60 cells is set at 1.

The specificity of this assay was obtained. Incubation with 5 mM glucose showed no change in AF intensity in time (Figure 4-6A).

A

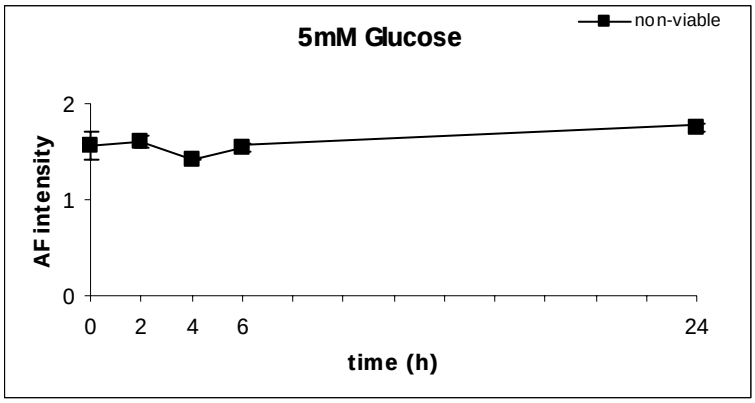

B

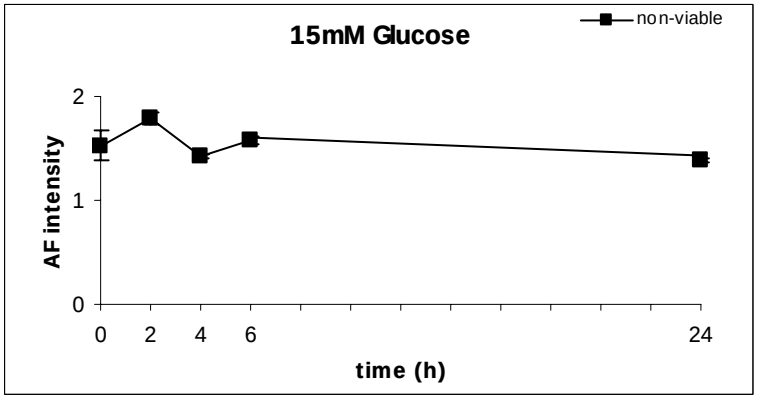

C

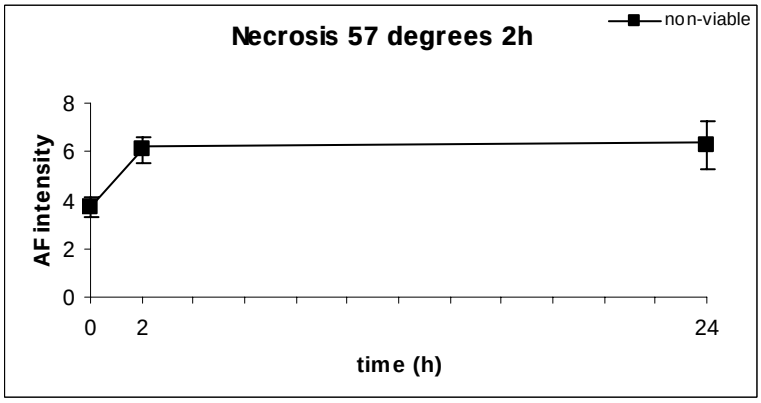

Figure 4-6. Autofluorescence (AF) intensity of HL60 cells incubated with 5 mM **(A)** or 15 mM glucose **(B)** or heated for 2h at 57°C to initiate necrosis **(C)**. AF intensity is in this case defined as the ratio of the mean fluorescence of the non-viable cells as compared to the mean fluorescence of the viable population. The plot represents the averaged number of one experiments performed in fourfold.

However, 15 mM glucose showed a minor decrease in AF intensity and therefore the $AF^{24/2}$ factor was slightly decreased (Figure 4-6B and table 4-1).

When HL60 cells were heated for 2h at 57°C to induce necrosis, the AF intensity increased with a factor 1.7 compared to untreated HL60 cells within 2h after heating. Thereafter, the AF intensity stayed at this level for 24h, which resulted in an $AF^{24/2}$ factor of nearly 1 (Figure 4-6) .

The results of the $AF^{24/2}$ factor are summarised in table 4-1.

	Early apoptotic (region 1)	**Late apoptotic (region 2)**	**Necrotic (region 3)**
Apoptosis			
- CPT	0.76	0.62	0.42
- TNF/CHX	1.14	0.49	0.68
- 6 Gray	1.10	0.52	0.47
- 10 Gray	0.96	0.51	0.38
	Non viable region		
Glucose			
- 5 mM	0.98		
- 15 mM	0.86		
Necrosis			
2h 57°C	1.03		

Table 4-1. $AF^{24/2}$ factor of HL60 cells incubated with different cell death inducers. HL60 cells were incubated with CPT or TNF-α/CHX, or irradiated with 6 or 10 Gray to initiate apoptosis. To test specificity, HL60 cells were incubated with 5 mM or 15 mM Glucose or heated for 2h at 57°C degrees to initiate necrosis.

4.4 Discussion

A new method is presented here in which AF intensity can be used to discriminate viable from apoptotic cells. HL60 cells were incubated with four different inducers of apoptosis, all acting at a specific point in the apoptotic cascade. Tumour necrosis factor α activates the cell death receptor at the surface of the plasma membrane,[19] while camptothecin arrest the cell cycle by inhibiting DNA topo-isomerase.[20] Irradiation induces apoptosis by acting on the mitochondria.[21] AF intensity was measured at the flow cytometer, so only the autofluorescence emerging from the flavins was analysed.[13-15] The progress of the AF intensity in time was the same for

all these apoptotic inducers, probably because all the apoptotic stimuli integrate at the mitochondria, which serves as a receiving platform.[22] The AF intensity increased the first 2h after incubation followed by a decrease up to 24h. Between 24 and 48h, the AF intensity again increased (Figure 4-4). An important cellular factor driving the cells to apoptotic cell death is the availability of cellular ATP.[23] Necrosis on the other hand is characterised by ATP depletion. In the first 2h after incubation with apoptotic stimuli, the oxidised NADH and flavins were responsible for this ATP. The oxidised form of flavins was measured with flow cytometry and was probably responsible for the increase in AF intensity. However, later in the apoptotic process, the ability of the cell to maintain cellular ATP levels was compromised, which resulted in a decrease in AF intensity. After 24h the AF intensity again increased. A possible explanation might be that the cell became necrotic, confirmed by light microscopy (Figure 4-1A 48h). When cells were heated for 2h at 57°C to induce necrosis, the AF intensity increased, which strengthens this hypothesis. However, during the process of necrosis, ATP is depleted, so one would expect a direct drop in AF intensity. Incubation of HL60 cells with a low glucose concentration (5 mM) did not show any change in AF intensity in time. The nutrients in the medium prevented the cell from taking up the extra nutrient, *e.g.,* glucose, so incubation with 5 mM glucose could be seen as an untreated sample. However, when HL60 cells were incubated with the higher glucose concentration (15 mM), a decrease in AF intensity became prominent. Many studies have already shown that high concentrations of glucose induce apoptosis in different cell types.[24-26] Furthermore, incubation of cells with glucose prevents necrotic killing, due to the fact that ATP depletion is diminished. In order to be able to translate the effects seen with flow cytometry to a microfluidic chip to be able to perform single-cell analysis, the $AF^{24/2}$ factor was introduced. For all four apoptotic inducers, the $AF^{24/2}$ factor was decreased (Table 4-1). This decrease was most prominent in the late apoptotic subpopulation, although HL60 cells in the necrotic stage of apoptosis also showed a large decrease in $AF^{24/2}$ factor compared to untreated HL60 cells. This effect was less powerful because the AF intensity of these cells was very low (Figure 4-4). Moreover, the decrease in $AF^{24/2}$ factor was specific for apoptotic cells, while necrotic HL60 cells had an $AF^{24/2}$ factor comparable to untreated HL60 cells. Though the AF intensity increased compared to untreated HL60 cells, this increase was limited to the first 2h after heating, and then stayed at this level, which

resulted in an $AF^{24/2}$ factor near 1. Considerable efforts have been made to use microfluidic devices to perform single-cell analysis.[7] Recent results have shown that it is possible to perform AF measurements on single cells in a microfluidic device.[27] Hence, no labelling with fluorescent probes is required, which limits sample preparation times and potential cell toxicity. Our goal is to translate the effects observed with flow cytometry to a microfluidic chip. Optical detection of a decrease in AF intensity will confirm the conventionally measured results as described in this chapter. HL60 cells were trapped in a microfluidic cell trap device as described by Valero *et al.*[28,29] by capillary flow. Cells were kept in the chip at room temperature and atmospheric CO_2 overnight. AF was detected with the mercury lamp. Figure 4-7 demonstrates that not all cells exhibited autofluorescence and differences in AF intensity could be observed. Furthermore, the cells that exhibited the green autofluorescence appeared in a morphologically different colour in the light microscopy pictures (Figure 4-7A white circles).

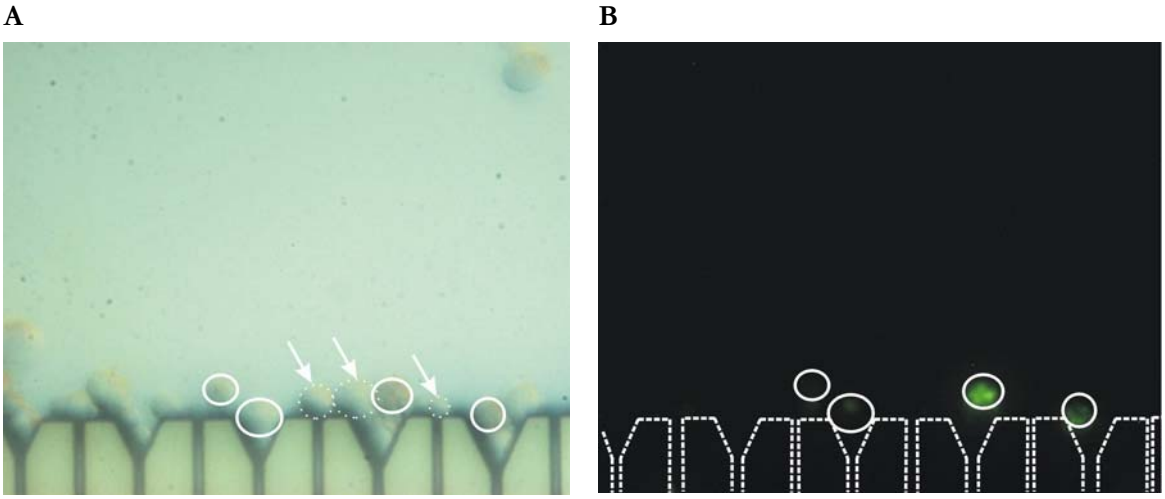

Figure 4-7. Light microscopy **(A)** and fluorescence microscopy **(B)** of HL60 cells trapped overnight in the microfluidic cell trap device.

The surface of these cells appeared a bit rough, which might indicate the blebbing of the plasma membrane. We would expect, because no stimuli were added, that all cells, being and staying viable overnight in the microfluidic cell trap chip, would exhibit autofluorescence. However, the environmental circumstances were different compared to conventional cell culture, in which cells were kept in a humidified atmosphere at 37ºC and 5% CO_2. Hence, a decrease in AF might have occurred (though no fluorescent pictures were taken at the start of the experiment),

indicating cells became either apoptotic or even necrotic. The HL60 cells further showed differences in size (Figure 4-7A white arrows and dashed circles), which strengthens this hypothesis. Further studies are needed to be certain that cells will feel happy in this new environment and will finally be able to perform sophisticated cell analysis on chip (chapter 6).

4.5 Conclusion

Our results have demonstrated the usefulness of analysing the AF intensity in time. Measuring the AF intensity is a rapid and simple technique to study the process of apoptosis in a specific manner. This study showed that in response to either irradiation or chemical agents used to activate the apoptotic process, a significant decrease in AF intensity was demonstrated between 2h and 24h, which resulted in a decreased $AF^{24/2}$ factor. This decrease in AF intensity was most pronounced in HL60 cells present in the late apoptotic phase, which reached the "point-of-no-return". For HL60 cells made necrotic, this decrease in AF intensity was not observed, showing an $AF^{24/2}$ factor comparable to untreated HL60 cells. For long-term real-time cellular based assays, toxicity of fluorescent dyes need to be avoided and measuring the AF intensity in time provides us with new possibilities to analyse the process of apoptosis at a single-cell level on chip.

4.6 References

1. Vermes I, Haanen C, Reutelingsperger C. Flow cytometry of apoptotic cell death. *J Immunol Meth* 2000; **243**: 167-190.
2. Vermes I, Haanen C. Apoptosis and programmed cell death in health and disease. *Adv Clin Chem* 1994; **31**: 177-246.
3. Reyes D, Iossifidis D, Auroux P, Manz A. Micro total analysis systems. 1. Introduction, theory, and technology. *Anal Chem* 2002; **74**: 2623-2636.
4. Aroux P, Iossifidis D, Reyes D, Manz A. Micro total analysis systems. 2. Analytical standard operations and applications. *Anal Chem* 2002; **74**: 2637-2652.
5. Van den Berg A, Lammerink T. Micro total analysis systems: microfluidic aspects, integration concept and applications. *Top Curr Chem* 1998; **194**: 21-49.

6. Andersson H, van den Berg A. Microfluidic devices for cellomics: a review. *Sens Actuat B* 2003; **92**: 315-325.
7. Andersson H, van den Berg A. Microtechnologies and nanotechnologies for single cell analysis. *Curr Opin Biotechnol* 2004; **15**: 44-49.
8. Guijt RM, Baltussen E, van der Steen G, Frank H, *et al.* New approaches for fabrication of microfluidic capillary electrophoresis devices with on-chip conductivity detection. *Electrophoresis* 2001; **22**: 2537-2541.
9. Blom MT, Chmela E, Oosterbroek RE, Tijssen R, van den Berg A. On-chip hydrodynamic chromatography separation and detection of nanoparticles and biomolecules. *Anal Chem* 2003; **75**: 6761-6768.
10. Vrouwe EX, Luttge R, van den Berg A. Direct measurement of lithium in whole blood using microchip capillary electrophoresis with integrated conductivity detection. *Electrophoresis* 2004; **25**: 3032-3042.
11. Dellinger M, Geze M, Santus R, Kohen E, *et al.* Imaging of cells by autofluorescence: a new tool in the probing of biopharmaceutical effects at the intracellular level. *Biotechnol Appl Biochem* 1998; **28**: 25-32.
12. Knight AW, Billinton N. Distinguishing GFP from cellular autofluorescence. Bioph Int September/October 2001.
13. Aubin JE. Autofluorescence of viable cultured mammalian cells. *J Histochem Cytochem* 1979; **27**: 36-43.
14. Benson RC, Meyer A, Zaruba ME, McKhann GM. Cellular autofluorescence-Is it due to flavins? *J Histochem Cytochem* 1979; **27**: 44-48.
15. DaCosta RS, Andersson H, Wilson BC. Molecular fluorescence excitation-emission matrices relevant to tissue spectroscopy. *Photochem Photobiol* 2003; **78**: 384-392.
16. Andersson H, Baechi T, Hoechl M, Richter C. Autofluorescence of living cells. *J Microsc* 1998; **191**: 1-7.
17. Petty HR, Worth RG, Kindzelskii AL. Imaging sustained dissipative patterns in the metabolism of individual living cells. *Phys Rev Lett* 2000; **84**: 2754-2757.
18. Brock R, Hink MA, Jovin TM. Fluorescence correlation microscopy of cells in the presence of autofluorescence. *Biophys J* 1998; **75**: 2547-2557.
19. Wallach D, Varfolomeev EE, Malinin NL, Goltsev YV, *et al.* Tumor necrosis factor receptor and Fas signalling mechanisms. *Ann Rev Immunol* 1999; **17**: 331-367.

20. Lui LF, Desai SD, Li TK, Mao Y, *et al.* Mechanism of action of camptothecin. *Ann N Y Acad Sci* 2000; **922**: 1-10.
21. Overbeeke R, Yildrim M, Reutelingsperger CPM, Haanen C, Vermes I. Sequential occurrence of mitochondrial and plasma membrane alterations, fluctuations in cellular Ca^{2+} and pH during initial and later phases of cell death. *Apoptosis* 1999; **4**: 455-460.
22. Parone PA, James D, Martinou JC. Mitochondria: regulating the inevitable. *Biochimie* 2002; **84**: 105-111.
23. Nieminen A. Apoptosis and necrosis in health and disease: Role of mitochondria. *Int Rev Cytol* 2003; **224**: 29-55.
24. Lorenzi M, Cagliero E, Toledo S. Glucose toxicity for human endothelial cells in culture. *Diabetes* 1985; **34**: 621-627.
25. Baumgartner-Parzer SM, Wagner L, Pettermann M, Grillari J, *et al.* High-glucose-triggered apoptosis in cultured endothelial cells. *Diabetes* 1995; **44**: 1323-1327.
26. Carpentier Y, Mayer P, Bobichon H, Desoize B. Cofactors in in vitro induction of apoptosis in HL60 cells by all-trans retinoic acid (ATRA). *Biochem Pharmacol* 1998; **15**: 177-184.
27. Emmelkamp J, Wolbers F, Andersson H, DaCosta RS, *et al.* The potential of autofluorescence for the detection of single living cells for label-free cell sorting in microfluidic systems. *Electrophoresis* 2004; **25**: 3740-3745.
28. Valero A, Merino F, Wolbers F, Luttge R, *et al.* Apoptotic cell death dynamics of HL60 cells studied using a microfluidic cell trap device. *Lab Chip* 2005; **5**: 49-55.
29. Valero A. Single cell electroporation on chip. *Thesis* ISBN 90-365-2416-4 Chapter **3**: 49-74.

5

Conventional apoptosis and proliferation assay for drug screening in breast cancer treatment

At present the ideal endocrine treatment for breast cancer still needs to be elucidated. *In vitro* studies are a low-cost, time-efficient option to make a selection of the most promising compounds that are to be used later in clinical trials. This way, they can provide valuable leads for novel therapeutic modalities. *In vitro* experiments are therefore necessary to analyse which agent (hormonal vs. non-hormonal), combination, the sequence of agent and the way of administering, will benefit the net effect of the drug on breast cancer cells. Therefore frequently used medicaments such as oestrogens, progestogens, the selective oestrogen modulator (SERM) tamoxifen and the aromatase inhibitors were administered to three different breast cancer cell lines and analysed for their effect on the balance between apoptosis and proliferation. Tamoxifen demonstrated a net apoptotic outcome irrespective of type of breast cancer and receptor status. Due to the negative side-effects of tamoxifen and patients becoming resistant to treatment, the aromatase inhibitors obtained growing interest in adjuvant therapy, although the best administering regime needs further evaluation.

5.1 Introduction

Breast cancer strikes more women than any other cancer. Worldwide, every year one million women are diagnosed with breast cancer, affecting especially older women.[1] The risk of breast cancer increases with age, and therefore breast cancer is less common in young women, though younger women tend to have more aggressive breast cancers than older women. Apart from age, hormonal conditions such as early menarche and postmenopausal hormone therapy have also been associated with an increased risk in developing breast cancer which is demonstrated in epidemiological as well as in clinical studies.[2-4] Non breast feeding mothers have also been reported to suffer an increased risk, whereas studies on oral contraceptive use and increased breast cancer risk are still uncertain.[4,5] The most plausible cause of the elevated risk associated with these conditions, is the level of oestrogen exposure, either due to a higher level or a longer duration of exposure. Many breast cancers, of which the vast majority is hormone-dependent, manifest during the postmenopausal period. This indicates that oestrogens play a crucial role in the development and evolution of breast cancer. Some evidence suggests that oestrogens are not only mitogenic but also have mutagenic effects.[6] Two recent studies, the Women's Health Initiative (WHI) and the Million Women Study (WMS), have raised concerns about the relationship between hormone replacement therapy (HRT) and the increased risk of breast cancer in postmenopausal women. The randomized trial of the Women's Health Initiative provides the best evidence to establish the effect of HRT on breast cancer incidence and mortality up till now. Combined oestrogen (*e.g.,* conjugated equine oestrogens) plus progestagin (*e.g.,* medroxyprogesterone acetate) demonstrated a 26% increase in the rate of occurrence of invasive breast cancer (*e.g.,* abnormal breast cells which have spread outside the breast duct or lobule where they originated), resulting in a hazard ratio of 1.26 (95% CI 1.00-1.59). No significant difference was observed for in situ breast cancers (*e.g.,* early cancer where abnormal breast cells are confined to the ducts or the lobules in the breast).[7] The increase in risk was greatest in women using combined HRT for longer periods, especially for having invasive lobular carcinoma and tumours positive for the oestrogen and progesterone receptor.[8] No increase risk in breast cancer mortality was reported, due to the relatively short follow-up time.[7] Single administering of conjugated equine oestrogens reported no

difference in breast cancer incidence in postmenopausal women (after hysterectomy because single administering of oestrogens increase the risk of endometrial cancer and therefore for women with a uterus a progestin is added for protection) compared to placebo after a follow up of 7 years.[9] However, this trial was stopped prematurely due to increased stroke incidence. Prior HRT use demonstrated a small but statistically significant increase in breast cancer risk as compared to non-users after exposure to conjugated equine oestrogens and medroxyprogesterone acetate. However, among prior hormone users no significant trend was seen as far as follow-up time and duration of prior use was concerned, whereas for non-users a significant increasing trend in breast cancer risk with follow-up time was demonstrated.[10] The other large (non-randomized) Million Women's Study confirmed these findings that current and previous use of HRT increased the risk of breast cancer, but this relative risk increased with increasing duration of use of HRT. Furthermore, this study demonstrated little consistent variation in which progestogen or oestrogen was administered.[11] The Million Women Study is noteworthy for the large numbers of women included in the study, although some controversy exists.[12,13]

Most breast cancers in postmenopausal women are oestrogen receptor (ER) positive, though for premenopausal women two-thirds of breast cancers is ER negative.[14] The goal of endocrine treatment in breast cancer is to block the action of oestrogen on tumour cells either by inhibiting oestrogen from binding to the specific oestrogen receptor (*e.g.,* SERMs) or by inhibiting its synthesis (*e.g.,* aromatase inhibitors).[15] The selective oestrogen receptor modulator (SERM) tamoxifen is presently the first choice for adjuvant treatment (administered after the initial surgery) in postmenopausal women with early breast cancer, due to the antagonistic effects of tamoxifen on the mammary gland.[16] Moreover, the positive (agonistic) effects of oestrogens, for example on bone, are retained. Tamoxifen is mainly cytostatic and slows the proliferation of breast cancer cells by inhibiting their progression from the G1 phase of the cell cycle. Best results appear to be achieved after 5 years of treatment, thereafter the beneficial effects decrease and toxicity increases.[17] Because of their antagonistic effects, SERMs and in particular tamoxifen aggravate or induce (severe) climacteric complaints.[18] Administering HRT in postmenopausal women with ER positive breast cancer when given concomitantly with tamoxifen did not increase the risk of breast cancer

recurrence.[19] This study did not reveal any increased risk for recurrence or mortality associated with HRT. Hence, because tamoxifen is weakly oestrogenic, it may not be optimally effective and increases the risk of endometrial cancer and stroke. Furthermore, patients may be refractory or may become resistant to tamoxifen treatment.[20] Aromatase inhibitors (AI) have the potential to be more effective than tamoxifen, as aromatase inhibitors block the oestrogen synthesis and have no intrinsic oestrogen activity.[15] Aromatization of androgens to oestrogens is the rate-limiting step in the oestrogen synthesis. In situ aromatization, rather than uptake of oestradiol from the plasma, is the key determinant of tumour oestradiol levels.[21] However, the possibility that circulating oestrogens contribute to intratumoral oestrogen cannot completely be refuted.[22] The conversion of the C19 androgens (androstenedione and testosterone) to the C18 oestrogens (oestrone and oestradiol) is mediated by the enzyme aromatase. The enzyme aromatase belongs to the family of cytochrome P450 enzymes. Aromatase is an excellent target for inhibition as it is the last step in steroid biosynthesis and therefore its blockade does not interfere with any steroid downstream. The AI present can be classified in steroidal and non-steroidal. Exemestane (Aromasin®, Pfizer, New York, NY, USA) is a steroidal AI, as exemestane competes with the natural substrate for the active site of aromatase, and the reaction intermediate binds irreversibly to the enzyme. In contrast, the non-steroidal AI anastrozole (Arimidex®, AstraZeneca, London, UK), is a competitive reversible inhibitor, which does not inactivate the enzyme. Recently, the ATAC (Anastrozole, Tamoxifen, Alone or in Combination) trial compared the established adjuvant hormone treatment, tamoxifen, with anastrozole alone and in combination with tamoxifen as adjuvant treatment for postmenopausal women with early breast cancer.[23,24] Single administering of anastrozole favoured the disease-free survival and time to recurrence compared to tamoxifen alone or the combination. Furthermore, anastrozole reduced the occurrence of distant metastases and contralateral breast cancers. Anastrozole was also associated with fewer gynaecological and vascular side-effects than tamoxifen (or the combination of anastrozole with tamoxifen), however, anastrozole caused more bone side-effects, such as an increase in fractures, especially in the spine. Furthermore, chronic deprivation of oestrogens might affect lipid metabolism and cognitive functions.[25] The negative effect of AI on bone metabolism, due to reduced oestrogen production, may be diminished by adding bisphosphonates to the current hormonal

therapy.[26] Bisphosphonates, which act by inhibiting osteoclastic bone resorption, also reduce the fracture risk in women with advanced breast cancer and clinically evident bone metastases. Some bisphosphonates may also reduce bone pain in women with advanced breast cancer and clinically evident bone metastases.[27] In addition to inhibiting osteoclastic bone resorption, bisphosphonates have also been shown to exhibit anti-tumour effects.[28] *In vitro*, bisphosphonates inhibited proliferation and induce apoptosis in cultured human breast cancer cells.[29] Apart from its use in early adjuvant therapy, AI demonstrated effective in a sequencing setting with tamoxifen during the first 5 years post-surgery as well as after 5 years of tamoxifen post-surgery.[30,31] In hormone-receptor positive advanced breast cancer, anastrozole is at least as effective as tamoxifen in first-line therapy.[30,31] Long-term safety and efficacy of AI relative to the present standard tamoxifen for 5 years are currently being evaluated in ongoing large trials. Furthermore, there might be important clinical differences between the various AI, which need a further detailed study. AI generally are not used alone in premenopausal or perimenopausal women with breast cancer, because functioning ovaries overcome oestrogen blockade by increasing production of luteinizing hormone (LH) and follicle-stimulating-hormone (FSH), resulting in increased oestrogen production and rendering the AI ineffective.[31] However, the use of AI is under investigation in combination with ovarian ablation/suppression in these peri- and premenopausal women.

This chapter will highlight the most important *in vitro* results for improving and fine-tuning existing forms of hormone replacement therapy and endocrine therapy for breast cancer treatment, since the ideal endocrine treatment is still to be elucidated. These results stem from a long collaboration between the department of Obstetrics and Gynaecology and the department of Clinical Chemistry of the Medisch Spectrum Twente. Although *in vitro* studies can only function as an experimental model, these studies are low-cost and time-efficient in making a selection of the most promising compounds that are to be used later in clinical trials. In this way, they can provide valuable leads for novel therapeutic modalities. The effects of the single administering of oestrogens[32,33], progestogens[32-34], tamoxifen[33,35] and aromatase inhibitors together with their combinations on tumour growth will be evaluated on different breast cancer cell lines by measuring the apoptosis/proliferation ratio. Cyclin D1 is measured as a proliferation marker. Several lines of evidence point to an important role for Cyclin D1 in breast cancer

formation.[36] Compared to normal ductal cells, Cyclin D1 is over-expressed in nearly 50% of breast cancer cells. Overproduction of Cyclin D1 mRNA and protein correlates strongly with oestrogen receptor synthesis. The DNA fragmentation assay, as described by Nicoletti *et al.*[37] is used to measure the amount of apoptosis in the presence of different drugs. Furthermore, future perspectives towards lab-on-a-chip and personalized medicine in breast cancer therapy will be discussed.

5.2 Materials and methods

5.2.1 Cell culture

Three human breast cancer cell lines were used in the experiments. The oestrogen receptor (ER) positive invasive lobular carcinoma cell line MCF-7 (DSMZ, Braunschweig, Germany), the ER positive invasive ductal carcinoma cell line T47D (ATCC, Rockville, MD, USA) and the ER negative invasive ductal carcinoma cell line MDA-MB 231 (ATCC, Rockville, MD, USA). All cell types were grown in Roswell Park Memorial Institute (RPMI)-1640 medium supplemented with 10% (v/v) foetal bovine serum (FBS) gold, 100 IU/ml penicillin, 100 μg/ml streptomycin, 2 mM L-glutamine and 0.4 μg/ml fungizone. Media and supplements were all obtained from Cambrex (Verviers, Belgium), except for FBS gold which was obtained from PAA (Pasching, Austria). Cell cultures were sustained in a 5% CO_2 humidified atmosphere at 37ºC. The medium was refreshed every 3-4 days and the cultures were split weekly at a ratio of 1:3 – 1:6 after treatment with versene in aqua dest. Versene consists of aqua dest. with 137 mM NaCl, 1.47 mM KH_2PO_4, 2.68 mM KCl, 7.37 mM $Na_2HPO_4.2H_20$ and 0.54 mM NA_2EDTA dissolved. Cells used for experiments were plated in a concentration of 0.2 x 10^6 cells/ml. Drug exposure experiments were performed by adding medium containing concentrations of 10^{-6} M drug to the cells for 6 days incubation.

5.2.2 Drugs

17β-oestradiol (E2) and dihydrodydrogesterone (DHD) were obtained from Solvay Pharma (Brussels, Belgium), medroxyprogesterone acetate (MPA) from Sigma (St. Louis, MO, USA), and tibolone from Organon (Oss, The Netherlands). Tamoxifen

was purchased from Pharmachemie (Teva Pharmaceuticals Ltd, Petach Tikva, Israel), and the aromatase inhibitors anastrazole (Arimidex®) from AstraZeneca (London, UK) and exemestane (Aromasin®) from Pfizer (Pfizer, New York, NY, USA).

5.2.3 Measurement of proliferation

Cell proliferation was measured by quantification of the expression of Cyclin D1 mRNA. The mRNA was measured quantitatively using competitive reverse transcription polymerase chain reaction (RT-PCR) technique as described previously by Heid *et al.*[38] and clarified in detail in chapter 6. Briefly, the cells were washed, lysed and RNA was isolated using the QIAamp RNA Blood Kit (Qiagen, Hilden, Germany). cDNA was synthesized and amplified using the required set of primers and probes (Applied Biosystems, Foster City, CA, USA) at the Taqman. The mRNA expression of Cyclin D1 was quantified using the ΔΔCt method.[39] The intra-assay variability was 3.9% and the inter-assay variability 5.2%. Results are plotted as a relative ratio of the amount of Cyclin D1 expression in the drug-treated sample compared to the Cyclin D1 expression in the untreated sample. A relative ratio of 1 indicates no change in Cyclin D1 expression compared to untreated cells.

5.2.4 Measurements of apoptosis

Cell death due to apoptosis was determined by using the DNA fragmentation assay according to the method of Nicoletti *et al.*[37] The cells were washed with PBS, detached with versene, centrifuged (350g) and fixed in ice-cold ethanol. The fixed cells were resuspended in 1 ml sodium citrate solution (1 mg/ml) containing 10 μg/ml propidium iodide (PI, Sigma, Deisenhofen, Germany) and 0.1% Triton X-100 (Merck, Darmstadt, Germany) and kept in the dark for 10 minutes incubation. In each sample the DNA content of 10,000 stained cells was measured by flow cytometry (FCM). The intra- and inter-assay variability was less then 5%. The results are plotted as a relative ratio of the percentage of apoptotic cells in the drug-treated sample compared to the percentage of apoptotic cells in the untreated sample. A relative ratio of 1 indicates no change in the number of apoptotic cells compared to untreated cells.

5.2.5 Statistical analysis

The cell proliferation marker Cyclin D1 and the DNA assay marker for apoptosis were measured in two separate experiments and duplicated for the apoptosis measurements and duplicated twice for the Cyclin D1 measurements. The results are expressed as the relative ratio as compared to untreated samples. From these values the ratio apoptosis/proliferation was calculated to define the outcome of the drug-treatment. A ratio apoptosis/proliferation > 1 indicates that the amount of apoptosis is higher than the amount of proliferation, which causes an apoptotic outcome of the drug. The reverse is the case for a ratio apoptosis/proliferation < 1, in which proliferation prevails. A ratio apoptosis/proliferation of 1 indicates no change in the presence of the drug compared to the untreated sample, though the cell turnover can be increased or decreased as a consequence of a same increase or decrease in apoptosis as in proliferation. Standard errors of the mean (SEM) of these ratios apoptosis/proliferation were calculated. The 95% confidence intervals (95% CI) were assessed and the p-values derived from these intervals were calculated with the one-sample t-test and considered statistically significant if they were less than 0.05.

5.3 Results and Discussion

5.3.1 Characteristics breast cancer cell lines

Table 5-1 summarizes the important characteristics of the three breast cancer cell lines used.

	MCF-7	**T47D**	**MDA-MB-231**
Type	invasive lobular	invasive ductal	invasive ductal
Morphology	epithelial	epithelial	epithelial
Receptor status			
• ER-α	60%	80%	0%
• PR-A	25%	100%	0%
Doubling time	50h (30-72h)	32h	42h

Table 6-1. Characteristics of the human breast cancer cell lines used for drug screening. Oestrogen (ER) and progesterone (PR) receptor status were established with immunohistochemistry (Laboratory for Microbiology, Twente-Achterhoek, Enschede, The Netherlands).

5.3.2 Oestrogens and progestogens

The relative ratios of the individual proliferation and apoptosis measurements of drug-treated versus untreated breast cancer cells with SD for the oestrogens and progestogens, are given in respectively figure 5-1 and figure 5-2. Analysis was performed after 6 days of incubation as progestogens have a biphasic action on the cell cycle. Acute progestogen exposure stimulates the cell through a first mitotic cell cycle. However, the chronic exposure of progestogens demonstrate a growth inhibition in the G1 phase of the second cycle.[40] 17β-oestradiol (E2) demonstrated proliferation independent of the type of breast cancer and the receptor status (Figure 5-1), whereas apoptosis was decreased, or showed no effect compared to control (Figure 5-2).

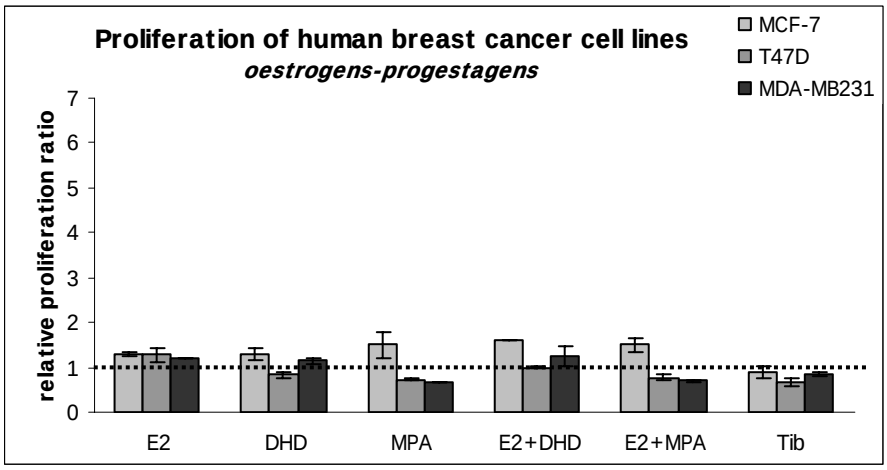

Figure 5-1. Relative proliferation ratio of Cyclin D1 of drug-treated cells versus untreated cells with SD. Three different breast cancer cell lines were incubated with oestrogens, progestogens, tibolone or combinations with a concentration of 10^{-6}M for 6 days. E2 = 17β-oestradiol; DHD = dihydrodydrogesterone; MPA = medroxyprogesterone acetate; Tib = tibolone.

The progesterone dihydrodydrogesterone (DHD), the major metabolite of dydrogesterone, and medroxyprogesterone acetate (MPA) (synthetic C21 derivate of progesterone) showed varying results in the three breast cancer cell lines. For MCF-7 cells an increase in the proliferation in the presence of the progestogens DHD and MPA was measured, whereas in T47D cells the proliferation was decreased (Figure 5-1). The amount of apoptosis was increased in ER positive cells in the presence of DHD, but MPA only increased the apoptosis in T47D cells (Figure 5-2). DHD increased the proliferation and MPA decreased the proliferation

in ER negative MDA cells, however for both progestogens the apoptosis was decreased. Combining oestrogens with progestogens, as performed in hormone replacement therapy, hardly any increase in proliferation was noticeable as compared to the single administering of progestogens. However, apoptosis was greatly increased in ER positive cells for the combination E2+DHD, and the combination E2+MPA in T47D cells. Tibolone decreased the proliferation and increased the apoptosis irrespective of the type of breast cancer and the receptor status.

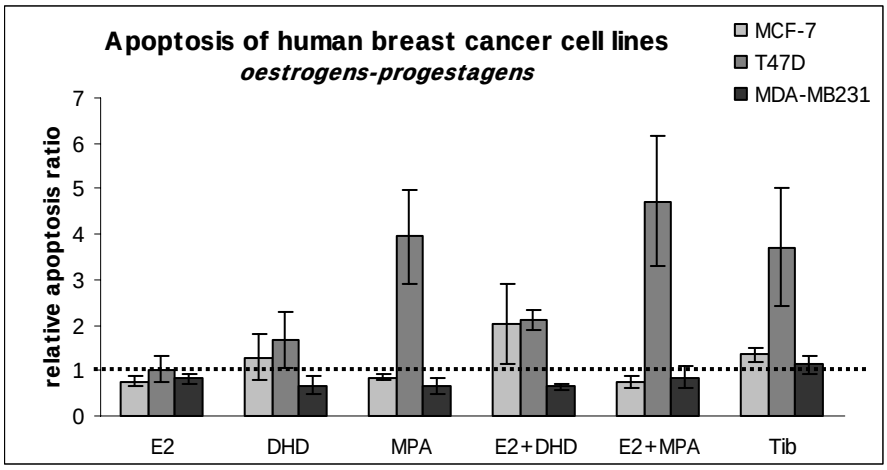

Figure 5-2. Relative apoptosis ratio of DNA fragmentation of drug-treated cells versus untreated cells with SD. Three different breast cancer cell lines were incubated with oestrogens, progestogens, tibolone or combinations with a concentration of 10^{-6}M for 6 days. E2 = 17β-oestradiol; DHD = dihydrodydrogesterone; MPA = medroxyprogesterone acetate; Tib = tibolone.

To determine the net effect of administering of oestrogens and progestogens on the three breast cancer cell lines, the ratio apoptosis/proliferation (Rap) was determined (Figure 5-3). A Rap > 1 indicates that the amount of apoptosis is higher than the amount of proliferation, which causes an apoptotic outcome of the drug. The reverse is the case for a Rap < 1, in which proliferation has the overhand. A Rap of 1 indicates no change in the presence of the drug compared to the untreated sample, though the cell turnover can be changed.

As described in literature, oestrogens exert proliferative effects on the breast[6], showing a Rap < 1 for all three breast cancer cell lines. On the other hand, the role of progestogens is more controversial. Not all progestogens act identically on breast cancer cells[34,41,42], as is also shown in figure 5-3. DHD and MPA showed a net apoptotic effect in T47D cells, whereas DHD in MDA cells and MPA in MCF-7

cells demonstrated a proliferative effect. As described in literature and confirmed by these results, MPA only has direct growth inhibitory effects (concentration dependent) on ER positive and PR positive human breast cancer cell (*e.g.,* T47D) *in vitro* and these effects can be accounted for by a decrease in the rate at which cells transverse the G1 phase of the cell cycle.[43,44] HRT has been associated with increased risk of breast cancer, though for breast cancer cells, not every oestrogen-progestogen combination proved harmful. In ER positive ductal carcinoma cells (T47D) both combinations of E2 with either DHD or MPA demonstrated a net apoptotic effect. However, ER positive lobular carcinoma cells (MCF-7) showed no response after administering of the combination E2+DHD, but the combination E2+MPA was highly proliferative. For ER negative invasive ductal cells (MDA-MB231) the combination E2+DHD was proliferative. From figure 5-3 it can be concluded that especially the progestogens determine the net outcome of the drug and perhaps due to the presence of more progesterone receptors the apoptotic effect is more pronounced in T47D breast cancer cells.

Tibolone can bind to both the oestrogen and the progesterone receptor and the metabolites of tibolone have oestrogenic as well as progestogenic activity.[45,46] Overall, tibolone demonstrated an apoptotic effect independent of the type of breast cancer and the receptor status.

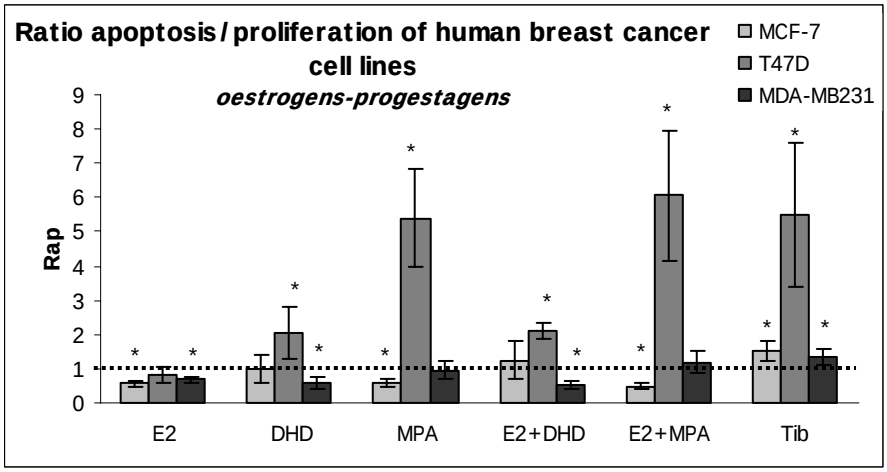

Figure 5-3. Relative apoptosis/proliferation ratio (Rap) drug-treated cells versus untreated cells with pooled SD. Three different breast cancer cell lines were incubated with oestrogens, progestogens, tibolone or combinations with a concentration of 10^{-6}M for 6 days. E2 = 17β-oestradiol; DHD = dihydrodydrogesterone; MPA = medroxyprogesterone acetate; Tib = tibolone. * = $p \leq 0.05$.

5.3.3 Tamoxifen

Generally, tamoxifen binds specifically to the oestrogen receptor thereby inhibiting the transition of breast cancer cells from the G1 to the S phase of the cell cycle. Tamoxifen demonstrated a decrease in proliferation for all three breast cancer cell lines (Figure 5-4). An increase in apoptosis was only shown after administering to T47D cells (Figure 5-5). Overall, tamoxifen caused a net apoptotic effect in all three breast cancer cell lines, however this effect was more pronounced, as expected, in breast cells expressing the oestrogen receptor (Figure 5-6). The mechanism of tamoxifen action cannot solely be explained via the ER receptor, since tamoxifen has an effect on ER negative cells. This is probably the reason why some ER negative tumours *in vivo* can respond to tamoxifen and hormonal manipulation too.[17] The classical genomic mechanism of oestrogens is based on the function of the oestrogen receptor (ER) as a ligand-dependent transcription factor that binds to oestrogen-response-elements (ERE) in promotors of target genes to initiate gene expression. However, ER also stimulates rapid non-genomic pathways, which are initiated at the cell membrane or in the cytosol and involve the activation of cytoplasmic signal transduction cascades, such as the ERK pathway. These pathway-selective oestrogen receptor ligands might represent a novel option for hormone replacement therapy.[47] In breast cancer cells, oestrogens can even activate early cell survival mechanisms in an ER independent fashion, at least in part through the G-protein coupled angiotensin II type I receptor (GPCR At1).[48] Due to the presence of non-genomic signalling pathways, even in an ER-independent fashion, the aromatase inhibitors may be beneficial in treating ER positive as well as ER negative breast cancer.

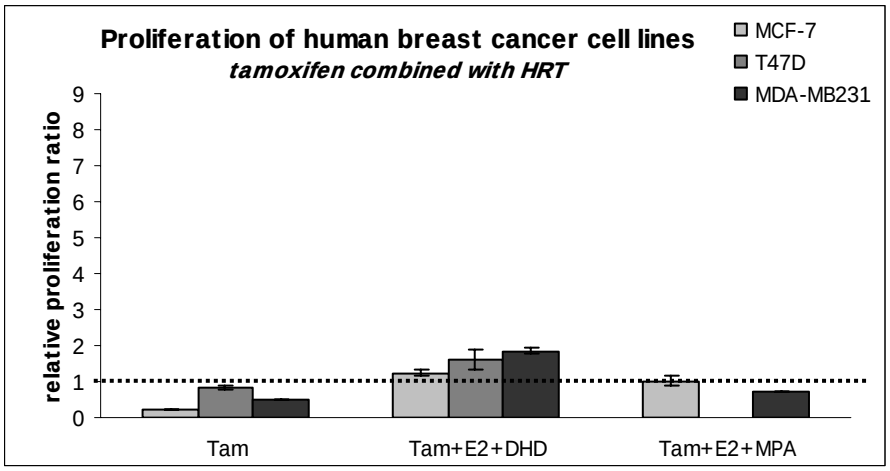

Figure 5-4. Relative proliferation ratio of Cyclin D1 of drug-treated cells versus untreated cells with SD. Three different breast cancer cell lines were incubated with tamoxifen alone or combined with HRT with a concentration of 10^{-6}M for 6 days. Tam = tamoxifen; E2 = 17β-oestradiol; DHD = dihydrodydrogesterone; MPA = medroxyprogesterone acetate.

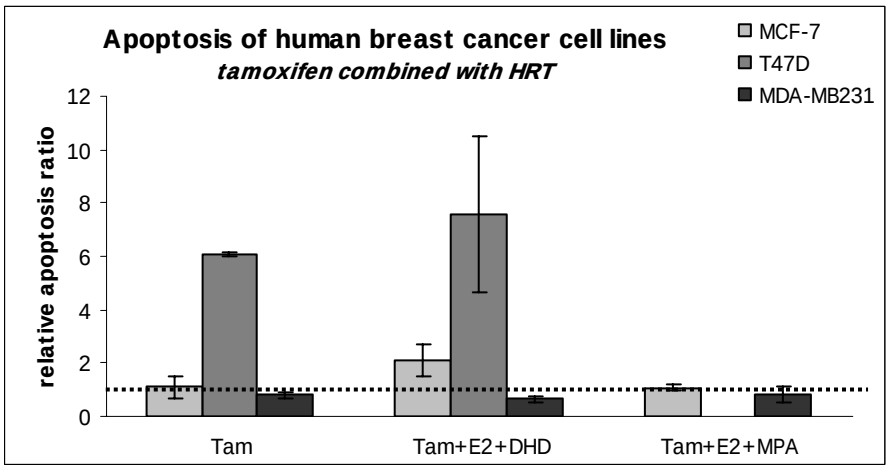

Figure 5-5. Relative apoptosis ratio of DNA fragmentation of drug-treated cells versus untreated cells with SD. Three different breast cancer cell lines were incubated with tamoxifen alone or combined with HRT with a concentration of 10^{-6}M for 6 days. Tam = tamoxifen; E2 = 17β-oestradiol; DHD = dihydrodydrogesterone; MPA = medroxyprogesterone acetate.

To minimize the climacteric symptoms accompanied with the administering of tamoxifen due to its agonistic effects, tamoxifen was combined with standard hormone replacement therapy. The combination of tamoxifen with E2 and DHD showed an increase in proliferation for all three breast cancer cell lines. In ER positive cells an apoptotic increase was seen. Moreover, this increase was larger than after administering only E2 and DHD especially in T47D cells (Figure 5-2).

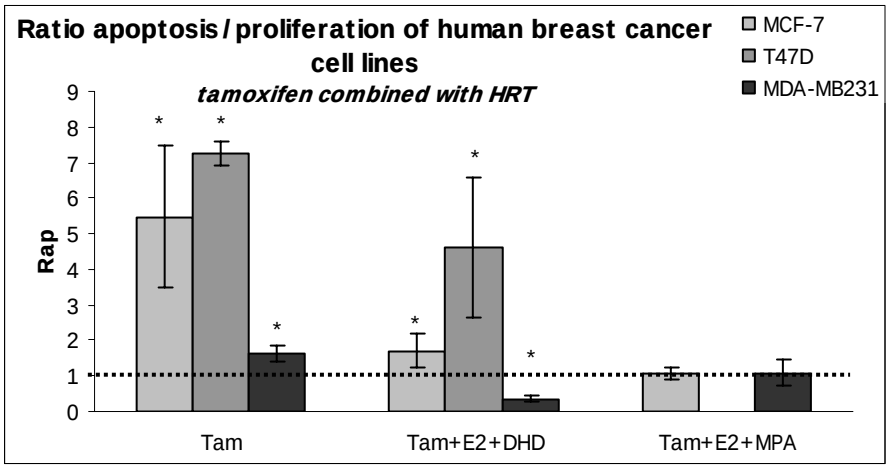

Figure 5-6. Relative apoptosis/proliferation ratio (Rap) drug-treated cells versus untreated cells with pooled SD. Three different breast cancer cell lines were incubated with tamoxifen alone or combined with HRT with a concentration of 10^{-6}M for 6 days. Tam = tamoxifen; E2 = 17β-oestradiol; DHD = dihydrodydrogesterone; MPA = medroxyprogesterone acetate.

For MDA cells a decrease in apoptosis was demonstrated. In ER positive cells, combined administering of tamoxifen with HRT did not lead to proliferation of tumour cells, showing a Rap > 1, indicating apoptosis (Figure 5-6). For ER negative cells the reverse was the case, in which the combination tamoxifen with E2 and DHD demonstrated proliferation. The combination tamoxifen with E2 and MPA had no effect on the Rap in MCF-7 cells and MDA cells. This combination was not analysed in T47D cells. So, adding HRT in combination with the SERM tamoxifen to ER positive or ER negative human breast cancer cell lines does not necessarily lead to the proliferation of tumour cells. This seems to be dependent in a substantial part on the hormone combination used. Adding tamoxifen to E2+DHD, the same trend could be observed compared to the single administering of E2+DHD. Especially the type of progestogen is of paramount importance in keeping the Rap above 1.[35]

5.3.4 Aromatase inhibitors

Aromatase inhibitors influence breast cancer proliferation and apoptosis, though their effect was not equal in the three breast cancer cell lines used. The aromatase inhibtors anastrozole and exemestane had hardly any effect on the proliferation compared to untreated cells (Figure 5-7). Combining with HRT, the administering

of tibolone to AI strongly increased the proliferation, whereas single administering inhibited proliferation (Figure 5-1).

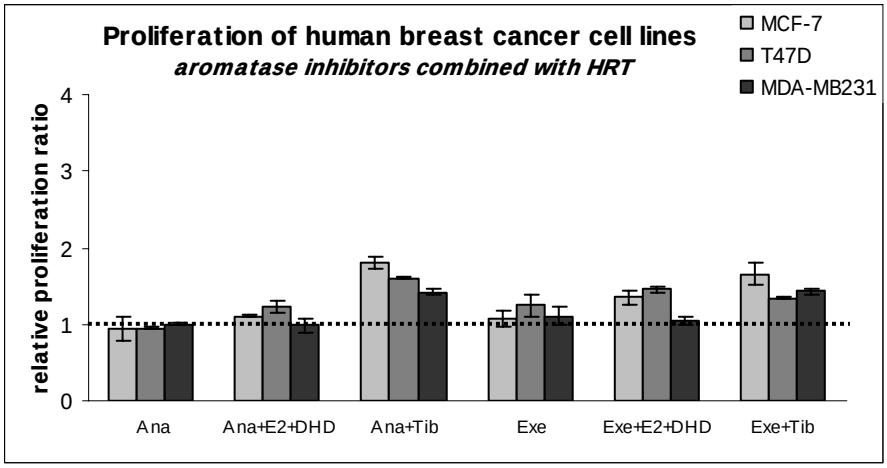

Figure 5-7. Relative proliferation ratio of Cyclin D1 of drug-treated cells versus untreated cells with SD. Three different breast cancer cell lines were incubated with aromatase inhibitors alone or combined with HRT with a concentration of 10^{-6}M for 6 days. Ana = anastrozole; Exe = exemestane; E2 = 17β-oestradiol; DHD = dihydrodydrogesterone; Tib = tibolone.

More pronounced effects of the AI alone and in combination with HRT were demonstrated at the apoptotic level. The AI anastrozole only induced apoptosis in the MCF-7 cell line (Figure 5-8).

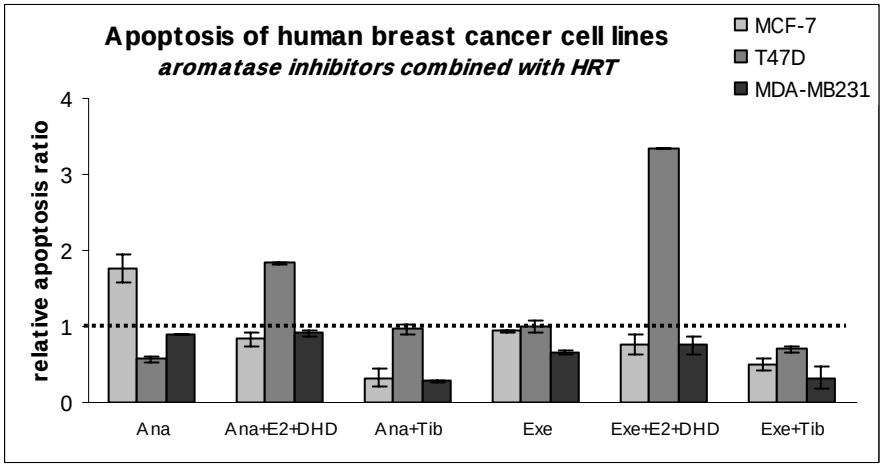

Figure 5-8. Relative apoptosis ratio of DNA fragmentation of drug-treated cells versus untreated cells with SD. Three different breast cancer cell lines were incubated with aromatase inhibitors alone or combined with HRT with a concentration of 10^{-6}M for 6 days. Ana = anastrozole; Exe = exemestane; E2 = 17β-oestradiol; DHD = dihydrodydrogesterone; Tib = tibolone.

The other ER positive cell line T47D demonstrated apoptosis after administering of the AI in combination with E2 and DHD. In all other cases, the apoptotic process was inhibited. Overall, anastrozole only demonstrated a favourable apoptosis/proliferation ratio in the MCF-7 cell line (Figure 5-9). In the T47D cell line both anastrozole and exemestane showed a decrease in cell growth when combined with E2+DHD, attributable mostly to the pro-apoptotic effect of E2+DHD (Figure 5-3). For MDA cells, the AI alone or in combination with HRT showed no change or a net proliferative effect, because of an increase in proliferation and a decrease in apoptosis (Figure 5-9).

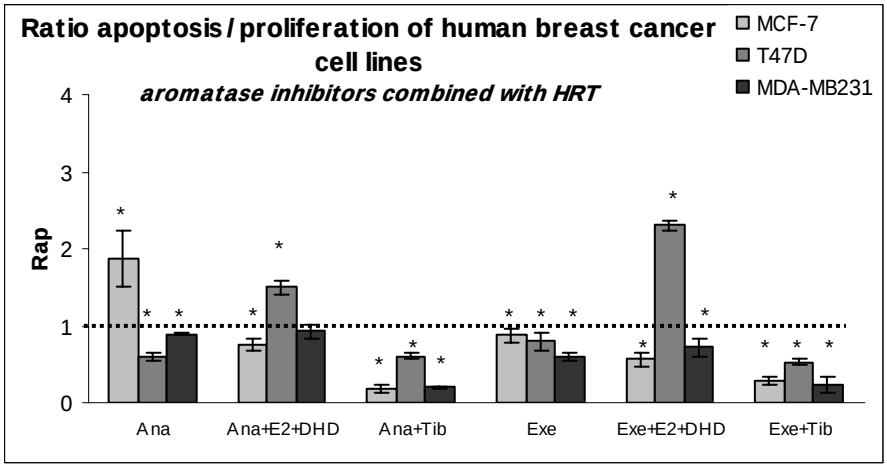

Figure 5-9. Relative apoptosis/proliferation ratio (Rap) drug-treated cells versus untreated cells with pooled SD. Three different breast cancer cell lines were incubated with aromatase inhibitors alone or combined with HRT with a concentration of 10^{-6}M for 6 days. Ana = anastrozole; Exe = exemestane; E2 = 17β-oestradiol; DHD = dihydrodydrogesterone; Tib = tibolone.

Aromatase inhibitors proved successful in many clinical and epidemiological studies in breast cancer treatment in different settings. To our knowledge, there are no *in vitro* studies analyzing the effect of AI on the balance between apoptosis and proliferation at present. Our *in vitro* measurements showed unexpected results. It was hypothesized that breast cancer cells in the presence of AI showed a Rap > 1. Combining AI with HRT, either E2+DHD or tibolone, decreased the Rap as compared to single administering of AI towards even proliferative effects. This is the case for the combination of AI with tibolone on all breast cancer cell lines and the combination AI with E2+DHD on the ER positive cell line MCF-7. However, the combination of AI with E2+DHD in T47D demonstrated a net apoptotic effect, as expected. MDA-MB231 cells are ER negative and therefore not expected

to depend on oestrogen for growth. However, for AI alone and in all combinations a Rap < 1 was measured, indicating proliferation. All breast cancer cell lines used in this study express the Cyp19 gene, encoding for the enzyme aromatase, in equal amounts when in culture. Moreover, AI therapy does, surprisingly, not influence ER levels, since oestrogen down regulates its own receptor and oestrogen deprivation increases the ER expression level, though PR levels are decreased.[22,49] Interpretation of the results published in this chapter is rather difficult and further analysis will be necessary as important clinical differences between the different AI could exist. Incubation of the three breast cancer cell lines with AI for a shorter time (*e.g.,* 24h) improved the Rap, demonstrating an apoptotic outcome in the presence of the AI exemestane on all three breast cancer cell lines, and the AI anastrozole on MCF-7 and MDA-MB231 cells. Furthermore, it is known from literature that aromatase inhibitors (anastrozole, letrozole) reduce cell growth by inducing growth suppression and cell cycle arrest at the G0-G1 phase.[50] A possible explanation for the differences seen in this study could be the duration of the cell cycle of the used cell lines. MCF-7 cells have the longest cell cycle duration (30-72 hour), compared to the T47D (32 hour) and the MDA (42 hour) cell line, so prolonging the incubation time of anastrozole, more cells will have reached the G1 phase in fewer cell cycles, augmenting the apoptotic effect. Perhaps the AI also have a kind of biphasic pattern as described for progestogens, showing differences between acute and chronic exposure. However, it seems feasible that an optimum in incubation time lies between 24 and 144h of incubation with AI. Furthermore, the AI will have to be analysed over a concentration range, in order to evaluate which concentration could favour apoptosis. In our study, all drugs were used in a concentration of 10^{-6}M, though the IC50 (concentration of the inhibitor required to inhibit enzyme activity with 50%) of anastrozole and exemestane in breast cancer homogenates is 8nM and 15nM respectively.[15]

AI demonstrated great advantages in terms of efficiency in the treatment of breast cancer. However, AI have major disadvantages on the bone due to oestrogen deprivation. Treatment with oestrogens might overcome this side-effect. Though administering a patient suffering from breast cancer with oestrogens may be controversial, since the role of oestrogens in the development of breast cancer is well recognized.[6] Combining oestrogens with progestogens demonstrated a beneficial role on the Rap in human breast cancer cells and is possible.[34] Nowadays,

bisphosphonates are prescribed to patients suffering from bone degradation. In addition to inhibiting bone resorption, bisphosphonates have also been shown to exhibit anti-tumour effects.[28] *In vitro*, bisphosphonates inhibited proliferation and induced apoptosis in cultured human breast cancer cells (MCF-7, T47D and MDA-MB231) after 6 days of incubation.[29] Our results on the combination of AI with bisphosphonates for 24h demonstrated that combined exposure of breast cancer cells to bisphosphonates and AI did not reduce the apoptotic effects seen after adding only AI. Even more so, the presence of bisphosphonates increased the apoptotic effects on breast cancer cells of which the combination zoledronate with exemestane seemed to be the most powerful in reducing overall cell growth in the ER positive cell line T47D and the combination zoledronate either with anastrozole or exemestane in the ER positive cell line MCF-7.

Currently, the ideal endocrine therapy for breast cancer treatment still needs to be elucidated. Many questions concerning the most effective future usage of tamoxifen and AI in the adjuvant setting are still being addressed in ongoing trials. These questions relate primarily to the optimal single agent or sequence, duration of treatment and selection of individual patients. However, according to the currently available data, 5 years of treatment with tamoxifen alone may no longer be considered a standard for postmenopausal women with receptor positive early breast cancer.[30] Furthermore, individual treatment regimes have to be set to define the best treatment possible for every patient. Especially, the current confusion and controversy that surrounds postmenopausal hormone therapy, makes it all the more important to individualize treatment. The specific objectives for each patient must be identified and the best treatment option (formulation hormonal or non-hormonal, dose, route of administering, lifestyle changes, medication or no medication) that meets the patient's goals has to be selected, a process that will require time-consuming patient-clinician dialogue.[13] Using patient's own breast (cancer) cells, obtained via biopsy, will help to determine the best individual treatment. Though the conventional techniques, as described in this chapter, to measure the balance between apoptosis and proliferation have numerous disadvantages. First, to obtain enough cells, many passages of cell culture are necessary, which cause cellular modifications. Furthermore, millions of cells are needed to perform flow cytometry analysis as well as RT-PCR for screening only one drug in one dosage. In order to analyse the effect of only one drug in one

dosage, let alone the work involved to measure different (combinations of) drugs in various dosages on different types of breast (cancer) cells for varying time periods is very time-consuming and extremely laborious with these conventional techniques. Moreover, limited number of breast (cancer) cells can be obtained via a biopsy, making these conventional techniques not suitable for *ex vivo* measurements to individualize treatment. With immunocytochemical analysis fewer cells are needed, but a patient first needs to be treated after which the outcome of the drug can be analysed.[51] Recently, the use of microtechnologies for cell biology applications receives rapidly growing attention.[52,53] As microfluidic dimensions equal the size of cells, these devices are very suitable for the analysis of many different biochemical processes, even on a single-cell level. Furthermore, due to smaller dimensions, fewer cells are needed, which will eliminate cell culture in conventional cell culture flask (*in vitro* vs. *ex vivo*). Moreover, using the patient's cells at different positions on the chip, different (combinations of) drugs can be screened at the same time as studying the dose-response relationship to explore drug specific pharmacokinetics, leading to high-throughput analysis. First steps in analyzing the apoptotic effects of different drugs on breast cancer cells (MCF-7) on chip, were taken and will be discussed in chapter 8.

5.4 Conclusion

Results from these *in vitro* studies warrant further pharmacological and clinical studies to analyse the different possibilities for endocrine therapy. Randomized trials with large research populations are necessary for representative *in vivo* experiments. As a result of genomics it is known today that polymorphisms in the DNA sequence cause genetic variation and therefore patients will show an individual response to the therapy. Using a patient's own breast (cancer) cells obtained by biopsy, and analysing the balance between proliferation and apoptosis upon drug treatment will overcome these disadvantages and offers the possibility to make an optimal selection of hormonal or cytotoxic treatment. Although the conventional techniques as described in this chapter are not suitable for these purposes, microfluidics have the potential to meet the requirements. Different drugs in various dosages can be screened to study dose-response relationships using

only a few of the patient's own cells to achieve individual treatment, which will provide further steps towards personalized medicine.

5.5 Acknowledgements

Of the department of Obstetrics and Gynaecology of the Medisch Spectrum Twente, Henk Franke, Anne-Fleur Jordaan, Renske Verdijk, Marielle Bronsema and Istvan Vermes of the department of Clincal Chemistry are acknowledged for their clinical input. Zehra Ciftci and Janneke Hilderink are thanked for their help in performing the experiments in the lab and Job van der Palen for statistical assistance. The Laboratory for Microbiology Twente-Achterhoek is gratefully acknowledged for the immunohistochemical staining procedures.

5.6 References

1. Parkin DM, Fernandez LMG. Use of statistics to assess the global burden of breast cancer. *Breast J* 2006; **12**: S70-S80.
2. Franke HR, Jordaan AF, Wolbers F, Vermes I, *et al.* Ex vivo measurements of cell apoptosis and proliferation in breast tissue of healthy women: influence of age and steroid status. An exploratory study. *Eur J Obstet Gynecol Reprod Biol* 2006; **129**: 92-99.
3. Pike MC, Krailo MD, Hendersson BE, Casagrande, Hoel DG. Hormonal risk factures, breast tissue age and the age incidence of breast cancer. *Nature* 1983; **303**: 767-770.
4. Clemons M, Goss P. Estrogens and the risk of breast cancer. *N Engl J Med* 2001; **344**: 276-285.
5. Marchbanks PA, McDonald JA, Wilson HG, Folger SG, *et al.* Oral contraceptives and the risk of breast cancer. *N Engl J Med* 2002; **346**: 2025-2032.
6. Russo J, Hasan Lareef M, Gabriela B, Guo S, Russo IH. Estrogen and its metabolites are carcinogenic agents in human breast epithelial cells. *J Steroid Biochem Mol Biol* 2003; **87**: 1-25.
7. Writing Group for the Women's Health Initiative Investigators. Risks and benefits of estrogen plus progestin in healthy postmenopausal women: principal

results from the Women's Health Initiative randomized controlled trial. *JAMA* 2002; **288**: 321-333.

8. Li CI, Malone KE, Porter PL, Weiss NS, *et al.* Relationship between long durations and different regimens of hormone therapy and risk of breast cancer. JAMA 2003; 289: 3254-3263.
9. Stefanick ML, Anderson GL, Margolis KL, Hendrix SL, *et al.* Effects of conjugated equine estrogens on breast cancer and mammography screening in postmenopausal women with hysterectomy. JAMA 2006; 295: 1647-1657.
10. Anderson GL, Chlebowski RT, Rossouw JE, Rodabough RJ, *et al.* Prior hormone therapy and breast cancer risk in the Women's Health Initiative randomized trial of estrogen plus progestagin. *Maturitas* 2006; **55**: 103-115.
11. Million Women Study Collaborators. Breast cancer and hormone replacement therapy in the Million Women Study. *Lancet* 2003; **362**: 419-427.
12. van der Mooren MJ, Franke HR. The Million Women Study: no new evidence to change current opinions. *Maturitas* 2003; **46**: 99-100.
13. Speroff L. The Million Women Study and breast cancer. *Maturitas* 2003; **46**: 1-6.
14. Habel LA, Stanford JL. Hormone receptors and breast cancer. *Epidemiol Rev* 1993; **15**: 209-219.
15. Mouridsen HT, Rose C, Brodie AH, Smith IE. Challenges in the endocrine management of breast cancer. *Breast* 2003; **12S2**: S2-S19.
16. Riggs BL, Hartmann LC. Selective estrogen-receptor modulators – mechanisms of action and application to clinical practice. *N Engl J Med* 2003; **348**: 618-629.
17. Early Breast Cancer Trialists' Collaborative Group. Tamoxifen for early breast cancer: an overview of the randomised trials. *Lancet* 1998; **351**: 1451-1467.
18. Canney PA, Hatton MQF. The prevalence of menopausal symptoms in women treated for breast cancer. *Clin Oncol* 1994; **6**: 297-299.
19. Dew JE, Wren BG, Eden JA. Tamoxifen, hormone receptors and hormone replacement therapy in women previously treated for breast cancer: a cohort study. *Climacteric* 2002; **5**: 151-155.
20. Jordan VC. Tamoxifen: toxicities and drug resistance during the treatment and prevention of breast cancer. *Annu Rev Pharmacol Toxicol* 1995; **35**: 195-211.
21. Yue W, Santen RJ, Wang JP, Hamilton CJ, Demers LM. Aromatase within the breast. Endocr Relat Cancer 1999; 6: 157-164.

22. Geisler J, Detre S, Berntsen H, Ottestad L, *et al*. Influence of neoadjuvant anastrozole (arimidex) on intratumoral estrogen levels and proliferation markers in patients with locally advanced breast cancer. Clin Cancer Res 2001; 7: 1230-1236.
23. The ATAC trialists' group. Anastrozole alone or in combination with tamoxifen versus tamoxifen alone for adjuvant treatment of postmenopausal women with early breast cancer: first results of the ATAC randomised trial. *Lancet* 2002; **359**: 2131-2139.
24. The ATAC trialists' group. Results of the ATAC trial after completion of 5 years' adjuvant treatment for breast cancer. *Lancet* 2005; **365**: 60-62.
25. Conte P, Frassoldati A. Aromatase inhibitors in the adjuvant treatment of postmenopausal women with early breast cancer: putting safety issues into perspective. *Breast J* 2007; **13**: 28-35.
26. Chien AJ, Goss PE. Aromatase inhibitors in and bone health in women with breast cancer. *J Clin Oncol* 2006; **24**: 5305-5312.
27. Pavlakis N, Schmidt R, Stockler M. Bisphosphonates for breast cancer. *Cochrane Database Syst Rev* 2005; **20**: CD003474.
28. Diel IJ. Antitumour effect of bisphosphonates: first evidence and possible mechanisms. *Drugs* 2000; **59**: 391-399.
29. Verdijk R, Franke HR, Wolbers F, Vermes I. Differential effects of bisphosphonates on breast cancer cell lines. *Cancer Lett* 2007; **246**: 308-312.
30. Mouridsen HT, Robert NJ. The role of aromatase inhibitors as adjuvant therapy for early breast cancer in postmenopausal women. *Eur J Cancer* 2005; **41**: 1678-1689.
31. Berry J. Are all aromatase inhibitors the same? A review of controlled clinical trials in breast cancer. *Clin Ther* 2005; **27**: 1671-1684.
32. Franke HR, Vermes I. The effect of continuous combined 17β-oestradiol and dihydrodydrogesterone on apoptotic cell death and proliferation of human breast cancer cells in vitro. *Eur J Cancer* 2002; **38**: S69-S70.
33. Franke HR, Kole S, Ciftci Z, Haanen C, Vermes I. In vitro effects of estradiol, dydrogesterone, tamoxifen and cyclophosphamide on proliferation vs. death in human breast cancer cells. *Cancer Lett* 2003; **190**: 113-118.
34. Franke HR, Vermes I. Differential effects of progestogens on breast cancer cell lines. *Maturitas* 2003; **46S1**: S55-S58.

35. Werner HMJ, Franke HR, Vermes I. Apoptosis and proliferation in breast cancer cells, cultured in vitro: effects of SERMs. *Climacteric* 2005; **8**: 294-299.
36. Foster JS, Henley DC, Ahamed S, Wimalasena J. Estrogens and cell-cycle regulation in breast cancer. *Trends Endocrinol Metabol* 2001; **12**: 320-327.
37. Nicoletti I, Migliorati G, Pagliacci MC, Grignani F, Riccardi C. A rapid and simple method for measuring thymocyte apoptosis by propidium iodide staining and flow cytometry. *J Immunol Meth* 1991; **139**: 271-279.
38. Heid CA, Stevens J, Livak KJ, Williams PM. Real time quantitative PCR. *Genome Res* 1996; **6**: 986-994.
39. Bijwaard KE, Aguilera NSI, Monczak Y, Trudel M, *et al.* Quantitative real-time reverse transcription PCR assay for cyclin D1 expression: utility in the diagnosis of mantle cell lymphoma. *Clin Chem* 2001; **47**: 195-201.
40. Groshong SD, Owen GI, Grimison B, Schauer IE, *et al.* Biphasic regulation of breast cancer cell growth by progesterone: role of the cyclin-dependent kinase inhibitors, p21 and p27 (Kip1). *Mol Endocrinol* 1997; **11**: 1593-1607.
41. Gompel A, Somai S, Chaouat M, Kazem A, *et al.* Hormonal regulation of apoptosis in breast cells and tissues. *Steroids* 2000; **65**: 593-598.
42. Moore MR, Spence JB, Kiningham KK, Dillon JL. Progestin inhibition of cell death in human breast cancer cell lines. *J Steroid Biochem Mol Biol* 2006; **98**: 218-227.
43. Sutherland RL, Hall RE, Pang GY, Musgrove EA, Clarke CL. Effect of medroxyprogesterone acetate on proliferation and cell cycle kinetics of human mammary carcinoma cells. *Cancer Res* 1988; **48**: 5084-5091.
44. Kramer EA, Seeger, H, Kramer B, Wallweiner D, Mueck AO. The effects of progesterone, medroxyprogesterone acetate, and norethisterone on growth factor- and estradiol-treated human cancerous and noncancerous breast cells. *Menopause* 2005; **12**: 468-474.
45. Kloosterboer HJ. Tissue-selectivity: the mechanism of action of tibolone. Maturitas 2004; 48: S30-S40.
46. Sadarangani A, Salgado AM, Kato S, Pinto M, *et al.* In vivo and in vitro estrogenic and progestagenic actions of tibolone. *Biol Res* 2005; **38**: 245-258.
47. Wessler S, Otto C, Wilck N, Stangl V, Fritzemeier KH. Identification of estrogen receptor ligands leading to activation of non-genomic signaling

pathways while exhibiting only weak transcriptional activity. J Steroid Biochem Mol Biol 2006; 98: 25-35.

48. Lim KT, Cosgrave N, Hill AD, Young LS. Nongenomic oestrogen signalling in oestrogen receptor negative breast cancer cells: a role for the angiotensin II receptor AT1. *Breast Cancer Res* 2006; **8**: R33
49. Salmon RJ, Alran S, Malka I, de Cremoux P, *et al.* Estrogen receptors evolution in neoadjuvant aromatase inhibitor (AI) therapy for breast cancer in elderly women: stability of hormonal receptor expression during treatment. Am J Clin Oncol 2006; 29: 385-388.
50. Thiantanawat A, Long BJ, Brodie AM, Signaling pathways of apoptosis activated by aromatase inhibitors and antiestrogens. *Cancer Res* 2003; **63**: 8037-8050.
51. Conner P, Soderqvist G, Skoog L, Graser T, *et al.* Breast cell proliferation in postmenopausal women during HRT evaluated through fine needle aspiration cytology. *Breast Cancer Res Treat* 2003; **78**: 159-165.
52. Andersson H, van den Berg A. Microfluidic devices for cellomics: a review. *Sens Actuat B* 2003; **92**: 315-325.
53. Andersson H, van den Berg A. Microtechnologies and nanotechnologies for single cell analysis. *Curr Opin Biotechnol* 2004; **15**: 44-49.

6

Viability studies of HL60 cells*

Transfer of classical biological experiments towards microfluidics

Transfer of classical biological experiments into the chip environment offers many advantages as stated in chapter 2 and 5. One has to realise, though, that the chip environment is quite different from the environment used to perform conventional cell-based assays. Differences in environmental parameters such as temperature and CO_2 concentration and the choice of chip material can influence the viability of the studied cells. Therefore, control viability experiments are required to be able to perform sophisticated cell analysis on chip. In this chapter the effect of culturing human promyelocytic leukaemic HL60 cells at atmospheric CO_2 and various temperatures was assessed. Furthermore, commonly used microchip materials were analysed for their effect on HL60 cells. During the first 24h, the atmospheric CO_2 concentration had no influence on the cell growth, however, changes in temperature needed to be avoided. All microchip materials (with the exception of copper) appeared to be suitable for HL60 cells. Pre-coating the microchip material surfaces with serum favoured the proliferation.

*parts of this chapter are published

F. Wolbers[1,2], P.M. ter Braak[1], S. Le Gac[1], Regina Luttge[1], H. Andersson[1], I. Vermes[2], A. van den Berg[1]. Electrophoresis 2006; 27: 5073-5080

[1]*Department of Sensorsystems for Biomedical and Environmental Applications, MESA+ Institute for Nanotechnology, University of Twente, P.O. Box 217, 7500 AE Enschede, The Netherlands*

[2]*Department of Clinical Chemistry, Medisch Spectrum Twente, Hospital Group, Enschede, The Netherlands*

6.1 Introduction

Today there is a huge interest and effort in analyzing complex biological systems, such as living cells, using micro- and nanotechnologies.[1,2] However, transferring classical biological experiments into the chip environment, problems concerning cell viability can occur. For example, due to the chip design, mechanical effects, such as shear stress or pressure, can occur. The experimental set-up (*e.g.*, flow rates, cell-handling) and the use of different materials as compared to conventional cell culture equipment can harm also cells. Although many scientists have already performed cellular experiments on a chip-level, only few cell viability control experiments have been performed. Most of these studies concern short-time experiments, such as the capture[3], lysis[4,5], separation[6], sorting, *e.g.,* optical[6-8] or immunological[9], counting[10], and analysis[11] of cells. Some of these groups have already performed viability experiments on chip checking cell morphology[6], membrane integrity[3,12] or using dyes such as fluorescein diacetate (FDA)[13] and propidium iodide (PI)[6]. Especially when performing long-term cultivation experiments, it is crucial to verify that cells are in good viable condition before performing any sophisticated cell analyses on lab-on-a-chip devices, because this generated environment can be quite different from the conventional culture flasks. Some data are available about long term cultivation.[14-17] However, only few managed to develop a system for long term cultivation of mammalian cells in combination with on-line monitoring under conditions which are comparable to conventional culture conditions and which enables the performance of different cell-based experiments.[18-22] First, differences in environmental conditions, such as temperature and CO_2, were analysed. Normally these conditions are tightly controlled, but may vary when performing cell analysis outside the incubator. HL60 cells were cultured at atmospheric CO_2 (0.03-0.06%) at different temperatures. Viability was assessed with light microscopy and flow cytometry measuring the autofluorescence (AF) intensity (chapter 4) and DNA fragmentation described by Nicoletti *et al.*[23] Furthermore, in lab-on-a-chip devices many different materials are used, however, when using cells, it is beneficial to be aware what the effect is of these materials on the viability of mammalian cells and so will be advantageous to choose for cellular studies. Therefore new viability control experiments were performed to ensure that cells feel comfortable when in contact with these

microchip materials. Human promyelocytic leukaemic HL60 cells were cultured in contact with commonly used microchip materials, *e.g.*, native silicon oxide (SiO_2), borosilicate glass and polydimethylsiloxane (PDMS) and their effect on the viability was analysed with three independent analytical assays. Copper-coated silicon was analysed for its toxicity and therefore served as a positive control. With real-time reverse transcriptase PCR the expression of both the proliferation marker Cyclin D1 and the apoptosis marker tissue transglutaminase (tTG) was measured. Cyclin D1 plays an important role in the transition from the G1 to the S phase in the cell cycle[24], whereas tTG prevents the leakage of intracellular compounds from the cell in the apoptotic cascade.[25] With flow cytometry, the distribution through the different phases of the cell cycle (PI)[26,27] and the apoptotic cascade (Annexin V in combination with PI)[28] were analysed.

6.2 Materials and methods

6.2.1 HL60 cells

Human promyelocytic leukaemic HL60 cells were obtained from the German Collection of Microorganisms (Braunschweig, Germany). Tissue culture equipment was supplied by Corning (Schiphol-Rijk, The Netherlands). HL60 cells were cultured in RPMI-1640 medium supplemented with 10% heat-inactivated and filter-sterilized Foetal Bovine Serum (FBS), 100 IU/mL penicillin, 100 μg/mL streptomycin, 2 mM L-glutamine and 0.4 μg/mL fungizone (RPMI$^+$ medium). RPMI-1640 medium was obtained from Cambrex (Verviers, Belgium). Supplements and antibiotics were all obtained from Life Technologies (Grand Island, NY, USA). Cell cultures were sustained in a 5% CO_2 humidified atmosphere at 37°C. The medium was refreshed every 3-4 days. Exponentially growing cells were used in the experiments.

6.2.2 Experimental design

6.2.2.1 Environmental conditions

HL60 cells at a concentration of 0.5 x 10^6 cells/ml (5 ml per experiment) were added to a falcon tube at atmospheric conditions at 2 different temperatures, respectively room temperature (rt) and 37ºC (waterbath). Control cultures (in conventional cell culture flasks) were cultured at a humidified atmosphere of 5% CO_2 and 37ºC in the incubator. After 4 and 24h, cells were analysed for their viability checking morphology (May Grünwald staining with light microscopy) and measuring the autofluorescence (AF) intensity (chapter 4.2.2) and DNA fragmentation with flow cytometry.

6.2.2.2 Materials

HL60 cells at a concentration of 1.0 x 10^6 cells/ml (500µl used per experiment) were plated in a 24 wells plate (Corning, Schiphol-Rijk, The Netherlands) in contact with different commonly used microchip materials. Slices of native silicon oxide (SiO_2, 1 cm^2), borosilicate glass (*e.g.,* microscope slides, 2 cm^2, Marienfeld, Germany), polydimethylsiloxane (2 cm^2, PDMS 10:1 ratio base to curing agent; Sylgard 184 kit Silicon Elastomer Dow Corning GmbH, Wiesbaden, Germany) and copper-coated silicon (1 cm^2, first a thin layer (thickness of 20 nm) of chromium was sputtered on a silicon wafer and then a layer (thickness 200nm) of copper sputtered on top) were placed in the corresponding wells and washed once with 100% ethanol (30 minutes incubation at room temperature). HL60 cells added to untreated wells (only polystyrene material) served as controls. After washing with PBS three times, slices of SiO_2, borosilicate glass, PDMS and Cu-coated silicon were incubated with 100% FBS and placed in the incubator for 20 minutes. HL60 cells were added and a sample was taken and analysed for the expression of Cyclin D1 and tTG with real-time reverse transcriptase PCR every day for three days. Furthermore, samples were analysed with flow cytometry to discriminate between the different stages of apoptosis with Annexin V in combination with PI, and to discriminate between the different stages of the cell cycle with the using PI.

6.2.3 RNA isolation and cDNA synthesis

Ribonucleic acid (RNA) isolation was performed using the QIAamp RNA Blood Mini Kit (QIAgen, Hilden, Germany) according to the manufacturer's instructions. The reaction mixture for the synthesis of complementary DNA (cDNA) contained 0.05 μg/μL random primers, 0.5 mM deoxyribonucleotide triphosphates (dNTP's), 10 mM dithiothreitol (DTT), 1 unit RNase inhibitor, 5 units mouse moloney murine leukemia virus (M-MLV) reverse transcriptase enzyme, 1 x First-Strand buffer and RNase-free water. All reagents were obtained from Invitrogen (Paisley, UK), with the exception of dNTP's (Amersham Biosciences, Freiburg, Germany) and RNase inhibitor (Roche, Mannheim, Germany). First, 20 μL of previously prepared RNA (1-3 μg) was heated for 5 min at 65°C to denature secondary RNA structures. Thereafter, 20 μL of reaction mixture was added to obtain a final volume of 40 μL. The programme for cDNA synthesis consisted of the following steps: 10 minutes at 25ºC, 60 minutes at 37ºC and 5 minutes at 95ºC.

6.2.4 Real-time RT-PCR

Expression of Cyclin D1 and tTG messenger RNA (mRNA) was determined using Taqman based real-time RT-PCR according to Heid *et al.*[29] The required primers and probes, reagents and equipment were obtained from Applied Biosystems (Foster City, CA, USA). A fragment of the Cyclin D1 gene was amplified using the forward primer 5'-CCGTCCATGCGGAAGATC-3' (Cycl.304F) and the reverse primer 5'-ATGGCCAGCGGGAAGAC-3' (Cycl.389R). The probe sequence 5'-CTTCTGTTCCTCGCAGACCTCCAGCAT -3' (Cycl.334TR) was labelled at the 5' end with the reporter fluorophore 6-carboxyfluorescein (FAM) and at the 3' end with the quencher fluorophore 6-carboxy-tetramethyl-rhodamine (TAMRA). A fragment of the tTG gene was amplified using a gene expression assay developed by Applied Biosystems (Hs00231133_m1). The probe was labelled at the 5'- end with the reporter fluorophore FAM and at the 3'- end with a non-fluorescent quencher. Quantification of the amount of cDNA that was put in the reaction was controlled using porphobilinogen deaminase (PBGD) as a household gene for reference. As a forward primer 5'-GGCATTGCGGCTGCAA-3' and as a reverse primer 5'-GGGTACCCACGCGAATCAC-3' were used. The probe sequence 5'-

CTCATCTTTGGGCTGTTTTCTTCCGCC-3' carried the VIC fluorophore as a reporter and the TAMRA fluorophore as a quencher. PCR reactions were performed in 96 wells plates in which 5 μL of cDNA was mixed with 20 μL of PCR mix. For Cyclin D1 and PBGD, the PCR mix consisted of 1 x Taqman Universal PCR Master Mix, primers, probe and RNase free water to obtain a final concentration of 300 nM for the primers and 200 nM for the probe. The PCR mix for tTG consisted of 1 x Taqman Universal PCR Master Mix, primers, probe and RNase free water to obtain a final concentration of 900 nM for the primers and 250 nM for the probe. Amplification reactions for Cyclin D1, tTG and PBGD were performed in separate wells in fourfold. The number of cycles that is needed for the amplification plot of every separate gene to reach the threshold is called the Ct-value (example is shown is figure 6-1) and this Ct value is needed for quantification of the amount of mRNA expression using the following formula (ΔΔCt method) (eq. 6-1 and 6-2):

$$(Ct_{\text{cyclin D1}} - Ct_{\text{PBGD}})_{\text{treated}} - (Ct_{\text{cyclin D1}} - Ct_{\text{PBGD}})_{\text{untreated}} \quad \text{eq. 6-1}$$

for measuring the Cyclin D1 expression

$$(Ct_{\text{tTG}} - Ct_{\text{PBGD}})_{\text{treated}} - (Ct_{\text{tTG}} - Ct_{\text{PBGD}})_{\text{untreated}} \quad \text{eq. 6-2}$$

for measuring the tTG expression

In these formula, 'treated' corresponds with the different microchip materials used, whereas 'untreated' corresponds with the culture plate only (polystyrene, PS), which serves as a control.

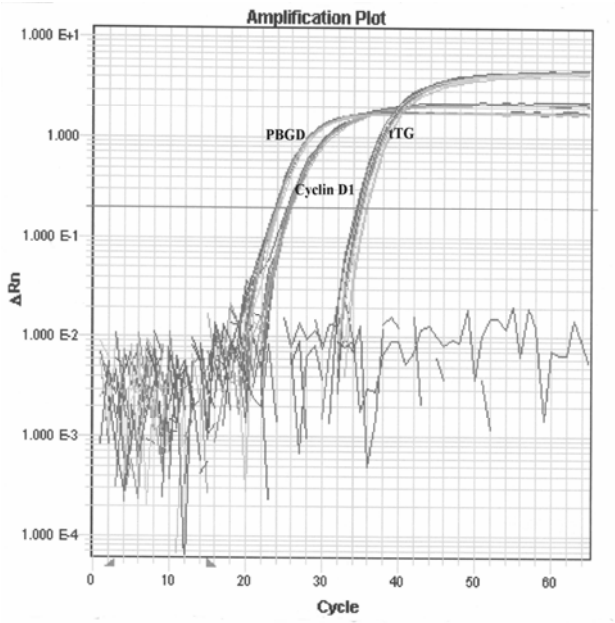

Figure 6-1. Amplification plot of HL60 cells. The amplification plot reflects the generation of the reporter dye (ΔRn) during amplification and is directly related to the formation of PCR products. Horizontal line refers to the threshold, which needs to be set in the linear phase of the plot. The number of cycles that is needed for the amplification plot of every separate gene to reach the threshold is called the Ct-value and can be read from the x-axis. First set of lines refers to the household gene PBGD, second to Cyclin D1, and the third to tTG.

6.2.5 Flow cytometry

6.2.5.1 The different stages of apoptosis with Annexin V and PI staining

Samples were collected and washed with PBS once. The pellet was resuspended in HEPES buffer containing 137 mM NaCl, 2.68 mM KCl, 10 mM HEPES, 1.7 mM $MgCl_2$, 25 mM Glucose and 2.5 mM $CaCl_2.H_2O$ (pH adjusted to 7.4). Annexin V (AV, FITC conjugate, generous gift from Dr. C. Reutelingsperger, PharmaTarget, Maastricht, the Netherlands) was added to give a final concentration of 0.01 μg/ml and samples were left in the dark for incubation for 20 minutes. Thereafter, PI was added (final concentration 0.2 μg/ml) and samples were immediately analysed with flow cytometry. Annexin V and PI fluorescence of individual cells were measured with a Beckman Coulter Cytomics FC500 flow cytometer. Excitation was elicited with the Argon laser at 488 nm and the fluorescence was measured using the FL-1 (Annexin V) and FL-3 (PI) channels.

6.2.5.2 Cell cycle analysis and DNA fragmentation with PI staining

Samples were collected and washed with PBS once. The pellet was resuspended in ice cold ethanol 70% for fixation. Samples were kept on ice for a minimal incubation time of 30 minutes. Samples were washed once with PBS and the pellet was resuspended in 1 ml PI stain consisting of 1.0 ml sodiumcitrate buffer (1 g/L; Merck, Darmstadt, Germany) containing 10 μg/ml propidium iodide (Sigma, St. Louis, MO, USA) and 0.1% (v/v) Triton X-100 (Merck). After incubation in the dark for 10 minutes, samples were analysed with flow cytometry. PI fluorescence was measured in the FL-3 channel.

6.2.5.3 Autofluorescence intensity

See chapter 4.2.4.

6.2.6 Statistical analysis

For the determination of the ratio apoptosis/proliferation, data represent results from four independently performed experiments. The cell proliferation marker Cyclin D1 as well as the apoptosis marker tTG were measured versus control (culture plate only, PS) and performed in fourfold. From these values the ratio apoptosis versus proliferation (R_{ap}) for every used microchip material was calculated. The 95% confidence interval (95% CI) was assessed and the p-values from these intervals were calculated and considered significant if they were 0.05 or less.

Flow cytometry data were analysed with the accessory CXP software and gates were set with several controls. In each sample, 10,000 events were measured. Results are shown as the mean ± standard deviation of the mean of 2 independently experiments performed in duplo. In the case of the AF intensity, the standard error of the mean (SEM) is shown.

6.3 Results and Discussion

Induction of apoptosis resulted in a reduced DNA stainability as measured with the Nicolleti method. This reduction in DNA stainability was the consequence of progressive loss of DNA from the cells due to the activation of endogenous endonuclease and the subsequent loss of molecular DNA from the cells. These apoptotic cells appeared as a sub-G0/G1 peak in the histogram, as cells were labelled with propidium iodide (Figure 6-2).

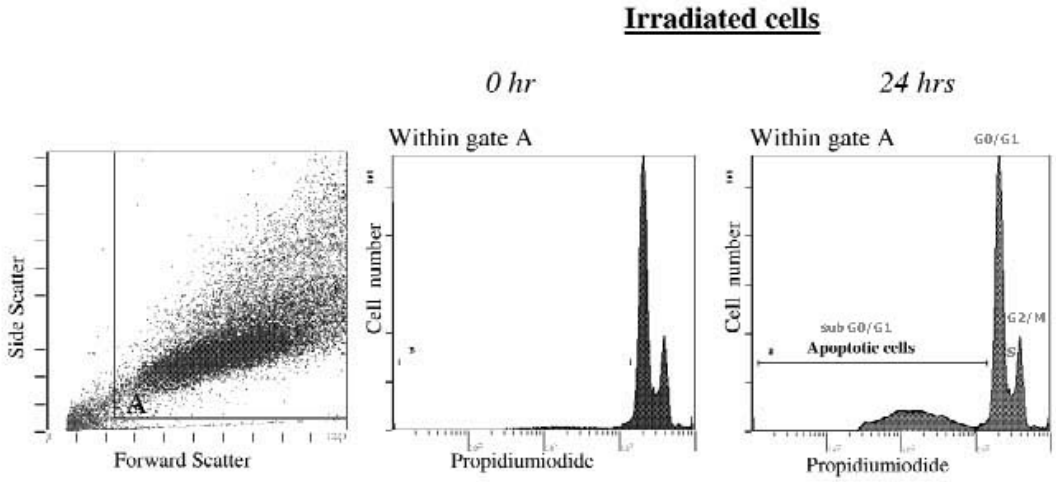

Figure 6-2. Flow cytometry of cellular DNA content: DNA fragmentation assay. Leukaemic white blood cells were irradiated to induce apoptosis and labelled with propidium iodide to stain the DNA. After 24h, a sub-G0/G1 peak appeared referring to apoptotic cells. G0/G1, S and G2/M indicate the different stages of the cell cycle. Published with the permission of Vermes *et al.* [28]

HL60 cells cultured at atmospheric pressure at room temperature showed an increase in the amount of apoptotic cells after 24h. This increase in DNA fragmentation was not obvious in cells cultured at 37ºC (Figure 6-3). These results were confirmed by measuring the autofluorescence intensity, in which HL60 cells cultured at atmospheric pressure and room temperature showed the largest decrease in AF intensity compared with control HL60 cells which were cultured in a humidified atmosphere of 5% CO_2 and 37ºC in the incubator (Figure 6-4).

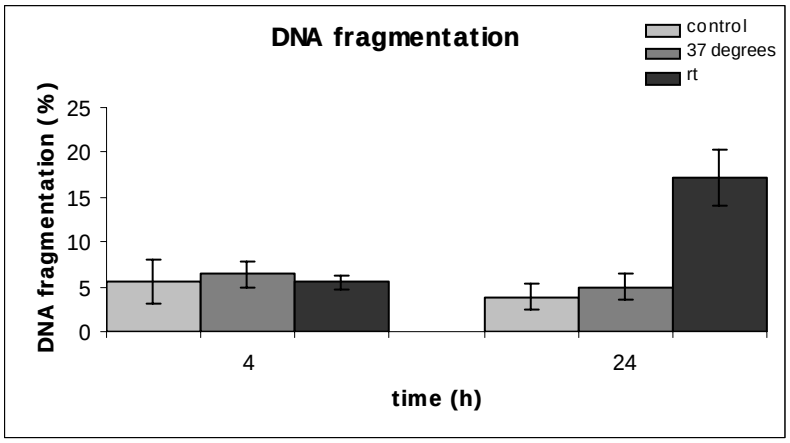

Figure 6-3. DNA fragmentation assay of HL60 cells cultured at atmospheric CO_2 either at room temperature (rt) or 37ºC. HL60 cells cultured in a humidified atmosphere of 5% CO_2 and 37ºC served as control. This figure represents data of two experiments performed in duplo for every time point and the mean ± standard deviation is shown.

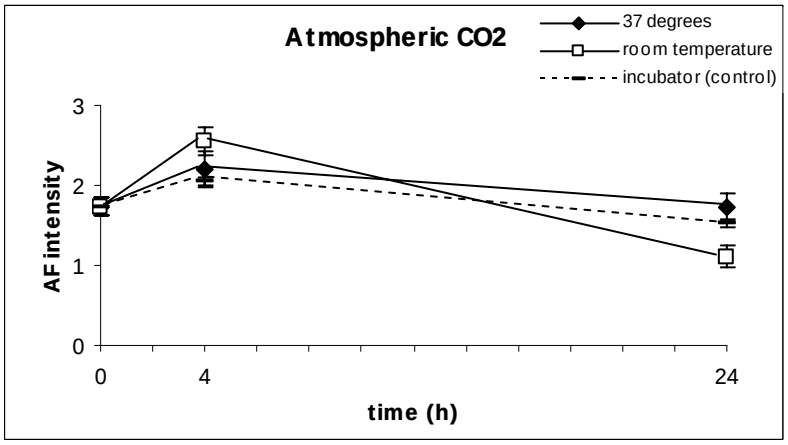

Figure 6-4. AF intensity of HL60 cells cultured at atmospheric CO_2 either at room temperature (rt) or 37ºC. HL60 cells cultured in a humidified atmosphere of 5% CO_2 and 37ºC served as control. The AF intensity defines the ratio of the mean fluorescence of the non-viable population compared to the mean fluorescence of the viable population, as described in chapter 4. This figure represents data of two experiments performed in duplo for every time point and the mean ± standard error of the mean is shown.

Furthermore, HL60 cells cultured at atmospheric conditions and room temperature appeared as shrunken cells with condensed chromatin and membrane blebbing (apoptotic bodies), all consistent with apoptosis (Figure 6-5).

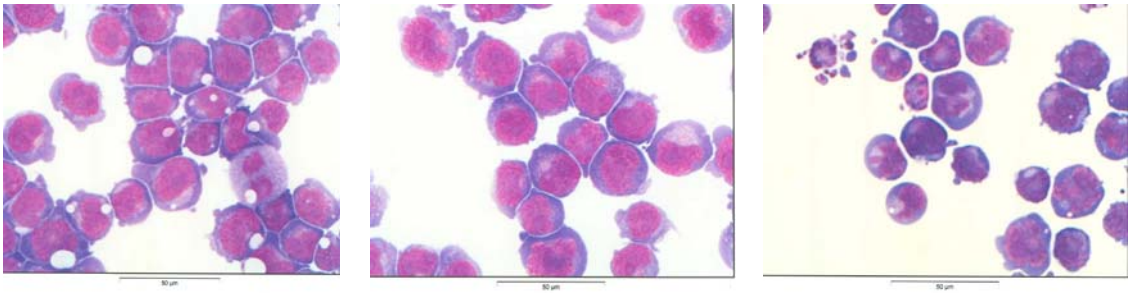

Control (humidified atmosphere) | **atmospheric CO_2 37ºC** | **atmospheric CO_2 room temperature**

Figure 6-5. Light microscopy of HL60 cells cultured under different conditions, *e.g.*, humidified atmosphere or atmospheric CO_2 at either 37ºC or room temperature after 24h. HL60 cells were stained with May Grünwald Giemsa staining.

Therefore, a difference in temperature induces apoptosis when culturing HL60 cells outside the incubator. Shimura *et al.*[30,31] reported that HL60 cells underwent apoptosis when exposed to room temperature. As demonstrated with the DNA fragmentation assay, the percentage of apoptotic cells was much higher after 24h than demonstrated in this study. Though during passaging the response of HL60 cells to the difference in temperature (*e.g.*, room temperature) becomes more prominent, so the HL60 cells used in this study probably had a lower passage number. Furthermore, our experiments were performed at atmospheric CO_2 (lid open), whereas Shimura's experiments were performed with the lid tightly shut. As stated by Shimura *et al.* the difference in oxygen consumption at room temperature generated reactive oxygen species, which might be a causative factor for the rt-induced apoptosis. Culturing cells as atmospheric CO_2 will raise the pH to 8, which will lead to impaired cell growth.[32,33] However, the first 24h cells were able to grow at maximal rate, so as also demonstrated in figure 6-3 cell viability will not be harmed. HL60 cells cultured at atmospheric CO_2 and 37ºC showed no increase in DNA fragmentation in comparison with control cells cultured in a humidified atmosphere. If long cell culture outside the incubator is necessary, then a specific medium (*e.g.*, CO_2 independent medium) is required to overcome changes in pH which will negatively influence cell growth. Besides variations in environmental conditions, the choice of chip material can have an effect on the viability of mammalian cells and therefore can influence the outcome of cellular studies. Figure 6-6 shows that HL60 cells in contact with native SiO_2 resulted in a $R_{ap} > 1$, meaning apoptosis, during the first 24h of incubation. However, in time R_{ap} turned towards proliferation. Pre-coating of native SiO_2 with 100% FBS benefited the

proliferation statistically. Borosilicate glass (microscope slides) did not affect the R_{ap}, which was comparable with conventional cell culture equipment (R_{ap} = 1, dashed horizontal line). Pre-coated borosilicate glass with 100% FBS showed proliferation after 48h. The best and stable proliferative results were obtained when HL60 cells were in contact with pre-coated PDMS. Copper-coated silicon demonstrated to be toxic for HL60 cells, causing extreme DNA damage, therefore we were unable to measure the R_{ap}.

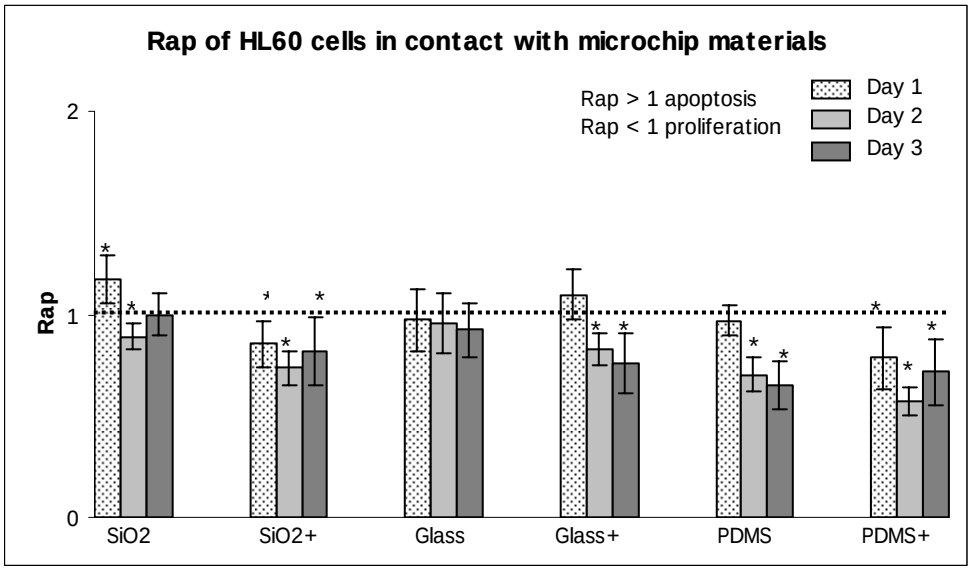

Figure 6-6. The apoptosis/proliferation ratio (R_{ap}) of HL60 cells in contact with microchip materials, measured with real-time RT-PCR. Dashed line refers to the control sample, meaning culture plate only (PS). * = statistical significant, $p \leq 0.05$. The figure represents data from 4 experiments performed in fourfold. Standard error bars reflect the 95% confidence interval. The symbol + behind the microchip materials refers to pre-coating with 100% FBS.

In order to determine the value of these results, flow cytometry assays were performed in which the effect of the different microchip materials on the distribution through the apoptotic cascade and the cell cycle was demonstrated. During the early stages of the apoptotic process, phosphatidyl serine, which is normally present on the inner leaflet of the cell membrane, flip-flops to the outer leaflet of the cell membrane, where annexin V can bind specifically. Together with PI, it is possible to discriminate between the different stages of the apoptotic cascade. Viable cells, which are AV^-PI^-, early apoptotic cells (AV^+PI^-), late apoptotic cells (AV^+PI^+), and necrotic cells (AV^-PI^+). Figure 6-7A shows that for all microchip materials used, with the exception of Cu, more than 90% of the HL60 cells were still viable after 72 hours. Therefore the slight differences seen in the

discrimination between the different stages of the apoptotic cascade (Figure 6-7B) were negligible and it can be concluded that the different microchip materials used, had no effect on the apoptotic process, in comparison with conventional cell culture. Nevertheless, for the Cu-coated silicon, over 90% decreased viability was demonstrated, thus confirming its toxicity. Copper is a potential useful material for electrodes to perform electrophysiological measurements.

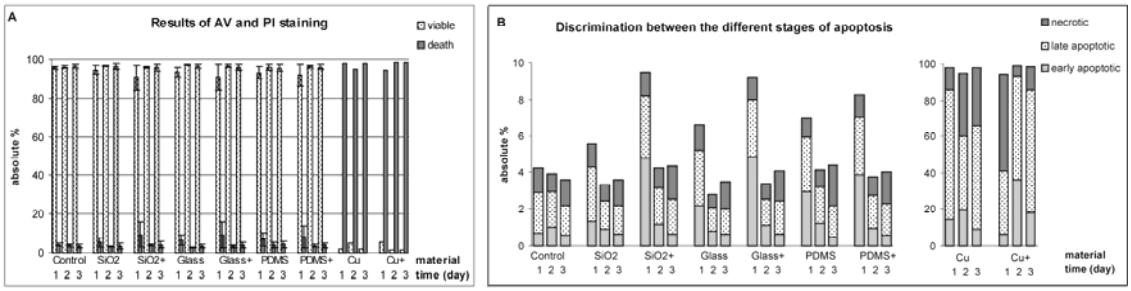

Figure 6-7. Discrimination between the different stages of the apoptotic cascade with Annexin V and PI staining. **(A)** Discrimination between viable and death population. **(B)** The 'death' population showed in A subdivided in the different stages of the apoptotic cascade. The figure represents data from 2 individual experiments and mean ± standard deviation is shown in figure 6-6A. The results obtained with Cu are from one individual experiment.

In order to analyze the effect of the microchip materials on the different phases of the cell cycle, PI was added to fixed-permeablized cells and the fluorescent intensity of the PI determined the amount of DNA present. G0/G1 phase cells have a normal amount of DNA (2n). In the S-phase of the cell cycle the DNA is replicated and therefore these cells have a DNA amount between 2n and 4n. Cells which are in the G2/M phase have a double amount of DNA (4n). As a result of the activation of endonucleases during the late stages of the apoptotic cascade, apoptotic cells exhibit a low DNA stainability (below the G0/G1 region) resulting in a sub G0/G1 peak (Figure 6-2). Figure 6-8 shows that the distribution in every phase of the cell cycle as for the apoptotic fraction for HL60 cells in contact with SiO_2, borosilicate glass and PDMS was comparable with conventional cell culture equipment (*e.g.,* control). The apoptotic fraction (Figure 6-8D) showed slightly increased values compared to the percentages shown in Figure 6-7B (late apoptotic and necrotic), though these differences were not significant. HL60 cells in contact with Cu demonstrated an increased apoptotic fraction in comparison to the other applied microchip materials.

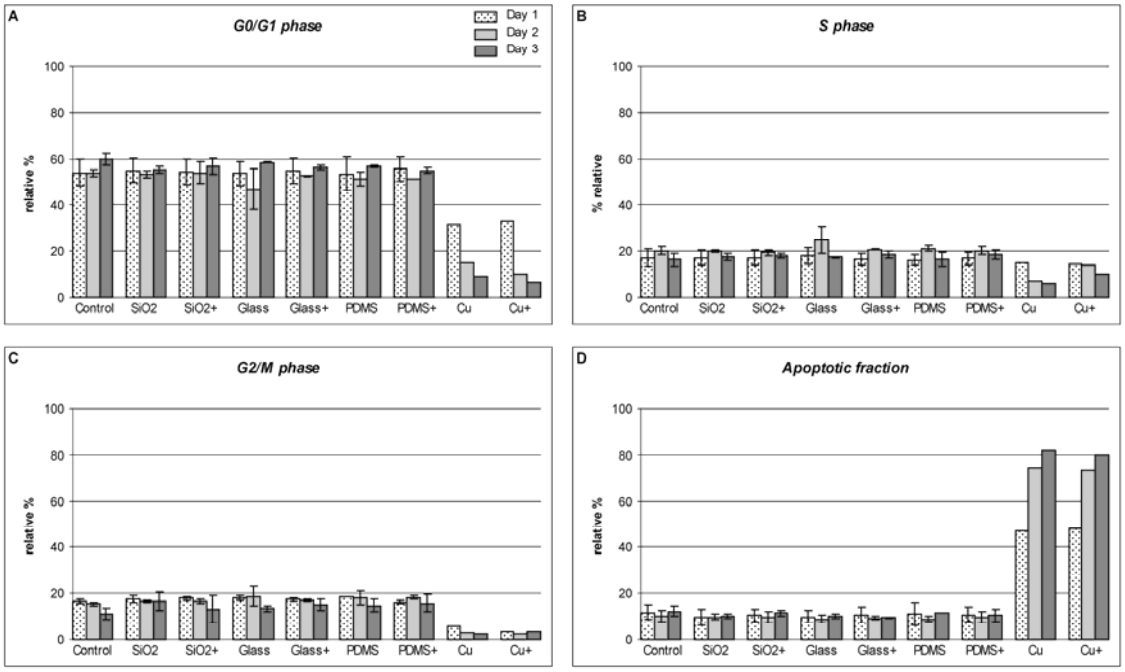

Figure 6-8. Discrimination between the different phases of the cell cycle and the apoptotic fraction with PI staining of fixed-permeabilized HL60 cells. **(A)** G0/G1 phase. **(B)** S-phase. **(C)** G2/M phase. **(D)** Apoptotic fraction. The figure represents data from 2 individual experiments and mean ± standard deviation is shown. The results obtained with Cu are from one individual experiment.

In this study different microchip materials were used with specific and modified (*e.g.*, serum coating) surface characteristics. Native SiO_2 and borosilicate glass are both hydrophilic, whereas PDMS is hydrophobic. Sasaki *et al.*[34] studied the interaction of the proteins, supplemented in cell growth media, with a hydrophobic and hydrophilic modificated silicon surface. The hydrophobic surface absorbed more protein than the hydrophilic surface, thus becoming relatively more hydrophilic upon protein absorption, whereas the hydrophilic surface became relatively hydrophobic. Though albumin is known to adsorb to both hydrophilic and hydrophobic surfaces, different modes of interactions play a role. Albumin absorbed onto hydrophobic surfaces, rapidly denatures and adheres strongly through van der Waals forces. Hydrophilic surfaces also adsorb protein, but the protein maintains its native structure in such a way that surface mobility and desorption is facile. Protein-modified hydrophobic surfaces are therefore good surfaces for cell attachment and cell growth. However, for this study, cells in suspension were used. Though adherence was not an issue, due to gravity (static experimental set-up), the HL60 cells interacted with their underlying surface. Incubation with FBS might form a thicker protein film on the hydrophobic PDMS

layer, making it relatively more hydrophilic. This alteration in surface characteristics might be the reason why HL60 cells showed a higher proliferation rate in contact with PDMS, though protein thickness was not measured in this study. Furthermore, PDMS is highly permeable to gases, biocompatible and several microfluidic systems have already been developed in PDMS for cellular based assays.[35] Moreover, the results obtained upon analyzing the viability using Annexin V in combination with PI and the cell cycle measurements, demonstrated that the microchip materials used, irrespective of their surface chemistry, were all suitable for HL60 cells. The assays here presented all measure different parameters which have an effect on the viability. This could be a reason why the beneficial results of pre-coating with FBS were not demonstrated with the flow cytometry assays. Furthermore, other microchip materials were analysed for their R_{ap} (fused silica, pyrex, borofloat (Figure 6-9A), SiO_2 dry (*e.g.*, dry etched oxide layer of 300nm), PECVD+SiO_2 and PECVD+SiN (Figure 6-9B)) and all shown suitable for HL60 cells and pre-coating with 100% FBS benefited the proliferation.

A

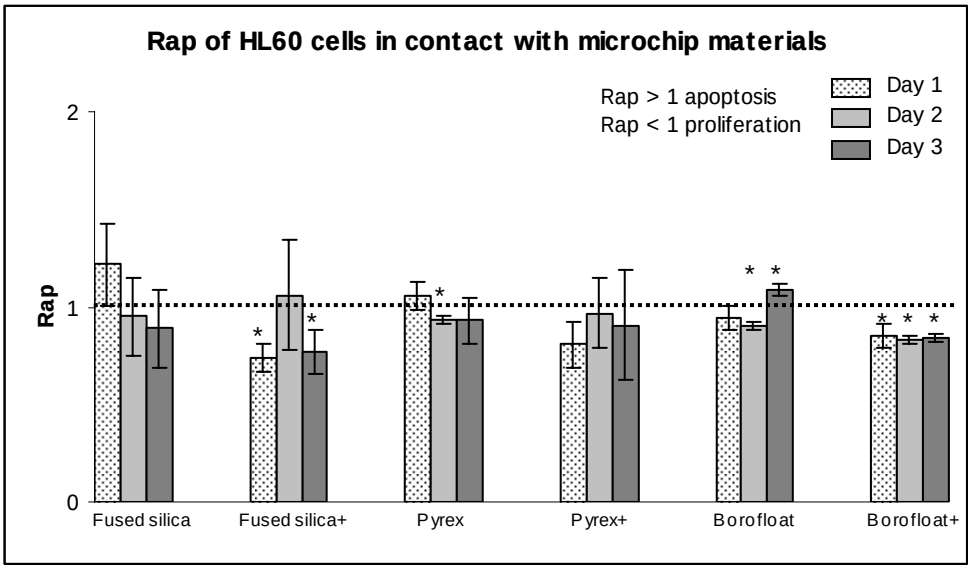

B

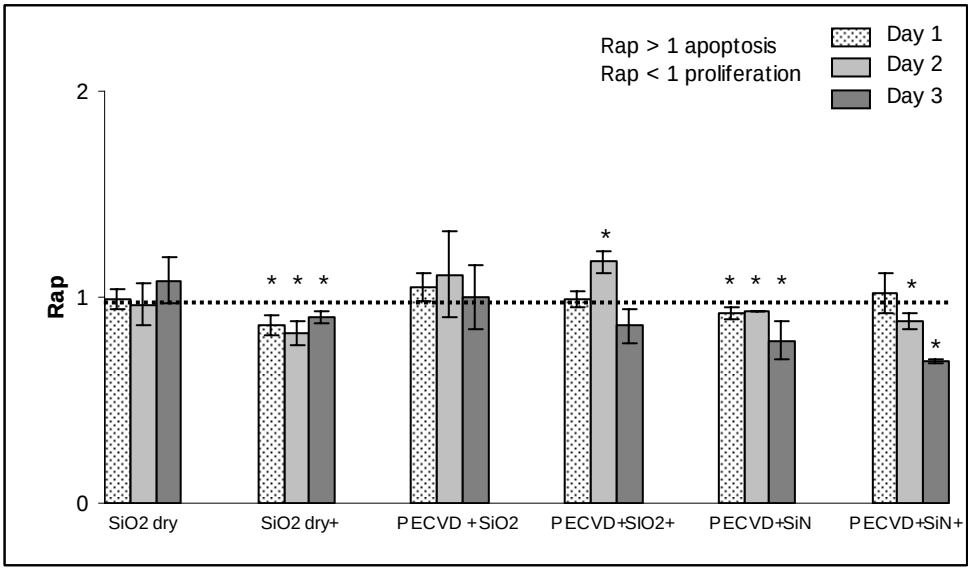

Figure 6-9. The apoptosis/proliferation ratio (R_{ap}) of HL60 cells in contact with microchip materials, measured with real-time RT-PCR. Dashed line refers to the control sample, meaning culture plate only (PS). * = statistical significant, $p \leq 0.05$. The figure represents data from one representative experiment performed in fourfold. Standard error bars reflect the 95% confidence interval. The symbol + behind the microchip materials refers to pre-coating with 100% FBS.

The Cu-coated silicon demonstrated toxic for HL60 cells, as referred in literature.[36,37] Our hypothesis is that the effect of microchip materials is more pronounced when using adherent cells. Patterning the PDMS with different substrates such as fibronectin and collagen or modifying the surface to render it hydrophilic (*e.g.*, oxygen plasma), makes this polymer useful for adherent cell studies.[38-40] Whitesides *et al.*[41] have already investigated the influence of the composition of PDMS on the attachment and growth of different adherent cell lines, to highlight the importance of examining the role of the surface chemistry of materials used for growing cells. The attachment and growth characteristics of cells differ for different cell types, cultured in similar environments. Therefore, in future experiments using adherent cell lines, first their viability (*e.g.*, attachment and growth characteristics) will have to be analysed. In conclusion, this study has demonstrated that when performing cell analyses with HL60 cells in lab-on-a-chip devices, the choice of material plays a minor role. Although Cu-coated silicon demonstrated toxic for HL60 cells. Coating the microchip material with FBS, benefited the proliferation, however, this advantageous effect was not seen in cell cycle measurements and viability experiments with Annexin V and PI, which

showed comparable results with conventional cell culture equipment (PS). Furthermore, changes in environmental conditions such as temperature and CO_2 needed to be avoided.

6.4 Conclusion

The enormous knowledge and practice in the field of micro- and nanotechnologies led to the transfer of many classical cell-based assays to lab-on-a-chip devices which yield a huge profit. However, it has to be kept in mind that this chip environment is quite different and can therefore influence the viability of mammalian cells negatively, producing misleading results. Environmental changes in temperature and CO_2 must be avoided. The choice of microchip material did not affect the cell viability of cells in suspension, with the exception of Cu. Nevertheless, the final chip design and experimental settings (*e.g.*, flow rate, cell handling) can still play a very important role. So, before performing any sophisticated cell analyses on chip, good control experiments have to be performed to ensure the validity of the obtained results.

6.5 Acknowledgements

Technical assistance of Jan van Nieuwkasteele and Johan Bomer is gratefully acknowledged.

6.6 References

1. Andersson H, van den Berg A. Microtechnologies and nanotechnologies for single-cell analysis. *Curr Opin Biotechnol* 2004; **15**: 44-49.
2. Lu X, Huang W, Wang Z, Cheng J. Recent developments in single-cell analysis. *Anal Chim Acta* 2004; **510**: 127-138.
3. Wheeler AR, Throndset WR, Whelan RJ, Leach AM, *et al.* Microfluidic device for single-cell analysis. *Anal Chem* 2003; **75**: 3581-3586.

4. Munce N, Li J, Herman P, Lilge L. Single cell analysis on a microchip platform using optical tweezers and optical scissors. *Proc Microfluidics BioMEMS and Medical Microsystems* 2003; **SPIE 4982**: 28-36.
5. Irimia D, Tompkins RG, Toner M. Single-cell chemical lysis in picoliter-scale closed volumes using a microfabricated device. *Anal Chem* 2004; 76: 6137-6143.
6. Munce NR, Li J, Herman PR, Lilge L. Microfabricated system for parallel single-cell capillary electrophoresis. *Anal Chem* 2004; **76**: 4983-4989.
7. Buhlmann C, Preckel T, Chan S, Luedke G, Valer M. A new tool for routine testing of cellular protein expression: Integration of cell staining and analysis of protein expression on a microfluidic chip-based system. *J Biomol Tech* 2003; **14**: 119-127.
8. Wolff A, Perch-Nielsen IR, Larsen UD, Friss P, *et al.* Integrating advanced functionality in a microfabricated high-throughput fluorescent-activated cell sorter. *Lab Chip* 2003; **3**: 22-27.
9. Furdui VI, Kariuki JK, Harrison DJ. Microfabricated electrolysis pump system for isolating rare cells in blood. *J Micromech Microengin* 2003; **13**: 164-170.
10. Son SU, Choi YH, Lee SS. Micro-cell counter using photoconductance of boron diffused resistor (BDR). *Sens Actuators Phys* 2004; **111**: 100-106.
11. Pantoja R, Nagarah JM, Starace DM, Melosh NA, *et al.* Silicon chip-based patch-clamp electrodes integrated with PDMS microfluidics. *Biosens Bioelectron* 2004; **20**: 509-517.
12. Huang Y, Sekhon NS, Borninski J, Chen N, Rubinsky B. Instantaneous, quantitative single-cell viability assessment by electrical evaluation of cell membrane integrity with microfabricated devices. *Sens Actuators Phys* 2003; **105**: 31-39.
13. Li PCH, de Camprieu L, Cai J, Sangar M. Transport, retention and fluorescent measurement of single biological cells studied in microfluidic chips. *Lab Chip* 2004; **4**: 174-180.
14. Potter SM, DeMarse TB. A new approach to neural cell culture for long-term studies. *J Neurosci Methods* 2001; **110**: 17-24.
15. Viravaidya K, Shuler ML. Incorporation of 3T3-L1 cells to mimic bioaccumulation in a microscale cell culture analog device for toxicity studies. *Biotechnol Prog* 2004; **20**: 590-597.

16. Tabuchi M, Baba Y. Self-contained on-chip cell culture and pretreatment system. *J Proteome Res* 2004; **3**: 871-877.
17. Tourovskaia A, Figueroa-Masot X, Folch A. Differentiation-on-a-chip: A microfluidic platform for long-term cell culture studies. *Lab Chip* 2005; **5**: 14-19.
18. Blau AW, Ziegler CMJ. Prototype of a novel autonomous perfusion chamber for long-term culturing and in situ investigation of various cell types. *Biochem Biophys Methods* 2001; **50**: 15-27.
19. Davidsson R, Boketoft A, Bristulf J, Kotarsky K, *et al.* Developments toward a microfluidic system for long-term monitoring of dynamic cellular events in immobilized human cells. *Anal Chem* 2004; **76**: 4715-4720.
20. Prokop A, Prokop Z, Schaffer D, Kozlov E, *et al.* NanoLiterBioReactor: Long-term mammalian cell culture at nanofabricated scale. *Biomed Microdevices* 2004; **6**: 325-339.
21. Ho C, Mou T, Chiang P, Weng C, Chow N. Mini chamber system for long-term maintenance and observation of cultured cells. *Biotechniques* 2005; **38**: 267-273.
22. Munoz-Pinedo C, Green DR, van den Berg A. Confocal restricted-height imaging of suspension cells (CRISC) in a PDMS microdevice during apoptosis. *Lab Chip* 2005; **5**: 628-633.
23. Nicoletti I, Migliorati G, Pagliacci MC, Grignani F, Riccardi C. A rapid and simple method for measuring thymocyte apoptosis by propidium iodide staining and flow cytometry. *J Immunol Meth* 1991; **139**: 271-279.
24. Stacey DW. Cyclin D1 serves as a cell cycle regulatory switch in actively proliferating cells. *Curr Opin Cell Biol* 2003; **15**: 158-163.
25. Volokhina EB, Hulshof R, Haanen C, Vermes I. Tissue transglutaminase mRNA expression in apoptotic cell death. *Apoptosis* 2003; **8**: 673-679.
26. Darzynkiewicz Z, Bruno S, Del Bino G, Gorczyca W, *et al.* Features of apoptotic cells measured by flow cytometry. *Cytometry* 1992; **13**: 795-808.
27. Darzynkiewicz Z, Bedner E, Smolewski P. Flow cytometry in analysis of cell cycle and apoptosis. *Sem Hematol* 2001; **38**: 179-193.
28. Vermes I, Haanen C, Reutelingsperger C. Flow cytometry of apoptotic cell death. *J Immunol Meth* 2000; **243**: 167-190.
29. Heid CA, Stevens J, Livak KJ, Williams PM. Real time quantitative PCR. *Genome Res* 1996; **6**: 986-994.

30. Shimura M, Ishizaka Y, Yuo A, Hatake K, *et al.* Characterization of room temperature induced apoptosis in HL-60. *FEBS Lett* 1997; **417**: 379-384.
31. Shimura M, Okuma E, Yuo A, Sasaki T, *et al.* Room temperature-induced apoptosis of Jurkat cells sensitive to both caspase-1 and caspase-3 inhibitors. *Cancer Lett* 1998; **132**: 7-16.
32. Mackenzie CG, Mackenzie JB, Beck P. The effect of pH on cell growth, protein synthesis, and lipid-rich particles of cultured mammalian cells. *J Biophys Biochem Cyto* 1961; **9**: 141-156.
33. Eagle H. Buffering combinations for mammalian cell culture. *Science* 1971; **174**: 500-503.
34. Sasaki DY, Cox JD, Follsteadt SC, Curry MS, *et al.* Glial cell adhesion and protein adsorption on SAM coated semiconductor and glass surfaces of a microfluidic structure. *Proc SPIE* 2001; **4265**: 152-163.
35. McDonald JC, Duffy DC, Anderson JR, Chiu DT, *et al.* Fabrication of microfluidic systems in poly(dimethylsiloxane). *Electrophoresis* 2000; **21**: 27-40.
36. Singh RP, Kumar S, Nada R, Prasad R. Evaluation of copper toxicity in isolated human peripheral blood mononuclear cells and it's attenuation by zinc: ex vivo. *Mol Cell Biochem* 2006; **282**: 13-21.
37. Bogner E, Dominizi K, Hagl P, Bertagnolli E, *et al.* Bridging the gap – Biocompatibility of microelectronic materials. *Acta Biomaterialia* 2006; **2**: 229-237.
38. Folch A, Toner M. Cellular micorpatterns on biocompatible materials. *Biotechnol Prog* 1998; **14**: 388-392.
39. Donzel C, Geissler M, Bernard A, Wolf H, *et al.* Hydrophilic poly(dimethylsiloxane) stamps for microcontact printing. *Adv Mater* 2001; **13**: 1164-1167.
40. Matsubara Y, Murakami Y, Kobayashi M, Morita Y, Tamiya E. Application of on-chip cell cultures for the detection of allergic response. B*iosens Bioelectron* 2004; **19**: 741-747.
41. Lee JN, Jiang X, Ryan D, Whitesides GM. Compatibility of mammalian cells on surfaces of poly(dimethylsiloxane). *Langmuir* 2004; **20**: 11684-11691.

7

Creating a microfluidic platform for measuring apoptosis

An overview

For performing sophisticated cell analysis on chip, the microfluidic device used and the experimental set-up used, both have to meet certain requirements. On the one hand, they should enable the analysis of the subject of interest, and on the other hand the cells should not be negatively influenced by the device or experimental set-up. Our ultimate goal is to analyse the apoptotic outcome of various drugs using different adherent cell types. The research in this chapter will investigate which microfluidic device and experimental set-up are best suited to meet our goal in terms of what do we need to measure apoptosis (e.g., detection, chip design, flow of apoptotic drugs) and what do the cells need (e.g., nutrients, oxygen, materials the cells can attach and grow on).

7.1 Introduction

This chapter focuses on the development of a microfluidic platform to measure apoptotic cell death in the presence of different drugs and monitor the apoptotic cascade in real-time. This device will provide us with fast and efficient analysis of the effects of various (new) drugs on many different cells or co-cultures of cells, with the possibility of using a patient's own cells. Furthermore, as stated in chapter 5, for postmenopausal women or breast cancer patients measuring the balance between proliferation and apoptosis on chip using a patient's own cells offers the possibility to make an optimal selection of cytotoxic or hormonal treatment.
Various requirements need to be implemented in the microfluidic platform to be able to perform sophisticated cell analysis on chip, in our case studying the effects of various drugs on the apoptotic pathway. Firstly, as adherent cells will be used, long-term cell culture is necessary. Secondly, the microfluidic chip has to be connected to a flow system to provide the cells with fresh culture medium and add various drugs. Thirdly, the chip needs to be mounted on a microscope stage to be able to monitor the process in real-time. Fourth, as biological materials, such as cells and culture medium, are used, all things have to be easy to clean and sterilize or preferably the whole microfluidic set-up should consist of disposables. In the next sections, these different requirements will be discussed, as well as the different microfluidic platforms that were analysed.

7.2 Long-term cell culture

It is not until recently that papers about long-term cell culture on chip appeared and there are still numerous challenges. In this area, long-term cell culture requires stringent cell maintenance of, for example, the pH and gas- and nutrient concentration. Whereas in conventional cell culture, the medium is refreshed twice a week, microfluidic cell cultures cannot be treated as static because the average volume of medium per cell is much smaller and therefore a continuous flow of nutrients is necessary. Furthermore, cells are kept in a humidified atmosphere of 5% CO_2 and 37ºC in an incubator. Hence, for culturing adherent cells in a microfluidic device, cells have to attach to the used material, in order to grow,

which needs flow of medium to supply the cells with the right concentrations of nutrients and gases, creating a platform where cell viability is maintained.[1] So, the biocompatibility of the materials used has to be analysed.[2-4] The very large surface area to volume (SAV) ratios existing in microchannels, is very advantageous because of the efficient mass transport of gases via diffusion to and from cells, assuming the microchannel is made of a gas permeable polymer.[5] Therefore, all devices designed so far have used the silicone elastomer poly(dimethylsiloxane) (PDMS), sometimes in combination with other materials, such as glass or silicon, for long-term cell culture. In most cases the material to which the cells attach, has been modified (for example with oxygen plasma) and/or pre-coated with proteins to promote stable cell adhesion under flow conditions and influence cellular function.[2,3] PDMS is mostly used for its biocompatibility and high gas permeability.[6] Furthermore, PDMS can be molded at low temperatures and by using rapid prototyping, chemists and biologists working with cells can easily and quickly fabricate cheap microfluidic devices.[7] PDMS is highly hydrophobic in its native state, but can be rendered hydrophilic by oxygen plasma, which causes a conversion of PDMS to oxidized forms of silicone, likely to include silanols (Si-OH).[2] Furthermore, oxygen plasma-treated PDMS (Ox-PDMS) becomes somewhat roughened compared to native PDMS which has a relatively smooth surface. Cell growth on native PDMS is completely inhibited, whereas Ox-PDMS is supportive of cell growth, comparable with other hydrophilic surfaces, such as tissue culture polystyrene used in conventional cell culture.[2,3] On the other hand, under flow conditions, hydrophobic PDMS promotes cell adhesion and fouling of the microfluidic device.[2] Moreover, the cell seeding density as well as the final chip design will influence the morphology of the cells.[4,8]

Tourovskaia *et al.*[9] were some of the first to describe a microfluidic system which maintained cell cultures for more than 2 weeks using gravitational flow. The microfluidic device was made in PDMS and sealed with a glass substrate, which consisted of cell-adhesive and cell-repellent micropatterns to produce cellular microstructures within the microfluidic environment. The murine skeletal muscle cell line C2C12 was successfully cultured and differentiated within this device. Besides gravitational flow for medium delivery, Leclerc *et al.*[10-12] used a perfusion system composed of a culture medium tank connected to a peristaltic pump to deliver the medium to the cells. The medium in the tank was refreshed every 2-3

days. Furthermore, the device included an oxygen chamber separated from the microfluidic channel network by a thin wall. With the help of the oxygen chamber, an increase in hepatic cell number was achieved without reducing the activity per single cell. The same device, though without the oxygen chamber, was also used to culture osteoblasts for bone tissue engineering.[13] Both the 3-D microstructure as well as performing the cell culture under dynamic conditions demonstrated an increase in the activity of the osteoblast cells. However, the cell number was not increased, probably due to the low flow rates, which did not provide the cells with proper nutrition as compared to conventional Petri dishes. In the examples described above, a conventional incubator was still necessary. To circumvent the need for external media and a CO_2 supply, Futai *et al.*[8] developed a microfluidic chip which combined Braille display modules, to actuate flow delivery and complete chip mounting, with an integrated transparent heater, hence favouring real-time monitoring of cells. Furthermore, basal cell culture media was modified to promote long-term cell culture outside the incubator. For C2C12 murine myeloblasts and MC3T3-E1 murine osteoblast, cell proliferation and myotube formation were recorded successfully.

To approach the *in vivo* situation, cells need to be cultured in 3-D. 3-D cell culture affects the behaviour of cells such as receptors, gene expression profiles and other biological activities more than in 2-D cell culture.[14] Moreover, cellular behaviour is significantly different from culture dimensions and cells can even lose their specific functions under standard 2-D cell culture conditions, as is the case for primary hepatocytes. Microfabrication technology can contribute to the fundamental understanding of cell biology by creating *in vivo*-like micro-environments and accelerating the outputs required for analysing complicated cellular behaviour, with high potency for tissue engineering. For 3-D microfluidic cell culture, different approaches were described, such as spheroids[15], hydrogels[16] or peptide scaffolds.[14] Spheroids are spherically symmetric aggregates in which cells are in close contact with each other, similar to the conditions in tissues. Torisawa *et al.*[15] developed a spheroid chip that consisted of on array of PDMS multichannels and wells on silicon. The medium within the channel was changed by withdrawing fluid from the outlet by using a micropipette. During the cell culture process, the spheroid chip was placed in a culture dish and incubated at 37ºC in a humidified atmosphere containing 5% CO_2. Viability assays were performed by measuring the oxygen

concentration. A lower oxygen concentration was measured around the microholes due to cellular respiration. Within this device, liver-specific functions could be preserved for 2 weeks. So maintaining the 3-D nature of the cells, this device can provide information on cellular activity and drug sensitivity under *in-vivo* like conditions, and therefore will be suitable in the development of a drug screening system for cancer and liver cells. Frisk *et al.*[16] used an extracellular matrix gel to embed, anchor, culture and study cells in 3-D, to resemble the *in vivo* situation closely, in which the extracellular matrix normally provides the tissue with support. Furthermore, the extracellular matrix is important for control of cell proliferation, motility and migration. COS 7 foetal monkey kidney cells were mixed with the extracellular matrix (*e.g.*, MATRIGEL) and added to the microchamber, which consisted of a microstructured silicon channel with pillars, which increased the stability of the gel allowing high surface flow rates without surface modifications. The microfluidic device was sealed with a glass cover for optical imaging of the cells. By increasing the temperature to 37ºC, the matrigel slowly polymerized, creating a flow path owing to a decrease in the volume of the gel. During cultivation the chip was placed in a petridish containing cell culture medium to allow for diffusion through the inlet and outlet ports into the chamber. Fresh culture medium was also perfused through the chamber once or twice a day, resulting in a complete exchange of fluids, though perfusion was slow as compared to 2-D cell culture. Cells were alive and viable after up to 6 days of incubation within the chamber, showing an increase in cell density. Kim *et al.*[14] used a peptide scaffold (*e.g.*, Puramatrix) to immobilize and culture liver cells in 3-D. In contact with culture media, the gel slowly polymerized from the liquid to the gel state, thereby self-assembling into a 3-D transparent scaffold which had a nanometer-scale fibrous structure. Hence, a linear concentration gradient existed across the peptide scaffold, enabling pharmacokinetic studies.

7.3 Flow

For long-term cell culture, as stated above, the continuous flow of medium is necessary to provide the attached cells with the appropriate amount of nutrients and oxygen, and to remove waste products. The applied flow rate will expose the cells to mechanical forces, such as the shear stress. Hence, for sophisticated cell

analysis, the cells need to be in contact with sufficient nutrients and oxygen and the necessary flow rate for this must not harm the cells, for example, cause the detachment of the cells. Furthermore, for analysing the effects of various drugs, it has to be ascertained that at the start of the experiment the set flow rate or a possible lack of nutrients and oxygen will not influence the outcome negatively. Nutrients and oxygen supply and the effect of shear stress will be discussed in the following section. Generally, the flow in microfluidic devices is laminar (low < 2300 Reynolds number) and viscous forces dominate.[17]

7.3.1 Nutrients and oxygen supply

Oxygen is a very important nutrient for cell culture, and its lower solubility in culture media makes it imperative that it is constantly monitored and supplied.[18] Today the oxygen concentration is strictly controlled in conventional incubators using conventional cell culture equipment. PDMS is highly permeable for gases[6], and because of this property passive permeation of oxygen through the PDMS (a thickness in the range of hundreds of μm to a few mm) is generally assumed to be sufficient for supplying the necessary amounts of oxygen to the cells. Therefore the oxygen concentration within microfluidic channels is not quantified. Furthermore, native PDMS is highly oxygen permeable, but this permeability is subject to change when proteins are absorbed on it or when the surface is modified by plasma oxidation to render the PDMS hydrophilic.[19] By manipulating the flow rate, the desired oxygen tensions within the microfluidic device can effectively be achieved. Besides the flow rate, the oxygen content depends on the cell density. Mehta *et al.*[19] demonstrated that measuring the oxygen content at two different points in a PDMS microbioreactor (thickness of 6 ± 2mm), a decrease in dissolved oxygen in the media was measured with increasing cell density and decreasing flow rates. The concentration of oxygen dissolved in media is 8.2 mg/L in the absence of cells. Increasing the cell density 4 times (from 1.92 x 10^8 till 8.01 x 10^8 cells/m^2) and decreasing the flow rate more than 400 times (from 0.22 μl/s till 0.0005 μl/s) showed a decrease in oxygen concentration of 8.2 mg/L till 1.76 mg/L over a length of 1 cm. These values are comparable to physiological values for mammalian cells (*in vivo* between 1-8 mg/L for a vessel with a diameter between 20 – 300 μm). These values are not uniformly transferable, because each PDMS device is made

under different conditions such as plasma oxidation and protein coating, though it provides general guidelines for designing PDMS devices in regards to their oxygen micro-environment for mammalian cell culture. Fluorescent dyes, such as ruthenium diimines (RDTP)[19] or porphyrines (PtOEPK)[20] were used for the time-lapse measurement of the oxygen concentration, of which the fluorescent dyes will be quenched in the presence of oxygen. However, with mathematical models[10,11,21] the oxygen consumption can be estimated in a microfluidic device without the need to perform experiments. The oxygen consumption can be calculated using the following equation (eq. 7-1)[10]

$$X_{O2\ consumption} = N_{cells/cm^2} \times X_{one\ cell} \times S_{device} \qquad \text{eq. 7-1}$$

where N_{cell/cm^2} denotes the cell density in the microdevice, $X_{one\ cell}$ the oxygen consumption by a single cell per second, and S_{device} the cell culture area. The oxygen consumption by a single cell per second is cell-type dependent but as an average is 1×10^{-16} mol/cell.s.[18] On the one hand, oxygen can be delivered through the medium flow, and on the other hand through the use of PDMS. The permeability of oxygen in PDMS (D_{PDMS}) is 41×10^{-6} cm^2/s[22] and using equation 7-2, the amount of oxygen that can be supplied into the microfluidic device through the PDMS (F_{max}) can be estimated as

$$F_{max} \approx D_{PDMS} \times (\Delta C/\Delta z) \qquad \text{eq. 7-2}$$

in which Δz denotes the thickness of the PDMS and ΔC the oxygen concentration gradient across the PDMS layer (between $2.0 - 2.5 \times 10^{-7}$ mol/ml).[21,23]
The solubility of oxygen in the medium without cells is ~ 8 mg/L = 2.5×10^{-4} mol/L = 2.5×10^{-10} mol/μl).[19] With equation 7-3, the amount of oxygen provided by the flow of medium can be estimated using a flow system to refresh the medium continuously.

$$O_{2\_flow} = Q \times S_{O2} \qquad \text{eq. 7-3}$$

in which Q defines the flow rate in μl/min and S the solubility of oxygen in medium in mol/μl.

The oxygen calculated, provided through the PDMS as well as through the medium flow, should be equal or higher than the oxygen needed to sustain the viability of the cells. At low flow rates, oxygen delivery to the cells via diffusion through the PDMS is a significant source of oxygen. At high flow rates, oxygen delivery occurs mainly via perfusion, and if it is sufficient enough it can eliminate the axial oxygen and nutrient gradients in the cell culture channel.[19,21]

7.3.2 Shear stress

Shear stress is defined as a stress state in which the stress is parallel to the surface. Hence, in our experimental set-up this is the effect of the flow (force) on the attached cells, which depend on the shear rate (G, the rate of change of velocity at which one layer of fluid (medium) passes over an adjacent layer (cells) = $\partial v/\partial x$) and the viscosity of the fluid (eq. 7-4).

Shear stress (τ) = shear rate (G) x viscosity (μ) eq. 7-4

For long-term cell culture, replacement of medium is needed to meet the nutrient requirements of mammalian cells. The maximum amount of shear stress that can be endured by cells depends on the cell type, since certain cells (*e.g.*, endothelial cells)[24-26] require shear stress for their development, whereas other cells are negatively affected by shear stress (such as chondrocytes).[27] Therefore, when developing a microfluidic platform which requires cell culture and flow of medium, the effect of shear stress have to be taken into consideration. For example, if you have two microfluidic channels with different heights but the same flow velocity, cells which are cultured in microfluidic channels with smaller heights will experience larger gradients in velocity over the membrane, thus having a higher shear stress.[5] Shear stress (for Newtonian fluids, defining fluids with a constant viscosity at a constant pressure and temperature, such as water) can be calculated with the following equation (eq. 7-5 and 7-6)

$\tau = 4\mu Q/\pi r^3$	round channels	eq. 7-5
$\tau = 6\mu Q/wh^2$	rectangular channels	eq. 7-6

in which τ defines the shear stress in dyne/cm^2, μ the dynamic viscosity of the fluid in dyne.s/cm^2 (~ 0.01 dyne.s/cm^2 for medium), Q the flow rate in ml/s (= cm^3/s), r the radius in cm, w the width of the channel in cm and h the height of the channel in cm. A shear stress of 1 dyne/cm^2 equals 0.1 Pa (1 Pa = 1 N/m^2 = 1 kg.m^{-1}.s^{-2}). In this study, the microfluidic devices that were designed, have a fixed geometry, so the shear stress, which act on the cells that have adhered to the surface, will depend on the applied flow rate.

Lu *et al.*[1,28] developed a microfluidic chip for quantitative analysis of cell adhesion varying the shear force, by changing channel geometry, and surface chemistry. First the microfluidic device was analysed for its geometry. The calculations demonstrated that more than 90% of the channel experienced a uniform shear stress distribution in the *y* direction, consistent with the general observation that the wall effect persists within one channel-height from the sidewall. Therefore, in microfluidic devices with high aspect ratio, most of the cells are subjected to a uniform shear stress. The presence of a non-flat cell in the microchannel changed the velocity distribution and correspondingly the shear stress and pressure distributions. The top of the cells experienced a higher shear stress than the edge, though the average shear stress was comparable to an empty channel. The adhesive strength of fibroblasts to PDMS greatly depended on the fibronectin surface density, as coating with 1 μg/ml fibronectin prevented cell detachment at a shear stress of maximal 2000 dyne/cm^2. Higher shear stress caused the detachment of cells within a few minutes. For long-term shear assays, Lu *et al.*[1,28] analysed the effect of the epidermal growth factor (EGF) on the adhesion of fibroblasts, as cell adhesion is not only regulated through adhesion to the matrix proteins (*e.g.,* fibronectin), but also through soluble molecules such as EGF. EGF has an established role in the disassembly of focal adhesions, thereby reducing cell adhesion. First, EGF signalling had to be returned to basal levels using an extended period of serum starvation (~ 12h), followed by EGF stimulation. EGF caused the

detachment of fibroblast in response to an increase in shear stress, as the control population (no EGF) exhibited higher resistance to shear stress.

Our interest is focused on the development of a microfluidic platform to measure apoptotic cell death in the presence of different drugs and monitor the apoptotic cascade in real-time, using first breast cancer cells as well as endothelial cells. Breast cancer cells are from epithelial origin, hence they do not require a (high) shear stress for development. Flow of the required nutrients and gases and removal of waste products is mainly performed by diffusion. Endothelial cells are constantly exposed to shear stress which modulates cell morphology and the expression of genes within these endothelial cells, including several pro-adhesive, pro-inflammatory and pro-thrombotic genes.[29] Thus epithelial cells are normally not exposed to shear stress, though they have demonstrated to be responsive to this. Low levels of shear stress (maximum of 5 dyne/cm^2) activate the expression of the *egr-1* gene, which in endothelial cells play a role in vascular remodelling after injury.[29] Moreover, the classical shear-stress response elements, such as ICAM and VCAM, which modulate gene expression in endothelial cells, are also active in renal epithelial cells under low shear stress (0.5-1.0 dyne/cm^2).[30] Furthermore, as breast cancer cells can metastasize to other parts of the body, the shear stress has an important role in inducing biochemical signals in the endothelial cells which can alter the surface expression of adhesion molecules on the endothelial cell and therefore influencing the ability of the endothelial monolayer to bind tumour cells.[31,32] The adhesion of circulating tumour cells to the endothelium is an essential prerequisite for extravasation of tumour cells from the blood stream to invade the tissue.[33] Furthermore, many cancers metastasize preferentially to certain organs, and this organ-specific nature of metastasis has attributed to interactions between endothelial ligands and specific receptors expressed on cancer cells.[34] Interaction of the protein fibronectin with intergrins present on the breast cancer cells initiates a cascade of reactions that up-regulate genes important for morphogenesis and tumour progression. Moreover, the expression of various integrin receptors on breast cancer cells is thought to be associated with differences in metastatic behaviour. The decreased expression of the $\alpha_2\beta_1$ integrin dimer is associated with a more malignant breast cancer phenotype.

In conclusion, epithelial cells can respond to shear stress, though they do not need this mechanical stimulation for development, as *in vivo* epithelial cells are not exposed to shear stress, as endothelial cells are. Therefore, shear stress, which will arise due to the flow of nutrients and drugs, have to be kept low when using epithelial cells. However, endothelial cells need shear stress for development and survival, and should therefore be kept at physiological shear stress levels (15 dyne/cm^2).

7.4 Microscope system

Optical detection was first used to analyse the effects of various drugs on the apoptotic process, checking cell morphology and fluorescence for specific dyes, such as Annexin V (AV) and propidium iodide (PI). The microfluidic device was mounted on to an X-Y-Z translation stage of an inverted wide fluorescence microscope (Leica DM IRM, Leica Microsystems, Wetzlar, GmbH, Germany). The microscope is equipped with a mercury lamp as an excitation source for fluorescence measurements, 20x, 40x, 50x, 63x objectives, and different fluorescence cubes (I3 filter cube with excitation BP of 450-490 and emission LP of 515 and a RGB filter cube with excitation BP 420/30 and emission BP 465/20 (blue); excitation BP 495/15 and emission BP 530/30 (green); excitation BP 570/20 and emission BP 640/40 (red)). In addition, a computer-controlled CCD camera (Leica DFC300 FX) is mounted on to the microscope for image recording, using the accompanied Leica Application Suite software (version 2.3.4 R2). The microscope is also equipped with a thermoplate (Leica MATS thermocontrol system Type E), to perform cell experiments at 37ºC.

7.5 Microfluidic devices

In order to be able to perform complex apoptosis studies on chip, various microfluidic devices were analysed, varying in materials, channel geometry and flow patterns. The fabrication process of each microfluidic device will be discussed, as will the experimental set-up and suitability for cell culture and finally apoptosis studies on chip, as performed in chapter 8.

7.5.1 Microfluidic cell trap chip

In order to manipulate single cells, cells have to be positioned in a specific location, allowing the analysis of the trapped cells in the presence of certain drugs. Trapping devices are especially suited for cells which grow in suspension. There are various ways to trap cells in microfluidic devices (*e.g.,* mechanical, optical, antibody-based, dielectrophoresis (DEP)). Mechanical trapping is used in this device. Mechanical cell trapping in microdevices is based on integrated microstructures with specific geometries which are capable of trapping cells that are transported in a fluid. This microfluidic chip consists of a filter used as a trapping site. The device is based on a cross-flow configuration of equally distributed flow channel length between the cross and the reservoirs. The schematic design, including channel dimensions, is shown in figure 7-1A and a SEM-picture of the trapping sites is depicted in figure 7-1B.

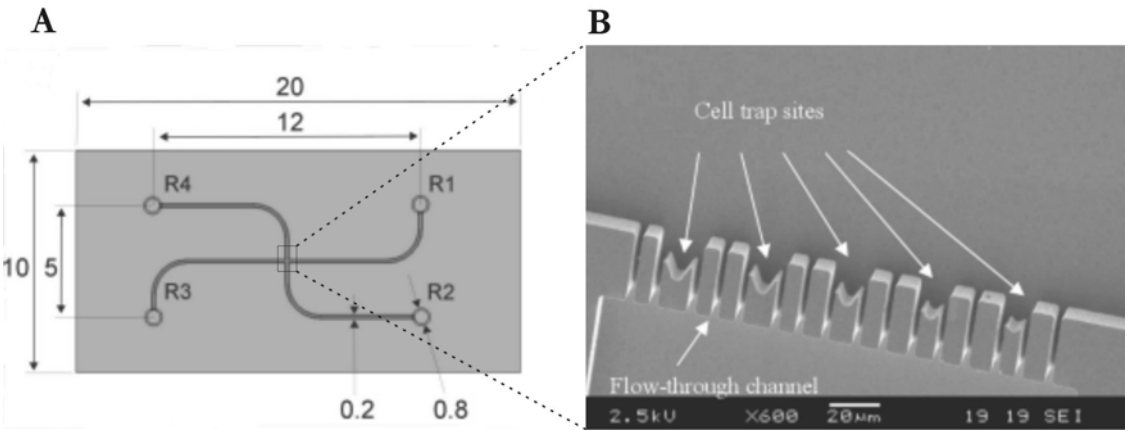

Figure 7-1. (A) Schematic drawing of the microfluidic cell trap device (dimensions in mm). **(B)** SEM picture of the trapping sites. Published with permission of A. Valero.[35]

The cell trapping microstructures act as a filter element. The fluid (medium) can flow through the traps and narrow slits, whereas the cells are captured in the cavities. This filter immobilizes cells in a predefined location where manipulation of the cells can be performed. For immobilization of cells, the cross-sectional dimensions of the traps have to be smaller than the average diameter of the cell. Several different geometries of the mechanical trap have been designed to determine their trapping efficiency in experiments. The trapping microstructures differ from each other in the shape, size, and the number of trapping sites as well as

the number of exits (narrow openings between the traps). The dimensions of the main channel are: length 12 mm, width 200 μm and depth 15 μm. The four access holes to the channels (denoted R1 to R4 in figure 7-1A) can be used as inlet, outlet, or blocked access that allows the configuration and modification of the flow direction.

7.5.1.1 Fabrication process

The microfluidic cell trap chip consists of a stack of 2 wafers, silicon and glass (Pyrex). The channel structures and trapping sites are patterned in silicon. Silicon is chosen as the material because of the significant high aspect ratio which can be achieved in silicon with deep reactive ion etching ((D)RIE)). Furthermore, (D)RIE is a well developed etching technique in the MESA$^+$ cleanroom, in contrast to dry etching of glass (*e.g.,* fused silica). The channels are covered with a non-patterned substrate, Pyrex glass, to close the channels, and to be able to optically visualize the channels and the trapping process, and monitor the effects of different drugs on the apoptotic process by using microscopy.
A schematic of the fabrication process is shown in figure 7-2. In the silicon substrate, the microfluidic channels and the trapping sites are etched by RIE using the Bosch process (a-d). Briefly, in the Bosch process, two different gas compositions (SF_6 and C_4F_8) are used. C_4F_8 creates a protective layer on the surface of the substrate, and SF_6 etches it. The protective layer is immediately sputtered away by the physical part of the etching (*e.g.,* ions with high enough energy knock out atoms out of the material to be etched, without any chemical reaction), but only on the horizontal surfaces and not on the sidewalls. Since the protective layer only dissolves very slowly in the chemical part (*e.g.,* the ions are accelerated towards and react at the surface of the material to be etched) of the etching, it builds up on the sidewalls and protects them from etching. In this way, high aspect ratios can be achieved. Access holes are powder blasted from the back of the silicon wafer (e). After this step, the silicon wafer is thermally oxidized at 1100ºC (g), hence losing the electrical conductivity of native silicon. Finally, a Pyrex wafer is anodically bonded to the silicon wafer (h), which allows optical monitoring.

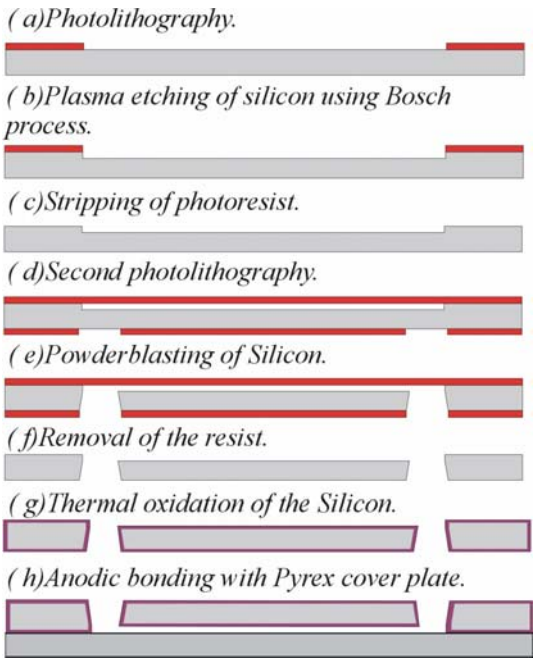

Figure 7-2. Schematic of the fabrication process of the microfluidic cell trap device. Published with permission of A. Valero.[35]

7.5.1.2 Experimental set-up

In experiments, cells were added in the microfluidic cell trap chip using a pipette. Due to capillary flow, cells moved to the trap. Then the chip was placed in a chip holder to be able to connect a flow system to the chip. Pressure driven flow was applied through a syringe pump. The connections between the chip and the syringe pump consisted of Nanoport™ assemblies and fused silica tubing. The connections are all from Upchurch Scientific (Oak Harbor, WA, USA) and specified in table 7-1. The syringes are from Hamilton (Reno, Nevada, USA) and are gastight with a cemented needle.

P-550 Column plug	10-32, X-long, PEEK™, natural
P-773 Y Connector	NANOTIGHT®, with 2 F-331 & sleeves, 360 µm OD, .004 in THRU, PEEK™
F-372x (yellow) and F-376x (green) Tubing sleeve	FEP, .0155 in (395 µm; green) and .007 in (180µm; yellow) x 1/32 in x 1.6 in
F-123Hx, Nut	NANOPORT™, Headless, 6-32 FB, 360 µm, PEEK™, natural
N-123-03x Ferrules	For N-123, 6-32, Flat, 360/510 µm OD
FS-110 Tubing	Fused silica, 100µm x 360 µm x 2m

Table 7-1. Characteristics of the necessities for connection of the microfluidic cell trap chip to the syringe pump.

The microfluidic cell trap device was used for cells in suspension and for adherent cells. The apoptotic process of HL60 cells was analysed using the fluorescent labelled inhibitor of caspases (FLICA) and the permeability dye propidium iodide (PI), as described in chapter 3. Moreover, HL60 cells were analysed for their autofluorescence, as described in chapter 4. The main focus in this chapter is to find the best microfluidic platform to perform apoptosis studies on adherent cells. In order to do this, experiments were performed to check the adhesion of adherent cells to the Pyrex glass and analysed for their viability, of which the importance is stated in chapter 6.

Two different adherent cell lines were checked for their adhesion to the Pyrex glass, as this would be the substrate the cells mainly attach to. Because of a limited depth of 15 μm, the silicon oxide layer will also play a role, but the adhesive effect to the silicon oxide was not analysed. Immortalized human microvascular endothelial cells (HMEC; a generous gift from Dr. P. Koolwijk, TNO, Leiden, The Netherlands) and the oestrogen receptor positive invasive lobular breast carcinoma cell line MCF-7 were plated in a 24 wells plate in contact with the Pyrex glass using a concentration of 0.5 x 10^6 cells/ml, as described in chapter 6.2.2.2. Adhesion to the material was checked by May Grünwald staining. MCF-7 cells which were added to untreated wells and HMEC cells which were added to wells pre-coated with 1% gelatine served as controls. Furthermore, cellular viability was checked in the microfluidic cell trap chip after different adhesion times and under different flow conditions. Preferably, adhesion times have to be as short as possible, and the flow has to start as soon as possible, to prevent lack of nutrients and oxygen which would damage the cells.

7.5.1.3 Results and discussion

In conventional cell culture, MCF-7 cells do not need a specific coating, as for example gelatine or fibronectin, in order to be able to attach and grow on to the surface of the culture plate (polystyrene). First, we checked if MCF-7 cells could also attach and grow to other surfaces, specifically Pyrex glass, as this will be the substrate the MCF-7 cells need to attach to when using the microfluidic cell trap chip. Figure 7-3 shows the light microscopy (LM) pictures of MCF-7 cells stained with May Grünwald staining in contact with either PS (control) or a Pyrex plate.

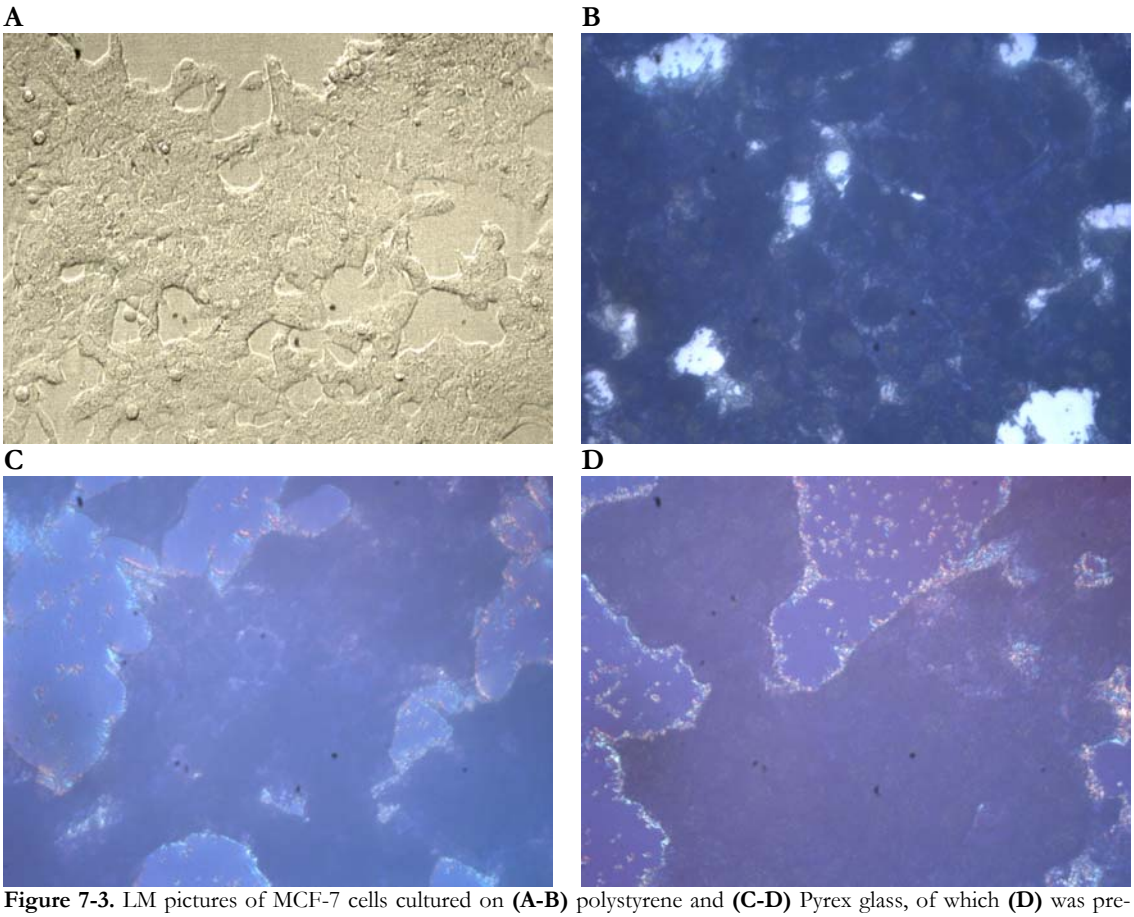

Figure 7-3. LM pictures of MCF-7 cells cultured on **(A-B)** polystyrene and **(C-D)** Pyrex glass, of which **(D)** was pre-coated with serum. **(B-D)** May Grünwald staining. Magnification **(A)** is 20x, **(B-D)** is 63x.

MCF-7 cells have an epithelial-like morphology and grow in colonies, forming aggregates, as it is the nature of tumours (Figure 7-3A). MCF-7 cells adhered well to the Pyrex glass. Adhesion was not increased with a pre-coat with serum. The colonies were denser on the Pyrex, than the colonies of MCF-7 cells grown on conventional cell culture PS. At the end of the experiment cells were not counted, thus no detailed statements on changes in cell growth could be made.

Conventionally, HMEC cells grow on 1% gelatine coated PS wells, showing a cobblestone appearance as they grow towards a confluent monolayer (Figure 7-4). In these LM pictures, it is clearly shown that with May Grünwald staining, the eosin stains the cytoplasm red, due to the binding of the acid eosin to the basic elements in the cytoplasm. The methylene blue, which is basic, binds to the acid components in the nucleus, showing a blue staining.

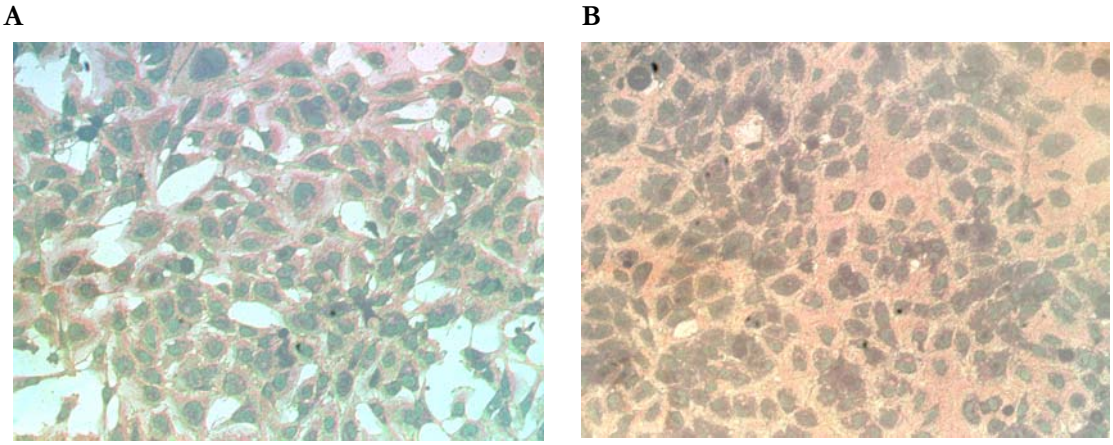

Figure 7-4. LM pictures of HMEC cells grown in 1% gelatine coated PS wells of a 24 wells plate. Cells were stained after **(A)** 24h and **(B)** 5 days with May Grünwald staining. Magnification is 20x.

HMEC cells did not attach to either uncoated Pyrex glass or Pyrex glass pre-coated with 1% gelatine. Gelatine has an iso-electric point (pI) between 4.7 and 5.2. With the pH of 1% gelatine being higher than the pI (pH = 7.02), the molecule has a negative charge, and therefore cannot form a layer on the Pyrex glass. Coating the Pyrex glass overnight at room temperature with 0.1 % (3-(2,3-epoxypropoxy)-propyl)-trimethoxysilan) (APS) in 100% ethanol, demonstrated attachment of HMEC cells, with no change in morphology. Fibronectin could also be used for coating the Pyrex glass to enhance adhesion and promote growth.

MCF-7 cells were used to perform viability experiments in the microfluidic cell trap chip, as these cells are easier to culture than HMEC endothelial cells. In these viability experiments the effect of adhesion time and flow rate was analysed. Figure 7-5A shows the LM picture of design.

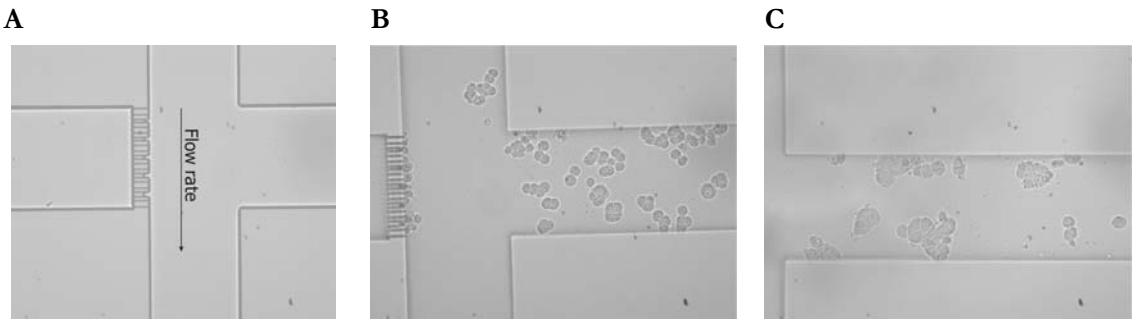

Figure 7-5. LM pictures of MCF-7 cells cultured in the microfluidic cell trap chip. **(A)** Design, **(B)** after adhesion of 2h in the incubator, **(C)** after 16h with a flow of 1µl/min. Magnification is 20x.

The access holes of the horizontal channel were blocked with PDMS. The chip was loaded with cells with a pipette, and when enough cells were present in the chip, the flow was stopped by placing the chip in a Petri dish covered with RPMI$^+$ culture medium. After 2h, the cells already were nicely attached to the Pyrex glass (Figure 7-5B). The chip was placed in the chip holder and connected to the syringe pump. A flow rate of 1 μl/min was applied in the direction as depicted in figure 7-5A, which accounted for a shear stress of 22 dyne/cm^2. Epithelial cells were cultured in the right side channel, thus experiencing much lower shear stress than existing in the main channel, still these cells were provided with fresh medium. The medium used, was CO_2 independent medium (Invitrogen, Grand Island, NY, USA), which is a non-HEPES proprietary medium suitable for supporting cell growth under atmospheric conditions. CO_2 independent medium function as the basal medium, to which supplements such as FBS and antibiotics are added. After 16h, MCF-7 cells formed colonies, and showed a viable morphology (Figure 7-5C). In another viability control experiment, MCF-7 cells adhered to the Pyrex plate for 5h in the incubator, after which a flow of 10 μl/h was applied, which corresponded to a shear stress of 3.7 dyne/cm^2. In this case, the flow of (CO_2 independent) medium was in direct contact with the attached cells, which was not the case in the experiment described above. As shown in the LM pictures, the attached MCF-7 cells reacted directly to the applied flow, as shown by a roughened morphology, though the cells remained attached (Figure 7-6). All access holes were open.

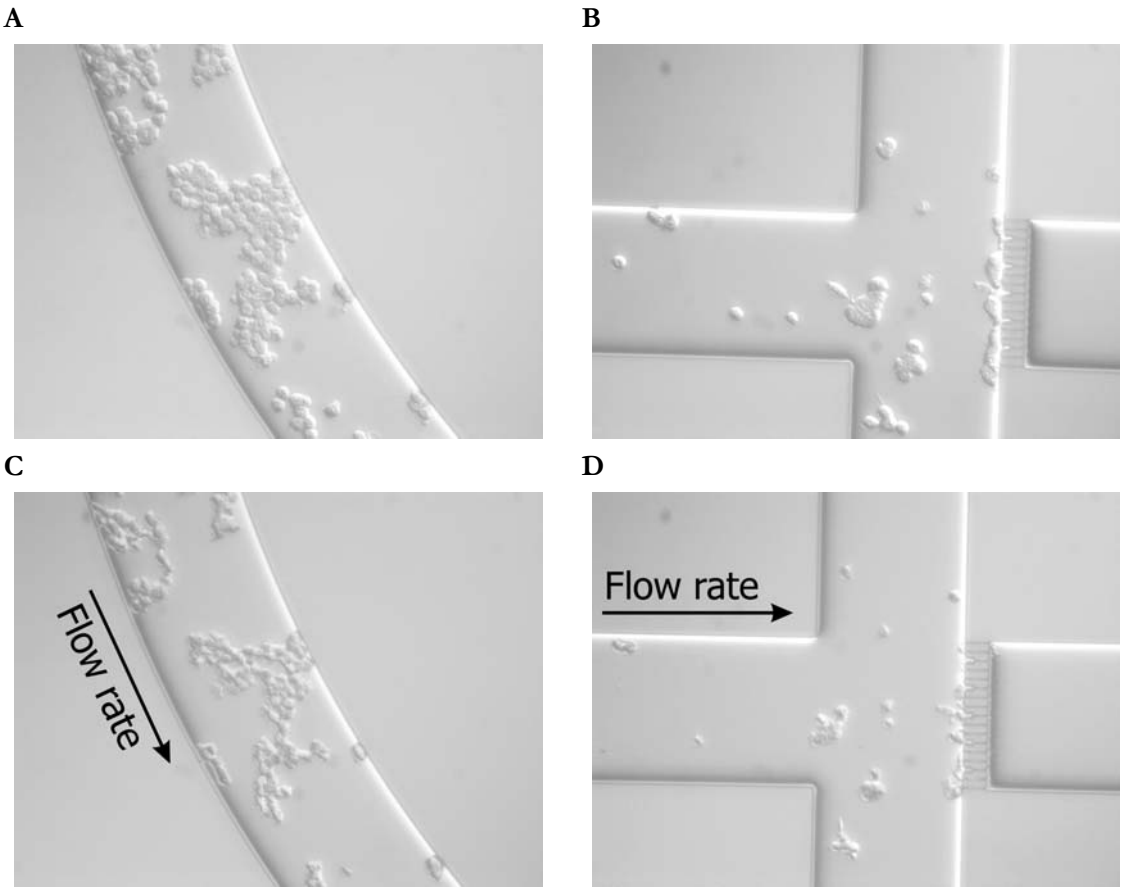

Figure 7-6. LM pictures of MCF-7 cells in the microfluidic cell trap chip. After adhesion of 5h in the incubator, a flow of 10 µl/h was applied. **(A)** and **(B)** after adhesion of 5h in the incubator. **(C)** and **(D)** after 30 minutes with a flow rate of 10 µl/h. Magnification is 20x.

In conclusion, this microfluidic cell trap chip can be used for apoptosis studies, though cells have to be cultured in the side channel, as demonstrated in figure 7-5B-C, and not be in direct contact with the flow. Lower flow rates than 10 µl/h (= 3.7 dyne/cm^2) were not analysed. As the trapping site is very suitable for positioning cells in suspension, it might change the adhesion properties and the morphology of adherent cells, due to the restricted space in the trap and furthermore change the flow as cells are trapped. Apoptosis studies within this device are performed and will be discussed in chapter 8.

7.5.2 Meander chip

This simple three-port microfluidic device was developed to show the potential of using cellular autofluorescence in combination with microfluidic devices for single-cell analysis. Within this microfluorescence activated cell sorter (μFACS), granulocytes were successfully differentiated from red blood cells based on differences in AF.[36] As a preliminary experiment, this device can be used for performing apoptosis studies, as the only necessities are a channel to which the cells can adhere and flow can be applied to.

7.5.2.1 Fabrication process

This simple μFACS consists of three-port microstructures patterned in Borofloat glass using isotropic wet-etching with hydrofluoric acid (HF). The channels are covered with a Borofloat plate of 1 mm thickness. Access holes are powder blasted. The channels have a depth of either 50 μm or 100 μm with a corresponding width of 102 μm or 202 μm, respectively. The length of the channel varies, as the number of loops differs. Chips with 5 loops have a channel length of 113.7 mm, 7 loops a length of 157.6 mm, and 10 loops a length of 201.6 mm. Figure 7-7 shows a photograph of the microfluidic device.

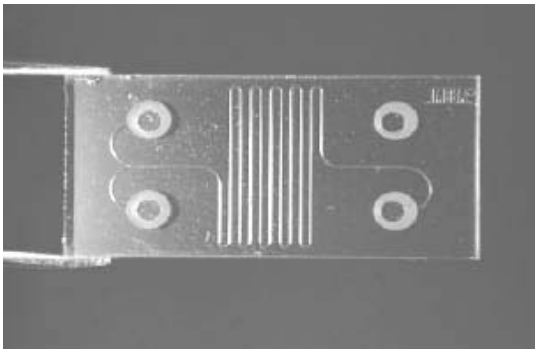

Figure 7-7. Photograph of the meander chip with 5 loops, showing the inlet on the right, and the two outlets on the left.[36]

7.5.2.2 Experimental set-up

For loading the meander chip with MCF-7 cells, the chip was first rinsed and filled with culture medium (RPMI$^+$ medium). 10 μl of MCF-7 cells in a concentration of

0.5 x 10^6 cells/ml were added to the inlet, and by gently sucking at the outlet, flow was initiated. When enough cells were present in the chip, the flow was stopped by placing the chip in a Petri dish, fully covered with $RPMI^+$ medium and placed in the incubator for cell adhesion. Various adhesion times in the incubator were analysed, to define after which time period adhesion is best. Before starting experiments (*e.g.,* analysis of different drugs on the apoptotic process), viability was assessed with propidium iodide (PI), making sure that cells were viable and that the effects demonstrated later were due to the presence of the drug, and not due to damaged cells already at the start of the experiment.

7.5.2.3 Results and discussion

The attachment of MCF-7 cells to the Borofloat glass was not analysed in the conventional manner as for the Pyrex glass, as both materials are borosilicate glass, though they differ in the composition of the trace elements. The time needed for MCF-7 cells to attach to the Borofloat was analysed in the Meander chip under different flow rates. The Meander chip with 5 loops and a depth of 100 μm was used. MCF-7 cells adhered to the Pyrex glass during 5½h in the incubator, after which the flow was connected to the chip. Connection of the chip to the syringe pump was the same as used for the microfluidic cell trap chip, only now specific ferrules for glass were used (type N123-04x, Upchurch Scientific). A flow rate of 25 μl/h, which accounted for a shear stress of 0.2 dyne/cm^2 (for a rectangular channel) was applied. Figure 7-8 shows the time-lapse recording. Already, within an hour after starting the flow with CO_2 independent medium, the cells demonstrated apoptotic characteristics (Figure 7-8B, dashed circle), such as rounding of the cells and membrane blebbing. Due to the channel depth of 100 μm, the cells were out of focus (Figure 7-8C) and detached (Figure 7-8D).

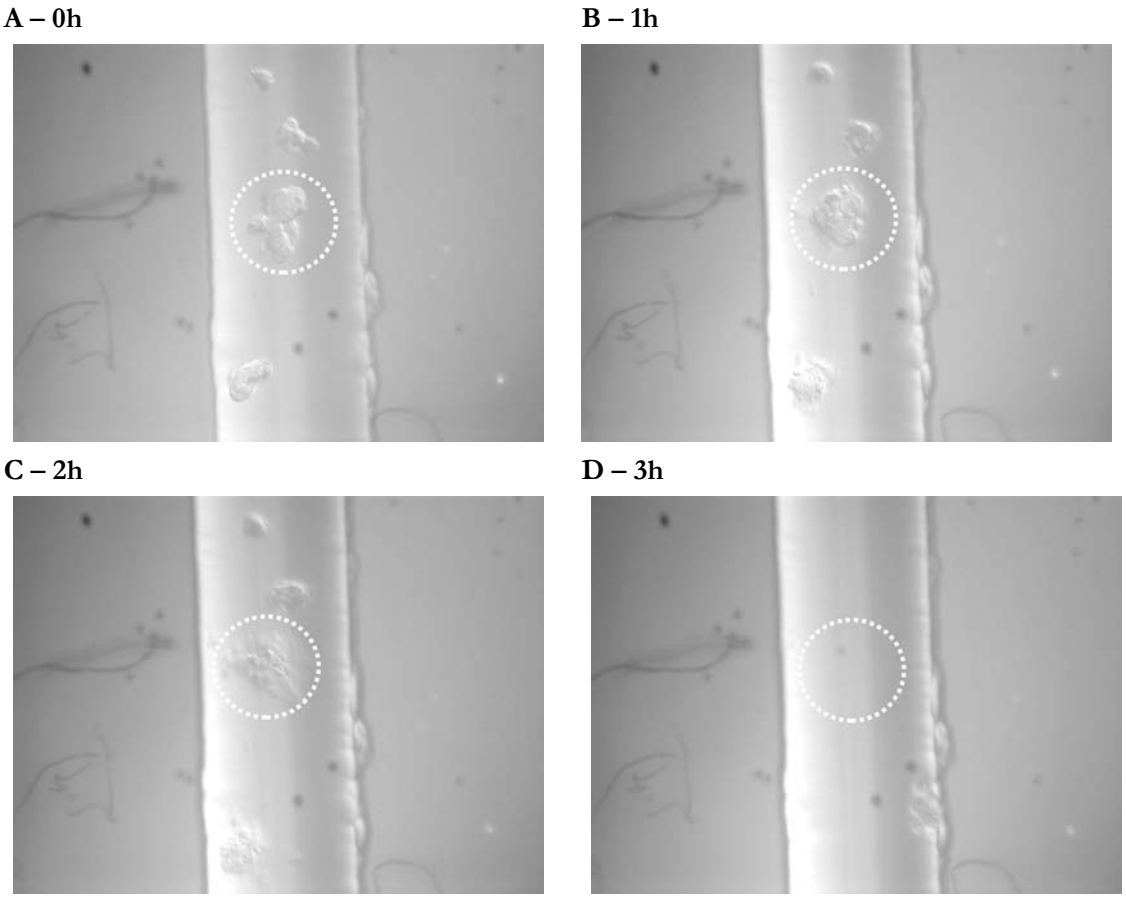

Figure 7-8. LM pictures of MCF-7 cells cultured in the Meander chip (5 loops, d = 100µm). After an adhesion time of 5½h in the incubator, a flow of 25 µl/h was applied and pictures were taken at **(A)** t=0h, **(B)** 1h, **(C)** 2h and **(D)** 3h. Magnification is 20x.

Detachment can have occurred due to the flow rate, which still might be too high or because of a lack of nutrients. Moreover, this did not seem plausible as the chip did not dry out and the depth of the channel is 100 µm. At such a low cell concentration in combination with those chip dimensions, there should be enough medium for such a short time period. The volume in the chip is 2.2742 µl. The solubility of O_2 in the medium is 2.5 x 10^{-4} mol/L, thus 5.6855 x 10^{-10} mol O_2 was present in the chip. The meander chip was loaded with about 100 cells. The oxygen consumption per cell per second is 1 x 10^{-16} mol. During the 5½h adhesion in the incubator, the total oxygen consumption was 1.8 x 10^{-10} mol, hence enough oxygen was present as 5.6855 x 10^{-10} mol was dissolved in the medium. Additionally, the medium was totally refreshed every 5.45 minutes in the chip (condensation of the medium not accounted), which provided the cells attached with enough medium, as

there was also enough oxygen in the medium during the 5½h adhesion in the incubator, where there was no flow. The attachment of the cells was probably not long enough. In the following experiment, we compared two different adhesion times, 5h and 24h, in the incubator. After 5h, a flow rate of 10 µl/h was applied, which corresponded to a shear stress of 0.08 dyne/cm^2 (for a rectangular channel).

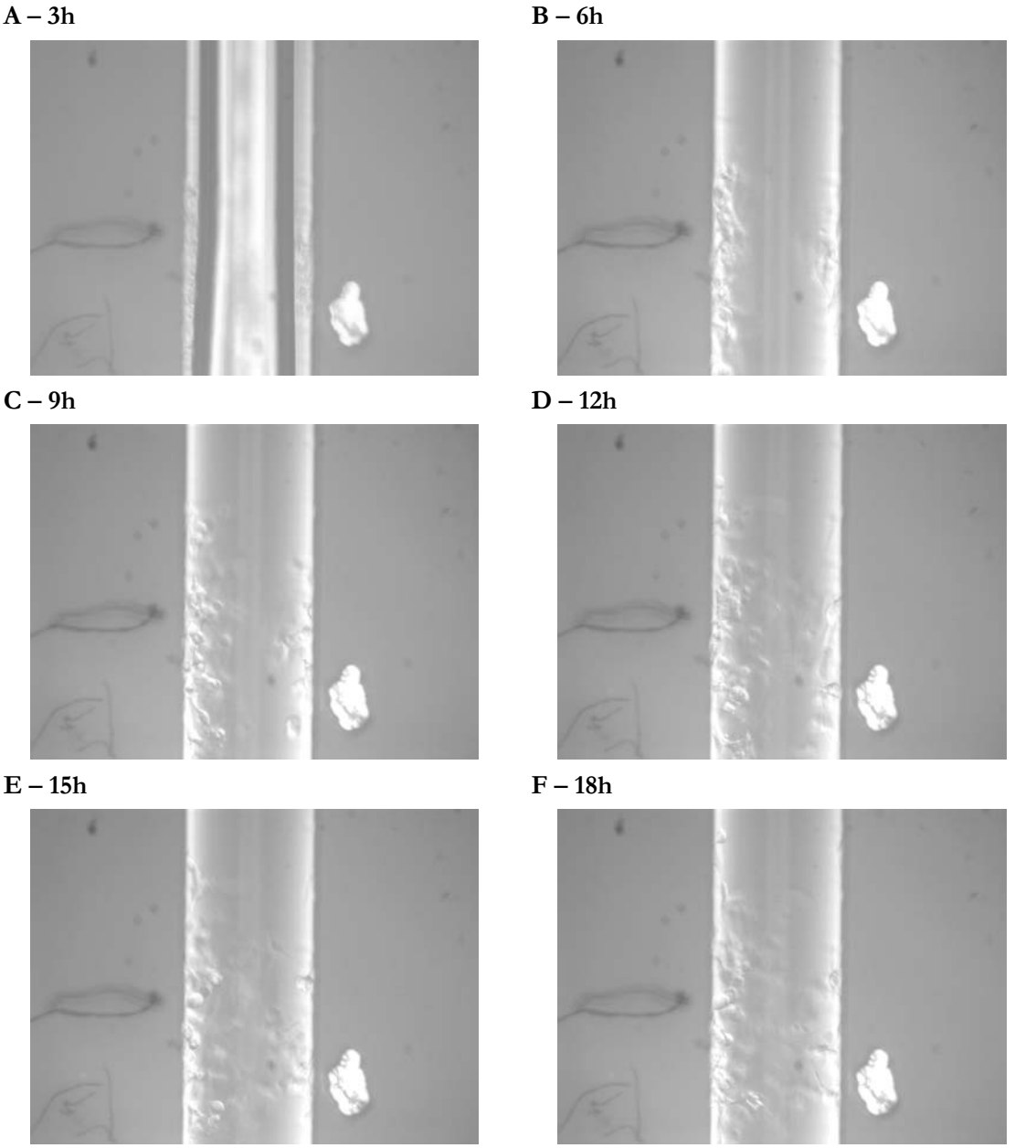

Figure 7-9. LM pictures of MCF-7 cells cultured in the Meander chip (5 loops, d = 100 µm). After an adhesion time of 5h in the incubator, a flow of 10 µl/h was applied and pictures were taken at **(A)** t=3h, **(B)** 6h, **(C)** 9h, **(D)** 12h, **(E)** 15h**,** and **(F)** 18h. Magnification is 20x.

Unfortunately, air bubbles disrupted the flow during 2h and 3h (Figure 7-9A) and detached a lot of cells. Nevertheless, some cells managed to survive at the sidewalls of the channel, and demonstrated spreading and migration in time (Figure 7-9B-F). Hence, the applied flow rate did not damage the cells.
The cells also survived adhesion during 24h in the Meander chip, with no medium change in between, as demonstrated in figure 7-10. Cell viability was checked with PI staining. Of the three cell colonies, which had attached to the Borofloat, only a few cells were PI positive.

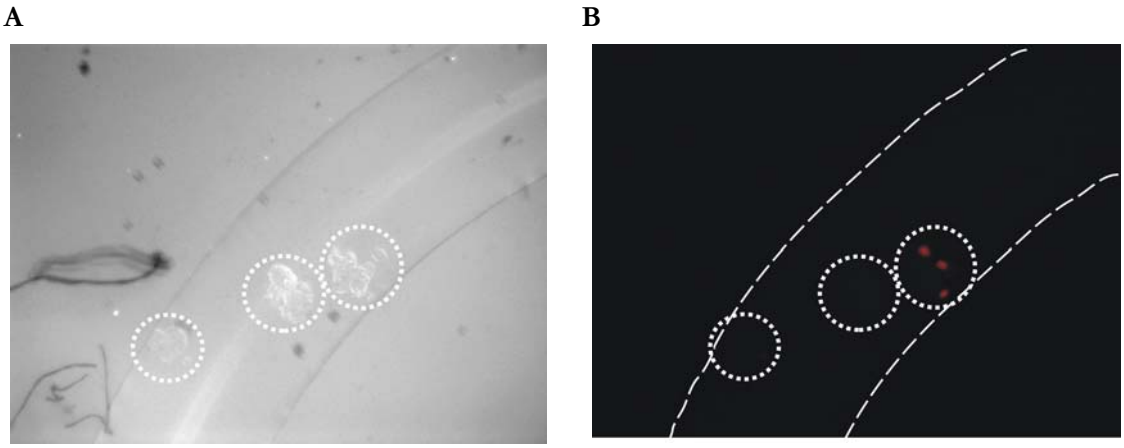

Figure 7-10. LM picture **(A)** of MCF-7 cells cultured in the Meander chip (5 loops, d = 100μm). Cells adhered for 24h in the incubator and fluorescence was checked with **(B)** PI. Magnification is 20x.

For 100 cells, the total oxygen consumption was 8.64 x 10^{-10} mol for an adhesion time of 24h. Furthermore, as the cells attached near the inlet, little diffusion probably preserved the cellular viability also.
In following experiments, overnight adhesion (between 16 – 24h) was preferred. Before starting apoptosis experiments, viability was checked with PI, to make sure that the cells which will be followed in time were viable. Overall, viability was over 80%.

7.5.3 Apoptosis chip

PDMS is widely used as the chip material used to perform (long-term) cellular studies, because of its biocompatibility and gas permeability. Furthermore, PDMS is a cheap material and chips can be made very easily, without the need of cleanroom facilities, apart from making the silicon mold. To improve environmental

conditions for the cells, 3 different chips were designed (*e.g.,* apoptosis chip #1, #2 and #3), in which either the cover was of PDMS (#1), or the structures were patterned in PDMS (#2 and #3). In all cases, PDMS (Sylgard 184) was obtained from Dow Corning (Midland, MI, USA). Curing – and base agent were mixed at a ratio of 1:10 for 10 minutes, degassed and cured for 2h at 60ºC on a Teflon-coated smooth silicon wafer (for #1) or on a FDTS-coated patterned silicon wafer (for #2 and #3), as FDTS formed a hydrophobic monolayer on the wafer.

7.5.3.1 Fabrication process

Apoptosis chip #1

This microfluidic device consists of a small culture chamber, with on each side a channel to apply a flow. The structures are patterned in Pyrex glass using isotropic wet-etching with hydrofluoric acid (HF). The channels have a depth of 15 μm, 30 μm, or 50 μm, with the corresponding width of respectively 32 μm, 62 μm and 102 μm. The culture chamber has dimensions of 230 μm x 230 μm for a depth of 15 μm, 260 μm x 260 μm for a depth of 30 μm, and 300 μm x 300 μm for a depth of 50 μm. Access holes are powder blasted. The outer dimensions of the chip are 10 mm x 20 mm, and therefore fit the same chip holder as used for the microfluidic cell trap chip and the Meander chip (Figure 7-11).

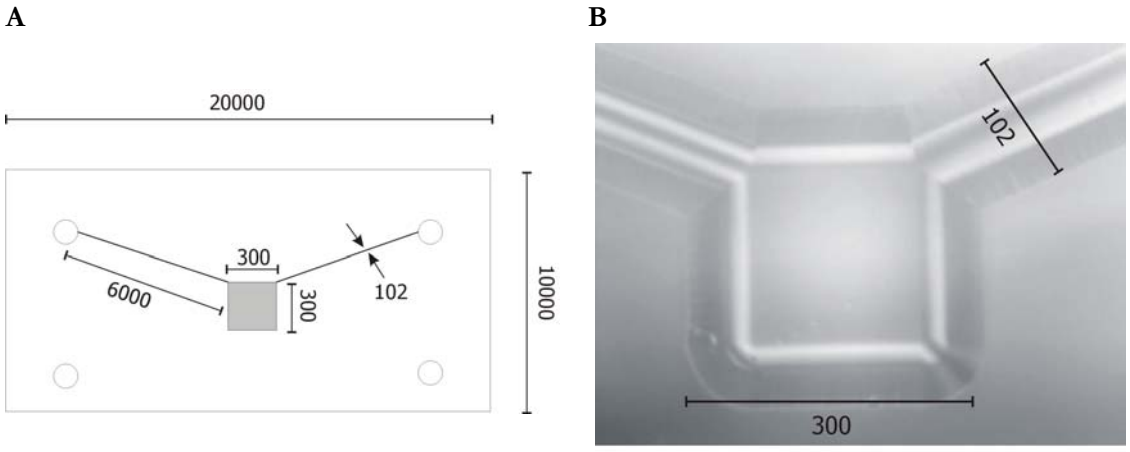

Figure 7-11. Design of apoptosis chip #1. **(A)** Dimensions in μm for a depth of 50μm and **(B)** LM picture. Magnification is 20x.

The channels can be either sealed with PDMS or with polypropylene (PP) foil (Optical adhesive covers, Applied Biosystems, Foster City, CA, USA). PP foil is

sticky, so only pressure is necessary to seal the chip. For sealing PDMS to the Pyrex chip, oxygen plasma is used. Therefore, both surfaces are thoroughly cleaned with acetone using an ultrasonic bath for ten minutes. Subsequently, both surfaces are rinsed with distilled water and placed back in the ultrasonic bath containing distilled water for 5 minutes. The surfaces are dried in the oven and placed in the plasma oxygenator (Harrick PDC001) for 4 minutes at a pressure of 400 mTorr and at RF 29.6 W (high). After sealing, PBS is introduced in the chip, to preserve the hydrophilicity of the PDMS and to facilitate cell loading.

Apoptosis chip #2

First, a silicon mold is fabricated, which mirrors the structures patterned in the PDMS. The design of the chip is a single channel with a length of 1 cm, a width of 200 μm, and a depth of 50 μm. The middle of the channel contains a trap structure, consisting of vertical PDMS columns, each having a width of 17 μm, a length of 10 μm, and a height of 40 μm. The distance between the columns is 5 μm (Figure 7-12).

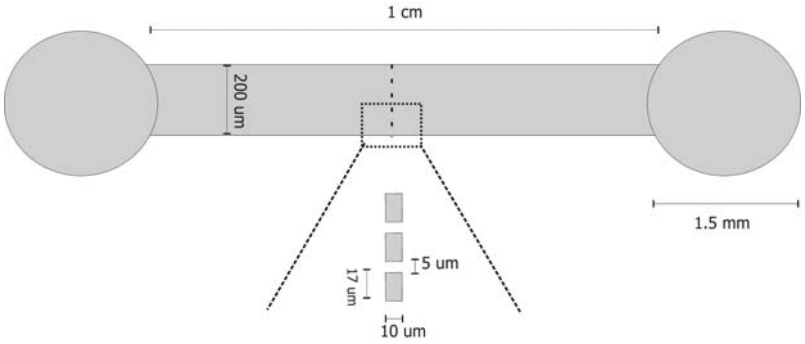

Figure 7-12. Design of apoptosis chip #2. The middle of the channel contains a trapping site, of which a small part is enlarged. The total trap consists of 9 vertical columns, hence 8 trapping sites.

PDMS is poured on the FDTS-coated silicon mold and cured for 2h at 60ºC. The thickness of PDMS varies from 0.1 mm by spinning, to 1 mm by pouring. Holes (diameter of 1.5 mm) are punctured in the PDMS, destined for inlet and outlet. PDMS chips are sealed to a piece of Pyrex of 2 by 1 cm using oxygen plasma as described above for apoptosis chip #1.

Apoptosis chip #3

A silicon mold is fabricated with structures which mirrors the structures patterned in the PDMS. Figure 7-13A shows the schematic of the chip, and figure 7-13B a picture of the final design in PDMS.

A **B**

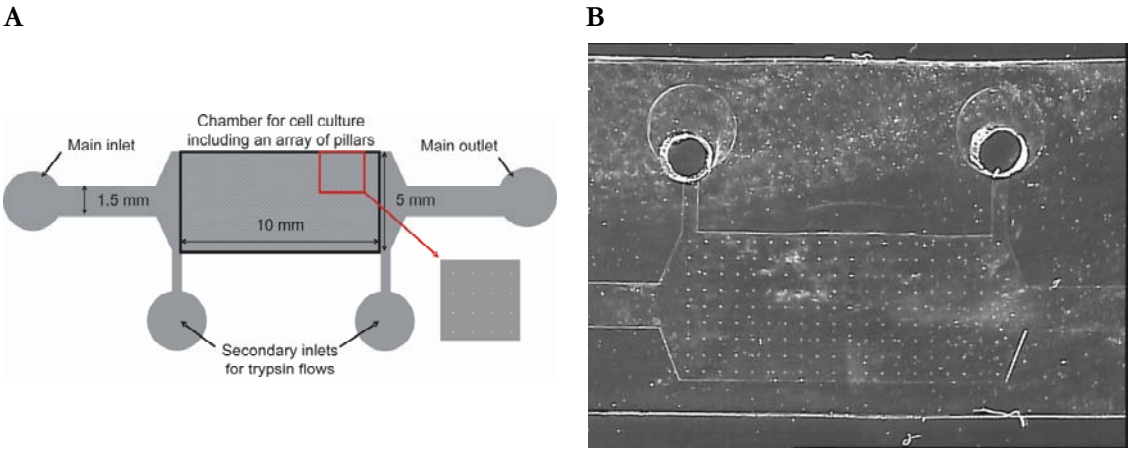

Figure 7-13. Design of apoptosis chip #3. **(A)** Schematic of the chip and **(B)** a picture of the final design in PDMS. Courtesy S. Le Gac 2007.

The inlet and outlet channel have a width of 1.5 mm and a depth of either 44 μm or 66 μm. The cell culture chamber has a length of 10 mm, a width of 5 mm and a depth of either 44 μm or 66 μm. The cell culture chamber includes an array of pillars with variable geometries and volumes, for increasing the stability of the chamber. Furthermore, the chip consists of two secondary inlets for, for example, trypsin, to remove the attached cells. The PDMS chip is sealed to a microscope slide (Figure 7-14), using oxygen plasma as described above for apoptosis chip #1.

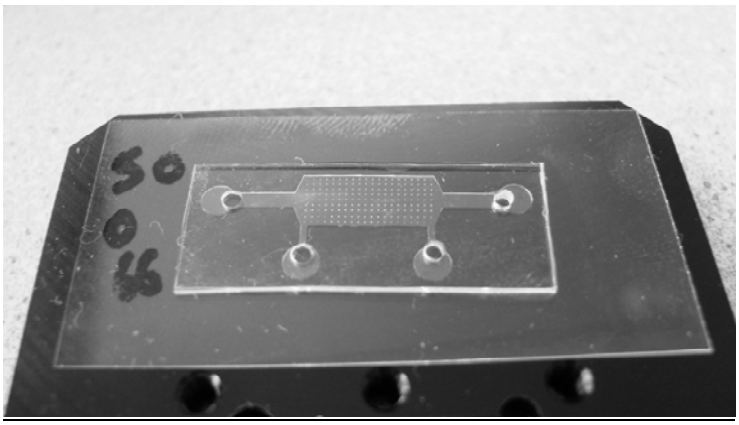

Figure 7-14. Final design of apoptosis chip #3. In this device, the pillars are round with a diameter of 50 μm. The depth of the channels is 66 μm. Courtesy S. Le Gac 2007.

7.5.3.2 Experimental set-up

Anoikis chip #1

Loading MCF-7 cells and HMEC cells was performed with a pipette, using the same procedure as in the microfluidic cell trap chip and the Meander chip. The chip was placed in a Petri dish to stop the flow and to let the cells adhere, preferably in the cell culture chamber. For applying a flow, the chip was placed in the chip holder and connected with the syringe pump using the standard equipment of Upchurch Scientific as described above for the Meander chip. First the adhesion of the two different cell lines to the PDMS was analysed.

Anoikis chip #2

Cell loading of MCF-7 cells was accomplished by pipetting 4 µl of 0.5 x 10^{-6} cells/ml in the inlet. Hydrostatic forces moved the cells into the channels and the cells were trapped at the trapping site. The chip was then covered with medium to prevent further flow. Long-term cell culture in this microfluidic chip was analysed and viability was checked with Calcein-AM (Molecular Probes Invitrogen, Carlsbad, CA, USA) and PI. Calcein-AM is a cell-permeant dye that can be used to determine cell viability in most eukaryotic cells. In live cells, the non-fluorescent Calcein-AM is converted to green-fluorescent Calcein, after acetoxymethyl ester hydrolysis by intracellular esterases. In this experiment, a new way of applying the flow was analysed, as this PDMS chip could not be placed in the chip holder. Therefore, small blocks of PDMS were sealed to the inlet and outlet, to heighten these access holes. A small polyamide tube (Liquid scan, Uberlingen, Germany) with an inner diameter of 0.25 mm and an outer diameter of 0.75 mm (Fluidmedic PA6) was connected to the heightened inlet. The tube was connected to a gastight syringe with a BD Microlance needle (30G x ½"; 0.3 mm x 13 mm, yellow). Cell loading of MCF-7 occurred as described above, and cells were allowed to attach in the chip in the incubator overnight.

Apoptosis chip #3

Cell loading of three different cell types was performed with a pipette. For human umbilical vein endothelial cells (HUVEC) and human microvascular endothelial cells (HMEC), the chip first needed to be pre-coated with 2 mg/ml fibronectin in

the incubator for at least 30 minutes. For every cell type (*e.g.,* HUVEC, HMEC and MCF-7), 20 µl of cell suspension with a concentration of ± 4 x 10^6 cells/ml was pipetted into the main inlet. Due to hydrostatic forces, the cells moved into the chip. For the endothelial cells, normal culture medium is EBM-2 medium, supplemented with growth factors, FBS and antibiotics (EGM-2 Bulletkit, CC-3162, Cambrex, Verviers, Belgium). After cell loading, the chip was placed in a Petri dish and covered with medium, either EGM-2 for endothelial cells, or $RPMI^+$ for MCF-7 cells. Cells were cultured for 2 days in the chip, though the medium in the chip was refreshed after one day. Flow was applied by using white pipette tips (Finntip 200Ext 5-200µl; Thermo Electron Corporation, Vantaa, Finland), in which the PA-6 (Liquid scan) tube fitted nicely. This tube was, at the inlet, connected to a BD plastic syringe (Becton Dickinson, Franklin Lakes, NJ, USA) with a BD Microlance needle (30G x ½"; 0.3 mm x 13 mm, yellow). At the outlet, the tube was connected to a 50 ml falcon tube, which served as a waste reservoir. Figure 7-15 shows pictures of the flow set-up. The secondary inlets will not be used during flow experiments, and therefore were closed with yellow pipette tips.

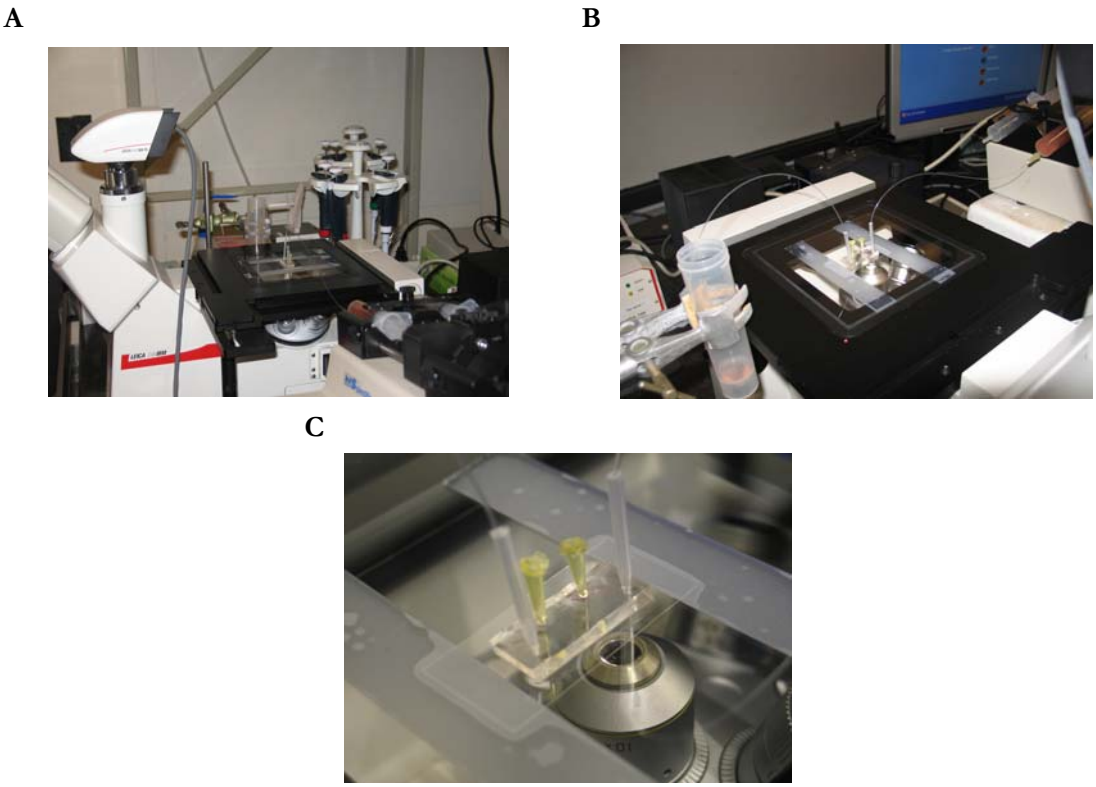

Figure 7-15. Experimental set-up of the flow system used for apoptosis chip #3. **(A)** Global overview, **(B)** focus on the microscope stage and **(C)** focus on the connections on the chip.

7.5.3.3 Results and discussion

Both the cell lines HMEC and MCF-7 adhered barely to the hydrophobic PDMS or PDMS pre-coated with either serum or polyethylene glycol (PEG). Therefore, during adhesion, the apoptosis chip #1 was turned upside down in the Petri dish to allow cells (because of gravity) to adhere to the Pyrex glass. Only a few MCF-7 cells managed to adhere overnight to the Pyrex glass and maintained attached with a flow rate of 20 µl/h (= 1.3 dyne/cm^2) (Figure 7-16).

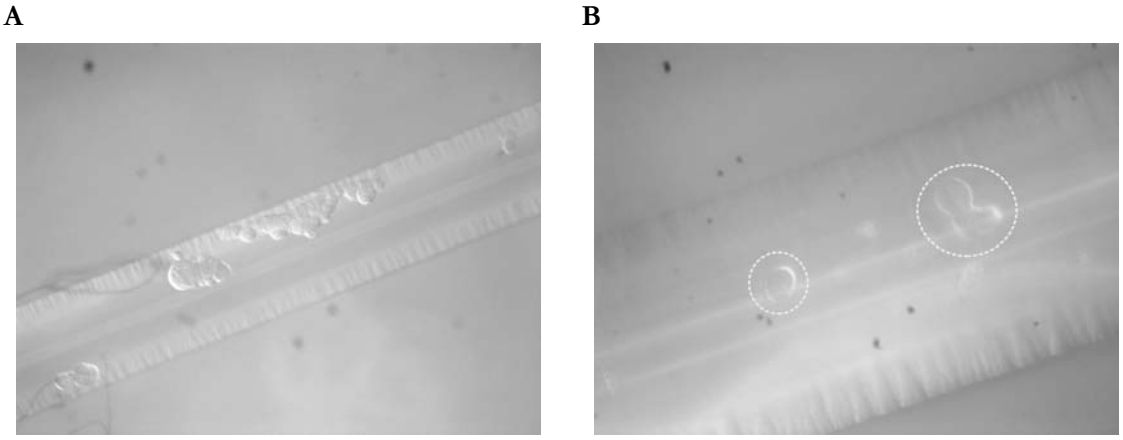

Figure 7-16. MCF-7 culture in apoptosis chip #1. **(A)** MCF-7 cells after overnight adhesion in the incubator. Magnification is 20x. **(B)** After applying a flow rate of 20 µl/h, most of the cells detached. Magnification is 50x.

When filling the chip with a pipette, the (capillary) flow in the chip was very high and cells moved with high speed past the culture chamber towards the outlet. Furthermore, the apoptosis chip #1 did not fit as nicely in the chip holder as the microfluidic cell trap chip and the Meander chip, because of the variable thickness and the flexibility of the PDMS. Therefore, a new chip was designed (apoptosis chip #2), using a different experimental set-up to apply the flow. By loading MCF-7 cells into the vertical inlet, only a few cells flowed through the channel because of hydrostatic forces. These cells were trapped at the trapping site. However, most of the cells stayed at the inlet, probably due to the fact that the MCF-7 cells in suspension were present in small aggregates, not as single cells, and these cells were quite sticky. Resuspending the cells present in the inlet did not yield extra cells in the channel and this could damage the cells mechanically. The cells present in the trap in time migrated out of the trap (Figure 7-17), when no flow was applied.

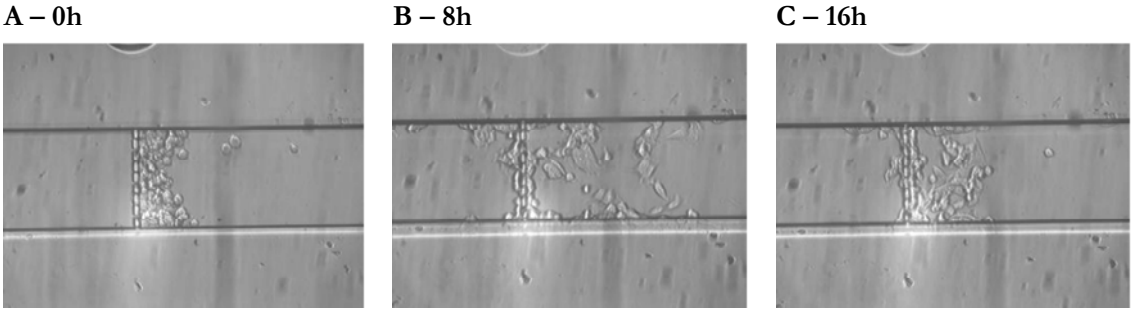

Figure 7-17. LM pictures showing the migration of MCF-7 cells in the chip. Cells were cultured in CO_2 independent medium at 37ºC on to microscope stage. Magnification is 10x.

Furthermore, the viability of long-term cell culture of MCF-7 cells was analysed, as it is probably better to culture the cells for 2-3 days before starting apoptosis experiments, because the cells are then in their exponentially growing phase (doubling time ±50h). To check viability, MCF-7 cells were stained with 2 μg/ml Calcein-AM (= 2 μM) and 10 μg/ml PI (= 15 μM). Medium in the chip was refreshed every day and for every time-point a new chip was used, as the fluorescent dyes were toxic for the cells.

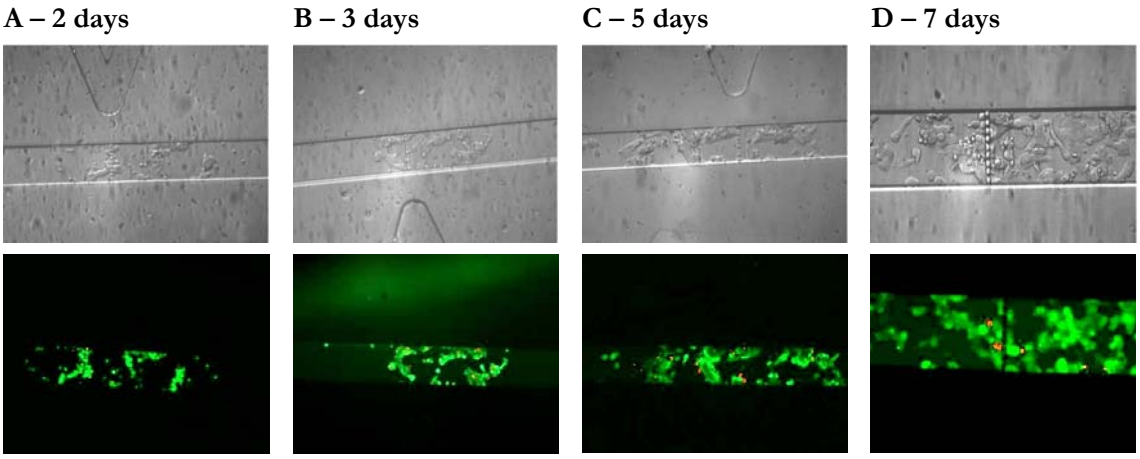

Figure 7-18. Long-term cell culture of MCF-7 cells in apoptosis chip #2. LM and fluorescence pictures of Calcein and PI were taken after **(A)** 2 days, **(B)** 3 days, **(C)** 5 days and **(D)** 7 days. Magnification of the pictures A-C is 10x and of picture D is 20x.

As demonstrated in figure 7-18, the majority of the MCF-7 cells were viable, showing green Calcein staining and rather no red PI fluorescence. MCF-7 cells migrated away from the trap, forming aggregates in the channel, and because of this clustered cell growth, quantifying the viability of the cells was difficult. The thickness of the PDMS (0.1-1.0 mm) and the distance from the trap to the inlet and

outlet did not have an effect on the cell-viability inside the channel, because there was hardly any diffusion of nutrients from the medium into the chip, as the chip was placed in a Petri dish covered with medium in the incubator for long-term cell culture. Cell growth was also better at the inlet and outlet, where the cells were in direct contact with the medium and had no PDMS on top (Figure 7-19).

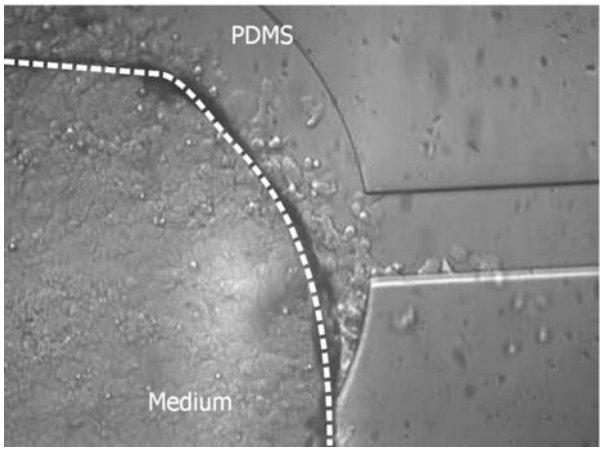

Figure 7-19. LM picture of the cell growth of MCF-7 cells at the inlet at day 5. Cell growth was better at the medium side, forming confluent cell clusters, whereas the cell growth under the PDMS was less pronounced. Magnification is 20x. The dotted line shows the dividing line between cells cultured under the PDMS or in direct contact with the medium.

Applying a flow using the heightened inlet and outlet, drops of CO_2 independent medium fell into the inlet and flowed though the channel, causing an increase in the medium-level at the heightened outlet. However, we did not manage to control the flow. The cell trap and the formation of cellular aggregates, which blocked the trap, caused a disturbed flow. Therefore, apoptosis chip #2 with the experimental flow set-up used, was not suitable, also because the flow set-up was not a closed system and the exact flow rate inside the chip was unknown. A new flow system was designed, in which pipette tips were punctured through the PDMS. This required larger channels, because puncturing with pipette tips caused a large displacement of liquid in the apoptosis chip #2, which damaged and detached the cells. In the apoptosis chip #3, three different cell types were used, *e.g.,* the endothelial cells HUVEC and HMEC, and the breast cancer cell line MCF-7. All three cell types were successfully cultured in apoptosis chip #3, as demonstrated in figure 7-20. After 2 days, the endothelial cells formed a monolayer, and the MCF-7 cells aggregates.

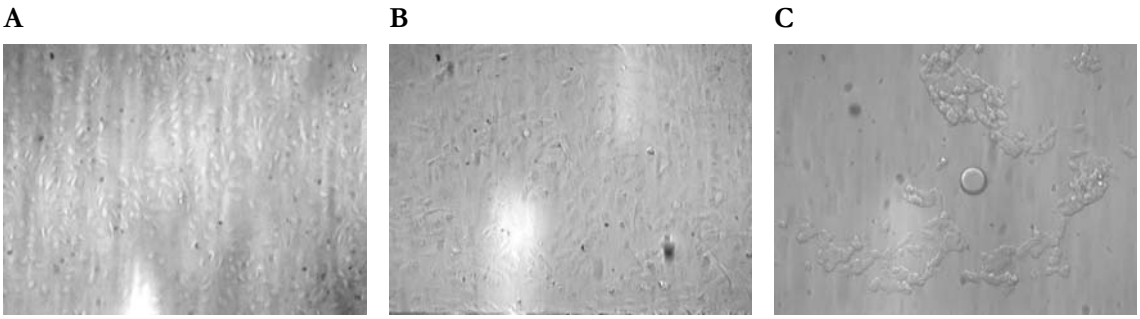

Figure 7-20. Three different cell types were successfully cultured in apoptosis chip #3. **(A)** HUVEC, **(B)** HMEC and **(C)** MCF-7.

Oxygen was provided by the medium as well as through diffusion through the PDMS. The total volume of the chip with a depth of 44 μm is 4.4 μl. The solubility of O_2 in the medium is 2.5 x 10^{-4} mol/L, hence 1.1 x 10^{-9} mol O_2 was dissolved in the medium. The total surface area of the chip is 100 mm^2, the averaged diameter of the cell is about 15 μm, and so about 400.000 cells can be cultivated in the chip. The oxygen consumption per cell per second is 1 x 10^{-16} mol, which for 400.000 cells after 24h gave a total oxygen consumption of 3.456 x 10^{-6} mol. As the medium did not provide the cells with sufficient oxygen, the rest of the oxygen should be provided by diffusion through the PDMS. With equation 7-2, 4.428 x 10^{-6} mol O_2 could flux through the PDMS per day. Hence, enough oxygen was provided.

Connecting the apoptosis chip #3 to the flow system was performed by puncturing the white pipette tips through the PDMS, as demonstrated in figure 7-15C. This caused a displacement of liquid in the chip. However, the cells stayed nicely attached, because in apoptosis chip #3, the larger surface area caused the net effect of liquid displacement on the cells to be smaller than compared to apoptosis chip #2. For the endothelial cells, the flow rate was set in such a way that the shear stress was around 10 dyne/cm^2, as endothelial cells need a shear stress for development and survival, as discussed in paragraph 7.3.2. For MCF-7 cells control experiments were performed to check the viability at different flow rates. Experiments were performed after an adhesion time of 2 days in the incubator. The shear stress has to be kept as small as possible, because *in vivo* the flow of the required nutrients and gases and the removal of waste products are mainly performed by diffusion. Unfortunately, air bubbles appeared after the flow was applied for > 6h. De-gassing the medium with either a vacuum pump or an

ultrasonic bath prior to experiments did not help. Probably, the medium underwent changes at room temperature, resulting in air bubble formation. Increasing the temperature lowers the gas solubility. Temperature changes from room temperature (syringe) to 37°C (chip), or the pressure needed to pump medium through the chip could account for the appearance of air bubbles. Larger tubing could prevent the formation of air bubbles. Nevertheless, a flow rate < 1.5 µl/min (< 0.5 dyne/cm^2 for a d of 44 µm) preserved the viability of MCF-7 cells (Figure 7-21). Moreover, the shear stress in the middle of the channel (with the pillars) was even smaller, because here the width is a factor 3.33 broader (1.5 mm vs. 5 mm). Hence, the viability of MCF-7 cells was preserved if the aggregate-like morphology was retained and MCF-7 cells did not become round in shape.

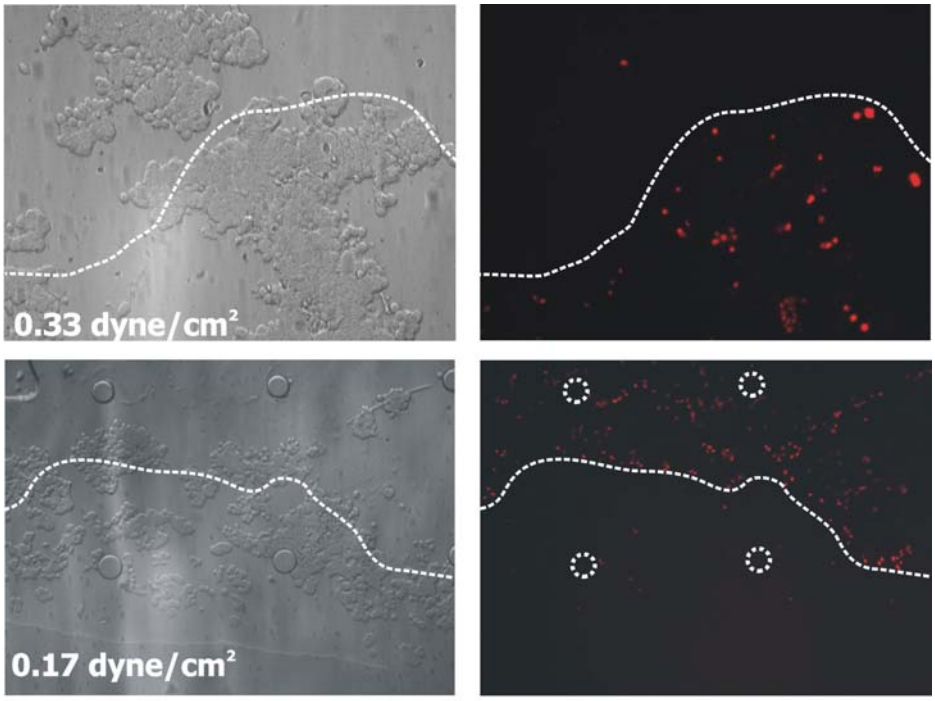

Figure 7-21. MCF-7 cells cultured in apoptosis chip #3 under continuous flow of 1 µl/min (0.33 dyne/cm^2) or 0.5 µl/min (0.17 dyne/cm^2). Left shows LM pictures with the corresponding PI fluorescent pictures at the right. Magnification is 20x.

7.6 Conclusion

In this chapter different microfluidic devices were analysed for their suitability to perform complex cell based analysis. In our case, demonstrating the effects of

different drugs on the apoptotic pathway, and establishing a platform to perform high-throughput drug screening, with future steps towards personalized medicine. First, microfluidic devices, which were present in our laboratory, were screened. In the beginning it was not certain which device would meet the requirements and proved the best to perform apoptosis studies using adherent cell types. Different factors, such as materials, channel geometry, and flow profile, influenced the set-up and outcome of the experiments. As the first apoptosis experiments performed on chip needed only a channel with an inlet and outlet to connect the flow, apoptosis chip #3 was favoured. Moreover, this microfluidic device met all the requirements to perform apoptosis studies using adherent cell types, such as long-term cell culture, the connection to a flow system, optical analysis and the use of disposable materials. Preliminary apoptosis studies were performed in the microfluidic cell trap device, the Meander chip and apoptosis chip # 3 and these results will be discussed in chapter 8.

7.7 Acknowledgements

For the overall fabrication of the different microfluidic devices and for technical assistance, Jan van Nieuwkasteele and Paul ter Braak are gratefully acknowledged. For the design of the microfluidic cell trap chip, Nicolas Demierre and for the Meander chip, Jurjen Emmelkamp is thanked. Lionix is acknowledged for the fabrication of apoptosis chip #1. Job Komen is acknowledged for the design and fabrication of apoptosis chip #2 and Severine Le Gac for designing and fabricating apoptosis chip #3.

7.8 References

1. Lu H, Jensen KF. Cellular and subcellular analysis on chip. In "Lab-on-Chips for Cellomics: Micro and nanotechnologies for Life Science", ed. H. Andersson and A. van den Berg, Kluwer Academic Publishers 2004.
2. Peterson SL, McDonald A, Gourley PL, Sasaki DY. Poly(dimethylsiloxane) thin films as biocompatible coatings for microfluidic devices: Cell culture and flow studies with glial cells. *J Biomed Mater Res* 2005; **72A**: 10-18.

3. Faid K, Voicu R, Bani-Yaghoub, Tremblay R, *et al.* Rapid fabrication and chemical patterning of polymer microstructures and their applications as a platform for cell cultures. *Biomed Microdevices* 2005; **7**: 179-184.
4. Prokop A, Prokop Z, Schaffer D, Kozlov E, *et al.* NanoLiterBioReactor: Long-term mammalian cell culture at nanofabricated scale. *Biomed Microdevices* 2004; **6**: 325-339.
5. Walker GM, Zeringue HC, Beebe DJ. Microenvironment design considerations for cellular studies. *Lab Chip* 2004; **4**: 91-97.
6. Merkel TC, Bondar VI, Nagai K, Freeman BD, *et al.* Gas sorption, diffusion, and permeation in poly(dimethylsiloxane). *J Polym Sci Part B – Polym Phys* 2000; **38**: 415-434.
7. McDonald JC, Duffy DC, Andersson JR, Chiu DT, *et al.* Fabrication of microfluidic systems in poly(dimethylsiloxane). *Electrophoresis* 2000; **21**: 27-40.
8. Futai N, Gu W, Song JW, Takayama S. Handheld recirculation system and customized media for microfluidic cell culture. *Lab Chip* 2006; **6**: 149-154.
9. Tourovskaia A, Figueroa-Masot X, Folch A. Differentiation-on-a-chip: A microfluidic platform for long-term culture studies. *Lab Chip* 2005; **5**: 14-19.
10. Leclerc E, Sakai Y, Fujii T. Cell culture in 3-dimensional microfluidic structure of PDMS (polydimethylsiloxane). *Biomed Microdevices* 2003; **5**: 109-114.
11. Leclerc E, Sakai Y, Fujii T. Microfluidic PDMS (polydimethylsiloxane) bioreactor for large-scale culture of hepatocytes. *Biotechnol Prog* 2004; **20**: 750-755.
12. Sakai Y, Leclerc E, Fujii T. Microfluidic cell-culture devices: Towards in vitro liver tissue reconstitution. In "Lab-on-Chips for Cellomics: Micro and nanotechnologies for Life Science", ed. H. Andersson and A. van den Berg, Kluwer Academic Publishers 2004.
13. Leclerc E, David B, Griscom L, Lepioufle B, *et al.* Study of osteoblastic cells in a microfluidic environment. *Biomaterials* 2006; **27**: 586-595.
14. Kim MS, Yeon JH, Park JK. A microfluidic platform for 3-dimensional cell culture and cell-based assays. *Biomed Microdevices* 2007; **9**: 25-34.
15. Torisawa Y, Takagi A, Nashimoto Y, Yasukawa T, *et al.* A multicellular sheroid array to realize spheroid formation, culture, and viability assay on a chip. *Biomaterials* 2007; **28**: 559-566.

16. Frisk T, Rydholm S, Andersson H, Stemme G, Brismar H. A concept for miniaturized 3-D cell culture using an extracellular matrix gel. *Electrophoresis* 2005; **26**: 4751-4758.
17. Brody JP, Yager P, Goldstein RE, Austin RH. Biotechnology at low Reynolds numbers. *Biophys J* 1996; **71**: 3430-3441
18. Fleischaker RJ, Sinskey AJ. Oxygen demand and supply in cell culture. *Appl Microbiol Biotechnol* 1981; **12**: 193-197.
19. Mehta G, Mehta K, Sud D, Song JW, *et al.* Quantitative measurement and control of oxygen levels in microfluidic poly(dimethylsiloxane) bioreactors during cell culture. *Biomed Microdevices*. Accepted for publication (2006).
20. Vollmer AP, Probstein RF, Gilbert R, Thorsen T. Development of an integrated microfluidic platform for dynamic oxygen sensing and delivery in a flowing medium. *Lab Chip* 2005; **5**: 1059-1066.
21. Mehta K, Linderman JJ. Model-based analysis and design of a microchannel reactor for tissue engineering. Biotechnol Bioeng 2006; 94: 598-609.
22. Charati SG, Stern SA. Diffusion of gases in silicone polymers: Molecular dynamics simulations. Macromolecules 1998; 31: 5529-5535.
23. Allen JW, Bhatia SN. Formation of steady-state oxygen gradients in vitro. *Biotechnol Bioeng* 2003; **82**: 253-262.
24. Kaiser D, Freyberg MA, Friedl P. Lack of hemodynamic forces triggers apoptosis in vascular endothelial cells. *Biochem Biophys Res Commun* 1997; **231**: 586-590.
25. Freyberg MA, Kaiser D, Graf R, Vischer P, Friedl P. Integrin-associated protein and thrombospondin -1 as endothelial mechanosensitive death mediators. *Biochem Biophys Res Commun* 2000; **271**: 584-588.
26. Li YSJ, Haga JH, Chien S. Molecular basis of the effects of shear stress on vascular endothelial cells. *J Biomech* 2005; **38**: 1949-1971.
27. Healy ZR, Lee NH, Gao X, Goldring MB, *et al.* Divergent responses of chondrocytes and endothelial cells to shear stress: Cross-talk among COX-2, the phase 2 response, and apoptosis. *PNAS* 2005; **102**: 14010-14015.
28. Lu H, Koo LY, Wang WM, Lauffenburger DA, *et al.* Microfluidic shear devices for quantitative analysis of cell adhesion. *Anal Chem* 2004; **76**: 5257-5264.
29. Schwachtgen JL, Houston P, Cambell C, Sukhatme V, Braddock M. Fluid shear stress activation of egr-1 transcription in cultured human endothelial and

epithelial cells is mediated via the extracellular signal-related kinase 1/2 mitogen-activated protein kinase pathway. *J Clin Invest* 1998; **101**: 2540-2549.

30. Kaysen JH, Cambell WC, Majewski RR, Goda FO, *et al.* Select de novo gene and protein expression during renal epithelial cell culture in rotating wall vessels is shear stress dependent. *J Membrane Biol* 1999; **168**: 77-89.
31. Summers Moss M, Sisken B, Zimmer S, Andersson KW. Adhesion of nonmetastatic and highly metastatic breast cancer cells to endothelial cells exposed to shear stress. *Biorheology* 1999; **36**: 359-371.
32. Gomes N, Berard M, Vassy J, Peyri N, *et al.* Shear stress modulates tumour cell adhesion to the endothelium. *Biorheology* 2003; **40**: 41-45.
33. Chotard-Ghodsnia R, Haddad O, Leyrat A, Drochon A, *et al.* Morphological analysis of tumor cell/endothelial cell interactions under shear flow. *J Biomech* 2007; **40**: 335-344.
34. Bartsch JE, Staren ED, Appert HE. Adhesion and migration of extracellular matrix-stimulated breast cancer. *J Surg Res* 2003; **110**: 287-294.
35. Valero A. Single cell electroporation on chip. *Thesis* 2006. ISBN 90-365-2416-4.
36. Emmelkamp J, Wolbers F, Andersson H, DaCosta RS, *et al.* The potential of autofluorescence for the detection of single living cells for label-free cell sorting in microfluidic systems. *Electrophoresis* 2004; **25**: 3740-3745.

8

Apoptosis chip for drug screening

Apoptosis is one of the most important topics in the field of cellular science, and plays a role in health and disease. In tumourigenesis, the process of apoptosis is disturbed, which provide tumour cells with the ability to metastasize to and invade other organs, hence having an anoikis-resistant phenotype. To explore the morphological mechanisms underlying this phenomenon, a microfluidic chip was developed to analyse the drug-specific responses of various apoptotic stimuli in real-time at a single-cell level. As a "proof-of-concept", MCF-7 breast adenocarcinoma cells and endothelial cells were treated with different apoptotic stimuli and analysed the conventional way with flow cytometry and a DELFIA® assay and in real-time on chip.

8.1 Introduction

Apoptosis plays a role in health and disease. The homeostatic balance between apoptosis and cell proliferation controls cell number and organ size. Suppression or enhancement of apoptosis is known to cause or contribute to many diseases, such as cancer, neurodegenerative diseases and AIDS.[1] As stated in chapter 2, apoptosis is a very complex biological process to study, as the duration of apoptosis is limited, involving single cells with morphological changes only after the "point-of-no-return", ending in phagocytosis without reaction in the neighbouring cell. Nowadays, a number of techniques are available to detect apoptosis, though they have limitations.[2] Microfluidic chip technology can overcome these limitations and enables the study of apoptosis in real-time at a single-cell level with high-throughput. This will give valuable additional and complementary information to existing conventional methods.[3,4]

Breast cancer strikes more women than any other cancer. Worldwide, every year one million women are diagnosed with breast cancer.[5] Currently, the ideal endocrine therapy for breast cancer still needs to be elucidated. 'Ideal' in this case refers to individual, because of genetic variation every patient will have an individual response to therapy. Therefore, *ex vivo* experiments need to be carried out using a patient's own breast cancer cells, obtained via biopsy, and analyse the balance between proliferation and apoptosis to make an optimal selection of cytotoxic treatment.

Apoptosis can be induced by numerous triggers, one of them being loss of cell anchorage, a process termed "anoikis", meaning "homelessness" in Greek.[6] Cell anchorage not merely provides structural anchorage for a cell, but mediates important survival signals to the cells.[6,7] The disturbance of cell anchorage will activate the cell death program immediately, thereby controlling tissue homeostasis. Moreover, adherent cells need to have the space to spread, as maintenance of the round phenotype will convict these cells to undergo apoptosis.[8] In tumourigenesis the homeostasis is disturbed, because malignant cells have acquired properties rendering them resistant to the loss of cell anchorage and anoikis.[9] Hence, these tumour cells are able to detach from the primary tumour without undergoing apoptosis and therefore are able to metastasize and invade other parts of the body, of which the precise mechanism still remains an enigma.[10]

The anchorage of cells to components of the extracellular matrix is mediated via integrins, and the cell-cell anchorage is mediated via cadherins. Cell-cell anchorage can overcome anoikis when loss of cell-matrix anchorage has occurred. Both the integrins and cadherins propagate signals into the cell activating various signal transduction cascades which connect adhesion to suppression of apoptosis.[7,11,12] At the core of this signalling pathway is focal adhesion kinase (FAK). After FAK, a web of signalling networks spreads.[7,11-13] The serin-threonin kinase protein kinase B (PKB)/AKT seems to have a central role in this cell survival signalling, as the integrin- , growth factor-, and cell-cell/matrix anchorage-mediated signal transduction mostly converge to the activation of this kinase.[7,12] PKB/AKT has multiple inhibitory effects on the apoptotic machinery, such as inactivation of caspase 9 and the pro-apoptotic protein Bad. Cessation of PKB/AKT signalling causes the translocation of Bad to the mitochondria, altering the Bad/Bcl-2 ratio, resulting in cytochrome c release and the activation of caspases.[7,13] However, this is not the only pathway influencing the process of anoikis. The activation of JNK and cleavage of the MAP/ERK kinase kinase -1 (MEKK-1) also plays a role in the initiation and execution of anoikis, which eventually merge in the activation of the caspases. In the signalling routes described above, apoptosis is controlled via the mitochondrial pathway. However, the Fas-receptor mediated signalling pathway also plays a role in anoikis, mediated via the interaction of Fas-ligand to the Fas-receptor, implicating a mitochondria-independent pathway resulting in caspase activation.[7,12,14] Overall, each cell type chooses it specific signal transduction pathway to activate the process of anoikis.

In mammary epithelial cells, the loss of cell-anchorage results in Bax distribution to the mitochondria, cytochrome c release, followed by caspase 3 activation and subsequently by cell death.[14] Hence, the death receptor mediated pathway to activate caspases is not involved. The opposite is the case for endothelial cells. Attached endothelial cells are resistant to Fas-mediated killing, though in response to specific stimuli (TNF-α) or injury these cells become sensitized for Fas- mediated apoptosis, via the up-regulation of the Fas receptor and the down-modulation of the endogenous caspase-8 inhibitor, c-Flip.[15]

In the course of malignant transformation, tumour cells have required resistance to anoikis, related to metastatic progression. Oncogenic growth involves irregularity of several pathways. In breast tumours, high levels of Bcl-2 and Bcl-X_L are frequently

found, though their effect depends on the genetic background of these tumours. Breast tumours with low adhesion ability which over-express Bcl-2 and Bcl-X_L have increased metastatic potential. This improved tumour cell survival, without cellular adhesion, enhances anchorage-independent growth, which might cause metastasis. This metastatic response is aborted in breast cancer cells that have not escaped the extracellular matrix control and die in non-adherent conditions, even when the anti-apoptotic proteins Bcl-2 and Bcl-X_L are overexpressed.[16] As acquisition of resistance to anoikis is an essential step in the development of the malignant phenotype, inhibitors of anoikis may provide a therapeutic strategy to selectively target malignant cells proliferating at inappropriate locations. MEKK-1 inhibitors render anoikis-resistant breast cancer cells sensitive to anoikis, particularly in breast cancer cells which depend on ERK for growth and survival.[17] Furthermore, TRAIL may be used to specifically target circulating tumour cells, before they attach and colonize to sites where they may have the potential to form tumours, as anchorage suppresses the expression and cytotoxic effects of TRAIL on breast cancer cells.[18]
Our focus is on evaluating the effects of various drugs on the apoptotic pathway in normal mammary epithelial cells and breast cancer cells. As in tumour cells, the process of apoptosis and anoikis are disturbed, this hopefully will help us in elucidating the mechanisms underlying these differences on a morphological basis. Microfluidic chip technology is used as an experimental platform, enabling dose-response analysis with high-throughput using different cell types and be monitoring drug-specific responses in real-time at a single-cell level, demands not easily performed with conventional techniques. First, the apoptotic response of the breast adenocarcinoma cell line MCF-7 in the presence of various drugs in a newly developed microfluidic chip is analysed, to evaluate and further optimise the experimental set-up. At the end preferably this microfluidic chip will be easily implementable in various clinical settings to improve not only breast cancer therapy, but fine-tune multiple therapies and treatment of diseases for further steps towards personalized medicine. To our best knowledge, such apoptosis experiments have not been performed on chip so far.

8.2 Materials and Methods

8.2.1 MCF-7

The estrogen receptor (ER) positive invasive lobular carcinoma cell line MCF-7 (DSMZ, Braunschweig, Germany) was grown in Roswell Park Memorial Institute (RPMI)-1640 medium supplemented with 10% (v/v) foetal bovine serum (FBS) gold, 100 IU/ml penicillin, 100 μg/ml streptomycin, 2 mM L-glutamine and 0.4 μg/ml fungizone. Media and supplements were all obtained from Cambrex (Verviers, Belgium), except for FBS gold which was obtained from PAA (Pasching, Austria). Cells cultures were sustained in a 5% CO_2 humidified atmosphere at 37°C. The medium was refreshed every 3-4 days and cultures were split weekly at a ratio of 1:3 – 1:6 after treatment with versene in aqua dest. Versene consists of aqua dest. with 137 mM NaCl, 1.47 mM KH_2PO_4, 2.68 mM KCl, 7.37 mM $Na_2HPO_4.2H_20$ and 0.54 mM NA_2EDTA dissolved.

8.2.2 Human umbilical vein endothelial cells (HUVEC)

Freshly isolated HUVEC were grown on 2 mg/ml fibronectin coated culture flasks. The culture medium consisted of EBM-2 medium, supplemented with 2% FBS, growth factors (*e.g.,* hFGF (human fibroblast growth factor), VEGF (vascular endothelial growth factor), R^3-IGF (insulin-like growth factor) and hEGF (human epidermal growth factor)), hydrocortisone, ascorbic acid, heparin and the antibiotics gentamicin sulphate/amphotericin B (EGM-2 Bulletkit, CC-3162, Cambrex, Verviers, Belgium). Cell cultures were sustained in a humidified atmosphere at 37°C and 5% CO2. The medium was refreshed every 3-4 days. Confluent cultures were subcultured after detachment with trypsin solution (0.05% trypsin/0.02% EDTA in PBS; Cambrex, Verviers, Belgium).

8.2.3 Human micro-vascular endothelial cells (HMEC)

HMEC (generous gift from Dr. P. Koolwijk, TNO, Leiden, The Netherlands) were grown on 2 mg/ml fibronectin coated culture flasks. The culture medium consisted of EBM-2 medium, supplemented with 2% FBS, growth factors (*e.g.,* hFGF

(human fibroblast growth factor), VEGF (vascular endothelial growth factor), R^3-IGF (insulin-like growth factor) and hEGF (human epidermal growth factor)), hydrocortisone, ascorbic acid, heparin and the antibiotics gentamicin sulphate/amphotericin B (EGM-2 Bulletkit, CC-3162, Cambrex, Verviers, Belgium). Cell cultures were sustained in a humidified atmosphere at 37°C and 5% CO2. The medium was refreshed every 3-4 days. Confluent cultures were subcultured after detachment with trypsin solution (0.05% trypsin/0.02% EDTA in PBS; Cambrex, Verviers, Belgium).

8.2.4 Conventional apoptosis assays

8.2.4.1 Annexin V and PI

MCF-7 cells were cultured in 6 wells plates (concentration 0.2 x 10^6 cells/ml) in the presence of different apoptotic inducers. Cells were treated with 3 nM TNF-α in combination with 50 μM CHX, 0.15 μM CPT, the protein kinase inhibitor staurosporine (SSP; Sigma) in a concentration of 1 μM and 20 μM, and the SERM tamoxifen in a concentration of 20 μM in the incubator for 6h and 24h. Untreated MCF-7 cells served as a control. After incubation, the supernatant and the MCF-7 cells were collected and washed with PBS once. The pellet was resuspended in HEPES buffer containing 137 mM NaCl, 2.68 mM KCl, 10 mM HEPES, 1.7 mM $MgCl_2$, 25 mM Glucose and 2.5 mM $CaCl_2.H_2O$ (pH adjusted to 7.4). Annexin V (AV, FITC conjugate, generous gift from Dr. C. Reutelingsperger, PharmaTarget, Maastricht, The Netherlands) was added to give a final concentration of 0.01 μg/ml and samples were incubated in the dark for 20 minutes. Thereafter, PI was added (final concentration 0.2 μg/ml) and samples were immediately analysed with flow cytometry. Annexin V and PI fluorescence of individual cells was measured with a Beckman Coulter Cytomics FC500 flow cytometer. Excitation was elicited with the Argon laser at 488 nm and measured with the use of the FL-1 (Annexin V) and the FL-3 (PI) channels.

8.2.4.2 DELFIA assay

MCF-7 and HUVEC cells were cultured in 24 wells plates (80.000 cells per well). For HUVEC the surface was pre-coated with fibronectin. Apoptosis was induced

using 3 nM TNF-α in combination with 50 μM CHX and 1 μM SSP for 6h and 24h. The DELFIA® assay was performed as described previously by Engbers-Buijtenhuijs *et al.*[19] Briefly, Annexin V (AV; generous gift from Dr. C. Reutelingsperger, PharmaTarget, Maastricht, The Netherlands) was labelled with Europium to obtain Eu^{3+}-labelled AV, which was purified with gel filtration, resulting in a final concentration of 0.4 g/L. The three fractions of the adherent cell cultures (*e.g.,* MCF-7 and HUVEC) grown in 24 wells plates, were prepared and analysed as represented schematically in figure 8-1.

A

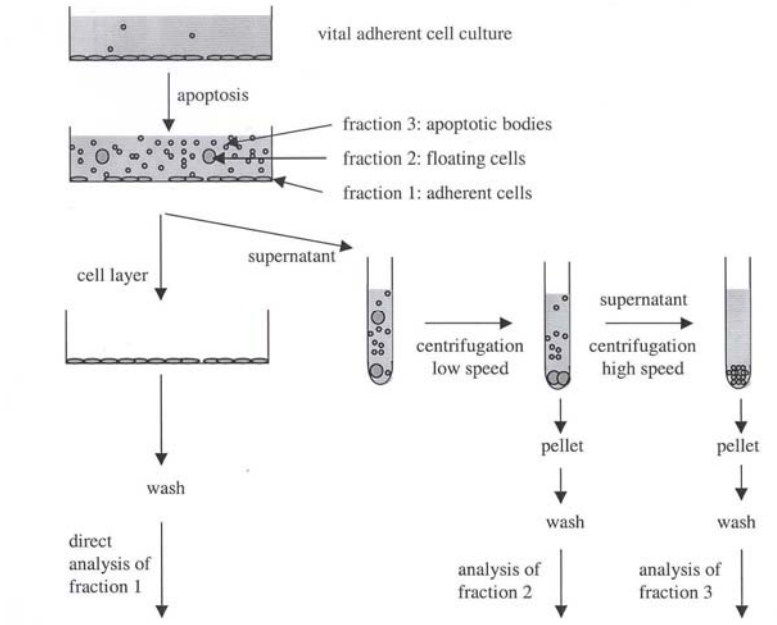

B

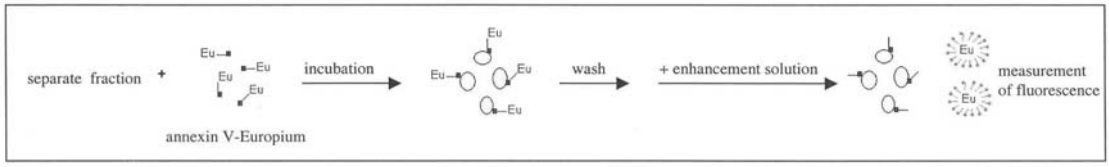

Figure 8-1. Work flow diagram of the different steps involved in the Europium-labelled AV time resolved fluorometric assay to analyse the cell death cascade. **(A)** Three fractions of the adherent cell cultures were prepared. Fraction 1 consisted of adherent cells, analysed while attached on their support, hence no treatment with trypsin or versene. Fraction 2 contained detached cells due to anoikis (floating cells) and fraction 3 contained apoptotic bodies. Both fractions 2 and 3 were present in the culture medium and isolated by differential centrifugation steps. **(B)** Apoptosis was then analysed in the three separate fractions by using the DELFIA® principle.[20] The DELFIA® assay utilises a Europium label which becomes highly fluorescent in the presence of enhancement solution. Published with permission of Engbers-Buijtenhuijs *et al.*[19]

The supernatant of the wells was collected and centrifuged at low speed (1'000 g, 3 min room temperature (RT)), to separate the floating cells (fraction 2) from the apoptotic bodies (fraction 3). The supernatant was centrifuged at high speed (3'500 g, 15 min, RT), and this pellet contained the apoptotic bodies. The three fractions were washed separately with HEPES buffer (see 8.2.4.1). Adherent cells (fraction 1) were then incubated with Europium-labelled AV in HEPES buffer in the dark (RT) for 30 minutes, to obtain a final concentration of 0.2 mg/ml. The pellets containing the floating cells (fraction 2) and the apoptotic bodies (fraction 3) were resuspended in Europium-labelled AV in HEPES buffer and incubated in the dark (RT) for 30 minutes, to obtain a final concentration of 0.2 mg/ml. The three separate fractions were washed with HEPES buffer and incubated with commercially available enhancement solution[20] at RT for 5 min to convert the Europium label to the highly fluorescent state. Time resolved fluorescence was measured in each sample on a Viktor fluorescence analyser (PerkinElmer, Waltham, MA, USA). Excitation and emission wavelengths were 340 and 615 nm, respectively. Fluorescence was normalised against untreated cultures and a-specific binding, using Europium-labelled IgG, was subtracted.

8.2.5 On-line apoptosis measurements

8.2.5.1 Time-lapse recording using conventional cell culture equipment

HMEC and MCF-7 cells were cultured in a Petri dish or in a Nunc culture chamber (Lab-Tek™ Chamber slide™ system, Roskilde, Denmark). For HMEC, the polystyrene surface (Petri dish) was precoated with 2 mg/ml fibronectin in the incubator for 1h and the borosilicate surface (Nunc chamber) with 0.1 % APS at room temperature overnight. Cells adhered in the incubator for 24h, prior to apoptosis treatment. Apoptosis was initiated with a mixture of 3 nM TNF-α and 50 μM CHX in CO_2 independent medium. The culture dish was placed at the microscope stage for time-lapse recording of the apoptotic process. For fluorescence measurements, cells were either incubated with solely the death dye PI, or incubated with a mixture of Annexin V in combination with PI. Annexin V (AV; FITC conjugate; NeXins-Molecular Probes, Eugene, Oregon, USA) was diluted 1:8

in HEPES buffer according to the manufacturer's instructions. PI was used in a final concentration of 1 μg/ml. The microscope system was described in detail in chapter 7 (paragraph 7.4).

8.2.5.2 Apoptosis on chip

Microfluidic cell trap chip

MCF-7 cells were loaded in the microfluidic cell trap chip with a pipette, placed in a Petri dish covered with $RPMI^+$ medium for adhesion in the incubator. Cells adhered to the Pyrex glass between 2h and 5h. The chip was placed in the chip holder and connected to the syringe pump, as described in paragraph 7.5.1. The flow rate was set at 1 μl/min or 10 μl/h. The medium used, was CO_2 independent medium, supplemented with 3 nM TNF-α and 50 μM CHX to initiate apoptosis. Morphological changes were assessed in time using the microscope system as described in chapter 7 (paragraph 7.4).

Meander

MCF-7 cells were loaded in the Meander chip (d= 100 μm) with a pipette. The (capillary) flow was stopped by covering the chip with $RPMI^+$ medium. The chip was placed in the incubator for overnight adhesion. Before the start of the experiment, the viability was checked with PI (1 μg/ml). Then, the chip was placed in the chip holder and connected to the flow, as described in paragraph 7.5.2. The flow rate was set at 5 μl/h. The medium used, was CO_2 independent medium, supplemented with 50 μM staurosporine (SSP). At the end of the experiment, cells were fluorescently labelled with Annexin V (AV; FITC conjugate; NeXins-Molecular Probes, Eugene, Oregon, USA), diluted 1:8 in HEPES buffer and PI (1 μg/ml). Light microscopy and fluorescent pictures were assessed using the microscope system as described in chapter 7 (paragraph 7.4).

Apoptosis chip #3

MCF-7 cells (~ 4 x 10^6 cells/ml) were loaded in apoptosis chip #3 (d = 44 μm) with a pipette. The chip was placed in a Petri dish, covered with $RPMI^+$ medium, to stop the flow and prevent the chip from drying out. The cells adhered for 2 days, with the medium in the chip replaced every day. Before the start of the experiment, the viability was checked with PI (1 μg/ml). The chip was connected to the flow, as

described in chapter 7.5.3.2 with some minor modifications. Instead of white pipette tips, yellow pipette tips were used, together with larger tubing (inner diameter 2 mm, outer diameter 4 mm). This tube-size directly fitted the plastic syringe, hence needles were not required. Larger tubing was used to prevent air bubbles, which disrupted the measurements. The medium used, was CO_2 independent medium, supplemented with 3 nM TNF-α and 50 μM CHX to initiate apoptosis. At the end of the experiment, cells were fluorescently labelled with Annexin V (AV; FITC conjugate; NeXins-Molecular Probes, Eugene, Oregon, USA), diluted 1:8 in HEPES buffer and PI (1 μg/ml). Light microscopy and fluorescent pictures were assessed using the microscope system as described in chapter 7 (paragraph 7.4).

8.3 Results and Discussion

The apoptotic response in breast cancer cells (MCF-7) and endothelial cells (HUVEC) in the presence of different inducers was first elicited using conventional techniques.

MCF-7 cells were incubated with 3 nM TNF-α in combination with 50 μM CHX, 0.15 μM CPT, the protein kinase inhibitor staurosporine (SSP) in a concentration of 1 μM and 20 μM, and the SERM tamoxifen in a concentration of 20 μM in the incubator for 6h and 24h. The collected supernatant and the cells were analysed for the presence of Annexin V (AV) and PI fluorescence using flow cytometry. However, MCF-7 cells are adherent cells, growing in aggregates, which made it difficult to distinguish between the different phases of the apoptotic process, *e.g.,* early apoptotic, late apoptotic and necrotic. Furthermore, for AV a clear positive peak was not demonstrated. Therefore, the change in either total AV or total PI fluorescence, compared to untreated cells (dashed line), was plotted in arbitrary units (a.u.) (Figure 8-2).

After 6h of incubation, TNF/CHX, CPT and tamoxifen showed a slight increase in AV as well as in PI fluorescence, however, the SD were quite high. The protein kinase inhibitor staurosporine (SSP) demonstrated no change in AV fluorescence after 6h, though PI fluorescence was greatly increased, especially for a SSP concentration of 20 μM. After 24h, most drugs demonstrated a decrease in the AV fluorescence and an increase in the PI fluorescence, with the exception of CPT and

tamoxifen. These drugs showed a decrease in PI fluorescence. CPT and tamoxifen were also the only drugs which showed a higher AV fluorescence compared to untreated cells after 24h. For all the other drugs, the AV fluorescence was below 1.

A

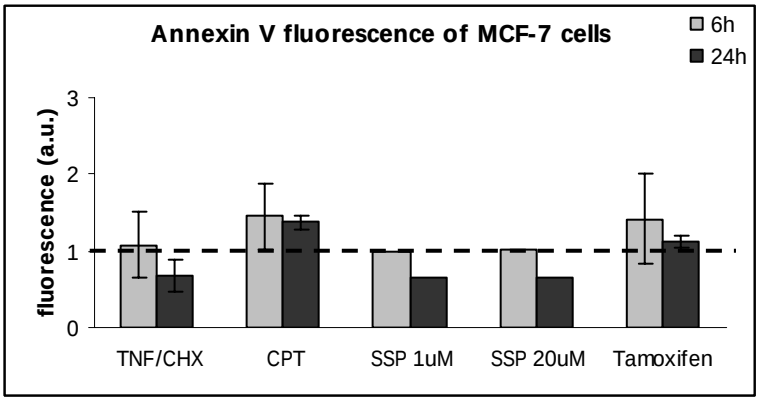

B

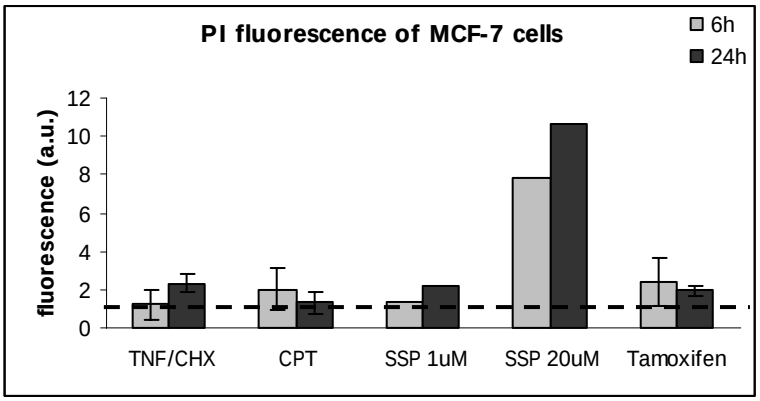

Figure 8-2. Annexin V (AV) and PI fluorescence of MCF-7 cells treated with different drugs. MCF-7 cells were incubated with 3 nM TNF-α in combination with 50 μM CHX, 0.15 μM CPT, the protein kinase inhibitor SSP (1 μM and 20 μM) and the SERM tamoxifen for 6h and 24h. The supernatant and the cells were collected and stained with **(A)** AV and **(B)** PI. Results are from 3 seperative experiments for TNF/CHX, CPT and tamoxifen and from one experiment for SSP. Mean ± SD is shown. Dashed line refers to untreated MCF-7 cells.

These results were compared with light microscopy pictures (Figure 8-3). In this case, the supernatant and MCF-7 cells were collected and spun on to a microscope slide, after which the cells were stained with May Grünwald staining. So, the aggregate-like morphology is not shown as demonstrated in figure 7-3A for untreated MCF-7 cells. The morphology of CPT- and tamoxifen-treated MCF-7 cells demonstrated no clear morphological differences compared to untreated MCF-7 cells, therefore only a slight increase in AV fluorescence was seen and no change in PI fluorescence. Probably these cells were still in the early apoptotic phase. For TNF/CHX-treated MCF-7 cells, the LM picture showed apoptotic

characteristics, such as blebbing of the plasma membrane and condensed nuclei. The flow cytometry data showed only an increase in PI fluorescence after 24h, *e.g.*, the necrotic phase of apoptosis, which did not correspond with the LM pictures, which showed MCF-7 cells in the early/late apoptotic phase of apoptosis. The LM pictures of SSP-treated MCF-7 cells showed necrosis, clearly seen for MCF-7 cells treated with 20 μM SSP for 24h, which corresponded with the flow cytometry data, demonstrating a large increase in PI fluorescence compared to untreated MCF-7 cells.

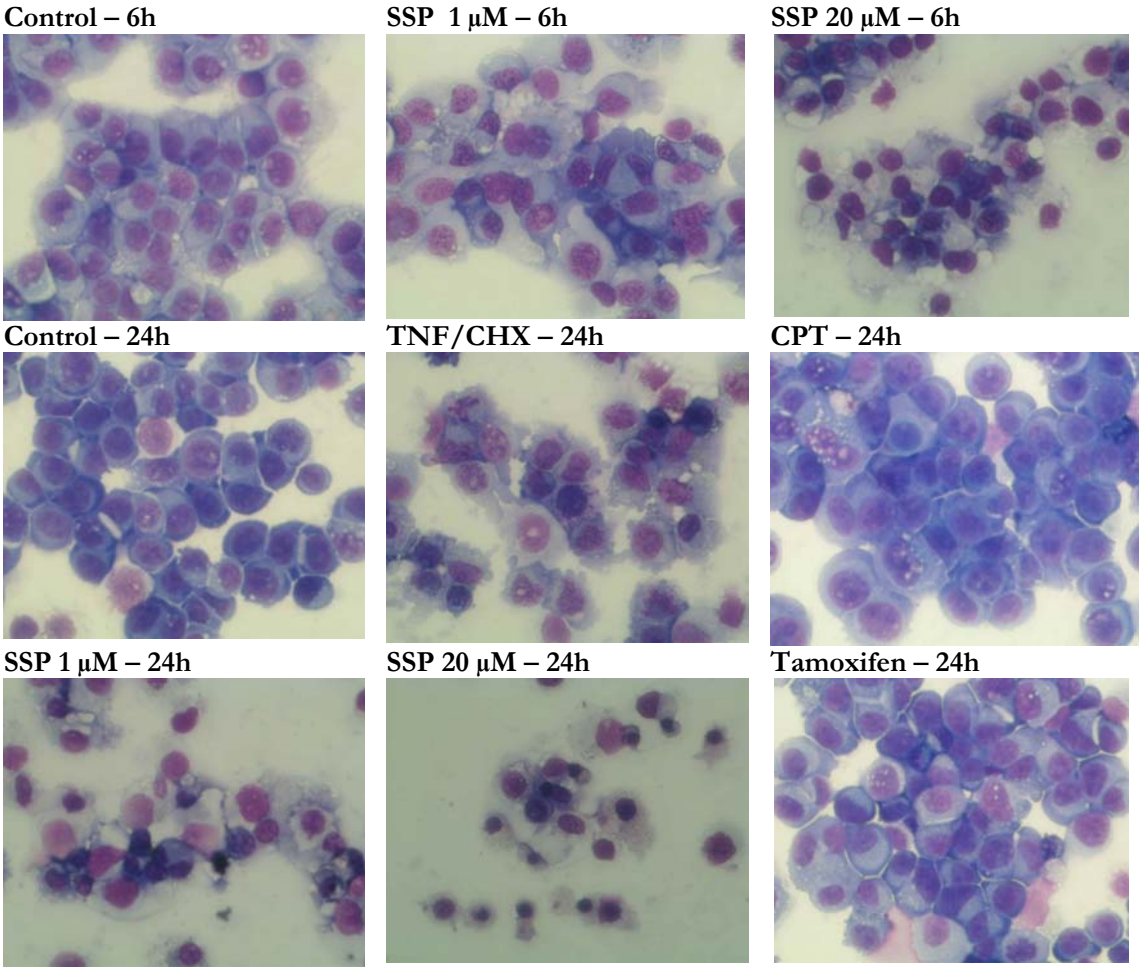

Figure 8-3. LM pictures of MCF-7 cells treated with different drugs. MCF-7 cells were stained with May Grünwald staining. Magnification is 40x.

Although MCF-7 cells lack caspase-3, these cells remain responsive to many apoptotic stimuli.[21] Apoptotic changes are detected as early as 4h in MCF-7 cells treated with 1 μM SSP.[22] MCF-7 cells demonstrate DNA fragmentation and an increase in the binding of AV, which continue to increase in time. These processes

are preceded by cytochrome c release (2h), loss of the mitochondrial membrane potential (3h; caspase-independent process) and Bax translocation to the mitochondrion (3h), which occur before caspases (caspase 6) are activated. Necrotic cell death is also suggested for SSP-treated MCF-7 cells.[23] TNF-α activates multiple signalling pathways, mediating cell survival as well as cell death.[24,25] Activation of the survival pathways results in the activation of the transcription factor NF-κB, resulting in the synthesis of anti-apoptotic proteins, such as Bcl-2. However, the activation of the NF-κB pathway is not sufficient to suppress TNF-α cytotoxicity in combination with the protein synthesis inhibitor CHX, most likely due to prolonged JNK activation. Though, the precise mechanism still needs to be determined, as JNK activation may promote, but is unable to initiate the apoptotic process. The balance between the pro- and anti-apoptotic regulators will define the apoptotic threshold of the cell.[24,25] The pro-apoptotic factor Bak participates in TNF-α-mediated apoptosis in caspase-3 deficient MCF-7 cells.[26] In case of the stimuli CPT and tamoxifen, a different form of programmed cell death plays a role. Apoptosis is the most common form of programmed cell death, nevertheless in recent years, alternative cell death programs have been receiving increasing attention, in particular autophagy has been proposed as an important non-apoptotic cell death mechanism.[27] Historically, autophagy is classified as type 2 programmed cell death (reversible), type 1 referring to apoptosis (irreversible). However, this is a matter of debate, as autophagy is well recognized as a survival mechanism during conditions of nutrient limitations. During the process of autophagy, cytoplasmic contents and organelles are encompassed in double or multi-membrane autophagosomes and subsequently delivered to the lysosomes for destruction. Here both nutrients and energy is generated to maintain the viability of the cell.[27,28] Persistence of autophagy will at the end destruct the cell by eating itself to death, or if normal cellular function cannot be restored, trigger the apoptotic machinery. Autophagic cell death is a process of days and notable for the presence of autophagic vacuoles in the dying cells, the nucleus and cytoskeleton remain intact. Various anti-cancer therapies induce autophagy in different cancer cell types.[29] However, whether autophagy in response to therapies is pro-death or pro-survival is still controversial. Tamoxifen and other anti-estrogens induce autophagy in breast cancer MCF-7 cells, and in this setting autophagy serves as a cell death program.[30] Ionizing radiation also induces autophagy in breast cancer cells, though here it

serves as a protective mechanism that allows cells to escape from apoptosis. High concentrations of tamoxifen (> 1 μM) induces rapid cell death within 60 minutes, showing cytochrome c release, a decrease in the mitochondrial membrane potential, and an increased production in reactive oxygen species (ROS). These are features of both the apoptotic and the necrotic cell death.[31] In our case, MCF-7 cells treated with 20 μM tamoxifen presented autophagic vacuoles after 24h (Figure 8-3), which increased in time (Figure 8-4A black arrows). The response of MCF-7 cells to CPT (0.15 μM) is both apoptosis and autophagy.[28] The process of apoptosis is rapid, with the peak apoptotic cell number observed within 60 minutes after drug administration. Autophagy developed at a much slower rate with continuous progression during the 24h exposure to CPT. Autophagy in the beginning serves a cytoprotective response for cancer cell survival, though as CPT stress persists, the apoptotic death machinery is switched on. In the LM picture both the apoptotic hallmarks as well as the autophagic vacuoles were demonstrated (Figure 8-4B).

A **B**

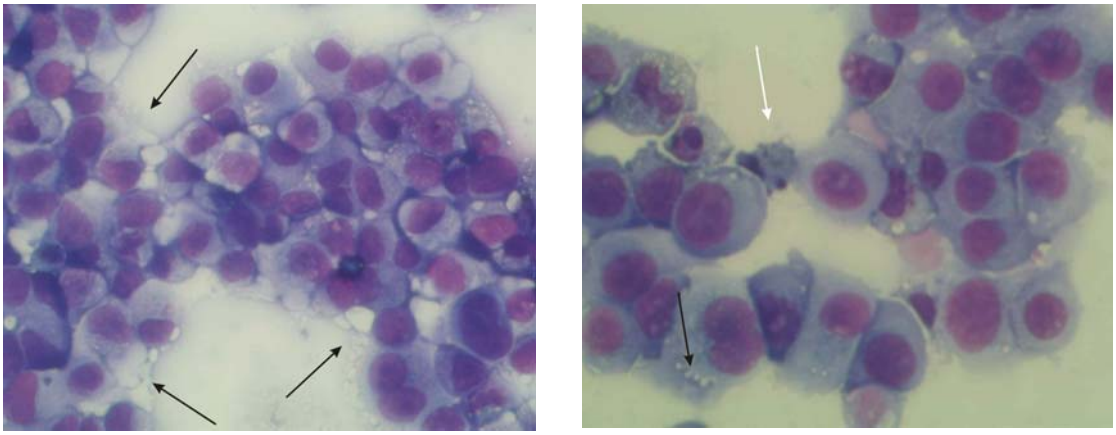

Figure 8-4. LM pictures of MCF-7 cells treated with **(A)** 20 μM tamoxifen or **(B)** 0.15 μM CPT for 48h. MCF-7 cells were stained with May Grünwald staining. Magnification is 40x. Black arrows point to autophagic vacuoles, the white arrow to an apoptotic cell.

It is suggested that the pro-apoptotic factor Bid serves as a molecular switch between apoptosis and autophagy. The expression of Bid (aggregated to Bax on the mitochondria) is crucial in triggering apoptosis in CPT-treated MCF-7 cells.[28,32] Aggregates of Bid/Bax promote the release of apoptogenic factors ("point-of-no-return"), such as cytochrome c and Smac/DIABLO.[33] In contrast to this rapid CPT-induced apoptotic response in MCF-7 cells, other studies have demonstrated that CPT-induced apoptosis develops more slowly in MCF-7 cells, with the AV and

DNA content remaining unchanged during the first 24h.[34] However, caspases become activated.[35] So the delayed apoptotic response and the fact that not all cells which detach from the surface shows activated caspases, reveals a possible role for autophagy.

Flow cytometry measurements are ideally suited to analyse the process of apoptosis in cells in suspension, such as HL60 cells. Though for adherent cells, the occurrence of membrane damage during harvesting these cells, induces apoptosis, producing false-positive results.[36] To circumvent this problem, MCF-7 cells need to be labelled with AV prior to detachment, and detached using mechanical scraping, because EDTA removes bound AV due to chelation of Ca^{2+}-ions. Moreover, sophisticated flow cytometry analysis is affected due to the aggregate-like growth of MCF-7 cells, preserved when cells are put in suspension. Therefore, we used a novel time resolved fluorometric assay using Europium-labelled Annexin V (AV) to measure the process of apoptosis and anoikis in adherent cells. This Dissociation Enhanced Lanthanide Fluoro Immuno Assay (DELFIA®, Wallac, Turku, Finland)[20] utilises a lanthanide metal (Europium) label which is practically non-fluorescent. However, after the binding of Europium-labelled AV to phosphatidyl serine, Europium is efficiently dissociated from the labelled compound (AV) because of the low pH (< 4) of the commercially available enhancement solution. The free Europium ions then rapidly form a new, high fluorescent and stable chelate with the components of this enhancement solution (Figure 8-1B).[19] This DELFIA® assay with Europium-labelled AV was used to measure the occurrence of apoptosis in two different adherent cell types, MCF-7 and HUVEC. Apoptosis was measured in cells which were still attached to the culture surface (fraction 1), in detached cells (floating cells, fraction 2), and cells in the final stage of the apoptotic pathway, *e.g.,* the apoptotic bodies (fraction 3), as represented schematically in figure 8-1A. MCF-7 cells were incubated with 3 nM TNF-α in combination with 50 μM CHX and with 1 μM SSP to induce apoptosis. HUVEC treated with 3 nM TNF-α in combination with 50 μM CHX served as a positive control, as these experiments were already performed by Engbers-Buijtenhuijs *et al.*[19] Figure 8-5 shows that the apoptotic inducers increased the amount of floating cells and apoptotic bodies in time for the two adherent cells types used. Apoptosis is expressed in arbitrary units (a.u.) and defines the increase/decrease in fluorescent intensity (counts) measured

on a Viktor fluorescence analyser. The obtained results of HUVEC treated with TNF-α in combination with CHX were comparable to the results obtained by Engbers-Buijtenhuijs *et al.*[19]

A

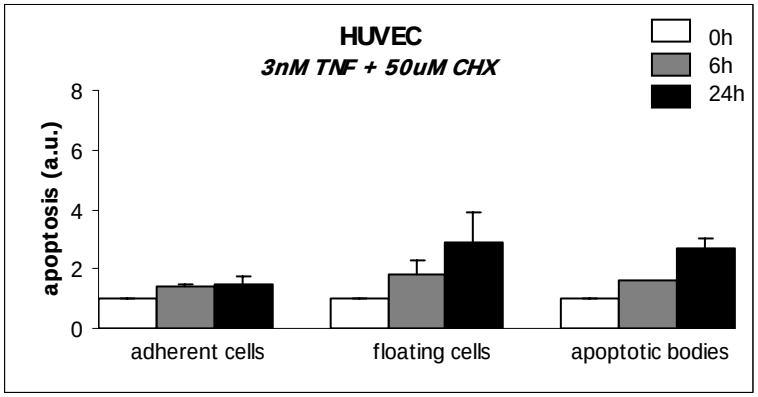

B

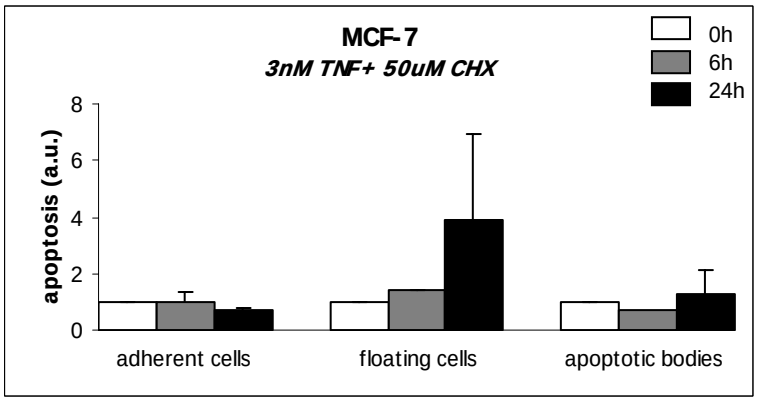

C

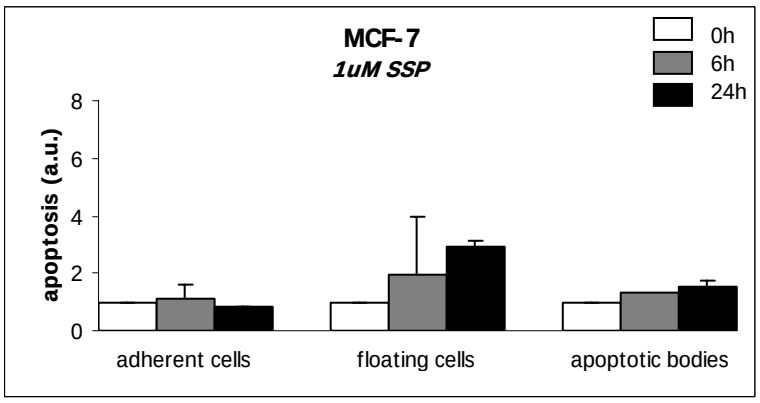

Figure 8-5. Apoptosis measured using the DELFIA® assay. HUVEC and MCF-7 cells were cultured and treated with **(A and B)** 3 nM TNF-α in combination with 50 μM CHX and with **(C)** 1 μM SSP for 6h and 24h. Europium-labelled AV fluorescence was measured in the three separate fractions. Results represent data from 2 individual experiments for each time point and mean ± SD is shown.

The apoptotic response in MCF-7 cells treated with both inducers was not so prominent, as observed in the LM pictures (Figure 8-3). For MCF-7 cells treated with TNF-α mixed with CHX, membrane blebbing and condensed nuclei were shown, and probably these cells were still attached to the surface, so present in the adherent cell fraction. For MCF-7 cells treated with SSP, no clear morphological differences were seen after 6h, and after 24h besides apoptotic characteristics (condensed nuclei), necrosis was also seen. Necrosis was, however, not measured in the DELFIA® assay. Though, for the adherent cell fraction of MCF-7 cells, no increase in fluorescence intensity was measured in the presence of both inducers. Due to detachment of apoptotic cells from their surface (anoikis), fewer cells were present and therefore hardly any increase or even a decrease in fluorescence intensity was demonstrated in this fraction. Figure 8-6 shows the fluorescence intensity of Europium-labelled AV of the MCF-7 adherent cell fraction corrected for the cell numbers. It was difficult to detach the MCF-7 cells after the fluorescence was measured, therefore cell numbers were measured in a separate experiment in which MCF-7 cells were cultured in 24 wells plate in the presence of the used inducers (TNF-α mixed with CHX and SSP). Cell numbers were calculated with a Bürker-Türk counting chamber. For correct cell numbers, this experiment had to be repeated many times to obtain a well-defined factor to correct the fluorescence intensity measured in the adherent cell fraction. Though, due to a lack of time, adherent MCF-7 cell numbers in the presence of different inducers were calculated only once. From these results, a clear trend towards an increase in Europium-labelled AV fluorescence in the adherent cell fraction was demonstrated.

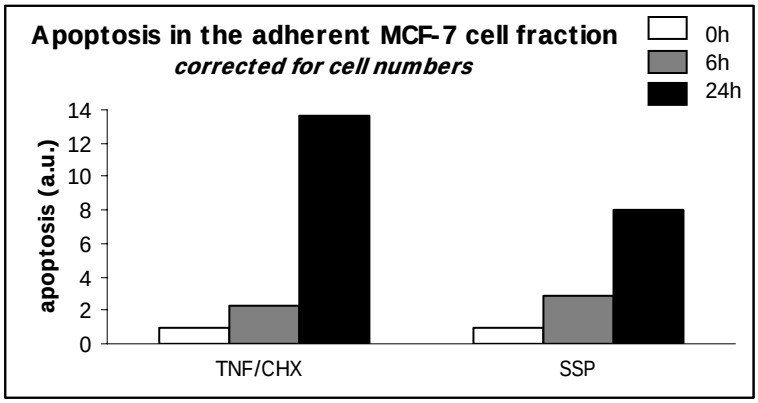

Figure 8-6. Fluorescence intensity of Europium-labelled AV of the MCF-7 adherent cell fraction corrected for the cell numbers.

In microfluidic experiments performed on chip, the adherent cells will not attach to the polystyrene (conventional cell culture equipment), but to different glass materials, such as Pyrex and borosilicate glass (microscope slides). Therefore, DELFIA® experiments were also performed to explore the effects of MCF-7 cells attached to Pyrex glass in the presence of the apoptotic inducers (Figure 8-7).

A

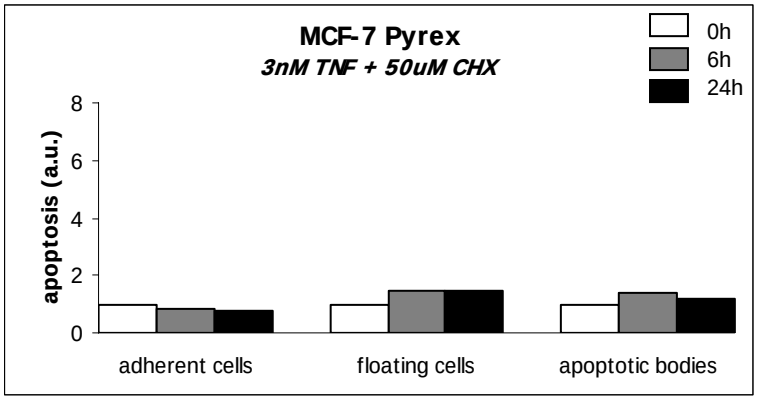

B

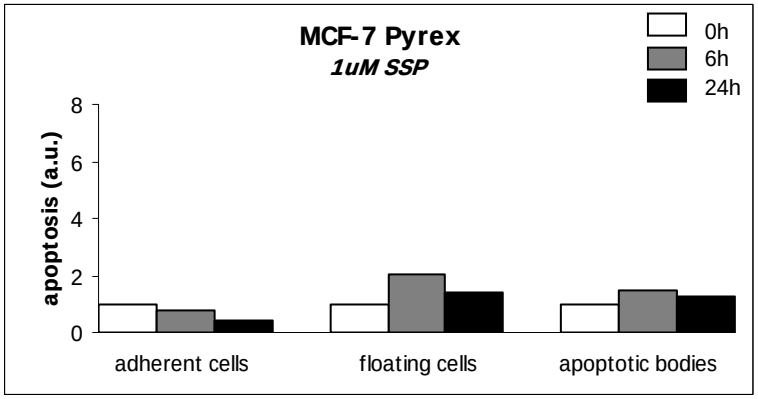

Figure 8-7. Apoptosis measured using the DELFIA® assay. MCF-7 cells were cultured on Pyrex slides and treated with **(A)** 3 nM TNF-α in combination with 50 μM CHX and with **(B)** 1 μM SSP for 6h and 24h. Europium-labelled AV fluorescence was measured in the three separate fractions. Results represent data from one experiment for each time point.

A slight increase in the fluorescence intensity was measured in the fraction with the floating cells and the fraction with the apoptotic bodies. Though, after correcting for the cell numbers in the adherent cell fraction, a large increase in Europium-labelled AV fluorescence was demonstrated (for TNF/CHX 7.29 after 6h and 16.59 after 24h; for SSP 1.71 after 6h and 4.92 after 24h). Probably, MCF-7 cells became apoptotic in response to the inducers, though did not detach. However, a

discrepancy existed in correcting for cell numbers. The fewer MCF-7 cells present in the adherent cell fraction would cause an increase in the number of cells present in the floating cell fraction and the fraction with the apoptotic bodies. However, after correcting for the cell numbers in the adherent cell fraction, the increase in fluorescence intensity was much larger than the total increase in fluorescence intensity in both fraction 2 and 3. Though, due to aggregates, it was difficult to count the MCF-7 cells in a counting chamber, especially the untreated cells. Repeated cell count experiments would overcome this bias. Furthermore, the growth of MCF-7 cells in colonies might also have influenced the outcome of the DELFA® assay, as the binding of Europium-labelled AV might be complicated and hence the fluorescent label did not easily reach every single MCF-7 cell. This did not account for human umbilical vein endothelial cells (HUVEC), as these cells grew in a monolayer.

Our interest is focused on analysing the effects of various drugs on the apoptotic pathway on the basis of morphological differences, using different cell types, for example normal cells vs. tumour cells. In response to apoptotic stimuli, normal (adherent) cells will activate the apoptotic cascade and detach from their surface. Though, will normal cells first become apoptotic and as a final stage detach from their surface in the form of apoptotic bodies? In this case the process is defined as apoptosis-induced anoikis. Or does the apoptotic stimulus function as a trigger for detachment, which will then activate the apoptotic process? This is defined as detachment-induced anoikis. And how is this process regulated in tumour cells, in which the process of apoptosis and anoikis is disturbed? Specific drugs might cause the detachment of tumour cells, but because of genetic modifications, these cells will not die, but instead metastasize to other parts in the body.[9] Though preferably, in response to other stimuli, the apoptotic pathway is stimulated in tumour cells, thereby preventing metastases. These questions cannot be answered with the DELFIA® assay. Therefore, to elucidate the mechanisms which might underlie the differences between normal and tumour cells, on-line monitoring was performed to analyse the differences in morphology and the expression of widely used fluorescent dyes in the presence of various stimuli, to finally characterize the apoptotic process.

First, the response of endothelial cells and breast cancer cells to the apoptotic inducer TNF-α in combination with CHX was analysed in real-time using conventional cell culture equipment.
In response to TNF-α mixed with CHX, HMEC cells got round and detached from their surface like colonies, not single-cells, as demonstrated figure 8-8, which shows the time-lapse recording. In this case, EBM2 medium was replaced by CO_2 independent medium, because the experiments were performed outside the incubator. Apoptosis-induced anoikis was demonstrated.

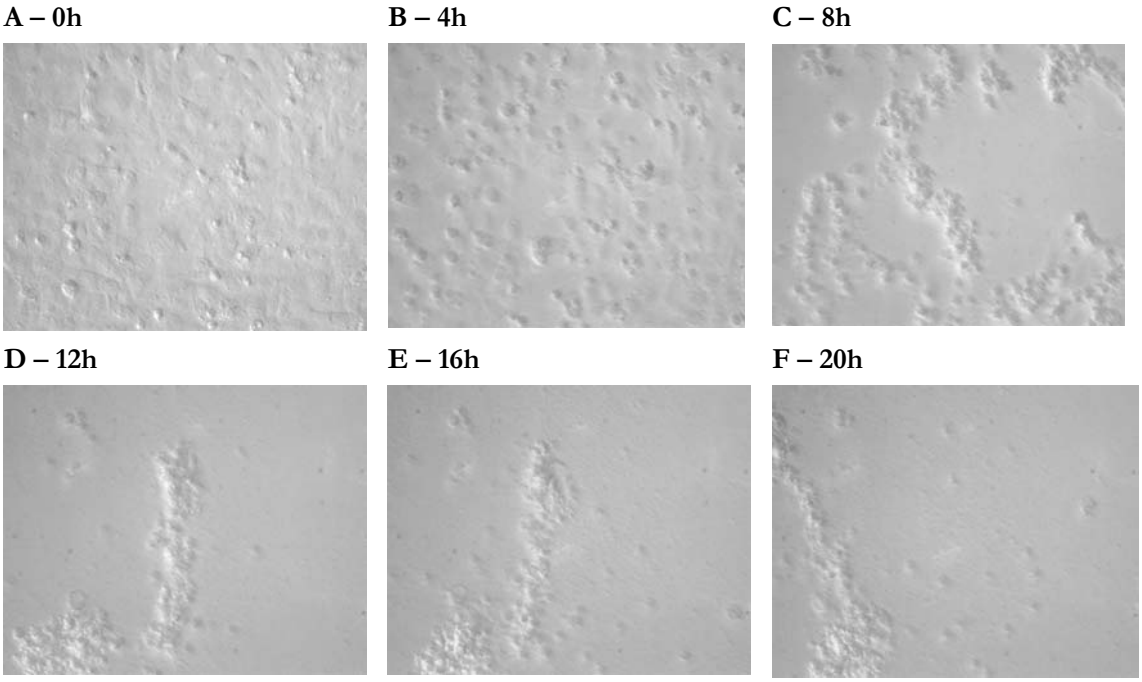

Figure 8-8. LM pictures of HMEC cells cultured in a Petri dish in the presence of the apoptotic inducer 3 nM TNF-α in combination with 50 μM CHX for **(A)** 0h, **(B)** 4h, **(C)** 8h, **(D)** 12h, **(E)** 16h and **(F)** 20h. Magnification is 20x.

Afterwards, the HMEC cells still attached to the surface, and the HMEC cells which detached, were stained with the death dye PI. Both demonstrated positive for PI (Figure 8-9). The detached cells were present in colonies. Aoudjit *et al.*[15] also noticed that during detachment endothelial cells got round and formed cell aggregates. They stated that this aggregation might be crucial for Fas/Fas-L interaction and induction of Fas-mediated apoptosis. Though, it might also be that due to their loss in membrane integrity, these endothelial cells became very sticky.

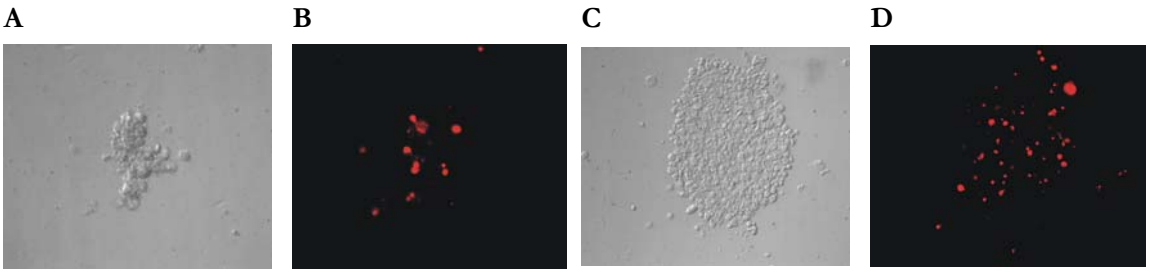

Figure 8-9. LM and fluorescence pictures of HMEC cells treated with a mix of 3 nM TNF-α and 50 μM CHX for 24h. HMEC cells still attached **(A and B)** on the surface of the Petri dish and detached cells **(C and D)** were separately imaged for their morphology **(A and C)** with light microscopy and positivity for PI **(B and D)** with fluorescence microscopy. Magnification is 20x.

Furthermore, the apoptotic process was analysed in more detail using the fluorescent probes AV (FITC-labelled) in combination with PI (Figure 8-10).

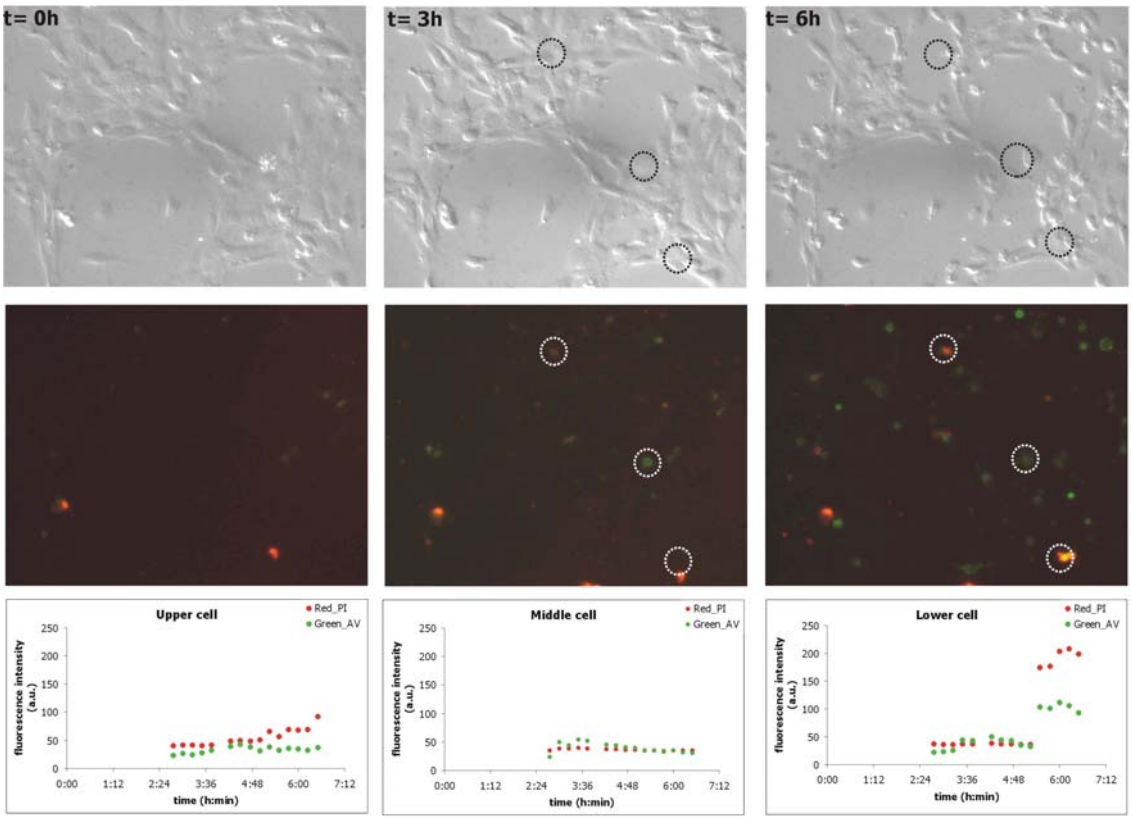

Figure 8-10. LM and fluorescence pictures of HMEC cells treated with a mix of 3 nM TNF-α and 50 μM CHX. HMEC cells were cultured in a Nunc culture chamber pre-coated with 0.1% APS. Dual fluorescence staining with AV and PI was accomplished and the change in fluorescence intensity for three different cells was plotted in time.

In this experiment, the cells detached as single cells (LM pictures black dashed circles), and not in colonies as demonstrated in figure 8-8. Moreover, the three selected cells (dashed circles) all had their specific response to the mixture of TNF-α and CHX. The upper cell demonstrated an increase in PI fluorescence in time, whereas hardly any change in AV fluorescence was shown. The middle cell only showed an increase in AV fluorescence after 3h, thereafter the green fluorescence diminished. The lower cell demonstrated a large increase in AV and PI fluorescence in time. These results confirmed the fact that apoptosis is a process that does not occur simultaneously in all the cells of a population, favouring analysis at the single-cell level. Furthermore, in immortalized endothelial cells (HMEC), in response to the apoptotic stimulus TNF-α, the death receptors were activated, which triggered the apoptotic cascade, resulting in AV and PI fluorescence. At the final stage, these cells detached from their surface, *e.g.,* apoptosis-induced anoiks. The round phenotype characterized cells undergoing apoptosis.[8,18,37]

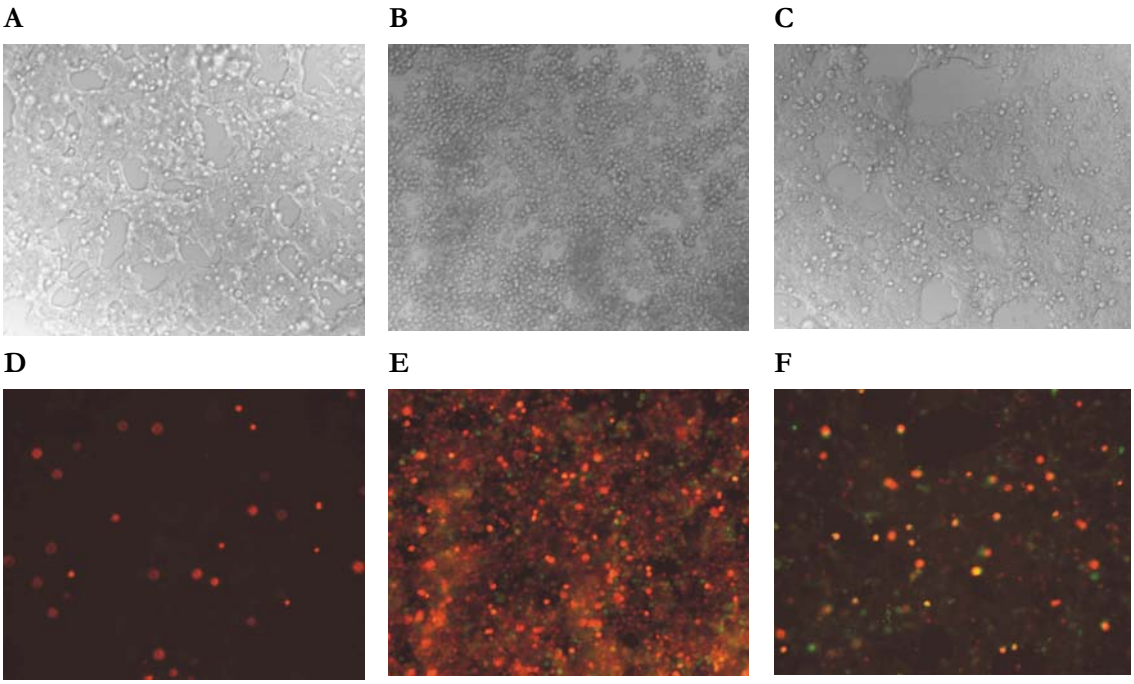

Figure 8-11. LM and fluorescence pictures of MCF-7 cells treated with a mix of 3 nM TNF-α and 50 μM CHX in CO_2 independent medium at room temperature. MCF-7 cells were cultured in a Petri dish. **(A-C)** LM pictures of treated MCF-7 cells at **(A)** t=0h and **(B)** t=24h and of untreated MCF-7 cells at **(C)** t=24h. **(D-F)** Dual fluorescence of MCF-7 cells with AV and PI of treated MCF-7 cells at **(D)** t=0h and **(E)** t=24h and of untreated MCF-7 cells at **(F)** t=24h. Magnification is 10x.

In MCF-7 cells treated with a mix of TNF-α and CHX to induce apoptosis, the morphology changed after 24h, demonstrating the rounding and the shrinkage of MCF-7 cells (figure 8-11B). This was accompanied by a large increase in AV and PI fluorescence (Figure 8-11E), expressed by the MCF-7 cells with altered morphology. The final stage, anoikis, was not (yet) demonstrated.
A part of this fluorescent increase accounted for the fact that this experiment was performed at room temperature (Figure 8-11C and 8-11F). This induced apoptosis, as demonstrated in chapter 6. Though, comparing figure 8-11E and 8-11F, the large increase in AV and PI was more pronounced in the presence of the mix TNF-α/CHX.
The increase in fluorescence demonstrated with fluorescence microscopy was more prominent compared to the flow cytometry data. The experiment using fluorescence microscopy was performed at room temperature, which sensitized MCF-7 cells, which in the presence of the apoptotic inducers might cause an additive effect. Moreover, the continuous presence of fluorescent dyes might also account for the increase in fluorescence. Furthermore, flow cytometry was not ideal for adherent cells, therefore (single-cell) apoptotic events might be missed, which were detected with fluorescence microscopy.
Hence, in response to TNF-α in combination with the protein synthesis inhibitor CHX, MCF-7 cells demonstrated apoptosis-induced anoikis, though the final stage, anoikis, was not observed.

The on-line monitoring results described above, could provide us already with a lot of information concerning the apoptotic response of different cell types in the presence of various drug. Though, for high-throughput dose-response analysis, microfluidic chip technology has greater potential. Drug-specific responses can be monitored in real-time at a single-cell level. Only a few cells are needed, favouring the use of primary (tumour) cells and hence perform *ex vivo* experiments. Furthermore, the applied flow provides the cells with the appropriate shear stress, which for endothelial cells is required for cell survival and development. Moreover, the flow system will provide the cells with the necessary nutrients and easily incubate the cells with different (doses of) drugs. Both the generation of drug gradients as well as multi-phenotypic cell arrays are performed on chip. Microfluidic gradient generators were fabricated on chip for high-throughput dose-response

analysis of quick electrophysiological effects of different concentrations of drugs on the activity of ion channels and receptors using scanning-probe patch-clamp measurements.[38] In this case cell culture was not required. Khademhosseine *et al.*[39] developed a microfluidic chip for the docking of cells in microwells. Due to reversible sealing of the PDMS containing the microchannels to the PDMS containing the microwells, the PDMS with the microchannels could be removed and replaced by a second piece of PDMS with the same channel structure, now orthogonally aligned on the PDMS with the microwells, resulting in channels that contained multiple cell types. Also in this case, cell culture was not necessary. Thompson *et al.*[40] designed a microfluidic platform consisting of a dilution module for obtaining drug-gradients as well as multiple cell culture chambers. This chip was developed for monitoring the dynamic gene-expression of NF-κB in response to different concentrations of TNF-α in cultured Hela S3 cells. This chip has great potential for multiple other applications, such as our apoptosis experiments, as various cell types can be cultured in the different cell culture chambers and monitored in time at a single-cell level in the presence of drug-gradients. Though, first we prefer a simple designed microfluidic chip to monitor the response of one cell type in response to a particular apoptotic stimulus to characterise the apoptotic pathway and optimise the experimental set-up, because at the beginning the best microfluidic platform is unknown. Furthermore, multiple cell culture chambers cannot be monitored optically at the same time, hence in our case for high-throughput analysis the optical set-up has to be replaced or combined with electrodes for electrical measurements, such as counting the cells that have detached from the surface.

Therefore in the first experiments, performed to characterise the morphological hallmarks during the apoptotic process, the microfluidic cell trap chip and the Meander chip were used. In the microfluidic cell trap chip, MCF-7 cells had to be cultured in the side-channel to retain a viable morphology in contact with a flow rate of 1 µl/min for 16h (Figure 7-5). Then, apoptosis was induced with a mix of TNF-α and CHX (Figure 8-12).

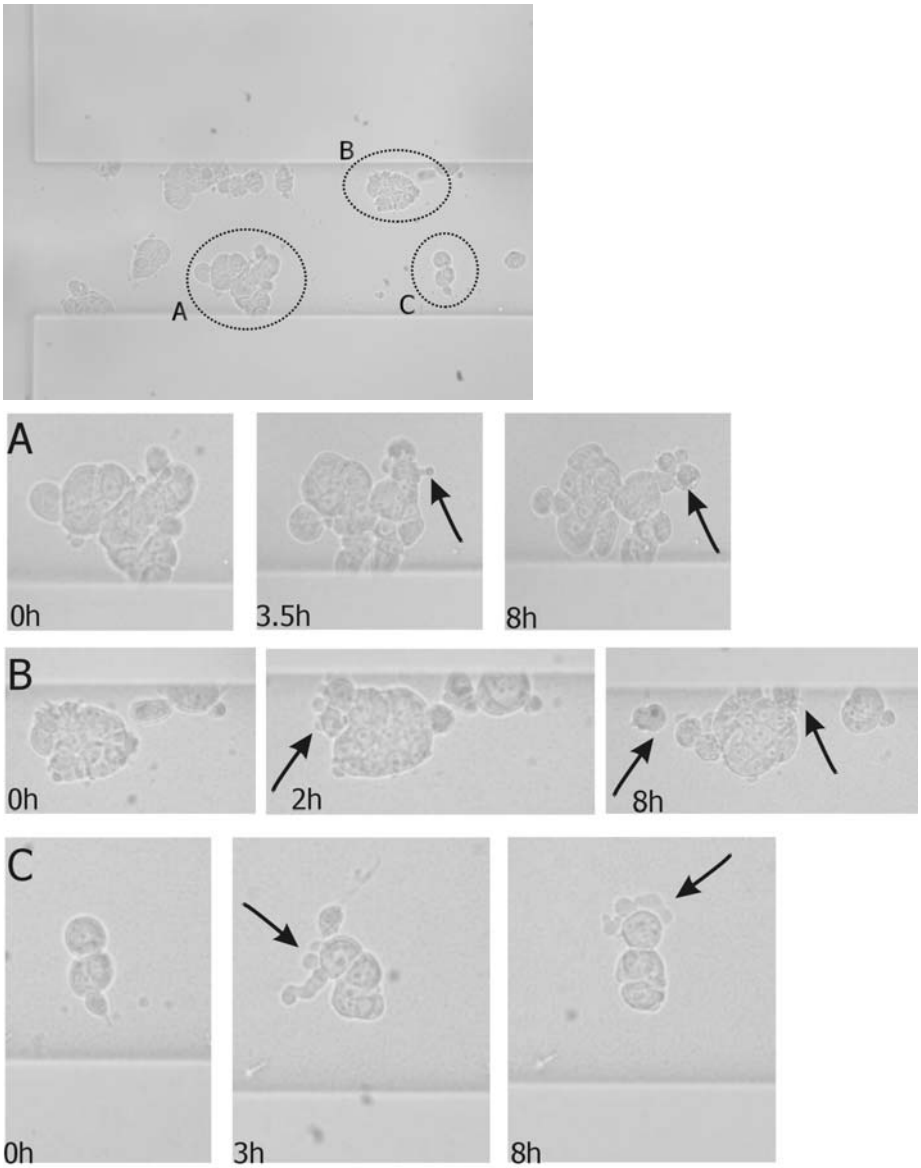

Figure 8-12. Snapshots of LM pictures of MCF-7 cells in the microfluidic cell trap chip treated with 3 nM TNF-α and 50 μM CHX under continuous flow of 1 μl/min for 8h. The first figure selected the three colonies of cells (*e.g.,* A, B and C) which were analysed in more detail for morphological changes during the apoptotic process. Magnification is 20x. Arrows point to the characteristic morphological changes during the apoptotic process, such as the rounding and the shrinkage of the cells and the formation of apoptotic bodies.

Induction of apoptosis with TNF-α and CHX showed all the morphological characteristics of apoptosis, such as the rounding of the cells accompanied with shrinkage, membrane blebbing and apoptotic body formation, as pointed out with the arrows in figure 8-12. Though, the cells did not detach. Even in contact with the mix of TNF-α/CHX for more than 45h, single-cell rounding appeared, but no clear detachment (Figure 8-13).

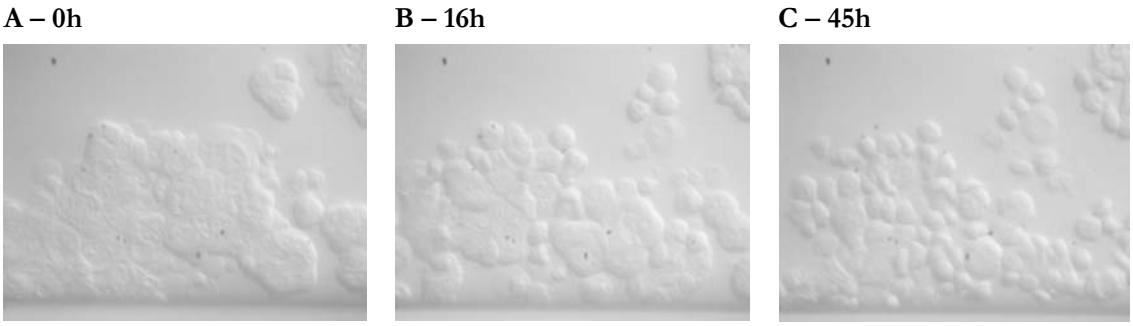

Figure 8-13. LM pictures of the time-lapse recording of MCF-7 in the presence of TNF-α in combination with CHX under continuous flow of 10 μl/h in the microfluidic cell trap chip. Magnification is 63x.

Detachment might be prevented because of the depth of the channels, which in this design is 15 μm, nearly the same dimension of MCF-7 cells. The meander chip has a depth of 100 μm. MCF-7 cells were allowed to attach in the Meander chip overnight, after which the flow (5 μl/h = 0.04 dyne/cm^2) was connected. Before the flow was applied, viability was checked with PI. The oxygen consumption of the approximately 100 cells present in the chip is 8.64 x 10^{-10} mol O_2, the oxygen provided through the medium is 5.6855 x 10^{-10} mol O_2 (paragraph 7.5.2.3). Although, there is a small difference, overall viability was > 90%, as checked with PI, though early apoptotic cells with preserved plasma membrane integrity were not included. The protein kinase inhibitor staurosporine (SSP; 50 μM) was used as the apoptotic inducer. This was a quite high concentration, as 20 μM SSP showed a necrotic morphology after 24h (Figure 8-3). However, with this high concentration, we would like to obtain quick morphological responses, and demonstrate the detachment of adherent cells. After 7h, the flow was stopped and cells were stained with AV and PI. Cells were still attached, but all positive for AV and PI, hence in the late apoptotic phase of the apoptotic process (Figure 8-14). It was clearly shown that AV bound to PS at the plasma membrane, demonstrating a green ring structure, whereas PI bound to the nucleotides in the nucleus, appearing as red spots. Nuclear fragmentation was not demonstrated.

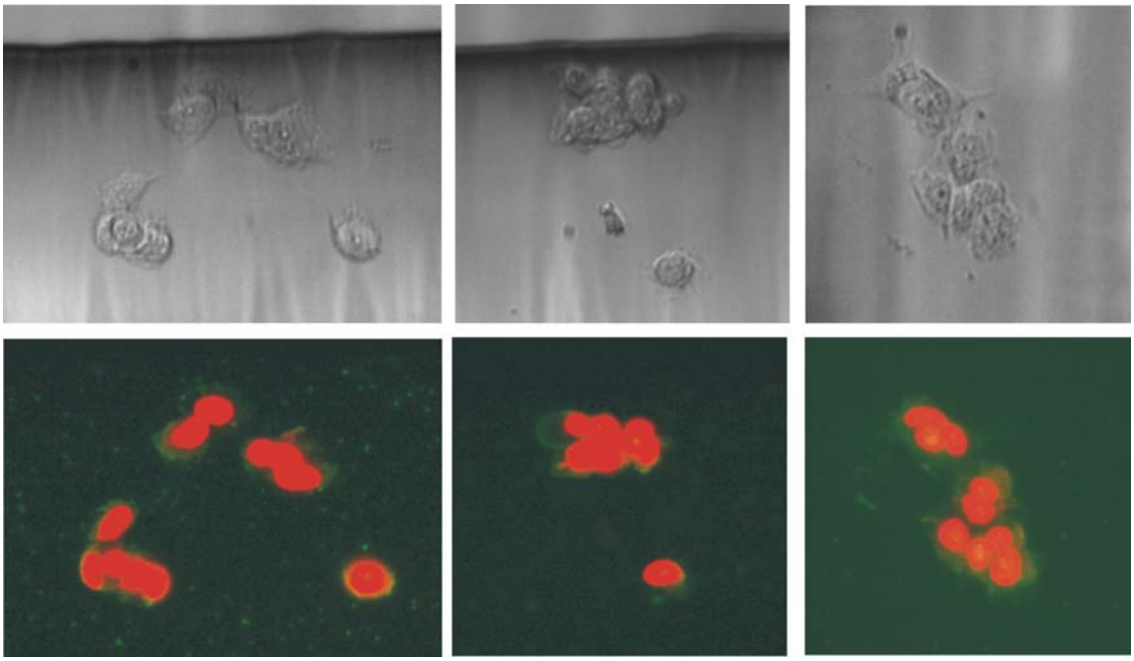

Figure 8-14. LM and fluorescent pictures of MCF-7 cells in the Meander chip treated with 50 μM SSP under continuous flow of 5 μl/h for 7h. Upper pictures show the LM with below the corresponding fluorescent pictures of the AV and PI staining. Magnification is 20x.

To improve the environmental and optical settings, a new microfluidic chip was developed, *e.g.,* apoptosis chip #3. This chip consists of PDMS which is recommended for cell culture and cell based assays, due to its biocompatibility and gas permeability. Especially, as demonstrated above, to fully characterize the apoptotic process, long incubations are necessary. Together with the time necessary for cell attachment, the cells will be present in the microfluidic device for days. Moreover, the whole experimental set-up utilizes disposables and no chip holder is required, which improves the optical settings. As demonstrated in chapter 7, endothelial cells and MCF-7 cells were successfully cultured in apoptosis chip #3 (Figure 7-20). MCF-7 cells were treated with 3 nM TNF-α in combination with 50 μM CHX to initiate the process of apoptosis. The flow rate was set at 1 μl/ min, corresponding to a shear stress of 0.33 dyne/cm^2 in the inlet and outlet channel. The shear stress in the middle of the channel was lower, due to broadening of the channel with a factor 3.33 (1.5 mm vs. 5 mm; figure 7-13).

In response to the mixture of TNF-α and CHX, the morphology of MCF-7 cells changed, demonstrating the rounding of the cells, accompanied with shrinkage, membrane blebbing and the pinching of of apoptotic bodies within 6h (Figure 8-15).

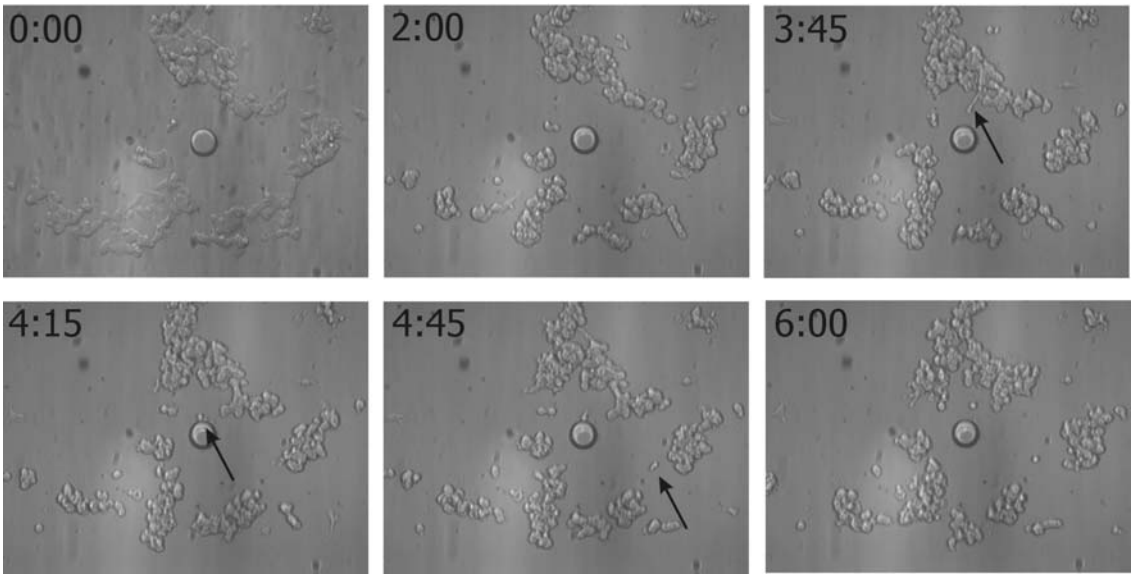

Figure 8.15. Time lapse recording of MCF-7 cells treated with 3 nM TNF-α in combination with 50 μM CHX in apoptosis chip #3 under a continuous flow of 1 μl/min. Magnification is 20x. Arrows point to the pinching of of apoptotic bodies.

After 6h air bubbles appeared in the chip, disrupting the morphological analysis of the apoptotic process. Some cells maintained attached to the surface, others detached, though managed to adhere at another place in the chip and recovered, as demonstrated in figure 8-16. These viable cells did not show fluorescence.

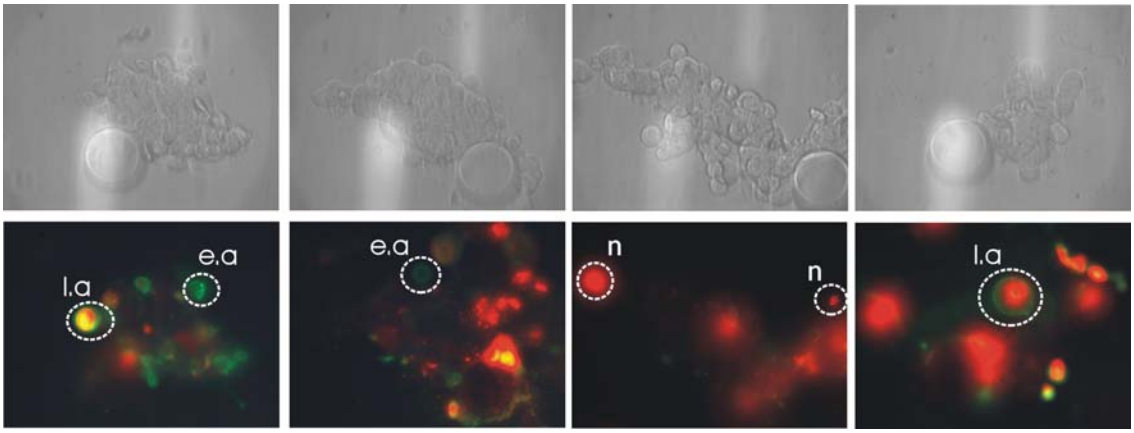

Figure 8-16. LM and fluorescent pictures of MCF-7 cells in apoptosis chip #3 treated with 3 nM TNF-α in combination with 50 μM CHX under a continuous flow of 1 μl/min for 18h. MCF-7 cells were stained with AV and PI, to characterize the different phases in the apoptotic process (e.a. = early apoptotic; l.a. late apoptotic; n = necrotic). Magnificance is 63x.

In the colonies of the cells, which have re-attached to the surface, some cells managed to stay viable (AV^-PI^-), while others were in one of the stages of the apoptotic process (AV^+PI^- early apoptotic, AV^+PI^+ late apoptotic or AV^-PI^+ necrotic), in the presence of the apoptotic inducer. This apoptotic process might be accelerated through the occurrence of air bubbles. Interesting was the phenomenon that MCF-7 cells, which are non-metastatic breast cancer cells[16], could detach from their surface and adhere to other places in the chip thereby preserving their viable morphology. Repeating the experiment with PFTE tubing (Teflon) did not prevent the formation of air bubbles (after 4h), and the same phenomenon, that disrupted cells managed to adhere at other places in the channel, retaining their viable morphology, was observed, Moreover, MCF-7 cells in the presence of TNF-α/CHX moved away from their colony and migrated to other spots in the chip (Figure 8-17 black arrows).

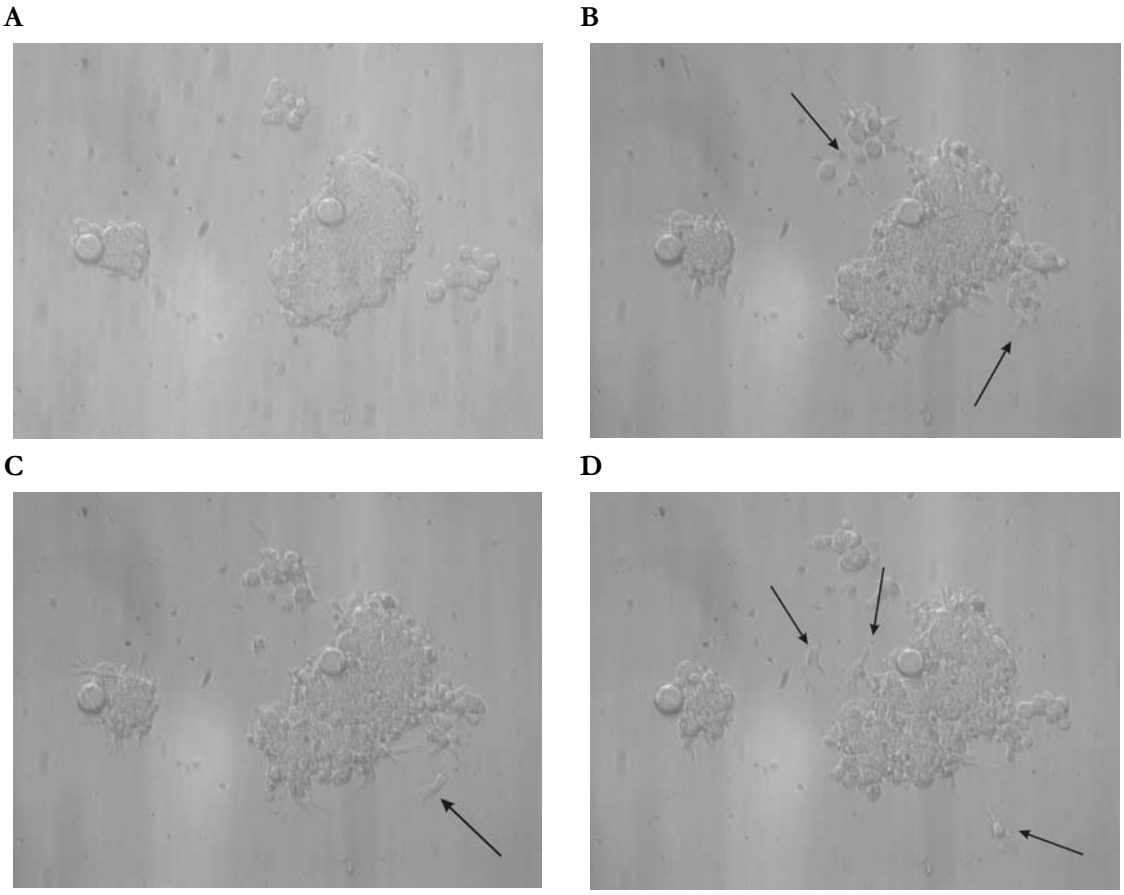

Figure 8-17. Time lapse recording showing LM pictures demonstrating the movement of cells away from their colony under continuous flow of 1 μl/min of TNF-α in combination with CHX at **(A)** 0h, **(B)** 2h, **(C)** 2.5h, and **(D)** 3.5h. Magnification is 20x.

This phenomenon was also once shown when MCF-7 cells were on-line monitored in the presence of 20 μM tamoxifen in a conventional Petri dish (Figure 8-18). During this migration, cell viability was maintained, as cells were positive for Calcein and hardly any PI fluorescence was observed.

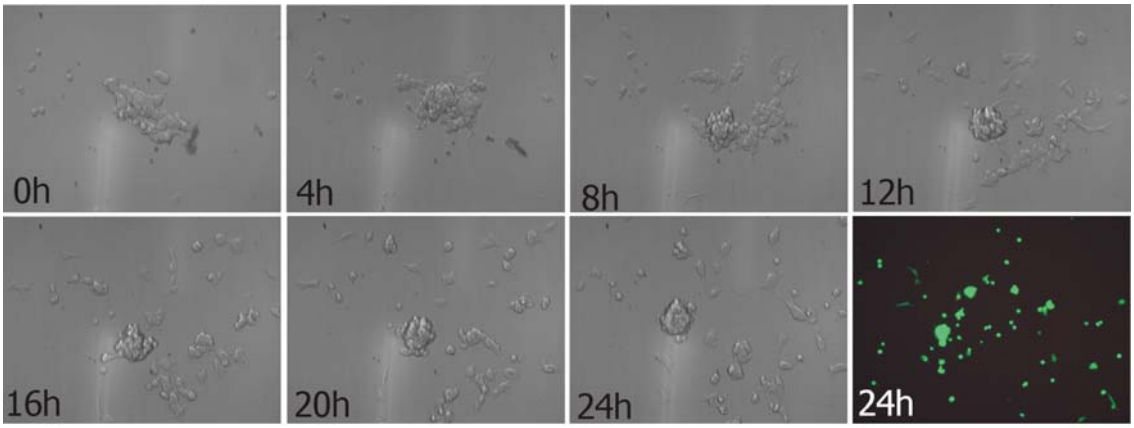

Figure 8-18. Time-lapse recording of MCF-7 cells in the presence of 20 μM tamoxifen cultured in a conventional Petri dish. LM pictures as well as the fluorescent picture of the dual staining with Calcein-AM and PI is shown. Magnification is 10x.

Hence, MCF-7 cells had the ability, in the presence of the right stimuli, to move away from their colony and migrate to other places, while retaining their viable morphology.

8.4 Conclusion

During tumourigenesis, the process of apoptosis and anoikis is disturbed, providing tumour cells with the ability to metastasize to and invade other organs. We intended to develop a chip to monitor the apoptotic cascade in real-time and evaluate drug-specific responses using different cell types. As a "proof-of-concept", MCF-7 breast cancer cells and immortalized endothelial cells (HMEC) were chosen to evaluate the mechanism underlying the process of apoptosis and anoikis. In response to the apoptotic stimulus TNF-α in combination with CHX, immortalized endothelial cells travelled through the apoptotic cascade, showing shrinkage and rounding of the cells, accompanied with AV and PI fluorescence. As a final stage, these cells detached from their surface, hence demonstrating apoptosis-induced anoikis. For the breast cancer cells MCF-7 in response to the mixture of TNF-

α/CHX, apoptosis was observed, though these cells did not detach from the surface. All the apoptotic characteristics were shown, such as shrinkage, cell rounding, membrane blebbing, and AV and PI fluorescence, however, the final stage, anoikis, was not observed. Moreover, MCF-7 cells in the presence of TNF-α/CHX moved away from their colony and migrated to other spots in the chip. Furthermore, MCF-7 cells which were disrupted from the surface, because of air bubbles, managed to adhere at another place in the channel, while maintaining their viable morphology. Immortalized endothelial cells are capable of extended proliferation, but possess no alterations in their genotype and tissue markers as compared to their parental tissue. Therefore, these cells, as expected, demonstrated apoptosis-induced-anoikis in response to apoptotic stimuli. However, MCF-7 breast adenocarcinoma cells are non-metastatic tumour cells, so probably these cells do not have a disrupted anoikis mechanism. However, disruption of these cells from their surface did not immediately mean that the process of apoptosis was activated, as some cells managed to remain their viable morphology. Moreover, in response to the right stimuli, the apoptotic response could be activated demonstrating various morphological apoptotic characteristics, though the final stage, the detachment, was not observed. Future experiments with other drugs and other cell types are necessary to evaluate these observations in more detail, and define its importance in cancer therapy.

8.5 Acknowledgements

For the overall fabrication of the microfluidic devices and for technical assistance, Jan van Nieuwkasteele and Paul ter Braak are gratefully acknowledged. For the design of the microfluidic cell trap chip, Nicolas Demierre and for the Meander chip, Jurjen Emmelkamp is thanked. Severine Le Gac is acknowledged for designing and fabricating apoptosis chip #3 and Andries van der Meer for help with the experimental set-up of apoptosis chip #3.

8.6 References

1. Vermes I, Haanen C. Apoptosis and programmed cell death in health and disease. *Adv Clin Chem* 1994; **31**: 177-246.
2. Wolbers F, Haanen C, Andersson H, van den Berg A, Vermes I. Analysis of apoptosis on chip: Why the move to chip technology. In "Lab-on-a-Chips for Cellomics: Micro and Nanotechnologies for Life Sciences", eds. H. Andersson and A. van den Berg, Kluwer Academics Publishers 2004.
3. Andersson H, van den Berg A. Microfluidic devices for cellomics: a review. *Sens Actuators B* 2003; **92**: 315-325
4. Andersson H, van den Berg A. Microtechnologies and nanotechnologies for single cell analysis. *Curr Opin Biotechnol* 2004; **15**: 44-49.
5. Parkin DM, Fernandez LMG. Use of statistics to assess the global burden of breast cancer. *Breast J* 2006; **12**: S70-S80.
6. Frisch SM, Francis H. Disruption of epithelial cell-matrix interactions induces apoptosis. *J Cell Biol* 1994; **124**: 619-626.
7. Grossmann J. Molecular-mechanisms of "detachment-induced apoptosis – anoikis". *Apoptosis* 2002; **7**: 247-260.
8. Chen CS, Mrksich M, Huang S, Whitesides GM, Ingber DE. Geometric control of cell life and death. *Science* 1997; **276**: 1425-1428.
9. Liotta LA, Kohn E. Cancer and the homeless cell. *Nature* 2004; **430**: 973-974.
10. Gupta GP, Massague J. Cancer metastasis: Building a framework. *Cell* 2006; **127**: 679-695.
11. Ruoslahti E, Reed JC. Anchorage dependence, integrins, and apoptosis. *Cell* 1994; **77**: 477-478.
12. Frisch SM, Screaton RA. Anoikis mechanisms. *Curr Opin Cell Biol* 2001; **13**: 555-562.
13. Valentijn AJ, Zouq N, Gillmore AP. Anoikis. *Biochem Soc Trans* 2004; **32:** 421-425.
14. Wang P, Valentijn AJ, Gilmore AP, Streuli CH. Early events in the anoikis program occur in the absence of caspase activation. *J Biol Chem* 2003; **278**: 19917-19925.

15. Aoudjit F, Vuori K. Matrix attachment regulates Fas-induced apoptosis in endothelial cells: A role for c-Flip and implications for anoikis. *J Cell Biol* 2001; **152**: 633-643.
16. Fernandez Y, Gu B, Martinez A, Torregrosa A, Sierra A. Inhibition of apoptosis in human breast cancer cells: Role in tumor progression to the metastatic state. *Int J Cancer* 2002; **101**: 317-326.
17. Fukazawa H, Noguchi K, Murakami Y, Uehara Y. Mitogen-activated protein/extracellular signal-regulated kinase kinase (MEK) inhibitors restore anoikis sensitivity in human breast cancer cell lines with a constitutively activated extracellular regulated kinase (ERK) pathway. *Mol Cancer Ther* 2002; **1**: 303-309.
18. Goldberg GS, Jin Z, Ichikawa H, Naito A, *et al.* Global effects of anchorage on gene expression during mammary carcinoma cell growth reveal role of tumor necrosis factor-related apoptosis-inducing ligand in anoikis. *Cancer Res* 2001; **61**: 1334-1337.
19. Engbers-Buijtenhuijs P, Kamphuis M, van der Sluijs Veer G, Haanen C, *et al.* A novel time resolved fluorometric assay of anoikis using Europium-labelled Annexin V in cultured adherent cells. *Apoptosis* 2005; **10**: 429-437.
20. Hemmila I, Dakabu S, Mukkala VM, Siitari H, Lovgren T. Europium as a label in time-resolved immunofluorometric assays. *Anal Biochem* 1984; **137**: 335-343.
21. Liang Y, Yan C, Schor NF. Apoptosis in the absence of caspase 3. *Oncogene* 2001; **20**: 6570-6578.
22. Mooney LM, Al-Sakkaf KA, Brown BL, Dobson PRM. Apoptotic mechanisms in T47D and MCF-7 human breast cancer cells. *Br J Cancer* 2002; **87**: 909-917.
23. Chen JSK, Konopleva M, Andreeff M, Multani AS, *et al.* Drug-resistant breast carcinoma (MCF-7) cells are paradoxically sensitive to apoptosis. *J Cell Physiol* 2004; **200**: 223-234.
24. Tang F, Tang G, Xiang J, Dai Q, *et al.* The absence of NF-κB mediated inhibtion of c-jun N-terminal kinase activation contributes to tumor necrosis factor alpha-induced apoptosis. *Mol Cell Biol* 2002; **22**: 8571-8579.
25. Machuca C, Mendoza-Milla C, Cordova E, Mejia S, *et al.* Dexamethasone protection from TNF-alpha-induced cell death in MCF-7 cells requires NF-kappaB and is independent from Akt. *BMC Cell Biol* 2006; **7**: 9-20.

26. Suyama E, Kawasaki H, Taira K. Identification of a caspase 3-independent role of pro-apoptotic factor Bak in TNF-α-induced apoptosis. *FEBS Lett* 2002; **528**: 63-69.
27. Debnath J, Baehrecke EH, Kroemer G. Does autophagy contribute to cell death? *Autophagy* 2005; **1**:66-74.
28. Motyl T, Gajkowska B, Zarzynska J, Gajewska M, Lamparska-Przybysz M. Apoptosis and autophagy in mammary gland remodeling and breast cancer chemotherapy. *J Physiol Pharmacol* 2006; **57S7**:17-32.
29. Kondo Y, Kondo S. Autophagy and cancer therapy. *Autophagy* 2006; **2**: 85-90.
30. Bursch W, Ellinger A, Kienzl H, Torok L, *et al.* Active cell death induced by the anti-estrogens tamoxifen and ICI 164 384 in human mammary carcinoma cells (MCF-7) in culture: role of autophagy. *Carcinogenesis* 1996; **17**: 1595-1607.
31. Kallio A, Zheng A, Dahllund J, Heiskanen KM, Harkonen P. Role of mitochondria in tamoxifen-induced rapid cell death of MCF-7 breast cancer cells. *Apoptosis* 2005; **10**: 1395-1410.
32. Lamparska-Przybysz M, Gajkowska B, Motyl T. BID-deficient breast cancer MCF-7 cells as a model for the study of autophagy in cancer therapy. *Autophagy* 2006; **2**: 47-48.
33. Gorka M, Godlewski MM, Gajkowska B, Wojewodzka U, Motyl T. Kinetics of Smac/DIABLO release from mitochondria during apoptosis of MCF-7 breast cancer cells. *Cell Biol Int* 2004; **28**: 741-754.
34. Del Bino G, Darzynkiewicz Z, Degraef C, Mosselmans R, *et al.* Comparison of methods based on annexin-V binding, DNA content or TUNEL for evaluating cell death in HL60 and adherent MCF-7 cells. *Cell Prolif* 1999; **32**: 25-37.
35. Smolewski P, Bedner E, Du L, Hsieh T, *et al.* Detection of caspase activation by fluorochrome-labelled inhibitors: multiparameter analysis by laser scanning cytometry. *Cytometry* 2001; **44**: 73-82.
36. van England M, Ramaekers FCS, Schutte B, Reultelingsperger CPM. A novel assay to measure loss of plasma membrane asymmetry during apoptosis of adherent cells in culture. *Cytometry* 1996; **24**: 131-139.
37. Streuli CH, Gilmore AP. Adhesion-mediated signaling in the regulation of mammary epithelial cell survival. *J Mammary Gland Biol Neoplasia* 1999; **4**: 183-191.

38. Pihl J, Sinclair J, Sahlin E, Karlsson M, *et al.* Microfluidic gradient-generating device for pharmacological profiling. *Anal Chem* 2005; **77**: 3897-3903.
39. Khademhosseini A, Yeh J, Eng G, Karp J, *et al.* Cell docking inside microwells within reversibly sealed microfluidic channels for fabricating multiphenotype cells arrays. *Lab Chip* 2005; **5**: 1380-1386.
40. Thompson DM, King KR, Wieder J, Toner M, *et al.* Dynamic gene expression profiling using a microfabricated living cell array. *Anal Chem* 2004; **76**: 4098-4103.

9

Summary and outlook

In this chapter the conclusions of the work described in the previous chapters are summarized. Furthermore, suggestions are given for future work concerning the performance and improvement of apoptosis studies for drug screening and the potential importance in clinical settings is highlighted.

9.1 Summary

This thesis described the process of the development towards a microfluidic platform to perform apoptosis studies on chip in real-time at a single-cell level.

Nowadays, there are many analytical assays are available for detecting apoptosis (chapter 2). Of those flow cytometry is highly recommended for studying the apoptotic cascade in relation to cell type, trigger and time. In chapter 3, the fluorochrome-labelled inhibitor of caspases (FLICA) was used to label human promyelocytic leukaemic HL60 cells and human umbilical vein endothelial cells (HUVEC) after caspase activation. This arrested further progress through the apoptotic cell death cascade, preventing cellular disintegration. Combining FLICA labelling with the membrane integrity dye propidium iodide (PI), the apoptotic cell death kinetics in the presence of various stimuli were obtained. The apoptotic turnover rate depended on the stimulus used to induce apoptosis, while the type of the cell determined the manner of transition through the apoptotic cascade. In the presence of tumour necrosis factor (TNF)-α in combination with cycloheximide (CHX), HL60 cells entered the apoptotic cascade much faster in comparison to camptothecin (CPT)-treated HL60 cells. Moreover, in HL60 cells the entrance rate into the apoptotic cascade was higher than in HUVEC, both treated with a mixture of TNF-α/CHX. Furthermore, a different transition pattern through the apoptotic cascade was shown. HL60 cells in the present of apoptotic stimuli transited from the viable quadrant to the early apoptotic quadrant and then to the late apoptotic quadrant, while the transition from the viable to the early apoptotic quadrant was skipped in HUVEC.

Fluorescent labels are very suitable in order to characterise the different events in the apoptotic cascade, however, for real-time monitoring the use of fluorescent labels must be prevented, because these dyes are toxic for cells. Therefore autofluorescence (AF) was presented as a new way to study the process of apoptosis in chapter 4. Induction of apoptosis with either irradiation or chemical agents (TNF-α/CHX and CPT) first resulted in an increase (first 2h) and then in a decrease in the AF intensity (up to 24h) in HL60 cells, especially in cells present in the late-apoptotic phase of the apoptotic cascade, resulting in a decreased $AF^{24/2}$

factor. This phenomenon was not observed in HL60 cells which were made necrotic and had an $AF^{24/2}$ factor comparable with untreated HL60 cells. Measuring the AF intensity provides new possibilities of analysing the process of apoptosis, even at a single-cell level, for which chip technology is required.

As stated in chapter 2, today, chip technology offers many advantages compared to the conventional methods used these days to analyse the process of apoptosis. For flow cytometry, a large number of cells are required, and in many cases cells are stained or fixed in order to analyse them, so intact single cells cannot be analysed. Minimal manipulation of cells (*e.g.,* detachment of adherent cells with trypsin) can induce apoptosis and staining with fluorescent dyes, kills the cells. On top of that, cell preparation for analysis requires additional time (at least 15-30 min) and therefore real-time monitoring of the cell death cascade is no option. In this case microtechnology is very advantageous for various reasons. Different cell manipulation methods (sorting, detachment, staining, fixing and lysis, etc.) can be integrated on one chip, less sample is needed, which is advantageously when only a few cells are available (*e.g.,* primary cells), and the dimensions favour single-cell analysis. In particular, apoptosis is extremely suited to analyse on chip, as apoptosis is a process that does not occur simultaneously in all the cells of a population, favouring analysis at the single-cell level. Furthermore, the process of apoptosis takes no more than a few hours, hence real-time monitoring will provide new insights into the apoptotic cascade. The integration of different detection techniques (electrical properties, cell size/morphology, and released cell content) can overcome the technical difficulties now existing in measuring programmed cell death. In this way, the different phases of the apoptotic cascade can be monitored in detail on one chip device.

Our goal, as described in this thesis, was developing a microfluidic chip for analysing the effects of various drugs on the apoptotic pathway and monitoring the morphological changes in real-time at a single-cell level using different cell types. Our main interest arrived at breast cancer cells. Up to now the ideal endocrine treatment for breast cancer still needs to be elucidated. Frequently used medicaments, such as oestrogens, progestagens, the selective oestrogen modulator tamoxifen and the aromatase inhibitors were administered to different breast cancer

cell lines and analysed for their effect on the balance between apoptosis and proliferation using conventional *in vitro* assays (flow cytometry and RT-PCR), as presented in chapter 5. Tamoxifen demonstrated a net apoptotic outcome, irrespective of the type of breast cancer and the receptor status. Due to the negative side effects of tamoxifen and patients becoming resistant to treatment, the aromatase inhibitors obtained growing interest in adjuvant therapy, however, our *in vitro* experiments showed unexpected results. The AI did not show in all cases an apoptotic outcome. Further detailed analysis concerning the best incubation time and concentration for administration is needed. Results from our *in vitro* studies warrant further pharmacological and clinical studies to analyse the different possibilities for endocrine therapy performed in large randomized trials. Nevertheless, as a result of genomics it is known that polymorphisms in the DNA sequence cause genetic variation and therefore patients will show an individual response to the therapy. Using a patient's own breast (cancer) cells, obtained via biopsy, will help to determine the best individual treatment in terms of formulation of the drug, dose and route of administration. The conventional techniques to measure the balance between apoptosis and proliferation upon drug treatment, as presented here, are not suitable for such *ex vivo* measurements to individualize treatment, however, microfluidics have the requirements. Therefore, drug-specific responses were analysed on a microfluidic chip.

Before proper cell analysis could be performed on chip, control experiments had to be performed to ensure the viability of the studied cells at the start of the experiments, as discussed in chapter 6. Both the environmental conditions as the choice of the chip material influenced the viability of the cells studied. HL60 cells had to be cultured at 37ºC, as room temperature caused an increase in DNA fragmentation and a decrease in the AF intensity between 2h and 24h, demonstrating the activation of the apoptotic cascade. Moreover, as experiments were performed outside the incubator, specific medium (CO_2 independent medium) was required to overcome changes in the pH. For HL60 cells, the commonly used microchip materials, such as native silicon oxide, dry etched silicon oxide, borosilicate glass, Pyrex glass, Borofloat and hydrophobic PDMS, all appeared suitable for HL60 cells and pre-coating these materials with serum favoured the proliferation. Of course, for adherent cells the choice of material is

more important because in this case the cells have to attach and grow on these materials (chapter 7). The breast adenocarcinoma cell line MCF-7 adhered to the Pyrex as wells as to the borosilicate glass, but barely adhered to hydrophobic PDMS or to PDMS pre-coated with either serum or polyethylene glycol (PEG). For the endothelial cell line HMEC, the Pyrex and the borosilicate glass needed to be pre-coated with fibronectin or 0.1% (3-(2,3-epoxypropoxy)-propyl)-trimethoxysilan (APS) to support adhesion. HMEC cells did not adhere to hydrophobic or pre-coated (serum or PEG) PDMS.

Apart from a proper cellular environment and a good supportive material for adhesion, the microfluidic platform must be connected to a flow system to provide the cells with fresh culture medium and oxygen, which is required for long-term cell culture and the addition of various drugs (chapter 7). The applied flow rate will expose the cells to mechanical forces such as the shear stress. Endothelial cells require a shear stress of approximately 15 dyne/cm^2 for survival and development. However, for epithelial cells this shear stress must be kept below 0.5 dyne/cm^2 to maintain cellular viability. For apoptosis studies, different microfluidic devices were investigated to select the device which best suited our goal. The microfluidic devices differed in chip materials and channel geometry, as described in chapter 7. In the microfluidic cell trap chip two channels, patterned in silicon, join together in a cross consisting of a trap structure. The channels are sealed with a Pyrex cover. The Meander chip consists of a long channel structure made in Borofloat glass. In apoptosis chip #3, the channel structure is patterned in PDMS, sealed to a microscope slide with oxygen plasma. PDMS is highly recommended for cell based assays, because of its biocompatibility and gas permeability. In all three microfluidic devices, the culture of MCF-7 cells and endothelial cells was achieved, however, for long-term cell culture apoptosis chip #3 proved the best. Furthermore, this device met all the other requirements for the performance of apoptosis studies, such as (easy) connection to a flow system, optical analysis and the use of disposable materials, preferably when biological materials are used.

In chapter 8, we describe how MCF-7 breast cancer cells and endothelial cells were treated with different apoptotic stimuli and analysed the conventional way with flow cytometry and an immunological DELFIA® assay and in real-time at a single-

cell level on chip. Different morphological mechanisms between breast cancer cells and endothelial cells were explored. In response to the apoptotic stimulus TNF-α in combination with CHX, immortalized endothelial cells travelled through the apoptotic cascade, showing shrinkage and rounding of the cells, accompanied with AV and PI fluorescence. In the final stage, these cells detached from their surface, hence demonstrating apoptosis-induced detachment, or in other words apoptosis-induced anoikis. During tumourigenesis, the process of apoptosis and anoikis is disturbed, which provide tumour cells with the ability to metastasize to and invade other organs. This is called an anoikis-resistant phenotype. For the breast cancer cells MCF-7 in response to the mixture of TNF-α/CHX or the protein kinase inhibitor staurosporine (SSP), apoptosis was observed. However, these cells did not detach from the surface. All the apoptotic characteristics were evident, such as shrinkage, cell rounding, membrane blebbing, and AV and PI fluorescence, however, the final stage, anoikis, was not observed. Moreover, MCF-7 cells in the presence of TNF-α/CHX or tamoxifen moved away from their colony and migrated to other spots in the apoptosis chip #3. Unfortunately, after a while, air bubbles appeared in the microfluidic device, detaching MCF-7 cells from the surface. However, some cells managed to re-attach in another place in the channel, maintaining their viable morphology. Future experiments with other drugs and other cell types are necessary to evaluate these observations in more detail, and define their importance in cancer therapy.

9.2 Outlook

As a 'proof-of-concept', apoptosis chip #3 demonstrated to be suitable for preliminary apoptosis studies on chip. First results demonstrated morphologically different mechanisms between breast tumour cells and endothelial cells in response to the mixture of TNF-α/CHX. To evaluate the importance of these results, these experiments will have to be repeated with other cell types (*e.g.,* immortalized epithelial cells, metastatic breast tumour cells) and other apoptotic stimuli and medicaments, such as cytostatics, or drugs influencing the cell-matrix anchorage. To improve the adhesion of MCF-7 cells to the surface, a laminin coating can be used, as this glycoprotein exerts the cell-matrix anchorage of epithelial cells *in vivo*.

Moreover, the appearance of air bubbles must be prevented by optimising the flow system and by using gas-tight connections.

For high-throughput drug screening, multiple culture chambers will need to be present on one chip, combined with a drug-gradient generator to perform dose-response analysis. In this case, optical monitoring should be combined with electrical measurements, using electrodes to count the cells which have detached from the surface (apoptotic index), or using nanowires to measure changes in conductance/resistance in cells which are either proliferating or transiting through the different phases of the apoptotic cascade (*e.g.,* rounding, changes in membrane integrity, detachment).

Finally, the importance in clinical settings must be highlighted through the use of primary breast (tumour) cells. Therefore, only a few of a patient's own cells need to be cultured in the microfluidic chip and different drugs in various dosages will be screened. First the apoptotic response will be monitored, and later the balance between apoptosis and proliferation to determine the net outcome upon drug treatment. This will select the best individual treatment for each patient and provide first steps towards personalized medicine. Eventually, this microfluidic chip can be implemented in various clinical settings, to improve not only breast cancer therapy, but fine-tune multiple therapies and the treatment of diseases, in which the process of apoptosis is suppressed or enhanced.

Samenvatting

Dit proefschrift beschrijft de ontwikkeling van een microfluïdisch platform voor het uitvoeren van apoptose studies op chip. Het mogelijke effect, dat diverse medicamenten in verschillende concentraties (dosis-response analyse) op het proces van apoptose hebben, zal in real-time op individuele cellen bestudeerd worden. Dit onderzoek richt zich voornamelijk op het evalueren van morfologische verschillen tussen cellen van diverse oorsprong, met speciale interesse voor borstkankercellen.

In de celbiologie bestaan 2 vormen van celdood, namelijk apoptose en necrose (Hoofdstuk 2). Necrose of ongecontroleerde celdood wordt veroorzaakt door bijvoorbeeld fysiek of chemisch aangebrachte schade. Tijdens het proces van necrose verliest de cel zijn specifieke permeabiliteit, waardoor deze direct zwelt en zijn inhoud de extracellulaire ruimte in lekt. Dit veroorzaakt een ontstekingsreactie. Apoptose of gecontroleerde/geprogrammeerde celdood is een mechanisme waarbij verouderde, slecht functionerende en ongewenste cellen opgeruimd worden en hun inhoud hergebruikt wordt door omliggende macrofagen of andere fagocyterende cellen. Apoptose wordt gekenmerkt door het krimpen van de cel en het ontstaan van blaasjes op het membraan ("membrane blebbing"). Uiteindelijk valt de cel uiteen in apoptotische lichaampjes die door middel van fagocytose door omliggende cellen worden opgeruimd. Gedurende dit apoptotisch proces spelen specifieke proteases (enzymen die eiwitten afbreken) in de cel, caspases genoemd, een prominente rol. Apoptose is belangrijke voor het behoud van een strak gereguleerd evenwicht (homeostase) tussen celdeling (proliferatie) en celdood (apoptose), waardoor het celaantal en de orgaangrootte in het lichaam nauwlettend worden gecontroleerd. Onderdrukking of een overmaat aan apoptose veroorzaakt of speelt een rol in verscheidene ziektes, waaronder kanker en neurodegeneratieve ziektes, zoals Alzheimer en de ziekte van Parkinson.

Tegenwoordig zijn er allerlei analytische methoden beschreven om apoptose te detecteren. Flow cytometrie heeft als meettechniek de voorkeur. Echter, om te kunnen bepalen hoe verschillende celtypes reageren in aanwezigheid van diverse

apoptotische stimuli (celdoodkinetiek), moet het proces van apoptose worden stilgelegd. Dit is vanwege het feit dat het proces van apoptose relatief kort is en een variabele tijdsduur in vergelijking tot de celcylcus heeft. De duur van het apoptotisch proces is afhankelijk van het celtype en de stimulus die gebruikt wordt om het apoptotisch proces te initiëren. Verder zijn morfologische kenmerken pas zichtbaar na "the point-of-no-return" en zijn de gevormde apoptotische lichaampjes klein en worden deze snel opgeruimd. Een nieuwe flow cytometrische bepaling is ontwikkeld, waarbij de caspases in de cel geremd worden door het gebruik van een fluorochroom gelabelde remmer van caspases (FLICA). In combinatie met propidium jodide (PI) kunnen de verschillende stadia in het apoptotisch proces in kaart worden gebracht en kan de celdoodkinetiek bepaald worden. Uit dit onderzoek blijkt dat de celdoodkinetiek afhangt van enerzijds het celtype en anderzijds de gebruikte stimulus. In aanwezigheid van dezelfde stimulus vertonen cellen die op een oppervlak groeien (adherente cellen, in ons geval endotheelcellen) een andere transitie door de verschillende stadia van het apoptotische proces en hierdoor een andere kinetiek dan cellen die in suspensie groeien (HL60 bloedcellen). Verder versnelt TNF-α, dat de apoptotisch cascade activeert via binding aan specifieke receptoren op de celmembraan, in combinatie met de eiwitsyntheseremmer cycloheximide (CHX) het apoptotische proces in vergelijking tot camptothecine (CPT), dat een effect op de kern heeft (Hoofdstuk 3).

Fluorescente labels zijn dus erg nuttig om de verscheidene stadia in het apoptotisch proces te karakteriseren. Echter wanneer men dit proces in real-time wil bestuderen moet de continue aanwezigheid van deze labels worden vermeden, omdat deze schadelijk zijn voor de cel. In hoofdstuk 4 is een nieuwe flow cytometrische techniek beschreven waarbij gebruik wordt gemaakt van de intrinsieke fluorescentie (autofluorescentie; AF) van cellen om het proces van apoptose te bestuderen. AF wordt veroorzaakt door metabolieten in de cel die betrokken zijn bij het regelen van de energiehuishouding en daarom is AF voornamelijk gelokaliseerd in de mitochondria. Het induceren van apoptose in HL60 cellen met straling of chemische stoffen, zoals TNF-α/CHX en CPT, resulteert gedurende de eerste 2 uur in een stijging van de AF intensiteit, gevolgd door een daling tot 24 uur, resulterend in een verlaagde $AF^{24/2}$ factor. Dit fenomeen is voornamelijk

waarneembaar in cellen die zich bevinden in de late fase van het apoptotisch proces. De daling in de $AF^{24/2}$ factor is specifiek voor apoptotische cellen. Necrotische cellen hebben een $AF^{24/2}$ factor vergelijkbaar met onbehandelde cellen. Vanwege de specificiteit en de eenvoud van deze methode, is het meten van de AF intensiteit in de tijd uitermate geschikt als detectietechniek voor het analyseren van het proces van apoptose in real-time.

Flow cytometrie is dus uitermate geschikt voor het analyseren van het apoptotisch proces voor zowel cellen die in suspensie groeien als adherente cellen. Echter er zijn ook enkele nadelen. Voor flow cytometrische analyse zijn veel cellen nodig die veelal voor analyse aangekleurd of gefixeerd moeten worden, waardoor intacte individuele cellen niet bestudeerd kunnen worden. Verder veroorzaakt minimale manipulatie van cellen (bijvoorbeeld het losmaken van adherente cellen van het oppervlak met trypsine) apoptose en is het gebruik van fluorescente labels, zoals veel gebruikt in flow cytometrie, schadelijk voor de cellen. De tijd voor het gereed maken van de cellen voor analyse is dusdanig dat real-time analyse niet mogelijk is. Na analyse zijn de cellen verloren en dus niet meer bruikbaar voor verder onderzoek. Daarnaast is de experimentele uitvoer veelal bewerkelijk en kost daardoor veel tijd. Voor het doel van dit onderzoek, het analyseren van het proces van apoptose in real-time in individuele cellen in aanwezigheid van verschillende (doses) van medicamenten, blijken de conventionele technieken zoals flow cytometrie dan ook niet geschikt. Microtechnologie biedt wel de vereiste mogelijkheden voor dit onderzoek. Diverse manipulatie technieken, zoals het sorteren, losmaken, aankleuren, fixeren en lyseren van cellen, kunnen geïntegreerd worden op één enkele chip, waardoor veel tijd en werk bespaard wordt. De afmetingen in de chip zijn vergelijkbaar met de afmetingen van cellen, waardoor individuele cellen eenvoudig onderzocht kunnen worden. Het analyseren van individuele cellen is vooral van belang wanneer het proces van apoptose wordt bestudeerd, omdat in aanwezigheid van een bepaalde stimulus niet alle cellen tegelijk in apoptose zullen gaan. Verder is er door de kleinere afmetingen minder monster nodig, hetgeen uitermate voordelig is als er maar een beperkt aantal cellen aanwezig is (bijvoorbeeld primaire cellen). Dezelfde cellen kunnen worden geïncubeerd met oplopende doses van eenzelfde medicament waardoor dosis-response analyse mogelijk wordt, maar ook een serie van diverse medicamenten kan

worden geanalyseerd. De integratie van verscheidene detectietechnieken (elektrische eigenschappen, celgrootte en morfologie, vrijgekomen celcomponenten) maakt het mogelijk om in één chip met de aanwezige cellen de verschillende fases in het apoptotisch proces te volgen. Het apoptotisch proces kan dus in detail in real-time in de chip gevolgd worden, hetgeen tot nu toe niet mogelijk was met de bestaande conventionele technieken (Hoofdstuk 2).

Deze studie richt zich op het evalueren van morfologische verschillen tussen cellen van verschillende oorsprong, met name gezonde cellen versus kankercellen, in ons geval borstkankercellen. Borstkanker is wereldwijd de meest voorkomende vorm van kanker. Elk jaar wordt er bij 1 miljoen vrouwen borstkanker gediagnosticeerd. Als adjuvante therapie zijn er meerdere vormen van endocriene therapie (hormoontherapie) bekend, maar de ideale vorm van adjuvante therapie is er nog niet. In hoofdstuk 5 zijn verschillende vormen van hormoontherapie (oestrogenen, progestagenen, tamoxifen en aromatase remmers) geanalyseerd voor hun effect op zowel de proliferatie als de apoptose. De ratio tussen proliferatie en apoptose bepaalt het netto effect van de diverse medicamenten op de gebruikte borstkankercellen. Tamoxifen wordt vaak voorgeschreven als adjuvante therapie. In dit (*in vitro*) onderzoek geeft tamoxifen op drie verschillende borstkanker cellen een apoptotisch effect. Het nadeel van tamoxifen is echter dat patiënten resistent kunnen worden voor deze vorm van behandeling. Hoewel de aromatase remmers (AI) in de kliniek een goed alternatief vormen, laat ons *in vitro* onderzoek, onverwacht, zien dat de AI niet in alle gevallen apoptose geven. Verder onderzoek naar AI is nodig voor het bepalen wat de beste dosis en incubatietijd is. Uiteraard geeft *in vitro* onderzoek alleen een idee wat voor een effect een bepaald medicament zal hebben, maar het is wel een belangrijke aanleiding voor grote gerandomiseerde trials om het effect van de behandeling bij groepen van patiënten te onderzoeken. Omdat ieder patiënt vanwege genetische variatie anders zal reageren op dezelfde vorm van therapie, heeft het de voorkeur om eigen patiëntenmateriaal, bijvoorbeeld enkele borstkankercellen verkregen uit biopsie, te onderzoeken (*ex vivo*) in aanwezigheid van verschillende vormen van therapie. Zo kan op individueel niveau voor ieder patiënt de beste therapie bepaald worden in termen van soort medicament, dosis en wijze van toediening. Vanwege de kleine celaantallen en de

mogelijkheid tot dosis-response analyse, is microtechnologie voor dergelijk onderzoek uitermate geschikt.

Voordat experimenten met cellen kunnen worden uitgevoerd op een chip, moet er eerst voor worden gezorgd dat deze nieuwe omgeving niet schadelijk is voor de cellen, oftewel de vitaliteit van de cellen moet worden onderzocht (Hoofdstuk 6). Zowel de omgeving (temperatuur, CO_2 concentratie) als het materiaal waaruit de chip is gemaakt heeft een effect op de vitaliteit van de cellen. Cellen moeten gekweekt worden bij 37°C, omdat bij kamertemperatuur het apoptotisch proces wordt geactiveerd. Verder is er specifiek medium nodig (CO_2 independent medium) als experimenten buiten de stoof worden uitgevoerd, om te zorgen dat de pH constant blijft. In de microtechnologie worden diverse materialen gebruikt, waaronder silicium-oxide, Pyrex glas, Borofloat glas en het polymeer polydimethylsiloxaan (PDMS). Al deze materialen zijn geschikt voor HL60 cellen en het behandelen van deze materialen met serum zorgt voor een proliferatief effect. Uiteraard speelt de materiaalkeuze een belangrijkere rol wanneer het gaat om cellen die aan het materiaal moeten hechten om zo hun vitaliteit te behouden. Borstkankercellen hechten en groeien op Pyrex glas en borosilicaat glas (microscoop glaasjes), maar niet op onbehandeld PDMS (hydrofoob) of PDMS behandeld met serum of polyethyleenglycol (hydrofiel). Endotheelcellen hechten en groeien op Pyrex glas en borosilicaat glas behandeld met fibronectine of 0,1 % (3-(2,3-epoxypropoxy)-propyl)-trimethoxysilaan (APS), maar niet op onbehandeld of behandeld PDMS (Hoofdstuk 7).

Naast het belang van de omgeving en de materiaalkeuze, moet het microfluïdisch systeem gekoppeld worden aan een flow-systeem, dat nodig is om de cellen te voorzien van vers medium en zuurstof en waarmee medicamenten aan de cellen kunnen worden toegediend. De snelheid waarmee de vloeistof over de cellen stroom, oefent een mechanische kracht uit op de cel, gedefinieerd als de schuifspanning (shear stress). Endotheelcellen hebben een bepaalde schuifspanning nodig om te overleven en zich te ontwikkelen. Voor epitheliale cellen, zoals borstkankercellen, moet deze schuifspanning zo laag mogelijk zijn om de vitaliteit van de cellen te waarborgen. In hoofdstuk 7 zijn allerlei chip-ontwerpen, onderling verschillend in materiaal en geometrie, bestudeerd, om uiteindelijk het beste ontwerp te bepalen. Apoptose chip #3 is het meest geschikt gebleken voor het uitvoeren van apoptose studies. De chip bestaat uit een aanvoer- en afvoerkanaal,

dat in het midden uitloopt tot een breder kanaal. Deze structuren zijn gemaakt in PDMS. PDMS is uitermate geschikt voor cellen vanwege zijn biocompatibiliteit en gaspermeabiliteit. Verder is de fabricatie van deze chips eenvoudig en snel uit te voeren. De kanalen worden gedicht door het PDMS te binden aan een microscoopglaasje. Dit is het materiaal waaraan de cellen zich hechten en zo kan ook het apoptotisch proces optisch geanalyseerd worden. Daarnaast is de connectie met het flow-systeem simpel. Het hele microfluïdische platform, bestaande uit de chip en het flow-systeem, gebruikt wegwerpartikelen, zoals gewenst is als er met biologisch materiaal wordt gewerkt.

In hoofdstuk 8 wordt beschreven hoe borstkankercellen en endotheelcellen behandeld worden met verschillende apoptotische stimuli en op zowel een conventionele manier (flow cytometrie en immunologische DELFIA® methode) als in real-time op individueel celniveau geanalyseerd. De morfologische verschillen tussen deze 2 celtypes is onderzocht. Van gezonde adherente cellen of goedaardige tumoren is bekend dat zodra deze cellen losraken van hun plek, door enerzijds mechanische (bijvoorbeeld luchtbellen) of anderzijds chemische oorzaak (bijvoorbeeld TNF-α), de apoptotische cascade wordt geactiveerd, een proces dat anoikis wordt genoemd. Van (kwaadaardige) tumorcellen is bekend dat het proces van apoptose en anoikis is verstoord. Hierdoor krijgen deze tumorcellen de mogelijkheid om hun plek van oorsprong te verlaten en te metastaseren naar een andere plek in het lichaam (anoikis-resistent fenotype). De combinatie TNF-α/CHX activeert het apoptotische proces in (onsterfelijk gemaakte) endotheelcellen, resulterend in het ronden en krimpen van deze cellen en in een toename van de fluorescentie van specifieke labels voor het detecteren van apoptose. In het laatste stadium van het apoptotisch proces laten de endotheelcellen los van hun oppervlak. Endotheelcellen vertonen dus een proces dat wordt gedefinieerd als apoptotisch-geïnduceerde anoikis. Borstkankercellen in aanwezigheid van TNF-α/CHX of de proteïne kinase remmer staurosporine (SSP) vertonen alle karakteristieken van apoptose, zoals het ronden, krimpen, membrane-blebbing en een toename in fluorescentie van de specifieke labels voor het detecteren van apoptose. Echter in het laatste stadium van het apoptotische proces laten deze cellen niet los van hun oppervlak. Het proces van anoikis wordt dus niet aangetoond. Daarentegen verlaten borstkankercellen in aanwezigheid van TNF-

α/CHX of tamoxifen hun kolonie en bewegen naar andere plekken in de chip. Luchtbellen zorgen ervoor dat borstkankercellen mechanisch van hun plek verwijderd worden. Toch induceert dit niet in alle borstkankercellen apoptose. Sommige cellen zijn in staat om op een andere plek in de chip te hechten en hierdoor blijft hun vitaliteit behouden. Verder onderzoek is nodig om deze observaties op hun waarde te schatten en om de mogelijke rol in de behandeling van kanker vast te stellen. Hiervoor zullen zowel verschillende medicamenten (cytostatica, medicamenten die de binding van cellen aan de matrix/oppervlak beïnvloeden) als diverse celtypes (normale epitheliale cellen, metastaserende epitheliale tumor cellen) bestudeerd moeten worden. Verdere aanbevelingen richten zich op onderzoektechnische aspecten als het voorkomen van luchtbellen, het gebruik van een speciale coating voor epitheelcellen om de hechting aan het oppervlak te bevorderen (laminine coating) en een chip te ontwikkelen waarop meerdere (apoptotische) analyses tegelijk kunnen worden uitgevoerd (high-throughput). Bij dat laatste moet de chip bestaan uit meerde kweekkamers gecombineerd met een gradiëntgenerator voor het creëren van aflopende concentraties van een medicament. Optische analyse is niet geschikt bij high-throughput analyse en zal moeten worden vervangen door elektronische analyse. Elektrodes geïntegreerd in de chip kunnen het aantal cellen dat heeft losgelaten tellen, of met behulp van "nanowires" kunnen verschillen in geleiding/weerstand worden gemeten die mogelijk ontstaan wanneer cellen zich delen, verplaatsen of dood gaan. Uiteindelijk moet blijken of microtechnologisch onderzoek met een chip een belangrijke bijdrage kan leveren voor de keuze van de meest optimale behandeling in de kliniek. Met slechts enkele cellen van de patiënt, gekweekt in de chip, kan het effect van verschillende medicamenten in diverse doses op het evenwicht tussen proliferatie en apoptose bepaald worden. Op deze wijze kan zorg op maat geleverd worden door voor iedere patiënt op individueel niveau de beste therapie te bepalen. Verder kan dit chip-ontwerp, naast het optimaliseren van de behandeling van borstkanker, van belang zijn voor andere vormen van kanker en ziektebeelden waarbij onderdrukking of een overmaat aan apoptose een rol speelt.

Dankwoord

Na meer dan 200 bladzijdes bewaar je het lastigste toch voor het laatst (viel achteraf reuze mee). Toch zijn dit de pagina's die in elk proefschrift altijd als eerste worden gelezen. Nu kan ik heel zakelijk en kort van stof zijn (à la me; kan ik ook niemand vergeten) en dit proefschrift eindigen met 3 woorden: DANK JE WEL! Zo hou je wel enkele minuutjes over om ook de rest van dit boekje wat aandacht te schenken. Maar na 4 jaar als PhD wil ik toch een paar mensen in het bijzonder bedanken.

Allereerst mijn 3 promotoren: een uitzondering.
Professor Albert van den Berg, beste Albert, bedankt dat ik deel mocht uitmaken van de BIOS groep. Eindelijk cellen in de groep! In de jaren als PhD heb jij mij veel vrijheid gegeven, wat ik altijd als erg prettig heb ervaren. En als leek in de microtechnologie, heb ik veel gehad aan je advies en ervaring. Samen met Istvan Vermes hebben we je enthousiast gemaakt voor celbiologisch onderzoek, en je hebt zelfs je sabbatical leave gewijd aan het proces van apoptose (sorry, ik ben een huismus, waar jij meer weg hebt van een trekvogel). Daarnaast bedankt voor het mogelijk maken van alle gezellige BIOS-uitjes, week in Denemarken, conferentiebezoeken en de BBQs bij je thuis.

Professor Istvan Vermes, beste Istvan, in het begin moest ik wel wennen aan uw Hongaarse temperament ("zo" betekent "nu"), maar ik ken geen begeleider die zo bekwaam en geïnteresseerd als u bent. Terwijl ik soms niet helemaal tevreden was over even een resultaat, was u altijd erg enthousiast. Bellen, mailen of even langs komen om te vragen waar ik mee bezig was, of alles goed ging, en dat ik toch altijd iets van me moest laten horen als ik weer een experiment had uitgevoerd. Hopelijk wilt u ook gedurende mijn nieuwe project als postdoc als adviseur blijven fungeren.

Professor Helene Andersson, dear Helene, supervision at a distance, though I could always call or email you for advice. And many thanks for the nice weather you always took with you, can't you come more often???

Lieve Ana en Marloes, mijn paranimfen, geweldig dat jullie samen met mij op het podium willen staan. Dear Ana, you have always been so enthusiastic and best room-mate ever! Always complimenting me about all sort of things ("que nice perfume, que chullo clothes, I love your haircolour"). I know it was difficult for you to leave all you friends behind, but I'm very proud of you that you have made the step and wish you all the best in Lausanne. I promise I will make an MSN account so we can chat! Lieve Marloes, mijn over-buurvrouw op het lab, wat kun je met jou lachen (niet dat ik boven jou uitkom, maar goed). Vol energie, altijd vrolijk, en voor alles in! Nu samen op de UT, op loopafstand voor lunch of een kopje thee (cream of island, the best), om bij te kletsen!

Gedurende mijn promotie heb ik op 2 locaties gewerkt: de BIOS groep van de UT en het lab van het MST. Je kunt de pech hebben dat je hierdoor buiten de boot valt en alles mist. Maar niets is minder waar, ik heb me altijd erg op m'n plek gevoeld. Deze 4 jaar zijn voorbij gevlogen!
Alle collega's van het lab hartstikke bedankt voor alle gezellige momenten in het kippenhok ("koffiekamer") en de vele lab-uitjes. "Dames van O&O", jullie zijn top! Met veel plezier denk ik terug aan onze geweldige weekendjes weg: zwoegen in de Ardennen (Judith, dankzij jou is onze aanwezigheid voor altijd verenigd in het hout), pictionary-en (sorry dames, mijn teken-kwaliteiten laten te wensen over), soppen in de drek (er waren wadlopers met een nog slechtere kledingkeuze, lees: sportbroekje), slapen in een "hutje op de hei", en laatst nog het zeilen (Ida, bedankt!). Het is maar een greep van wat we allemaal hebben gedaan, en hoewel we nu allemaal op een andere plek zitten, hoop ik toch dat deze uitstapjes een blijvertje zijn. Naast natuurlijk de daghap om toch op de hoogte te blijven van alles wat reilt en zeilt.
Dr. Henk Franke, beste Henk, vol met nieuwe experimenten en hormonen die de moeite waard zijn om getest te worden. Soms was tijd de beperkende factor. Altijd erg geïnteresseerd hoe het met mijn promotie ging en altijd bereikbaar voor hulp. Ik ben daarom ook erg blij dat je deel wilt uitmaken van mijn commissie. Ik hoop dat het project een doorstart maakt, en als ik nog van nut kan zijn, je weet me te vinden.
Beste Job van der Palen, bedankt voor het beantwoorden van al mijn statistiek vragen.

Lieve (ex-)BIOS-ers, wat een geweldige groep om deel van uit te mogen maken! Allemaal je eigen vakgebied, maar nooit beroerd om anderen te helpen en ervaringen te delen. Bedankt voor de gezellige momenten in de koffiekamer (wat is het vol: is er taart???; sorry voor de tosti-stank) en de leuke uitjes! Ad, Albert, Ana, Anil, Arjan, Björn, Celio, Daniël, Doro, Edwin, EdwinO, Eddy, Egbert, Elwin, Erik F., Erik K., Gabriël, Georgette, Han, Hien-Duy, Ida, Iris, Jacob, Jan E., Jan van N., Johan, Joke, Jurjen, Kevin, Lingling, Mathieu, Monica, Paul, Piet, Regina, Roald, Rob, Sebastiaan, Séverine, Steven (en Saron), Sumita, Svetlana, Ton, Vincent, Wim, Wojciech, Wouter O., en Wouter S. (meester in het maken van vage opmerkingen), BEDANKT! Blij dat ik nog even mag blijven. Jurjen (hoi, goeie 's middags, komt binnen wanneer ik me tas pak om huiswaarts te keren, maar als we dan samen waren bedankt voor de dropjes, slechte muziek-keuze, hoewel je radio 3 nu ook gevonden hebt, en dat ik je paranimf mocht zijn), Egbert (Eggie, weer terug op je oude stek, betere muziek-smaak, geen ochtendmens, hoewel je het toch soms speciaal voor mij hebt geprobeerd) en Ana (hola, mijn lieve paranimf), dank je wel dat jullie mijn kamergenootjes zijn/waren. Paul ("polletje"), bedankt voor alle gezellige momenten met de cellen in "ons" kweekhok. Jan van N., ik weet je werd soms gek van mij, maar bedankt voor het maken van de vele chips. Hermine, bedankt voor al het regelwerk. Ralph (ICT) bedankt voor het installeren van mijn laptop en router en het oplossen van mijn vele computerproblemen.

Daarnaast wil ik natuurlijk alle arts-assistenten en studenten, die ik heb begeleid bedanken voor al hun hulp, inzet en enthousiasme. Janneke, the best student ever! Wat een gezellige meid! Wat heb jij het werken in het laboratorium snel opgepakt. En wat gun ik het jou dat je artikel toch nog wordt gepubliceerd, 3x is scheepsrecht! Job, niks voor zo aannemen, altijd kritisch en vol nieuwe ideeën. Bedankt, dit houd je als begeleider scherp, en zo zie je ook iets vanuit een ander perspectief.

Els Weir, bedankt voor het beoordelen van mijn Engelse schrijfkunsten. De avonden bij jou thuis heb ik als heel plezierig (lekker wijntje) en erg leerzaam ervaren. Ik waardeer het ontzettend dat je hier zo veel tijd in hebt willen steken, zeker omdat het onderwerp niet in je vakgebied ligt, wat het goed beoordelen lastig maakt.

Ik ben erg van het scheiden van werk en privé (goh, echt?!). Maar je hebt een goede thuisbasis nodig om op je werk te kunnen presteren.
Ola daddy en mams, terwijl ik toch heel bescheiden ben en niet heel uitgebreid over mijn werk praat, zijn jullie altijd erg geïnteresseerd, vol belangstelling, en willen jullie alles weten. Troste ouders, trotse dochter (alias ola-loortje)! Lieve broertjes, kus van je-zus. Lieve Veldhuisjes, een warmer schoonfamilie-nest kan ik me niet wensen. Lieve Nicole, bedankt voor onze momenten lekker thuis op de bank of samen in de kroeg. We kunnen uren niks zeggen of juist de hele avond kletsen over van alles en nog wat. Je bent geweldig! Wanneer gaan we Oldenzaal weer eens onveilig maken? En natuurlijk bedankt voor het lopen van de een-daagse van Nijmegen met mij (een unicum, hebben wij weer), we gaan ooit nog voor de 4! Lieve Robbin, Jonne, Gijs en David, bedankt voor alle prachtige tekeningen en kleffe zoenen! Nichtjes en neefjes zijn geweldig, kun je zelf ook weer eens kind zijn! Vrienden, hoewel we toch allemaal onze eigen weg zijn gegaan en elkaar toch wat minder zien, zijn de momenten samen heel gezellig. De harde kern blijft altijd over!
Last but not least, Dick. Je weet, ik ben niet het type (jij trouwens al helemaal niet) om nu in geuren en kleuren aan dit lezerpubliek te gaan schrijven hoe geweldig je bent. Bijna 10 jaar samen, dus dan weten we wel wat we aan elkaar hebben en kunnen woorden niet beschrijven hoe gelukkig ik ben met jou. Ik ga niet voor niks met gierende banden om half 5 op hoes an! Luv you!

Floor

P.S. Voor degenen die ik ben vergeten, niks persoonlijks, en daarom bij deze hartstikke bedankt!